

## Chapter 15

# 100 Years of Progress in Tropical Cyclone Research

KERRY EMANUEL

*Lorenz Center, Massachusetts Institute of Technology, Cambridge, Massachusetts*

### ABSTRACT

A century ago, meteorologists regarded tropical cyclones as shallow vortices, extending upward only a few kilometers into the troposphere, and nothing was known about their physics save that convection was somehow involved. As recently as 1938, a major hurricane struck the densely populated northeastern United States with no warning whatsoever, killing hundreds. In the time since the American Meteorological Society was founded, however, tropical cyclone research blossomed into an endeavor of great breadth and depth, encompassing fields ranging from atmospheric and oceanic dynamics to biogeochemistry, and the precision and scope of forecasts and warnings have achieved a level of success that would have been regarded as impossible only a few decades ago. This chapter attempts to document the extraordinary progress in tropical cyclone research over the last century and to suggest some avenues for productive research over the next one.

### 1. Introduction

By the time that the American Meteorological Society (AMS) was founded in 1919, mariners, engineers, and scientists had made great strides in characterizing the climatology of tropical cyclones, including their favored formation regions, tracks, seasonal variability, and surface wind field. By the middle of the nineteenth century, these characteristics had been compiled into a number of treatises, most notably by Sir Henry Piddington, whose 1848 work *The Sailor's Horn-Book for the Law of Storms*, which built on earlier research by William Redfield and Lieutenant Colonel William Reid, laid out a strategy by which ships at sea could avoid or more safely ride out tropical cyclones (Piddington 1848). Observations were sparse, although by the late nineteenth century Father Benito Viñes, a Jesuit priest and director of Havana's Belén Observatory, had established a rudimentary network of observations in the Caribbean Sea region and argued for the importance of upper-level winds in steering hurricanes (Viñes 1885).<sup>1</sup>

---

<sup>1</sup>A summary of Viñes's contribution is provided by Guadalupe (2014).

As valuable as these contributions were, almost nothing was known about the vertical structure of tropical cyclones, or the basic physical mechanism that drives them. Indeed, up through the 1930s, it was widely believed, on the basis of the observed rapid diminution of surface winds after landfall, that their circulation extended upward only 3 km or so, while the reigning theory for their power source was that of James Pollard Espy, who had surmised by the middle of the nineteenth century that cyclones in general were powered by latent heat release in a conditionally unstable atmosphere, a belief that persists even today.<sup>2</sup>

The first century of AMS's existence saw much progress in measuring, understanding, and forecasting tropical cyclones. This chapter attempts to document that progress and to set it in the context of important developments in the broad field of meteorology. Indeed, the magnitude and breadth of that progress is so large as to present a challenge to anyone who would attempt to summarize it in single chapter. Here I have attempted to document what, in my view, were the most significant advances, aiming more for readability than for comprehensiveness, and emphasizing historical significance, even in the case of the odd dead-end research path. Of necessity, many important references are omitted.

---

<sup>2</sup>See Kutzbach (1979) for a detailed account of Espy's work.

---

*Corresponding author:* Kerry Emanuel, emanuel@mit.edu

DOI: 10.1175/AMSMONOGRAPHS-D-18-0016.1

© 2018 American Meteorological Society. For information regarding reuse of this content and general copyright information, consult the [AMS Copyright Policy](#) ([www.ametsoc.org/PUBSReuseLicenses](http://www.ametsoc.org/PUBSReuseLicenses)).

The breadth of this topic also poses an organizational challenge. I have chosen to begin chronologically, but I shift, in discussing events at the end of the twentieth century, to a more topically based structure.

## 2. Watershed years: 1943–68

On 27 July 1943, Army Air Corps Colonel Joseph B. Duckworth, with navigator Lieutenant Ralph O'Hair, took an Air Force AT-6 trainer from an airfield in Texas and became among the first aviators to penetrate the eye of a hurricane. By the late 1940s, airborne reconnaissance of hurricanes and typhoons had become routine. This marked the beginning of a highly productive era of direct measurements of tropical cyclones above the surface; before this time what few measurements were made came from chance passages of storms over ships, islands, and coastal regions. While these earlier encounters sufficed to establish a general climatology of tropical cyclones as well as the structure of their surface wind, rain, and pressure fields, almost nothing was known about their three-dimensional structure. An important advance was, however, made by Bernhard Haurwitz (Haurwitz 1935), who inferred that the perturbation pressure could not vanish at altitudes much below 10 km, based on application of the hydrostatic equation to temperature measurements in typhoon eyes as they passed over high mountains. Further advances would await the advent of aircraft-based measurements.

The rapid implementation of routine airborne reconnaissance was largely motivated by a series of wartime U.S. naval disasters involving violent storms. Among these were the sinking of the destroyer USS *Warrington* in the Great Atlantic Hurricane of September 1944, with the loss of 248 mariners. Although too late for the *Warrington*, that hurricane was the first to be surveyed by meteorological radar as the storm later passed east of the U.S. Naval Air Station at Lakehurst, New Jersey. Scarcely three months later, Admiral William Halsey unwittingly sailed Task Force 38 of the U.S. Third Fleet directly into the center of vicious Typhoon Cobra, which sank three destroyers and took the lives of 790 sailors. Some of the ships were outfitted with radar, and thus Cobra became the second tropical cyclone recorded on radar. An image from such a radar, reproduced in Fig. 15-1, shows an unmistakable rain-free eye, an eyewall, and spiral rainbands, but radar operators of that era had no training to interpret images like these.<sup>3</sup>



FIG. 15-1. Radar image of Typhoon Cobra captured from one of the ships of Admiral Halsey's Third Fleet, east of the Philippines. This was only the second tropical cyclone captured on radar. (Source: NOAA Photo Library; original photograph was taken by the U.S. Navy.)

This incident in particular motivated the establishment of a U.S. Navy reconnaissance and forecasting operation which later became the Joint Typhoon Warning Center and which continues to provide valuable forecasts and warnings today. Routine airborne reconnaissance of western Pacific Ocean tropical cyclones began shortly after the Third Fleet disaster and continued through 1987.

The wealth of new data from reconnaissance missions helped stimulate renewed interest in tropical cyclone science. Among those who took an intense interest was Herbert Riehl.<sup>4</sup> Riehl was a German Jew whose mother got him out of Germany in 1933 as the Nazi regime consolidated power. After brief stints as a stockbroker in New York, a scriptwriter in Hollywood, and back to New York as an assistant to a green grocer, Riehl decided in 1940 to join the Army Air Corps, where he was directed to New York University's cadet program in meteorology. After graduating first in his class, he met Carl-Gustaf Rossby, who secured for him a meteorology job at the University of Washington. In 1942, he was hired as an instructor in the University of Chicago's recently founded Institute of Meteorology, where he joined such luminaries as Rossby, Horace Byers,

<sup>3</sup> Drawings on ancient vases from the Caribbean region suggest that pre-Columbian cultures may have understood that tropical cyclones were vortices and possessed spiral structure (Ortiz 1947; Emanuel 2005a).

<sup>4</sup> Lewis et al. (2012) is a wonderful short biography of Riehl.

Helmut Landsberg, Victor Starr, George Platzmann, George Benton, and Verner Suomi. The opening of the Pacific theater of World War II (WWII) created an urgent need to forecast tropical weather; in response Rossby developed the Institute of Tropical Meteorology (ITM) in Rio Piedras, Puerto Rico, operated jointly by the University of Chicago and the University of Puerto Rico. Riehl was sent there in July 1943, joining such notable colleagues as Clarence Palmer, Gordon Dunn, and Reid Bryson. Riehl's experience at the ITM was transformative, propelling him into the serious study of tropical meteorology, culminating in the publication of a textbook of the same name (Riehl 1954).

A seminal paper from that time is "A model of hurricane formation" (Riehl 1950), which, to my knowledge, is the first published paper that explicitly acknowledges the critical role of heat transfer from the ocean in powering tropical cyclones. Like Horace Byers before him (Byers 1944), Riehl recognized that some of the transfer occurs when air does not cool at the dry adiabatic rate as it spirals down the surface pressure gradient, and the rest is owing to latent heat transfer from the surface. He illustrated the energy cycle on tephigrams, but did not try in that paper to quantify the energy cycle specifically or to develop a relation for the peak wind or central pressure.

That was left to another German scientist, Ernst Kleinschmidt. A contemporary of Herbert Riehl's, Kleinschmidt was based in Germany for his whole life; of course, he traveled and was invited by Rossby to visit the University of Stockholm in 1951 and by Riehl to visit the University of Chicago in 1959–60. Kleinschmidt was by all accounts an idiosyncratic scientist, developing ideas that were usually considered eccentric at the time, but some of which later came to be widely appreciated.<sup>5</sup> He published a single paper on tropical cyclones (Kleinschmidt 1951), which was the first to develop a quantitative formula for peak wind speed as a function of the thermodynamic energy cycle. Like Riehl, Kleinschmidt recognized the crucial role of surface heat transfer: "The heat removed from the sea by the storm is the basic energy source of the typhoon," and his formula for peak wind speed was

$$V^2 = 2E \frac{q^2}{1 - q^2}, \quad (15-1)$$

where  $E$  is the available energy calculated from a tephigram by assuming moist adiabatic ascent in the

eyewall, starting from saturation at sea surface temperature, and  $q$  is the fraction of the velocity that would occur if air conserved its angular momentum in the inflow. Kleinschmidt did not attempt to calculate that fraction from boundary layer considerations, but he did regard the steady hurricane vortex as having constant moist entropy along angular momentum surfaces (zero saturated potential vorticity), as did Douglas Lilly and the present author in the 1980s.

Kleinschmidt's paper foreshadowed the modern understanding of tropical cyclone physics, but, perhaps because it was written in German, it was not widely read at the time and might have disappeared into obscurity had it not been resurrected by Alan Thorpe at the University of Reading and his colleagues at the U.K.'s Meteorological Office. For a detailed comparison between Kleinschmidt's work and that of the author of this chapter, some 35 years later, see Gray (1994).

The work of Riehl and his colleagues, most notably Joanne Malkus, culminated in the publication of two papers in the early 1960s: Malkus and Riehl (1960) and Riehl (1963b). The first of these once again emphasized that the radial temperature gradients that sustain tropical cyclones arise from heat transfer from the ocean. Using simple hydrostatics coupled with the assumptions of a moist adiabatic lapse rate and undisturbed geopotential height at 100 hPa, they derived a simple relationship between the pressure drop from the undisturbed environment to the inner edge of the eyewall and the increase in boundary layer equivalent potential temperature  $\theta_e$  over the same interval:

$$\delta p_s = -2.5\delta\theta_e, \quad (15-2)$$

where the pressure drop is in hectopascals and the  $\theta_e$  increase is in kelvins. This explicitly quantifies the relationship between storm intensity and radial gradients of boundary layer moist entropy, but assumes that moist isentropic surfaces are vertical (rather than being congruent with angular momentum surfaces, as Kleinschmidt had assumed) and assumes a specific level (100 hPa) at which geopotential perturbations vanish. Malkus and Riehl (1960) is a quirky paper and includes demonstrably incorrect inferences such as "the pressure gradient along the [boundary layer] trajectory is thus limited by the input rate of sensible heat from sea to air." They come very close to deriving what is now generally regarded as a correct relationship between storm intensity and surface enthalpy fluxes. Specifically, they wrote a budget equation for equivalent potential temperature along a boundary layer streamline in an

<sup>5</sup> See Alan Thorpe's summary of Kleinschmidt's scientific achievements (Thorpe 1992).

assumed steady flow. Combining their (17), (18), and (33) gives

$$V \frac{\partial \theta_e}{\partial s} = C_k V \frac{(\theta_{e0}^* - \theta_e)}{h}, \quad (15-3)$$

where  $V$  is the magnitude of the velocity along a streamline,  $s$  is distance along a streamline,  $C_k$  is the surface enthalpy exchange coefficient (but note that Malkus and Riehl did not assume as I have here that the exchange coefficients for sensible and latent heat are equal),  $\theta_{e0}^*$  is the saturation  $\theta_e$  of the sea surface,  $\theta_e$  is that of the boundary layer air, and  $h$  is the boundary layer depth (which Malkus and Riehl unaccountably omitted from their equivalent equation). They then combined (15-2) with (15-3) to obtain

$$\frac{\partial p_s}{\partial s} = -2.5 C_k \frac{(\theta_{e0}^* - \theta_e)}{h}. \quad (15-4)$$

This is equivalent to the equation that follows their (33). Their (35) expresses a relationship between pressure gradient along a streamline and dissipation of kinetic energy:

$$V \frac{\partial p_s}{\partial s} = \frac{-C_D}{h} \rho V^3, \quad (15-5)$$

where  $C_D$  is the drag coefficient and  $\rho$  is the air density. They might have eliminated the pressure gradient between (15-4) and (15-5) to obtain

$$V^2 = 2.5 \frac{C_k}{C_D} \frac{(\theta_{e0}^* - \theta_e)}{\rho}, \quad (15-6)$$

but they did not, instead switching to a peculiar discourse on the nature of boundary layer air trajectories and returning to their contention that the pressure drop is proportional to only the sensible heating of the boundary layer, which is a contradiction to (15-2) that appeared earlier in the same paper. Had they just taken the simple step of combining their equivalent of (15-4) and (15-5), they would have been the first to discover that the intensity varies directly with  $C_k$  and inversely with  $C_D$  and would have confirmed Kleinschmidt's finding that the true driver is the net enthalpy disequilibrium between the tropical atmosphere and oceans and not just the temperature difference.

Later, Riehl (1963b) derived an equation similar to (15-6) but without the explicit dependence on the exchange coefficients, and with a factor that depends on the ratio of some outer radius to the radius of maximum winds. This paper marked the end of a remarkably productive sequence of papers addressing the steady-state structure and energetics of tropical cyclones that

began with Riehl (1950). Herbert Riehl himself would go on to make many important contributions to tropical meteorology and hurricane science, not the least of which were his students, who would constitute the core of research on tropical cyclones for several decades. These included T. N. Krishnamurti, William Gray, Robert Simpson, Noel LaSeur, Russell Elsberry, Charles Jordan, Klaus Fraedrich, José Colón, and Elmar Reiter.<sup>6</sup> Joanne Malkus (later Simpson) would also significantly advance tropical meteorology, but neither scientist returned to the issue of the energy cycle of tropical cyclones.

Rossby enticed a steady stream of distinguished visitors to the University of Chicago; among whom was the Finnish atmospheric scientist Erik Palmén, who was resident there during 1946–47. He would go on to co-author papers with Riehl and with Riehl's student Charles Jordan. Of particular note is his paper "On the formation and structure of tropical hurricanes" (Palmén 1948), a work of which he was particularly proud (Palmén 1985). He expressed the view that the energy for tropical cyclones comes from the conditional instability of the tropical atmosphere, a line of thought dating back to the work of Espy (1841); Palmén does not mention the local flux of enthalpy from the ocean. But he produced what this author believes to be the first published vertical cross section through a hurricane, based on a single radiosonde ascent in the eye of a 1944 hurricane, on a tropical mean sounding presumed to represent the undisturbed environment, on his knowledge of the character of the surface wind field and on basic notions of thermal wind balance. His Fig. 9 is reproduced here as Fig. 15-2. Palmén's depiction is remarkably prescient, showing the eyewall as a kind of front, the amplification of the temperature anomaly with altitude, and the inference that air in the eye is descending. He even shows a slight cold anomaly at the storm center in the lower stratosphere, a feature seen in recent observations by very-high-altitude aircraft and in some numerical simulations.

In the same paper, Palmén demonstrated, using surface data and soundings from the tropical Atlantic Ocean, that hurricanes only develop over ocean water where the air temperature exceeds 27°C, but not within 5° of latitude of the equator. He also showed that these regions are conditionally unstable, whereas other parts of the tropics (or during other seasons) are generally stable.

<sup>6</sup>These and many other aspects of the "family tree" of tropical researchers may be found in the informative and engaging work of Hart and Cossuth (2013).

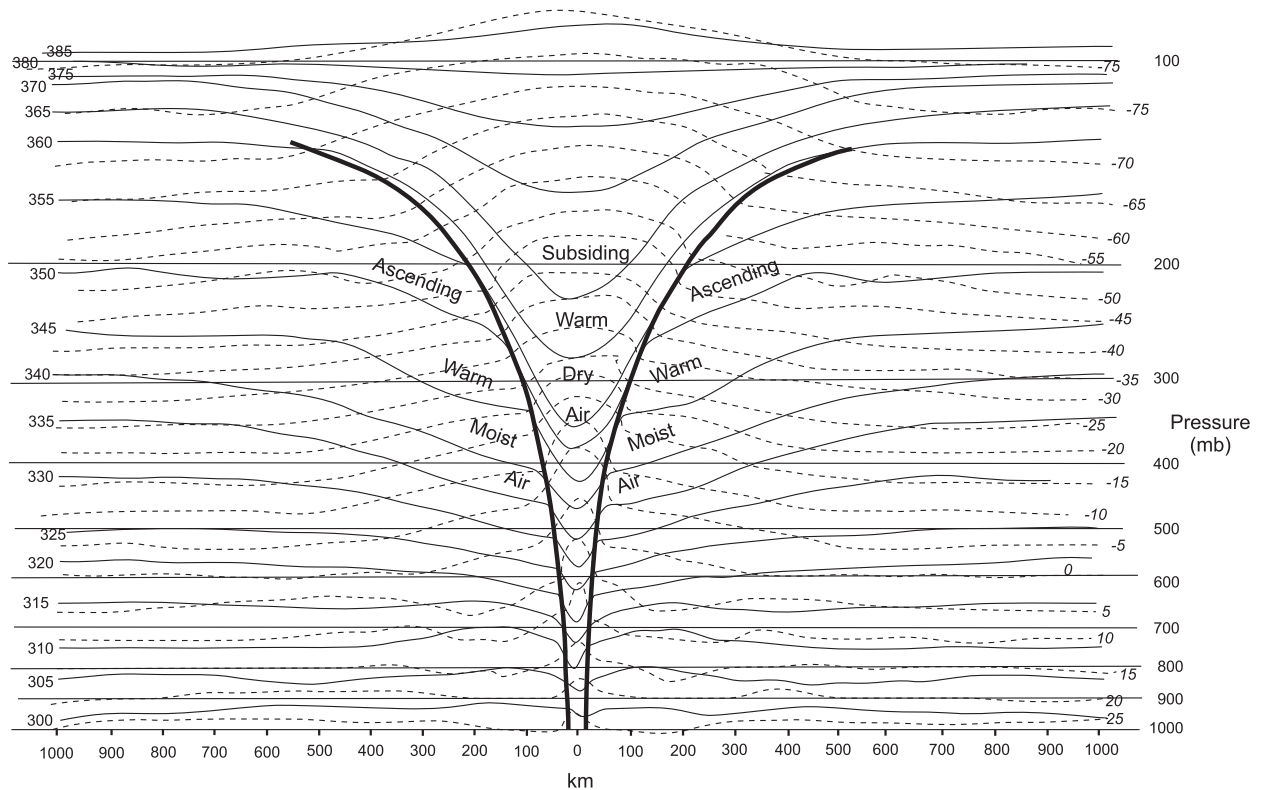


FIG. 15-2. Cross section through a hurricane. The abscissa is radial distance from storm center (km), and the ordinate is pressure (hPa; right). Solid curves show potential temperature (K; left), and dashed curves show temperature (C), with the values given by the italicized numbers at the right. (Note that a temperature minimum occurs between the two uppermost isotherms.) The two thick solid lines show the position of the inner edge of the eyewall. [Source: After Palmén (1948).]

Rossby himself made one interesting contribution (Rossby 1948) to the University of Chicago research on tropical cyclones. He reasoned that the different magnitudes of the Coriolis acceleration acting on the north and south sides of a closed vortex would exert a force on the vortex that would cause it to drift poleward. This effect is sometimes referred to as “Rossby drift,” but his idea has since been shown to be incorrect. The correct explanation was developed by physical oceanographers (Firing and Beardsley 1976; McWilliams and Flierl 1979) and was first applied to tropical cyclones by Holland (1983). These researchers deduced that closed barotropic cyclonic vortices would advect the planetary vorticity in such a way as to create an anticyclonic gyre poleward and eastward of the vortex center and a cyclonic gyre equatorward and westward of the center. (These gyres have since been nicknamed “beta gyres.”) The flow between these two gyres would advect the closed vortex poleward and westward. Holland’s calculations showed that the poleward and westward drift induced by the effect has a magnitude of a few meters per second, and there has been much work further elucidating beta drift (e.g., Smith and Ulrich 1990).

Meanwhile, Riehl, Palmén, and others had noticed by this time that tropical cyclones usually, if not always, develop out of preexisting disturbances. In what is, in my view, a prescient work, Tor Bergeron (Bergeron 1954) tackled the problem of why tropical cyclogenesis seems to require a finite-amplitude seed disturbance. Citing recent findings from the Thunderstorm Project (Byers and Braham 1948), Bergeron pointed out that groups of convective storms are always accompanied by *cool, anticyclonic outflow* near the surface, which stabilizes the atmosphere and mitigates against the formation of a cyclone. He postulated that, were this to occur over a sufficiently warm ocean, the evaporatively cooled outflow would be reheated by contact with the sea, leading in some cases to what he termed the “inverting” of the cyclone, during which enough enthalpy is added from the ocean to initiate convection and inflow of high-enthalpy air. Following the earlier work of Riehl and Kleinschmidt, he again emphasized the need to increase the enthalpy of the inflowing air. Bergeron anticipated by more than three decades the finding that cold, low-entropy convective downdrafts prevent most tropical disturbances from becoming tropical storms.

The 1950s and 1960s saw the rapid development of techniques for quantitative forecasting of tropical cyclone motion. Charney, Fjørtoft, and von Neumann (Charney et al. 1950) had shown that the numerical integration of the barotropic vorticity equation was feasible using newly developed digital computers, but the severe limitations of the computers of that generation did not allow regional grid meshes with spacing of much less than 300 km, which was rightly deemed inadequate for tropical cyclone prediction. To get around this limitation, pioneers in tropical cyclone prediction attempted first to remove the vortex from the vorticity field and then to predict the residual flow using the barotropic vorticity equation on a coarse mesh. For example, Sasaki and Miyakoda (1954) showed that short-term predictions could be made by calculating the vorticity tendencies from the barotropic vorticity equation and then graphically adding the increments to the original residual flow. Syōno (1955) did something similar, but using a semi-analytic approach to computing the vorticity tendencies. Finally, Kasahara (1957) solved the vorticity tendency equation numerically, after once again having removed the tropical cyclone from the initial fields.

Research on tropical cyclones in the United States was indirectly accelerated by a troika of severe hurricanes, Carol, Edna, and Hazel, that caused widespread devastation in 1954. Hazel, in particular, did much damage in Washington, D.C., and attracted the attention of lawmakers, who responded by creating, in 1955, the National Hurricane Research Program (NHRP) funded under the U.S. Weather Bureau and directed by Robert Simpson. With an initial staff of 20 located at West Palm Beach, Florida, the project was loaned three aircraft by the U.S. Air Force. NHRP conducted its first reconnaissance mission on 13 August 1956, into Hurricane Betsy over the Turks and Caicos Islands. A year later, the organization moved to Miami, and over subsequent years it used aircraft observations to map out the time-evolving, three-dimensional structure of hurricanes. Thus began a new and highly productive era of hurricane reconnaissance, leading to many important discoveries.

Although Kleinschmidt and the Chicago School had provided persuasive evidence that tropical cyclones are driven primarily by surface enthalpy fluxes, the idea that such storms represent a mode of release of energy stored in a conditionally unstable atmosphere proved tenacious. In the late 1950s, Banner Miller (Miller 1958) developed a theory for the minimum central pressure in hurricanes. Miller started by assuming a moist adiabatic eyewall but explicitly ignored any increase in entropy from the outer region into the eyewall, opting instead to assume that the air in the eyewall starts out with the sea

surface temperature, a standard surface pressure of 1010 hPa, and a relative humidity of 85% (not much different from a typical tropical boundary layer value). Miller then estimated a vertical profile of temperature in the eye itself by assuming dry adiabatic descent modified by mixing with the eyewall air. Once the eye temperature profile is constructed, the central surface pressure is calculated hydrostatically, assuming a level of zero horizontal pressure gradient at the standard pressure level nearest the level of neutral buoyancy for undiluted pseudo-adiabatic ascent in the environment. The calculated central pressures were in good agreement with the minimum pressures recorded in a limited sample of intense hurricanes. Miller regarded the hurricane as resulting from the release of conditional instability of the ambient atmosphere, requiring no enhanced air–sea enthalpy flux. He quotes Horace Byers' statement that compared the hurricane to "one huge parcel of ascending air" and states in his opening sentence that "the principal source of energy of the tropical storm is the release of the latent heat of condensation." Miller's approach was further developed by Holland (1997).

The resurgence of the idea that tropical cyclones are a mode of release of conditional instability led to a series of frustrated attempts to simulate numerically the intensification of such storms. The first of these, to the best of my knowledge, was that of Kasahara (1961), and this was followed by several others, notably Rosenthal (1964), Kuo (1965), and Yamasaki (1968). Kasahara initialized his model with an unstable sounding and could only integrate out to about 3 simulated hours. He specified a constant evaporative flux from the surface. Convective updrafts developed in the interior, and the initial disturbance amplified, but the integration could not be carried out long enough to ascertain whether a hurricane-like vortex actually developed. Rosenthal (1964) reasoned that the rapid growth of convection could be limited simply by choosing a coarse radial resolution. He also initialized his model with an unstable sounding; although he included surface sensible heat flux, he did not allow for evaporation from the surface. He was able to integrate out to 9 simulated hours, during which a vortex grew very rapidly (far too rapidly, as he realized) owing to the unstable initial sounding. Kuo (1965) was able to integrate out to 36 h by using only two levels in the vertical direction. As with the work of Kasahara and Rosenthal, he began with a weak barotropic vortex in a conditionally unstable atmosphere, but, unlike the others, he included a wind-dependent latent as well as sensible heat flux from the surface. His initial vortex developed to a maximum wind speed of  $25 \text{ m s}^{-1}$  by 36 h, and the radius of maximum wind contracted inward. His discussion makes it clear that he

ascribed the intensification to release of latent heat, and although he included surface heat fluxes, he did not discuss their possible role in the development. Yamasaki's four-level model did not allow for surface fluxes of sensible or latent heat and parameterized moist convection. It is not clear how unstable his initial condition was, but his linear stability analysis showed rapidly growing small-scale stationary modes that undoubtedly represented moist convection, with heating of the various layers occurring with a fixed vertical structure. He was able to integrate out to 10 days and his initial weak barotropic vortex developed into a hurricane-like cyclone with peak winds near  $40 \text{ m s}^{-1}$  and a radius of maximum winds of around 10 km.

In hindsight, what development did occur in these simulations represented the release of conditional instability, confined in an axisymmetric framework. The development was either too fast, as in Rosenthal's simulations, or controlled by strong lateral mixing. It is notable that none of the four works described here cited any of the work of Kleinschmidt or the Chicago School on the role of surface enthalpy fluxes, working from the premise that tropical cyclones are a mode of release of conditional instability. They effectively rediscovered the definitive result of Bjerknes (1938) and Lilly (1960) that moist instability, like its dry counterpart, is released in the form of very rapidly growing, small-scale convection. The state of affairs in 1964 is nicely summarized in a comprehensive review by Michio Yanai (Yanai 1964). The hunt began for a mechanism that would force this instability to be realized at the scale of tropical cyclones rather than that of individual cumulus clouds.

That search culminated in a pair of papers published in the same year, one by Vic Ooyama (Ooyama 1964) and the other by Jule Charney and Arnt Eliassen (Charney and Eliassen 1964), that introduced the idea of conditional instability of the second kind (CISK). Ooyama had spent some time at the Massachusetts Institute of Technology in 1963, discussing his ideas with Charney, but in the end they published separate papers. Charney and Eliassen (1964) and Ooyama (1964) argued that tropical cyclones represent an organized mode of release of conditional instability, with the convergence of the cyclone's Ekman boundary layer serving as the organizing agent. They maintained that the rate-limiting factor for the growth of the cyclone-scale circulation was the advective supply of latent heat. According to Charney and Eliassen (1964),

We should look upon the pre-hurricane depression and the cumulus cell not as competing for the same energy, for in this competition the cumulus cell must win; rather, we should consider the two as supporting one another—the cumulus cell by supplying the heat energy for driving

the depression, and the depression by producing the low-level convergence of moisture into the cumulus cell.

The key feedback here is between the frictionally induced convergence and the release of latent heat. The mathematical innovation was to specify the vertical distribution of latent heat release and relate its magnitude to low-level moisture convergence. This allowed for simple, linear analytic treatments of latent heat release and led to an explosion of papers on CISK, applied to tropical cyclones and to other phenomena.

As with the papers by Kasahara, Kuo, Rosenthal, and Yamasaki, neither Charney and Eliassen nor Ooyama cite the work of Kleinschmidt or the Chicago School, and they do not attach any importance to surface enthalpy fluxes. It is as though the previous work had simply ceased to exist. While CISK became a highly influential theory, it made predictions that were inconsistent with observations and did not address the fact that even liberal estimates of moist available potential energy stored in the tropical atmosphere implied very modest peak wind speeds, as pointed out earlier by, for example, Riehl (1954).

Despite the reemergence of the conditional instability theory of tropical cyclone formation, work on the original idea of hurricanes as heat engines continued sporadically. Of particular interest was a paper presented by Robert Simpson and Herbert Riehl at the technical conference<sup>7</sup> on hurricanes in 1958 (Simpson and Riehl 1958). They used aircraft observations of Hurricanes Carrie (1957) and Daisy (1958) to show that air was moving in and out of the core of the storms at middle levels, in effect ventilating the cores with low-entropy air from the midlevel environment. They argued that such ventilation would weaken the cyclones by damping the radial entropy gradient. This idea has emerged more recently as a leading candidate for why vertical wind shear tends to weaken tropical cyclones (e.g., Tang and Emanuel 2010).

One interesting project that began as a result of the NHRP was Project STORMFURY, an experiment to test the hypothesis that seeding tall cumulus clouds in the periphery of tropical cyclones could reduce the peak winds in the storms by promoting freezing and latent heat release outside the eyewall. Begun in 1962, the project was funded jointly by the U.S. Navy, U.S. Weather Bureau, and National Science Foundation, and it continued through 1983. Many Atlantic hurricanes were seeded (e.g., see Simpson and Malkus 1963; Gentry

<sup>7</sup>This proved to be the first of a long and highly productive series of technical conferences that have since become the biannual Conference on Hurricanes and Tropical Meteorology run by AMS.

1970), but, as summarized by Willoughby et al. (1985), STORMFURY never produced definitive findings on whether cloud seeding could actually reduce tropical cyclone intensity. On the one hand, we now know that the development of new, outer eyewalls can at least temporarily weaken storms, although they also lead to an expansion of the wind field (see section 3b) so that it is not clear that the overall hazard is diminished. On the other hand, there is somewhat less supercooled water and more natural ice in tropical cyclones than had been anticipated during the design of STORMFURY. Despite the lack of a definitive result, STORMFURY's numerous reconnaissance missions into Atlantic hurricanes produced a wealth of data that proved to be a boon to research.

The 1950s and early 1960s also produced two important revolutions in observations of tropical cyclones. Beginning in 1957, the U.S. Weather Bureau deployed a new generation of radars—the WSR-57—around the United States, focusing initially on coastal regions subject to hurricanes. This allowed forecasters to more precisely locate and assess the structure and intensity of hurricanes about to make landfall. In 1961, Atlantic Hurricane Esther became the first major tropical cyclone to be discovered in satellite imagery, photographed from *TIROS III*. By the late 1970s, virtually all tropical cyclones on the planet were being detected from satellite.

The rapid development of aircraft reconnaissance, radars, satellites, and digital computers in the post-WWII era, along with research advances that stemmed at least in part from these new tools and from a generation of highly gifted researchers, many of whom were introduced to meteorology as a result of the war, led to what we might think of as the modern era of tropical cyclone research, described in the next section. The state of tropical cyclone research up through about 1980 is nicely summarized by Anthes (1982).

### 3. The modern era

By the late 1960s and early 1970s, most of the key technology and some of the fundamental physical understanding on which contemporary tropical cyclone research is based was in place. While both technology and understanding improved rapidly after the 1960s, radar, satellites, and airborne reconnaissance were all well underway, and a basic understanding of tropical cyclone physics developed in the early 1950s was about to undergo a renaissance. In this section, I provide an overview of research, and to a much lesser extent, operational developments in various subtopics of tropical cyclone research and forecasting. This section is organized

by topic, with developments within each topic discussed more or less chronologically.

#### a. Continued advances in observational technology

Observational technology made substantial strides forward in the modern era. Beginning in 1987, National Weather Service ground-based radars were replaced with NEXRAD Doppler radars, enabling accurate assessment of tropical cyclone wind fields as storms approached landfall (see Stith et al. 2019). Unfortunately, in that same year, the U.S. Navy discontinued airborne reconnaissance of tropical cyclones in the western North Pacific, leaving the North Atlantic as the only basin in which tropical cyclones are routinely reconnoitered by aircraft, although storms near Taiwan are surveyed by a jet aircraft (e.g., C.-C. Wu et al. 2005).

In 1982, Hurricane Debby became the first tropical cyclone to be surveyed by airborne Doppler radar (Marks and Houze 1984). Advanced Doppler radars mounted on NOAA's WP-3D aircraft, the Electra operated by the National Center for Atmospheric Research (NCAR), and later a Naval Research Laboratory (NRL) WP-3D, have become an important means of quantifying tropical cyclone winds in three dimensions, for both operations and research (see section 3b for an example of airborne Doppler-derived airflow).

Dropsondes deployed from research and reconnaissance aircraft have provided much valuable information about the thermodynamic and kinematic structure of tropical cyclones. A large advance was made in 1997, when the Omega system, which tracked sondes using ground-based radio transmission, was replaced by the global positioning system (GPS), enabling wind measurements of much higher accuracy and frequency.

Perhaps the most remarkable advances were in satellite remote sensing (see Ackerman et al. 2019 and Fu et al. 2019). Over the decades since the 1970s, passive radiometers continued to improve in quality and both spatial and spectral resolution, providing unprecedented details of tropical cyclone structure in near-real time. By the mid-1970s, Vern Dvorak had developed a technique for inferring tropical cyclone characteristics, especially intensity, from visual and infrared measurements (Dvorak 1975, 1984), and this was further developed to take advantage of improving measurements from space (Velden et al. 2006; Olander and Velden 2007). Observations of tropical cyclones from space made a leap forward in 1978 with the launch of *Seasat*, the first satellite to carry a microwave scatterometer designed to detect the amplitude and orientation of capillary waves on the ocean surface, from which the direction and magnitude of surface wind stress can be inferred. Surface winds inferred from sea surface scatterometry

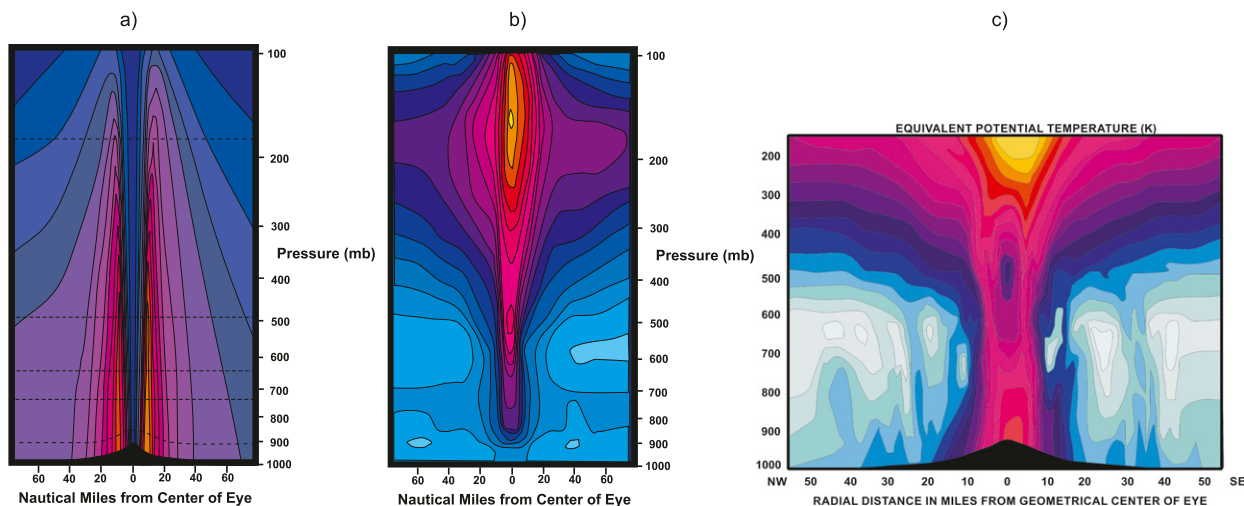


FIG. 15-3. Cross sections through Hurricane Inez of 1966, showing (a) storm-relative horizontal wind speed, (b) temperature perturbation from the distant environment at the same pressure level, and (c) equivalent potential temperature. In (a) the wind speeds vary from a minimum of 10 to a maximum of 130 kt, in (b) the temperature perturbation varies from a minimum of  $0^{\circ}$  to a maximum of  $16^{\circ}\text{C}$ , and in (c) the equivalent potential temperature varies from a minimum of 336 to a maximum of 376 K. The horizontal black dashed lines in (a) show the flight altitudes of the research aircraft used to make the measurements. [Source: After Hawkins and Imbembo (1976).]

proved to be a boon to forecasters and researchers. Better spatial and temporal resolution may be obtained from the constellation of Cyclone Global Navigation Satellite System (CYGNSS) satellites launched in 2017 (Ruf et al. 2016). These satellites receive forward-scattered GPS signals, whose wavelength is sufficiently long to avoid appreciable attenuation by rain.

In recent years, unmanned aerial vehicles (UAV) have been used to measure conditions in tropical cyclones. In 2005 the eyewall of Typhoon Longwang was sampled by an aerosonde (a small, lightweight, and inexpensive UAV), and the National Aeronautics and Space Administration (NASA) Global Hawk has been used to deploy dropsondes to sample tropical cyclones (Braun et al. 2013). A Coyote UAV (Patterson et al. 2014) was more recently air launched into North Atlantic Hurricane Edouard of 2014 (Cione et al. 2016). These developments may usher in a new area of inexpensive and highly effective platforms for making in situ and near-field remote sensing measurements of tropical cyclones and will allow relatively less developed nations, institutions, and corporations to reconnoiter tropical cyclones.

### b. Axisymmetric structure

The new observational tools and an increasing abundance of aircraft reconnaissance data fostered rapid advances in delineating tropical cyclone structure, propelled forward largely by two programs: the NHRP, whose research arm later became NOAA's Hurricane Research Division, and William Gray and his research team at Colorado State University. Of particular note

is a series of papers on tropical cyclone structure originating in the NHRP (Hawkins and Rubsam 1968; Hawkins and Imbembo 1976). These showed the structures of Atlantic hurricanes, as sampled by aircraft, with an unprecedented level of detail. Figure 15-3 shows cross sections of horizontal wind speed, temperature perturbation, and equivalent potential temperature through Hurricane Inez of 1966, a small but intense storm. These cross sections reveal the striking warm-core structure of a mature hurricane, with almost no temperature perturbation at the surface but a whopping  $16^{\circ}\text{C}$  anomaly near the tropopause. As dictated by the constraint of thermal wind balance, the strongest winds are near the surface and decay upward, becoming anticyclonic at large radii near the storm top. The equivalent potential temperature shows a pronounced inward increase near the radius of maximum winds, supporting the inferences by Riehl (1950) and Kleinschmidt (1951) that tropical cyclones are powered by enthalpy fluxes from the ocean.

The axisymmetric structure of tropical cyclones was further elucidated by detailed examination of observations by William Gray and his students at Colorado State University. Shea and Gray (1973) and Gray and Shea (1973) composited NHRP aircraft data with respect to the radius of maximum winds and were able to compare the radial wind and pressure structures of a handful of Atlantic storms. In a pair of papers, Gray's student William Frank (Frank 1977a,b) extended the earlier composite structure to a much larger radius using radiosonde data from the western North Pacific, showing,

among other things, the unmistakable presence of large-scale anticyclones near the tropopause. Weatherford and Gray (1988a,b) made use of U.S. Air Force reconnaissance data from the western North Pacific to further delineate the axisymmetric structure of wind, temperature, and pressure; quantify the relationship between peak winds and central surface pressure; and show that the inner core region and outer wind field could behave somewhat differently under some circumstances.

Early on, it was recognized that the overall diameter of tropical cyclones, as measured, for example, by their radii of gale-force winds or the radii of the outermost closed surface isobar, varies widely, and Merrill (1984) showed that, in general, tropical cyclone diameter follows a lognormal distribution and is systematically greater in the western North Pacific region than in the Atlantic. The lognormal character of the frequency distribution of tropical cyclone diameters was confirmed by Dean et al. (2009), who used enhanced historical datasets (Demuth et al. 2006; Kossin et al. 2007), and by Chavas and Emanuel (2010), who used QuickSCAT sea surface scatterometer data.

Theoretical understanding of axisymmetric structure was relatively slow to catch up with observations. Emanuel (2004) and Chavas and Emanuel (2014) argued that the radial profile of azimuthal wind outside the rain area has to be such that the resulting Ekman suction velocity at the top of the frictional boundary layer matches the radiative subsidence velocity in the stratified air above the boundary layer, else mass would accumulate at the top of the boundary layer in the steady state. The resulting wind profile obeys a Riccati equation, whose numerical solution was shown by Chavas and Emanuel (2014) to very well match observed outer wind profiles. The theoretical understanding of the inner core wind profile is still debated, and to this author's knowledge, the only theoretical treatment is that of Emanuel and Rotunno (2011), who argued that the temperature stratification of the outflow sets the radial profile of gradient wind in the inner core and that such thermal stratification is in turn set by small-scale turbulence in the outflow, which drives the Richardson number toward a critical value for the onset of turbulence.

Regardless of the physics underlying the axisymmetric part of the storm structure, by the early 1980s there were enough reconnaissance data to develop empirical wind profiles that were and remain in high demand by, for example, risk modelers. A particularly popular generic profile was developed by Holland (1980) and later refined (Holland et al. 2010).

By the 1950s it had been clearly recognized that the idea of a simple axisymmetric, steady structure was an overidealization of reality in many cases. For example,

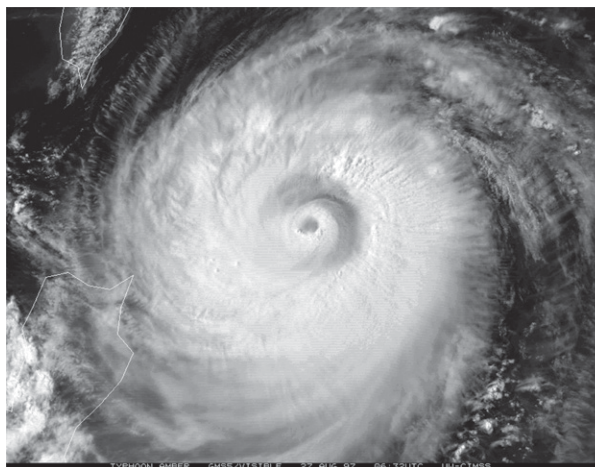


FIG. 15-4. Geostationary Meteorological Satellite-5 (GMS-5) visible image of Typhoon Amber on 27 Aug 1997, showing a double eyewall structure. (Source: Cooperative Institute for Meteorological Satellite Studies of the University of Wisconsin–Madison Space Science and Engineering Center.)

Fortner (1958) analyzed the structure of western North Pacific Typhoon Sarah of 1956 and showed that at various times it exhibited two eyewalls, and that intensity fluctuated on a diurnal time scale. By the early 1980s, the existence of double eyewalls had been firmly established from radar and aircraft observations, and Willoughby et al. (1982) showed that such features were usually time-dependent structures, with a secondary eyewall forming outside the existing eyewall, contracting inward over time, and eventually strangling the inner eyewall, thereby replacing it. Such concentric eyewall cycles are associated with profound fluctuations in the maximum wind speed and central pressure of tropical cyclones, and are particularly common in intense storms. Hawkins and Helveston (2004) performed a global climatology of concentric eyewalls based on passive microwave imagery and found that of tropical cyclones whose maximum wind attained at least 120 kt ( $1 \text{ kt} = 0.51 \text{ m s}^{-1}$ ), 40% of Atlantic and 80% of western North Pacific storms experienced at least one episode of concentric eyewalls. Kossin and Sitkowski (2009) showed that secondary eyewalls are more likely to form when the midtropospheric humidity is high, there is not much vertical shear of the environmental horizontal wind, and the ocean mixed layer is relatively deep. There is some evidence that secondary eyewalls are more likely to form in tropical cyclones with broad wind fields and to lead to a further expansion of the circulation (Huang et al. 2012; Rozoff et al. 2012).

By the 1990s, high-resolution visible and microwave imagery from satellites could be used to detect concentric eyewall cycles in near-real time. Figure 15-4 shows a

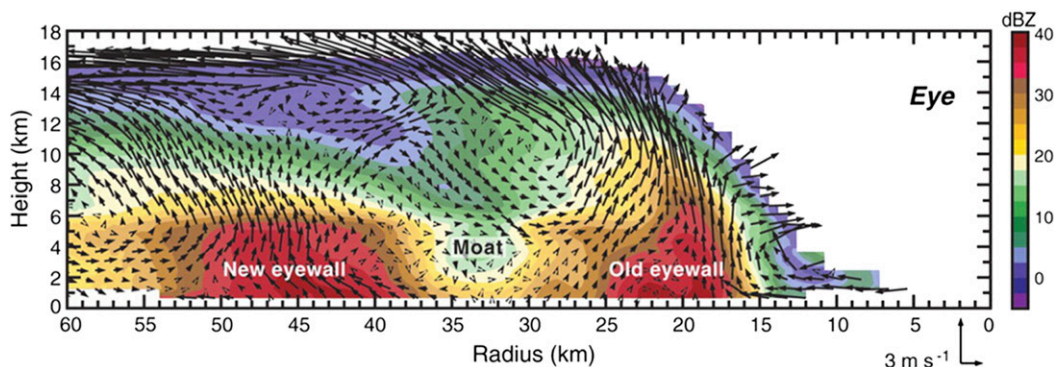


FIG. 15-5. Vertical cross section through Hurricane Rita of 2005, as surveyed by the NCAR Electra Doppler Radar (ELDORA) mounted on NRL's P-3 aircraft. The cross section extends 60 km out from the storm center located at the right edge of the figure, and from the surface to 18-km altitude. The color shades show the radar reflectivity. The black arrows show the flow in the radius–height plane, with the scale given at the lower right. The outer reflectivity maximum and associated upward motion reveal a secondary eyewall that will move inward and eventually replace the primary eyewall. A reflectivity minimum with downward motion is evident between the two eyewalls. (Source: Houze et al. 2007; reprinted with permission from the American Association for the Advancement of Science.)

visible image of western North Pacific Typhoon Amber of 1997 that clearly exhibits a double eyewall structure, and Fig. 15-5 shows a vertical cross section of radar reflectivity and airflow, derived mostly from airborne Doppler radar, in Hurricane Rita of 2005.

A large and growing literature addresses the physical cause of concentric eyewall cycles, but as of this writing a solid consensus has not yet emerged. An important question that remains on the table is whether such features are externally forced (e.g., by interactions with surface features or neighboring weather systems) or result from internal instability of the basic vortex (or, possibly, both). Kuo et al. (2004, 2008) proposed that concentric eyewalls result from the interaction between the tropical cyclone and nearby, weaker vorticity anomalies. Nong and Emanuel (2003) performed simulations with a simple axisymmetric model, in which the wind-induced surface heat exchange (WISHE) mechanism seemed to be necessary for secondary eyewall development, but also showed that external triggers operating through the outflow could be important. Other proposed mechanisms include accumulation of vortex Rossby waves at the radius at which their refractive index vanishes (Abarca and Corbosiero 2011) and complex nonlinear boundary layer processes in a conditionally unstable atmosphere (Abarca and Montgomery 2013; Kepert 2013). Whatever the precise mechanism, an expanding wind field is conducive to secondary eyewall formation (Rozoff et al. 2012).

### c. Axisymmetric energetics

By the end of the 1960s, the CISK theory of tropical cyclones had temporarily overshadowed the earlier work of Kleinschmidt and the Chicago School, and

numerical simulations of tropical cyclones that were based on the idea that such storms were driven at least initially by the release of available potential energy either failed altogether or produced storms that were too small. This changed with the work of Vic Ooyama (Ooyama 1969), who produced what is now generally regarded as the first successful numerical simulation of a tropical cyclone. Ooyama used an axisymmetric model whose vertical structure consists of a boundary layer of fixed thickness surmounted by two layers of variable thickness. Surface heat fluxes and drag are calculated using bulk aerodynamic formulae, assuming a fixed ocean temperature. Cumulus convection is represented by a scheme whose rate of convective heating depends on boundary layer moisture convergence, the degree of conditional instability, and the relative humidity above the boundary layer.

Ooyama presented a series of experiments that showed for the first time (but consistent with the Riehl–Malkus–Kleinschmidt view) that the peak intensity of the model storm varies directly with the coefficient of heat transfer and inversely with the drag coefficient. Yet Ooyama left an opening for adherents of CISK, which he had helped invent. The initial condition in the numerical experiments was strongly conditionally unstable—an ambient boundary layer parcel would be about 10 K warmer than its environment when lifted to the top layer. This produced a small intensification of the initial vortex, even when the surface enthalpy exchange was omitted. Earlier axisymmetric models with no surface heat fluxes whatsoever and enough conditional instability did indeed produce intense vortices, and simulations driven by ambient instability were performed

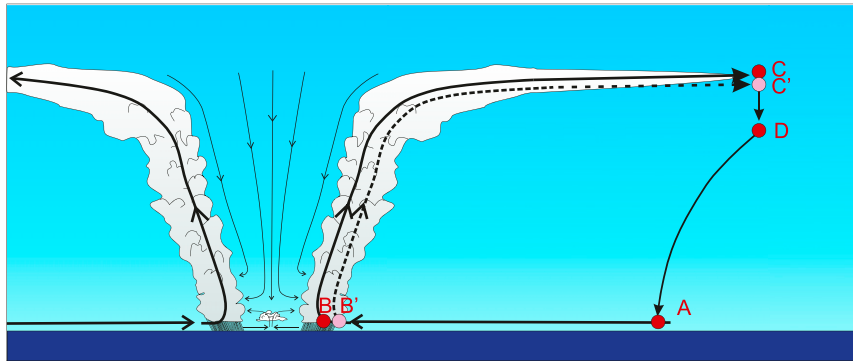


FIG. 15-6. Energy cycle of a mature, steady, axisymmetric tropical cyclone. See the text for a description.

as recently as the late 1970s (Yamasaki 1977). Dengler and Reeder (1997) showed that had Ooyama taken his initial state to be conditionally neutral he would have found that development would only occur if a vortex of sufficient amplitude is used in the initial condition, an aspect more in keeping with observations.

Ooyama's work was extended to a multilevel primitive equation model by Rosenthal (1971). Consistent with Ooyama's findings, Rosenthal found that the peak intensity of cyclones in his model varied directly with the surface exchange coefficients of sensible and latent heat transfer, and inversely with the drag coefficient. But Rosenthal also found that the rate of intensification of his cyclones increased with the drag coefficient, a finding supported by later simulations (e.g., Montgomery et al. 2010; Peng et al. 2018), although other work shows only a small sensitivity of intensification rate to drag coefficient (Craig and Gray 1996; Peng et al. 2018).

On the more theoretical side, Shutts (1981) solved for the structure of a balanced, axisymmetric vortex with the radial profile of the surface gradient wind specified and the structure aloft determined by an assumption of zero potential vorticity. As first pointed out by Bennetts and Hoskins (1979), this is equivalent to a vortex that is everywhere neutral to slantwise convection, a generalization of the principle of convective neutrality to include the effects of centrifugal accelerations. He rederived the same equation for the slope of absolute angular momentum surfaces that had first been derived by Kleinschmidt (1951), except that Kleinschmidt took the moist rather than the dry entropy as being constant along angular momentum surfaces. Shutts showed that given a reasonable radial profile of surface gradient wind, the assumption of zero potential vorticity gives a reasonable solution for the gradient flow and temperature aloft.

This approach was extended by Lilly (unpublished manuscript) in the early 1980s and by Emanuel (1986; see also Emanuel et al. 1985). Like Kleinschmidt, Lilly and Emanuel assumed that saturation moist entropy is constant along angular momentum surfaces (analogous to Shutts's assumption that the dry entropy is constant on such surfaces), but held that this was so everywhere, not just in the eyewall. They extended the earlier work by incorporating a dynamical lower boundary condition in which the gradient of moist entropy with respect to angular momentum in the boundary layer is determined by surface enthalpy and momentum fluxes. This results in an expression for the maximum wind speed that is proportional to the square root of the ratio of the surface enthalpy exchange coefficient to the surface drag coefficient. Emanuel (1986) described the results in terms of a Carnot heat engine, as illustrated in Fig. 15-6. I summarize this view, adding a few wrinkles here.

Air spirals in from point A toward the eyewall (B), acquiring enthalpy from the ocean at nearly constant temperature. Dissipation of turbulence kinetic energy also adds entropy along this leg, and this is not negligible. The air then rises moist adiabatically from B to C. In natural storms the outflowing air is exchanged with the environment, opening the energy cycle, but in models with outer walls, the air slowly subsides, first in the lower stratosphere (from C to D), where the descent is nearly isothermal, and then back down to A. Although the air loses entropy by infrared radiation along D–A (as well as C–D), it maintains a moist adiabatic lapse rate to match that of the undisturbed environment. Thus, its saturation entropy remains constant and D–A is equivalent to moist adiabatic descent.

The four legs just described are those of an ideal Carnot heat engine: (nearly) isothermal expansion, adiabatic expansion, isothermal compression, and adiabatic compression. The cycle converts heat energy into

mechanical energy, which in this case is the kinetic energy of the winds, and in the textbook case this mechanical energy is used to perform work on some external system. But here, the only real recipient of mechanical energy is the ocean. Some of the work done on the ocean is used to generate surface and internal waves, which transport energy to the far environment; this has been estimated to be roughly 15% of the mechanical energy generated by the thermal cycle (I. Ginis 2013, personal communication). Dissipation of turbulence energy in the ocean is likewise thought to be relatively small compared to that in the atmosphere, where the velocities are much larger. These sources of dissipation are usually neglected, and in the simplest formulation all of the mechanical dissipation is assumed to occur in the atmospheric boundary layer.

Integrating the product of absolute temperature and the net entropy source around the four legs A–B–C–D and equating the resulting net heating to the net loss of mechanical energy yields an integral constraint on the storm intensity. Note, however, that we could have equally well formulated the cycle to be A–B'–C'–D–A, where the points B' and C' are chosen to be directly adjacent to B and C. We do not redefine points A and D because, owing to the absence of strong gradients in the far environment, the properties of these points will not be very sensitive to their exact location. By contrast, the properties at points B and C, which exist in regions of strong horizontal and vertical gradients, respectively, will be sensitive to their location. By subtracting the second integral from the first and letting B' approach B and C' approach C, we can derive a local expression for the intensity:

$$|\mathbf{V}_s|^2 = \frac{C_k}{C_D} \frac{T_s - T_o}{T_o} (k_0^* - k), \quad (15-7)$$

where  $C_D$  is the surface drag coefficient,  $C_k$  is the dimensionless surface exchange coefficient for enthalpy,  $|\mathbf{V}_s|$  is the magnitude of the surface wind,  $T_s$  is the input temperature (in this case, the sea surface temperature), and  $T_o$  is usually referred to as the *outflow temperature*, which here is the absolute temperature at point C in the cycle. The quantity  $k$  that appears in (15-7) is the enthalpy per unit mass, defined as

$$k \equiv c_p T + L_v q, \quad (15-8)$$

in which  $c_p$  is the heat capacity at constant pressure,  $L_v$  is the latent heat of vaporization, and  $q$  is the specific humidity. In (15-7),  $k_0^*$  is the saturation enthalpy at the sea surface. The effect of the dissipative heating has been to replace the surface temperature by the outflow temperature in the denominator of the efficiency term in

(15-7). The wind speed given by (15-7) or various similar expressions that may be found in the literature is often referred to as the *potential intensity* (PI).<sup>8</sup>

Several important points must be made about the PI as given by (15-7). First, it is not a closed expression, since the value of the boundary layer enthalpy is not known, nor is the surface pressure which is needed to calculate the surface saturation enthalpy or the outflow temperature. The pressure dependence of the surface saturation specific humidity, together with the decrease in temperature that occurs as inflowing air attempts to cool adiabatically as it flows down the pressure gradient, increases the enthalpy disequilibrium ( $k_0^* - k$ ). This is a positive feedback, as increasing intensity yields a greater pressure drop in the ascent zone, increasing the disequilibrium term. This is a quantitatively important feedback in the tropical cyclone thermodynamic cycle, and becomes more so as the surface temperature increases (Emanuel 1988). At sufficiently high temperature (or low outflow temperature) this positive feedback runs away, implying that dissipation outside the boundary layer must become important. Storms that develop in this regime were nicknamed “hypercanes” and were numerically simulated by Emanuel et al. (1995).

A second important point about (15-7) is that it is specifically an expression for the surface wind speed and not the maximum wind speed that may (and usually does) occur above the surface. Expressions of similar but not identical form, based on the thermal wind equation coupled with boundary layer budgets (e.g., Emanuel 1986, 1988) and in some cases including corrections for nonbalanced flow (D. K. Lilly, unpublished manuscript; Bister and Emanuel 1998; Bryan and Rotunno 2009a,b; Bryan 2012), usually pertain to the maximum azimuthal wind speed in the domain. One advantage of the Carnot cycle derivation is that it makes no assumptions of hydrostatic or gradient balance. We know from detailed numerical simulations (Persing and Montgomery 2003; Bell and Montgomery 2008; Bryan and Rotunno 2009a) that the maximum winds above the surface layer can greatly exceed the value given by (15-7), especially when the parameterized lateral mixing is small; here the nonbalance terms are important (Bryan and Rotunno 2009a; Bryan 2012).

A final point about (15-7) is that its derivation here does not consider heat transport and dissipative heating associated with falling precipitation, other irreversible

<sup>8</sup>This is also often called the maximum potential intensity, but the words “maximum” and “potential” appear to be redundant in this expression.

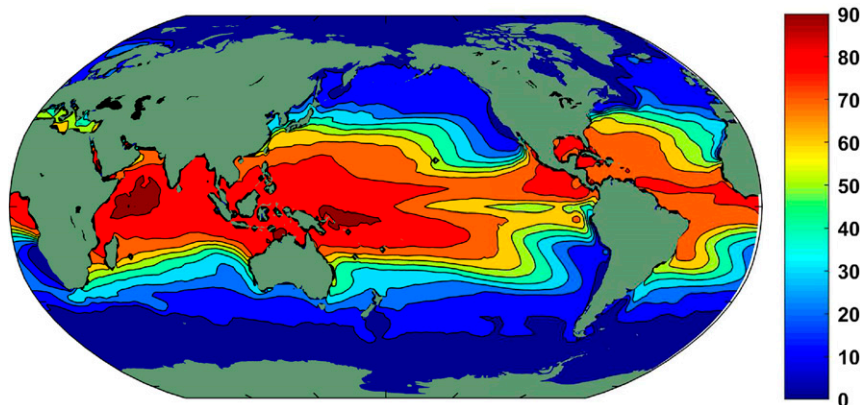


FIG. 15-7. Annual maximum of the potential intensity ( $\text{m s}^{-1}$ ) calculated from the algorithm of Bister and Emanuel (2002) using ERA-Interim data averaged over 1979–2016. The spatial resolution of the data is  $1.5^\circ$ .

influences on moist entropy, or the work done in lifting water substance. Variations on the basic formulation of potential intensity have considered the effects of ambient convective available potential energy (Frisius and Schönemann 2012), ocean mixing (Lin et al. 2013), and the work done in lifting water (Sabuwala et al. 2015; Makarieva et al. 2018).

A commonly used algorithm for calculating potential intensity from sea surface temperature and vertical profiles of temperature and humidity (Bister and Emanuel 2002) makes the ansatz that the relative humidity of the boundary layer at the radius of maximum winds is the same as that of the unperturbed environment. Given this assumption, the pressure effects on the surface saturation enthalpy are calculated iteratively: once an initial estimate is made for the potential intensity, this is used to estimate the surface pressure under the eyewall, and this is in turn used to revise the initial estimate of the saturation enthalpy. The iteration converges except in the hypercane regime. Figure 15-7 shows a map of the annual maximum potential intensity calculated using this algorithm applied to ERA-Interim data averaged over the period 1979–2016. Values as high as  $90 \text{ m s}^{-1}$  are found, and the potential intensity becomes small at high latitudes. The Carnot argument presupposes a vortex circulation and thus produces results at and near the equator, where steady tropical cyclones are mechanically impossible. Otherwise, the distribution of potential intensity captures the main belts where tropical cyclones are observed to develop, although they may travel substantially away from high potential intensity regions as they spin down, and may cause significant damage if they redevelop as baroclinic or hybrid storms. Empirically, genesis is seldom observed for PI values less than about  $40 \text{ m s}^{-1}$ .

Histograms of the lifetime maximum wind speed of observed tropical cyclones, divided by the potential intensity at the place and time of maximum observed intensity, show a distinctly bilinear behavior (Emanuel 2000). At subhurricane intensities, the exceedance frequency drops off quickly (but linearly) with normalized intensity, while the decline is somewhat less steep for storms of hurricane intensity, reaching zero at a normalized intensity of around unity. Thus, very few real storms achieve their theoretical intensity, and the reasons for this will be discussed in sections 3h and 3i.

One attempt to come up with a genuinely closed theory for both PI and storm structure in the ascent region was made by Emanuel and Rotunno (2011), who postulated that the outflow temperature varies with angular momentum in such a way as to render the outflow neutral to Kelvin–Helmholtz instability. This is based on observations from high-altitude aircraft that the outflow is generally turbulent, and from model simulations that also show active turbulence in the outflow. Emanuel and Rotunno assumed that this turbulence is efficient enough to keep the Richardson number near its critical value. This assumption leads to a closed form of the PI, expressing it in terms of environmental enthalpies and a function of the ratio of surface exchange coefficients of enthalpy and momentum. It also gives a reasonable solution for the structure of the vortex in the ascent region.

All of these ideas point to a system maintained by surface enthalpy fluxes, which are the sine qua non of the tropical cyclone. Most textbook descriptions of tropical cyclone physics continue to state that such storms are driven by latent heat release—a notion at odds with the successful simulation of dry hurricanes in a radiative–dry convective atmosphere in both two dimensions

(Mrowiec et al. 2011) and three (T. Cronin 2018, personal communication).

#### *d. Intensification physics*

While a steady-state theory is useful in illuminating the energetics and to some extent the dynamics of tropical cyclones, the physics behind the intensification of such storms are important both from the point of view of basic understanding and forecasting. Here we regard intensification as beginning when the inner core ascent region becomes approximately saturated. In models (e.g., Emanuel 1989; Nolan 2007) this usually marks the onset of more rapid intensification after a gestation period that we here consider to be part of the genesis process (see section 3k). For simplicity, we here consider the intensification process in the absence of retarding factors such as environmental wind shear (section 3i) and ocean interaction (section 3h).

Observations (Kowch and Emanuel 2015) show clearly that the probability density of observed and modeled intensification rates is nearly perfectly exponential, with no indication of any significant breaks or changes in the exponential shape of the distribution. This suggests that there are no significant changes in the physics of intensification once it is underway, even though the peak intensity probability distribution does show a clear break at approximately hurricane strength.

A simple nonlinear model of axisymmetric intensification was developed by Emanuel (1997) and later extended to include variable outflow temperature (Emanuel 2012). These models assume that the flow above the boundary layer is always neutral to slantwise moist convection and is in gradient wind and hydrostatic balance, and that the spinup in this region, similar to what happens in an Eady model of baroclinic instability, is driven by the nonbalanced flow response of the interior region to a changing distribution of moist entropy in the boundary layer. This latter assumption has been questioned by Smith et al. (2009), Montgomery and Smith (2014), Smith and Montgomery (2015), and Peng et al. (2018), who argue that vertical advection of supergradient angular momentum out of the boundary layer is a significant contributor to interior spinup. As long as the interior flow remains quasi-balanced, it is not clear whether the route to angular momentum increase above the boundary layer makes a tangible difference to, for example, the rate of intensification of the cyclone. In either case, the boundary layer flow near the radius of maximum winds is strongly frontogenetical, with convergence of the Ekman boundary layer flow guaranteed by the large radially inward increase of inertial stability as the vorticity rapidly increases inward. This strongly converging flow increases the radial gradient of the

boundary layer moist entropy, which further intensifies the vortex, leading to stronger Ekman convergence, and so on. Were it not for lateral mixing, a discontinuity would form in a finite time, similar to what happens in classical semigeostrophic frontogenesis (Hoskins and Bretherton 1972). Even without feedbacks to the pressure gradient, the nonlinear dynamics of the boundary layer may lead to the formation of shock-like structures (Williams et al. 2013).

In finite-difference axisymmetric models, this strong frontogenesis is halted by lateral diffusion of heat and momentum by parameterized three-dimensional turbulence and, perhaps to some extent, by numerical truncation error as the velocity and entropy gradients challenge the radial resolution of the models. Perhaps not surprisingly, the peak intensity of such models is sensitive to the mixing lengths used as parameters in the turbulence schemes (Bryan and Rotunno 2009a,b; Bryan 2012; Rotunno and Bryan 2012). On the other hand, Hakim (2011) showed that these superintense peak winds are actually transient features of a longer-term evolution, whose true steady state is insensitive to lateral mixing and whose intensity conforms more closely to potential intensity theory. Hakim was also the first to show that fully interactive radiation in a cloud-permitting model can lead to spontaneous cyclogenesis (section 3k).

Both full-physics models (e.g., Kilroy et al. 2017; Peng et al. 2018) and simple models [Emanuel (2012), but see the corrigendum to this paper] show that, remarkably, the rate of intensification actually increases with the drag coefficient, even though the steady-state intensity decreases with increasing drag. Kilroy et al. interpret this as highlighting the importance of Ekman convergence in organizing the convection, although Emanuel gets qualitatively the same result by assuming instantaneous moist convective neutrality.

Another interesting issue is whether there are substantial differences between strictly axisymmetric intensification and intensity change in three dimensions, absent external asymmetrizing influences such as vertical wind shear and ocean interaction, whose specific effects will be explored shortly. Montgomery and Kallenback (1997), Möller and Montgomery (2000), Hendricks et al. (2004), and Montgomery et al. (2006) proposed that tropical cyclone intensification might proceed via a three-dimensional route whereby rotating convective cells, called vortical hot towers, develop through local conditional instability and then migrate up the mean vorticity gradient into the core, where they are absorbed, yielding upscale angular velocity fluxes and mean flow intensification. But detailed analysis of three-dimensional numerical simulations of tropical cyclones

(Nolan and Grasso 2003; Nolan et al. 2007a; Kwon and Frank 2008; Miyamoto and Takemi 2013) show that injection of localized temperature perturbations outside the storm core generally leads to a mild weakening of the primary circulation and that the energy flow is from the mean flow to eddies, suggesting either that vortical hot towers, if they exist, extract energy from the mean flow or that competing three-dimensional processes that extract energy from the mean flow overwhelm the vortical hot tower effects. On the other hand, O'Neill et al. (2015) show that the vortical hot tower mechanism may be responsible for Saturn's polar vortices.

Much of the theory of tropical cyclone intensification and steady-state intensity is framed in a coordinate system in which the Coriolis parameter is constant. Peng et al. (1999) show that relaxing this assumption in a numerical model that includes the variation of the Coriolis parameter with latitude leads to slower intensification and weaker final intensity.

The dynamics of tropical cyclone intensification remain a highly active topic of research. It should be mentioned here that there is a growing literature on the subject of rapid intensification, defined as intensification rates greater than 30 kt in 24 h. While such a concept may be valuable in forecasting and communication tropical cyclone hazards, the lack of any breaks in the probability distributions of intensification rates (Kowch and Emanuel 2015) suggests that no special physics are operating at high intensification rates. Models and basic theory suggest that tropical cyclones will intensify rapidly if nothing by way of environmental interactions (e.g., wind shear or ocean feedback) prevents it.

#### *e. Eye dynamics*

The strong frontogenesis at the eyewall would result in a cylindrical vortex sheet if unimpeded by cross-frontal mixing. Across such a front, the azimuthal velocity would jump from zero in the eye to its maximum velocity at each level, while the saturation moist entropy would jump from a high value in the eye to a lower value dictated by thermal wind balance. Such a vortex sheet is strongly unstable to three-dimensional shearing instabilities (Montgomery and Shapiro 1995), however, and detailed stability analyses show instability for azimuthal wavenumbers greater than 2 (Rotunno 1978). While the strong deformation in the radius–height plane that exists during rapid intensification may suppress such instabilities (Bishop and Thorpe 1994; Le Dizes et al. 1996; Nolan and Farrell 1999; Nolan 2001), once the swirling flow begins to stabilize, multiple vortices may be expected to develop, and these are indeed observed (e.g., Black and Marks 1991), often taking the form of polygonal eyewalls (e.g., Lewis and Hawkins

1982; Muramatsu 1986). An example of a polygonal eyewall in radar imagery is shown in Fig. 15-8. There is a rich literature on the dynamics of eyewall mesovortices (e.g., Rotunno 1978; Willoughby 1988a; Schubert et al. 1999; Kossin and Schubert 2001; Nolan and Montgomery 2002; Naylor and Schechter 2014). In addition to mesovortices, strong horizontal shears of the vertical flow coupled with radial shear of the azimuthal flow may give rise to smaller-scale eddies (Leibovich and Stewartson 1983; Staley and Gall 1984), and these too have been observed in real tropical cyclone eyewalls (Bluestein and Marks 1987).

The three-dimensional vortices that form in the inner edge of the eyewall act to diffuse angular velocity into the eye itself, causing it to begin rotating cyclonically. The spinup will be faster and to a larger angular velocity at the base of the eye than at its top, as the strongest eyewall azimuthal winds are near the surface and decay with altitude, while the radius of maximum winds slopes outward. To maintain thermal wind balance, radially inward temperature gradients must develop (Smith 1980, 2005), and subsidence warming causes the eye to become warmer than the eyewall, with excesses over the unperturbed environment of more than 18°C observed at high levels (Simpson 1952b).

Thus, during intensification, the eye spins up largely owing to eddy shearing stresses that first develop near the eyewall, mechanically driving a thermally indirect circulation that warms the eye while causing it to spin cyclonically. As the storm reaches its peak intensity, the eye temperature stabilizes, but weak subsidence continues so as to balance the clear-sky radiative cooling of the exceptionally warm, dry air in the eye. In the steady state, reduction of angular momentum by radial outflow near the top of the boundary layer in the eye is balanced by inward eddy fluxes of angular velocity.

At the same time, the cyclonic airflow in the eye near the surface causes Ekman inflow, although this is much weaker than outside the radius of maximum winds, owing to the very strong inertial stability of airflow in the eye. This forces ascent near the core of the eye, cooling its base and usually leading to shallow clouds there. The eye airflow in the height–radius plane is sketched in Fig. 15-6. Where the Ekman-forced ascent meets the mechanically forced subsidence, a strong temperature inversion forms (e.g., Franklin et al. 1988; Willoughby 1998; Halverson et al. 2006). In principle, the height of the inversion should reflect the relative dominance of the mechanically forced subsidence and the Ekman-induced ascent. The former will be roughly proportional to the rate of intensification while the latter will more reflect the intensity itself. Thus, a rapidly intensifying but relatively weak storm should have a low inversion

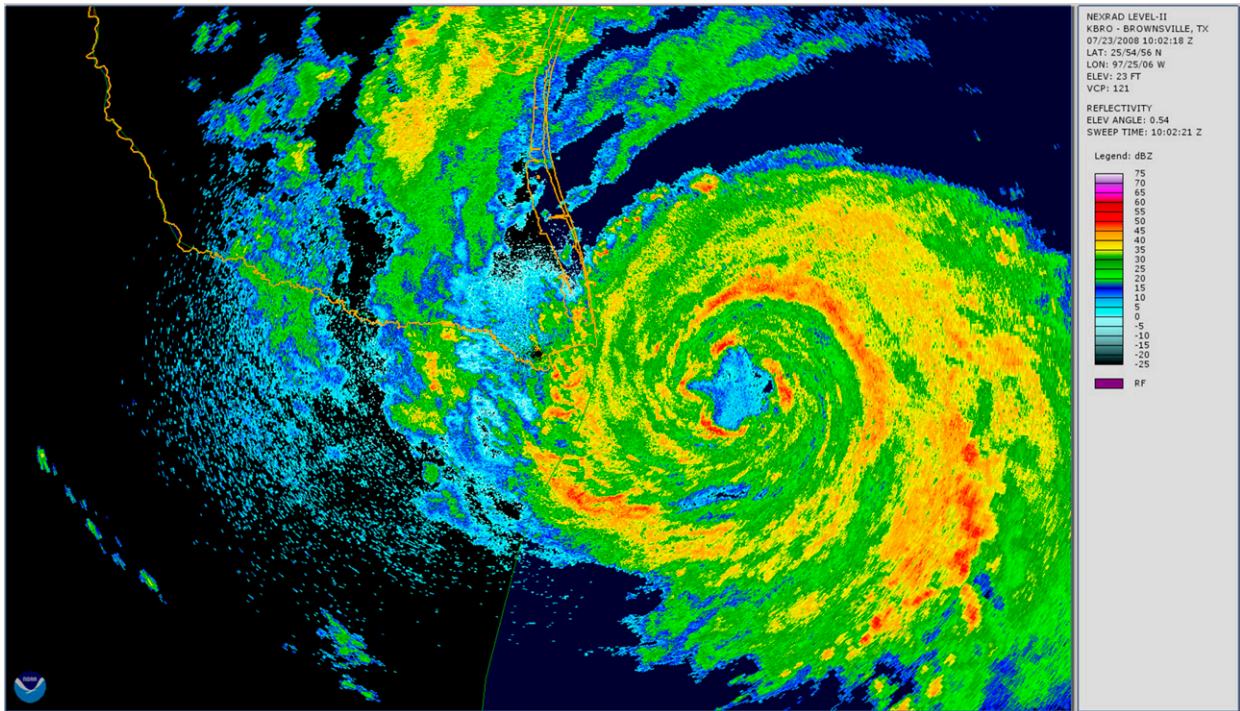


FIG. 15-8. NOAA/NEXRAD image from Brownsville, Texas, showing Hurricane Dolly approaching the Texas–Mexico border on 23 Jul 2008. The radar reflectivity scale (dBZ) is given at the right. A polygonal eyewall is evident at this time, and spiral bands envelope the storm at several different radii. (The software for the figure was obtained from <https://www.ncdc.noaa.gov/wct/install.php>.)

while an intense but decaying storm might be expected to have a high inversion, and observations (Jordan 1961; Willoughby 1998) and numerical simulations (Stern and Zhang 2013) of tropical cyclone eyes support this idea. During rapid intensification, both the vertical component of vorticity and the moist entropy peak in the eyewall, but after sufficient lateral mixing, both quantities tend to peak at the storm center (Kossin and Eastin 2001).

#### f. Spiral rainbands

Arguably the most visually spectacular features of tropical cyclone images from space and radar are the spiral bands of cloud and rain evident from just outside the eyewall to very large radii. There is some evidence that the pre-Columbian inhabitants of the Caribbean region had deduced the spiral structure of hurricanes, given the character of their graphic depictions of the god Huracán (Ortiz 1947), but it was not until coastal radars were deployed in the 1940s that the presence of spiral bands became well documented (Wexler 1945, 1947). Since then, there have been many observational studies of spiral bands (e.g., Senn and Hiser 1959; Barnes et al. 1983; Powell 1990; Gall et al. 1998; Corbosiero et al. 2006; Didlake and Houze 2013), culminating in the Hurricane Rainband and Intensity Change Experiment (RAINEX) of 2005 (Houze et al. 2006), devoted to

measuring and understanding concentric and spiral rainbands.

Spiral bands can be seen in Fig. 15-8, a radar image of Hurricane Dolly of 2008. Outside the eyewall itself, rain (as indicated here by radar reflectivity) is often organized in spirals, both within the region of azimuthal mean ascent in the storm's core and outside the core, where the bands often take the form of spirals of strongly three-dimensional convective storms. These storms sometimes produce tornadoes (Gentry 1983; Schultz and Cecil 2009), which pose a serious hazard in landfalling cyclones. Analysis of the nearby environment of tornadic storms within tropical cyclone circulations suggests that they occur in environments of low or modest convective available potential energy (CAPE) and very strong low-level shear associated with the frictional retardation of the boundary layer flow (McCaul 1991; Onderlinde and Fuelberg 2014).

In some cases, one spiral band stands out in comparison to others, and this is generally referred to as the *principal band* (Willoughby 1988a). In general, spiral bands appear to fall into roughly four categories: principal bands, secondary bands, distant bands, and inner bands (Houze 2010); some of these are illustrated in Fig. 15-9. Spiral bands are readily apparent in three-dimensional numerical simulations (e.g., Diercks and

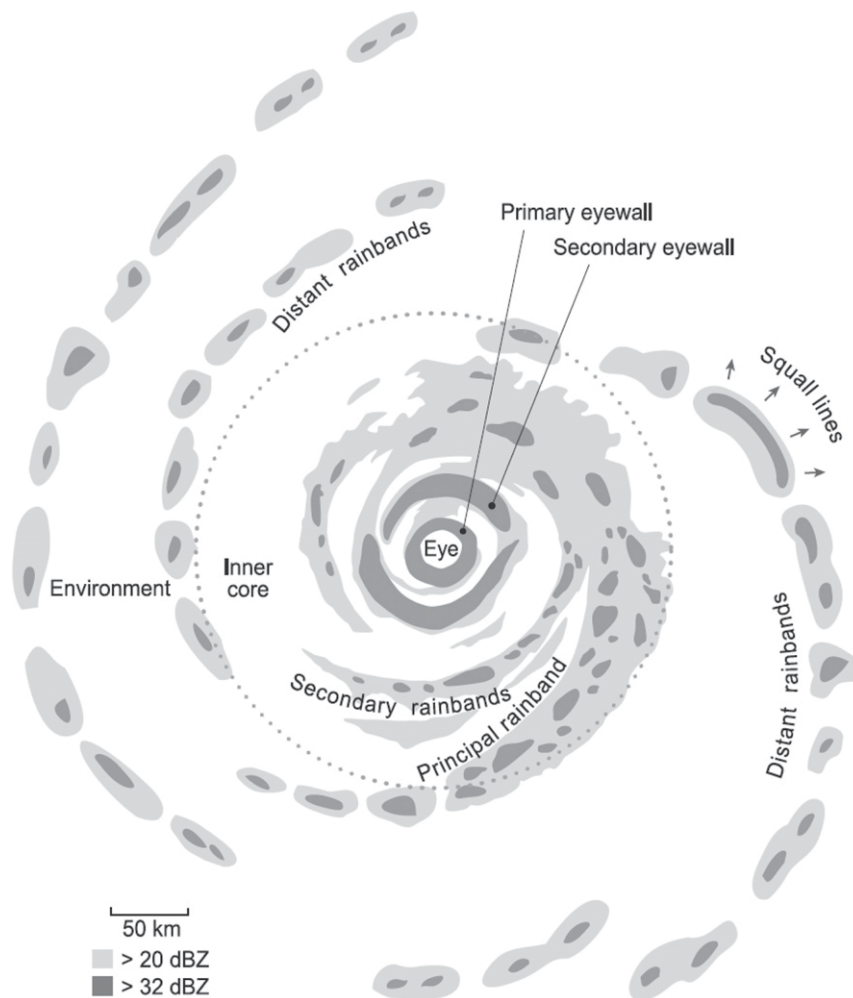


FIG. 15-9. Schematic view of the radar reflectivity in a Northern Hemispheric tropical cyclone that exhibits a primary and secondary eyewall. [Source: Houze (2010), “adapted liberally from [Fig. 1 of] Willoughby (1988a).”]

Anthes 1976; Kurihara 1976; Wang 2002; Chen et al. 2003; Wang 2009; Moon and Nolan 2015a).

Despite the wealth of observations and numerical simulations of spiral bands, a strong consensus about their underlying mechanism has yet to emerge, and there may be more than one type of spiral band from a dynamical point of view. Abdullah (1966) was perhaps the first to suggest that spiral bands are manifestations of inertia–gravity waves propagating outward from convective sources in the storm’s core. He suggested that these are partially ducted by the strong discontinuity of thermal stratification at the tropopause, and subsequent studies (e.g., Chane Ming et al. 2014) have confirmed the existence of a rich spectrum of inertia–gravity waves in the upper troposphere and lower stratosphere. Waves with similar characteristics have been observed at lower levels and successfully reproduced in numerical

simulations by Nolan and Zhang (2017). There is abundant evidence of diurnal pulsing of cloud tops in satellite imagery (Kossin 2002; Dunion et al. 2014), and three-dimensional numerical simulations show a strong diurnal signal in many variables, including precipitation (O’Neill et al. 2017). Both observations and models of the diurnal signal show that it is focused at the tropopause and originates well outside the eyewall (~200 km), propagating outward to large radii. While such waves clearly modulate the precipitation outside the core, there is little evidence that they are responsible for the existence of the spiral bands.

On the face of it, it seems unlikely that waves trapped near the tropopause can be responsible for organizing convection whose updrafts originate in the boundary layer. Willoughby (1977) and O’Neill et al. (2017) show that inertia–gravity waves whose energy propagation is

outward are unlikely, owing to the requirement that the intrinsic wave frequency lie between the buoyancy and local inertial frequencies. However, Willoughby (1977) derived cyclonically curved linear normal modes on a circular barotropic vortex whose energy propagation is inward but whose phase velocity is outward and that transport angular momentum outward. Thus, inertia-gravity waves whose source lies outside the tropical cyclone may conceivably organize convection into spiral bands. The work of Kurihara (1976) suggests that some of these modes may be destabilized by the horizontal shear of the tropical cyclone wind field.

One problem for the argument that spiral bands represent convectively coupled inertia-gravity waves is that the coupling to convection is generally missing from theoretical treatments. The waves observed by Chané Ming et al. (2014) and Nolan and Zhang (2017) are too fast to be convectively coupled; these papers do not claim a relationship of such waves to spiral rainbands.

The strong radial vorticity gradients in tropical cyclones provide a refractive index for Rossby waves, which provide a more promising candidate for convective coupling, as first pointed out by MacDonald (1968). The character of Rossby waves in a simple, barotropic circular vortex was examined by Guinn and Schubert (1993), who showed, using numerical simulations, that sufficiently strong vortex Rossby waves could break, leading to long, trailing spiral bands of vorticity that resemble spiral rainbands. They also showed that the interaction of two barotropic vortices, in which one is substantially weaker than the other, could lead to the distortion of the weaker vortex into a single spiral band that merges into the stronger vortex, forming what looks like an outer band. They postulated that inner bands could be manifestations of breaking Rossby waves while outer bands developed from the interaction between the tropical cyclone and external weather systems.

Rossby waves with opposite signed intrinsic frequencies can, under the right circumstances, become phase locked, leading to baroclinic instability. Necessary (but not sufficient) conditions for such instability were developed by Charney and Stern (1962) and by Fjørtoft (1950), assuming either two-dimensional or quasigeostrophic flows. Montgomery and Kallenbach (1997) extended these theorems to perturbations on a circular baroclinic vortex, including the effects of the strongly curved basic state flow. They were able to demonstrate that, as in the cases considered by Fjørtoft and Charney and Stern, instability of quasi-balanced perturbations requires that the radial gradient of the effective potential vorticity, which includes potential temperature gradients on the upper and lower boundaries, changes sign. This can happen, for example, when the eyewall

frontogenesis leads to a vorticity maximum in the eyewall, with positive vorticity gradients inside and negative gradients outside the eyewall (associated with a U-shaped radial profile of azimuthal wind), and indeed as reviewed in section 3e, this configuration is often unstable and leads to mesovortices in the eyewall. Outside the eyewall, the radial vorticity gradient is usually single signed, unless a secondary eyewall develops, and what surface temperature gradient exists would lead to Eady edge waves whose intrinsic phase speed is of the same sign as the internal Rossby waves so that the Montgomery-Kallenbach necessary condition for instability is not satisfied. On the other hand, Eady edge waves at the tropopause could conceivably phase lock, in an unstable way, with either or both the internal Rossby waves or lower Eady edge waves.

Montgomery and Kallenbach pointed out that their analysis really only pertains to azimuthal wavenumber-1 disturbances, which are the only ones that may be considered to be quasi-balanced. Indeed, higher wavenumbers may be unstable even if the Montgomery-Kallenbach sufficient condition for stability is satisfied, as argued, for example, by Ford (1994), who showed, using a linear stability analysis of rotating, shallow water equations, that a circular patch of uniform potential vorticity inside an infinite region of uniform, but lower, potential vorticity is always unstable. The instability involves the interaction of a Rossby wave on the boundary of the patch with gravity waves that are well outside the patch, and it is thus filtered from quasi-balanced systems. The idea that less-balanced modes might be unstable even if Charney-Stern-Fjørtoft-like sufficient conditions for stability are satisfied is strongly supported by the work of Zhong et al. (2009), who showed using linear shallow water theory that while Rossby-type and inertia-gravity-type oscillations are clearly separable in the eye and outer regions of tropical cyclone vortices, mixed Rossby-gravity waves can occur in and near the eyewall, giving rise to spiral-like structures. A weakness of the theoretical work on relatively low frequency wave disturbances to tropical cyclone-like vortices is that there is no attempt to couple to deep convection. This shortcoming may not be as much of a qualitative problem as it might appear, given the fact that simple linear shallow water modes of the equatorial waveguide are readily apparent in wavenumber-frequency decompositions of satellite outgoing long-wave radiation (Wheeler and Kiladis 1999), but the latter work also shows that growth rates and phase speeds are strongly affected by coupling. The strong vertical coupling that results from the weak effective stratification resulting from convective coupling may, for example, allow for a strong interaction between the

surface and tropopause Eady edge waves of a circular warm-core vortex, giving rise to baroclinic instability.

Several other ideas have been proposed to explain one or more of the types of spiral banding illustrated in Fig. 15-9. Moon and Nolan (2015b) showed that the inner spiral bands that form in a numerical simulation of a tropical cyclone do not conform to expectations based on either Rossby or inertia-gravity wave theory and suggested that they are simple manifestations of convection in an environment of strong mean-flow deformation. Alignment of ordinary (non-tropical cyclone) tropical cloud bands with the local deformation axis was demonstrated by Bluestein (1976). Noting the propensity for ordinary squall lines to align themselves normal to the low-level shear vector (Thorpe et al. 1982; Barnes and Sieckman 1984; Bluestein and Jain 1985; Rotunno et al. 1988), Robe and Emanuel (1996) proposed that outer spiral bands are simply squall lines aligned normal to the boundary layer shear of the tropical cyclone and presented some numerical simulations (albeit in nonrotating, Cartesian coordinate frameworks) that support that idea. Finally, laboratory experiments using unstratified vortices with Ekman layers (e.g., Faller 1963; Tatoo and Mollo-Christensen 1967) demonstrate two classes of spiral instability modes which Lilly (1966) identified as arising from the change in sign of the vertical gradient of horizontal vorticity, and with a kind of inertial instability of Ekman layer flows. Fung (1977) suggested that the inflection point (or Rayleigh) mode of instability identified by Lilly (1966) and seen in laboratory vortices could couple to deep moist convection, explaining spiral bands. The Faller-Lilly-Fung mechanism and the Rotunno-Klemp-Weisman mechanism predict the same basic orientation of the spiral bands as perpendicular to the boundary layer shear vector, but the latter mechanism would predict an additional propagation from the cold to the warm side of the band. One topic that deserves further exploration is whether Ekman layer instabilities can couple to interior Rossby, inertia-gravity, or mixed oscillations in the presence of deep convection.

There is a rich and ever-expanding literature on spiral bands in tropical cyclones, including detailed observations from field programs, comprehensive numerical simulations (most recently using cloud-permitting models), and many different theories. Progress in understanding the underlying dynamics of such bands has been impeded by a combination of the strong background flow, the inapplicability to higher-frequency modes of traditional balance constraints (that underlie, e.g., “PV thinking”), the complications of strong boundary layer shear and instabilities, and the intractability of coupling to deep moist convection. Thus,

despite much effort, it would be premature to claim that we have a good understanding of the various types of spiral bands, with the possible exception of the observed and simulated high-frequency spiral modes that are not coupled to convection. Spiral banding will no doubt remain a vital area of research for some time.

*g. The tropical cyclone atmospheric boundary layer and air-sea interface*

The boundary layer lies at the heart of tropical cyclone physics. Boundary layer turbulent fluxes of enthalpy drive the storms, while dissipation of turbulence kinetic energy in the atmospheric boundary layer is the main sink of energy. Especially in the mature state, much of the secondary circulation of the storm, including the all-important eyewall, is driven by the frictionally induced inflow in the boundary layer. Boundary layer processes may drive secondary eyewalls (section 3b) and spiral bands (section 3f). And, of course, virtually all of the damage done by a tropical cyclone occurs within its boundary layer.

The simplest bulk representation of frictionally driven inflow in the boundary layer is obtained from the steady-state angular momentum equation applied to a specified radial and vertical distribution of angular momentum, neglecting any vertical advection of angular momentum:

$$\rho u \frac{\partial M}{\partial r} = -r \frac{\partial \tau_{z\theta}}{\partial z}, \quad (15-9)$$

where  $\tau_{z\theta}$  is the vertical turbulent flux of azimuthal momentum,  $\rho$  is the air density, and  $u$  is the radial component of velocity. This representation also neglects the turbulent radial flux of azimuthal momentum, which is important in the eyewall region. We can integrate (15-9) in the vertical direction up to some depth  $h$  that is defined to be an altitude at which the vertical turbulent flux of azimuthal momentum vanishes or becomes small; the depth can be a function of radius:

$$\int_0^h \rho u \frac{\partial M}{\partial r} dz = r \tau_{\theta s}, \quad (15-10)$$

where  $\tau_{\theta s}$  is the turbulent stress at the surface. If we define  $\frac{\partial M}{\partial r}$  as the radial velocity-weighted vertical mean radial gradient of angular momentum in the boundary layer and use the classical aerodynamic drag formula for the surface stress, then (15-10) becomes

$$\int_0^h \rho u dz = \frac{-C_D \rho r |\mathbf{V}_{10}| V_{10}}{\frac{\partial M}{\partial r}}, \quad (15-11)$$

where  $C_D$  is the drag coefficient,  $|\mathbf{V}_{10}|$  is the magnitude of the horizontal wind at the surface (10 m), and  $V_{10}$  is

the surface azimuthal wind. Thus the total frictionally driven mass inflow in the boundary layer is given by (15-11), with the caveat that vertical advection and horizontal diffusion of angular momentum have been neglected. If we integrate the mass continuity equation in the vertical direction and use (15-11) for the radial mass flux, we obtain

$$(\rho w)_h = \frac{1}{r} \frac{\partial}{\partial r} \left( \frac{C_D \rho r^2 |\mathbf{V}_{10}| V_{10}}{\partial \bar{M} / \partial r} \right), \quad (15-12)$$

where  $(\rho w)_h$  is the vertical mass flux at the top of the boundary layer. This is a generalized Ekman pumping expression for nonlinear circular vortices. Note that to evaluate (15-11) and (15-12) one needs to know both the radial and vertical distributions of angular momentum in the boundary layer and both components of the surface wind.

Whatever the quantitative deficiencies of (15-11) and (15-12), they do show that there should be large radial inflow where the surface winds are strong but the inertial stability is small (i.e.,  $V$  decreases with radius), which is especially the case just outside the radius of maximum winds, while inside that radius the inertial stability is very large and the inflow will be correspondingly weak. The strong decrease of radial inflow inward across the radius of maximum winds entails strong frontogenesis and yields large upward velocities there.

The above formulation is too restrictive in that it prescribes the azimuthal flow, which is one of the most important quantities to calculate in the boundary layer. One step up from such a simple formulation is to average the steady form of the momentum and continuity equations over the boundary layer so as to calculate the depth-averaged horizontal and vertical velocities, given a prescribed distribution of gradient wind (e.g., the horizontal pressure gradient). This approach to tropical cyclone boundary layers, which have come to be known as slab boundary layers, was pioneered by Smith (1968) and further refined by Leslie and Smith (1970), Bode and Smith (1975), Smith (2003), and Smith and Vogl (2008), who introduced variable boundary layer depth. Shapiro (1983) extended the slab boundary layer to nonaxisymmetric flow induced by the translation of the vortex over the lower boundary.

Solutions of the slab boundary layer equations for tropical cyclone-like gradient wind profiles often yield stronger winds in the boundary layer than can be found in the balanced flow above the boundary layer. This happens in the core of the storm, where inflowing parcels advect angular momentum inward faster than it can be diminished by surface torque. The strongest azimuthal winds in the boundary layer actually exceed the local gradient wind.

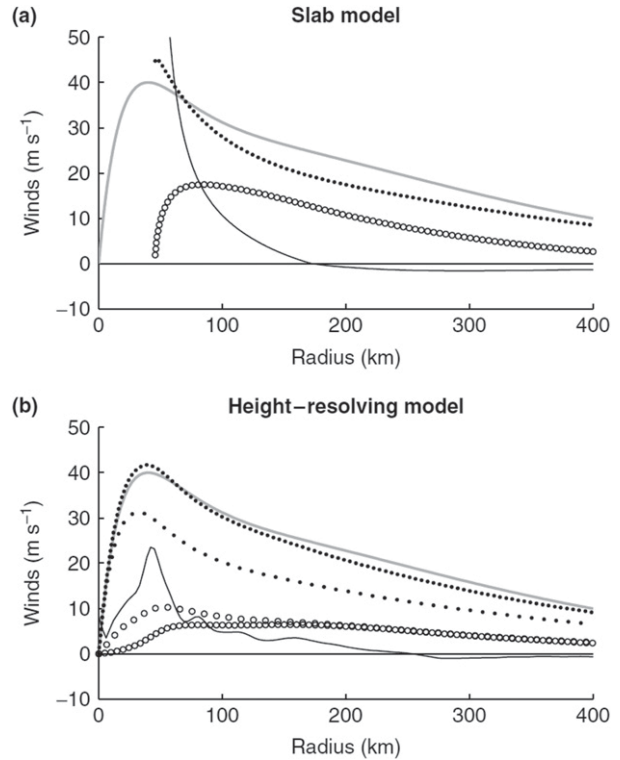


FIG. 15-10. (a) Axisymmetric boundary layer flow according to the slab model. Gradient wind (solid gray), boundary layer mean azimuthal (dots), inward (open circles), and upward (thin black, multiplied by 100) flow components are shown. Parameter values are as in Smith et al. (2008), including the boundary layer height which is fixed at  $h = 800$  m. (b) Simulation of the same vortex as in (a), except with the height-resolving model. Curves with closely spaced symbols are averaged over the lower 800 m, and those with less-dense symbols show the flow at 10-m height. The vertical velocity is at 800-m height. [Source: The figure and caption (before AMS editing) are from Kepert (2010); © Royal Meteorological Society.]

The steady, axisymmetric equations with prescribed gradient wind can also be solved as a function of altitude and radius (e.g., Montgomery et al. 2001; Foster 2009). These show that the radial flow can and often does change sign with altitude in the tropical cyclone core, as inflowing air attains supergradient wind speeds, ascends, and then is driven outward by its excess of centrifugal over pressure-gradient forces. Kepert (2010) showed that the height-resolved equations produce quite different results for the radial and vertical flows, and that the azimuthal wind is not as strongly supergradient as in slab models. Figure 15-10 compares a slab model calculation with the vertical mean of the equivalent height-dependent model. The height-resolved model produces more realistic radial profiles of depth-averaged radial and vertical wind, and the depth-averaged azimuthal wind is closer to the imposed gradient wind.

Note that none of the representations of the tropical cyclone boundary layer reviewed here include radial diffusion, which must become important in the eyewall region owing to the strong frontogenesis there (section 3d). Radial diffusion may be expected to have first-order effects on storm intensity and on radial profiles near the eyewall (Rotunno and Bryan 2012). Even outside the eyewall, boundary layer processes may cause shock-like structures to develop (Williams et al. 2013). In regions of shock and front formation one must be cautious in applying simple diffusion schemes to represent what is in fact a complex rearrangement of vorticity and angular momentum by three-dimensional eddies (Kossin and Schubert 2003).

It is just now becoming computationally feasible to carry out large-eddy simulations (LESs) of the tropical cyclone boundary layer, in which much of the radial as well as vertical turbulent diffusion can be explicitly simulated and in which the effects of nonclassical features such as boundary layer roll vortices are naturally included. An early example of a large-eddy simulation of a tropical cyclone boundary layer is that of Zhu (2008), who embedded an LES within the larger domains of the Weather Research and Forecasting (WRF) Model of a landfalling hurricane. The LES domain was over land and outside the core of the storms, but was able to simulate features such as boundary layer roll vortices that have been observed in many storms (e.g., Wurman and Winslow 1998; Katsaros et al. 2000; Morrison et al. 2005; Ellis and Businger 2010).

While much can be learned from simple models in which the pressure gradient (gradient wind) is specified, in reality there is a strong two-way interaction between the boundary layer and the interior, quasi-balanced flow. Inversion of a balanced, zero-moist-potential-vorticity interior (e.g., Emanuel 1986) requires as a lower boundary condition the gradient of moist entropy with respect to angular momentum, and this gradient is determined by boundary layer processes. The pressure gradients that ultimately drive the boundary layer are in turn related to the interior dynamics, and the feedback between the two leads to frontogenesis if the basic vortex is sufficiently strong (Emanuel 1997, 2012). In an axisymmetric model, the frontogenesis can only be halted by radial diffusion, and this in turn should affect the radial gradient of moist entropy with respect to angular momentum ( $ds/dM$ ) of the air emerging from the boundary layer.

Indeed, the region near the radius of maximum wind remains a *terra incognita* (or perhaps *aqua incognita*) of tropical cyclone physics, involving nonclassical boundary layers in which radial turbulent diffusion is important and into which enthalpy and momentum are

transported through a highly perturbed air–sea interface.

The nature of the air–sea interface at high wind speeds, and the formulation of fluxes of enthalpy and momentum across it, have received much attention in the last few decades. At ordinary wind speeds, the ocean surface is mildly perturbed by capillary and surface gravity waves, and field experiments show that as the surface wind speed increases, these waves increase in amplitude and the effective roughness length likewise increases, yielding an increase in the surface drag coefficient, as well quantified by field experiments (e.g., Smith et al. 1992; DeCosmo et al. 1996). The adjustment time of the capillary wave field to changing winds is very short, and therefore the two can be considered to be in equilibrium. However, the surface wave field, and especially the longer swells, adjust on time scales longer than the variation of the tropical cyclone winds and so are generally not in equilibrium with the local winds (e.g., Wright et al. 2001).

As the surface wind speed increases beyond roughly  $10 \text{ m s}^{-1}$ , waves begin to break, sending spume into the air and injecting air bubbles into the sea. The spume breaks into droplets, and bursting bubbles also inject small spray droplets into the air. As winds increase toward hurricane force, a spray layer forms, and the ocean surface begins to resemble an emulsion. At sufficiently high wind speeds, the notion of a sea surface becomes amorphous and the transition from solid water to pure air becomes gradual, with bubbled-filled water transitioning to spray-filled air. Relating fluxes of enthalpy and momentum to the driving horizontal pressure gradient in the atmosphere is exceptionally challenging but of critical importance to understanding and forecasting tropical cyclone intensity.

Riehl (1954) was perhaps the first to suggest that sea spray might enhance enthalpy transfer from the sea surface. As detailed in Andreas and Emanuel (2001), when a droplet is ejected into the air, it first cools slightly to the air temperature, giving up its sensible heat to the air. It then continues cooling rapidly to the local wet bulb temperature, transferring latent heat to the air at the expense of its own heat content. In cooling to its local wet bulb temperature, the droplet loses roughly 1% of its mass. If it then falls back into the sea, it cools the latter, demonstrating that re-entrant spray transfers enthalpy from the sea to the air. If it continues to evaporate, however, the heat of vaporization is supplied by the air and if it evaporates completely it will reabsorb in sensible heat all the latent heat it gave up in its initial cooling; in that case, the only net enthalpy transfer is owing to the initial sea–air temperature difference. Thus, to a first approximation, only reentrant spray

transfers appreciable enthalpy from the sea to the air, and the maximum transfer occurs when a droplet re-enters the sea after losing roughly 1% of its mass.

When spray is ejected into the air, it is accelerated toward the local horizontal wind speed, and this exerts a drag on the air regardless of whether the drop falls back into the sea. (In fact, vapor resulting from evaporation of surface water must also be accelerated to the local wind speed and thus exerts a stress: surface evaporation causes drag.) At the same time, the spray layer increases the effective density stratification of the surface layer of the atmosphere, and this would tend to reduce the overall drag coefficient. On the basis of detailed tropical cyclone wind profiles from air-deployed GPS dropsondes, Powell et al. (2003) deduced that the effective drag coefficient increases up to roughly hurricane-strength winds but then declines with wind speed for stronger winds. This behavior has also been seen in laboratory experiments using long wind-wave flumes (e.g., Donelan et al. 2004) and deduced from detailed upper-ocean momentum budgets (Jarosz et al. 2007) and atmospheric angular momentum budgets (e.g., Bell et al. 2012). Theoretical explanations of reduced drag at high wind speeds have been proposed and tested against experimental and field observations (e.g., Soloviev and Lukas 2010; Soloviev et al. 2014, 2017). Most of the approaches taken so far suggest that the surface drag coefficient peaks at approximately marginal hurricane force and then either levels off or actually declines. Soloviev et al. (2017) suggest that it reaches a second minimum at wind speeds of around  $60 \text{ m s}^{-1}$  and argue that the particular dependence of the drag coefficient on wind speed might explain the observed bimodal distribution of Atlantic hurricane intensity. Moon et al. (2004) and Holthuijsen et al. (2012) argue that the coupled response of the wave field is important in setting the temporal and spatial distribution of surface stress and also find that the drag coefficient levels off or declines at very high wind speeds.

Estimating the behavior of the surface enthalpy transfer coefficient has proved far more difficult. Haus et al. (2010) and Jeong et al. (2012) performed laboratory experiments using a long wind-wave flume and found little evidence for an increase in the enthalpy transfer coefficient with wind speed, but at least some of the spray blew out the end of the flume before it could reenter the water, compromising estimates of the enthalpy transfer. By contrast, Richter and Stern (2014) applied Monin–Obukhov similarity theory to thousands of dropsonde profiles collected in Atlantic hurricanes and showed that the scaling of the turbulent enthalpy flux with wind speed was more consistent with predictions based on the spray model of Andreas et al.

(2008) than with the aforementioned tank results. In 2003, the Office of Naval Research sponsored the Coupled Boundary Layer Air–Sea Transfer Experiment (Black et al. 2007) in an effort to obtain better understanding and quantitative estimates of air–sea enthalpy and momentum exchange. On the basis of densely packed radial arrays of dropsondes spanning the eyewalls of several Atlantic hurricanes, Bell et al. (2012) made estimates of the surface enthalpy fluxes and drag as residuals of angular momentum and energy budgets, but the error bars on these estimates were too large to allow definitive conclusions about the behavior of the surface exchange coefficients, although the central estimates were not dissimilar to conclusions based on wind profiles and laboratory experiments.

Emanuel (2003) applied dimensional analysis to a simple hypothetical system consisting of a semi-infinite layer of unstratified atmosphere overlying a semi-infinite, unstratified body of freshwater, with a constant horizontal pressure gradient applied to the atmosphere. In equilibrium, the surface stress, as represented by a friction velocity  $u_*$ , is entirely determined by the imposed pressure gradient and is therefore an external parameter of the system. He showed that the character of the system is controlled by just three nondimensional numbers, two of which are functions of gravity and the molecular properties of air and water. The third,

$$R_u \equiv u_*^4/(\sigma g),$$

must govern the dependence of the system, including the surface exchange coefficients, on the applied surface stress. Here  $\sigma$  is the kinematic surface tension and  $g$  is the gravitational acceleration. He made the ansatz that at very high applied stress the system behavior should become independent of  $R_u$ , leading to definite predictions, for example, that the depth of the spray layer should scale with the Charnock length  $u_*^2/g$ .

Early recognition of the potential importance of sea spray not only to tropical cyclone physics but to air–sea exchange of enthalpy, momentum, and trace gases in general led to many attempts to develop spray parameterizations (e.g., Wu 1990; Lighthill 1999; Andreas and Emanuel 2001; Andreas and Decosmo 2002; Fairall et al. 2003; Andreas 2004; Andreas et al. 2008; Andreas 2010; Bao et al. 2011; Andreas et al. 2015). These parameterizations are beginning to be used in research and operational forecast models, and unsurprisingly, they have noticeable influences on storm intensity and structure (e.g., Wang et al. 2001; Gall et al. 2008; Green and Zhang 2013; Zweers et al. 2015). Braun and Tao (2000) showed that numerical simulations of Atlantic Hurricane Bob were somewhat more sensitive to the

formulation of surface fluxes than to the representation of turbulent transport within the interior of the boundary layer.

It is clear that the physics of surface exchange in tropical cyclones continues to present a fascinating challenge to science, and one with important consequences for understanding and predicting tropical cyclones in general.

#### *h. Ocean response and interaction*

The violent winds of tropical cyclones elicit a profound response from the ocean. Not only do such storms extract enormous quantities of heat from the sea, they also cool the ocean mixed layer through turbulent entrainment of colder water from below the seasonal thermocline. In the region influenced by the high-wind core of the cyclone, turbulent mixing within the ocean is usually the dominant source of surface cooling.

Perhaps the first detailed observational study of ocean surface cooling by tropical cyclones was that of [Leipper \(1967\)](#), who documented surface temperature decreases of over 5°C following Hurricane Hilda of 1964. Observations like these inspired some early attempts at tropical cyclone simulation with coupled models, through these were at first limited to stationary storms ([O'Brien 1967](#); [O'Brien and Reid 1967](#); [Chang and Anthes 1979](#)) or used linear ocean models (e.g., [Geisler 1970](#)). The Chang and Anthes study used axisymmetric atmospheric and ocean models with 60-km radial grid spacings, and the turbulent entrainment of cold water through the seasonal thermocline was modeled based on an assumption that a certain fraction of the turbulence kinetic energy produced in the ocean mixed layer was consumed in turbulent entrainment. The spatial resolution together with the environmental conditions used in the experiments produced weak storms with peak wind speeds of around 30 m s<sup>-1</sup>, and ocean coupling led to a diminishment of this peak by only a few meters per second, despite producing surface temperature declines of around 3°C. The authors concluded that sea surface cooling would not noticeably affect the intensity of a translating tropical cyclone. In hindsight, this inference, which ultimately proved erroneous, stemmed from the small intensity of the control cyclone and to the coarse resolution of the model, but it was sufficiently widely accepted to impede recognition of the important role of ocean feedback on storm intensity, and even today, some research and operational forecasting efforts use uncoupled models.

[Elsberry et al. \(1976\)](#) were among the first to consider the ocean response to a moving cyclone. They parameterized mixing by arbitrarily partitioning the input of wind energy to the ocean between acceleration of currents and

dissipation of turbulence kinetic energy and showed that upwelling and mixing dominated the temperature response near the track of the imposed cyclone.

Hydrographic surveys through tropical cyclone wakes clearly revealed a pronounced rightward bias (in the Northern Hemisphere) of the storm-induced cooling ([Leipper 1967](#); [Federov et al. 1979](#); [Pudov and Federov 1979](#)). [Ichiye \(1977\)](#) demonstrated that an imposed, translating cyclone excites near-inertial oscillations to the right of the storm track (in the Northern Hemisphere), where the local surface winds change direction with time in near resonance with such oscillations, but he did not consider their effect on mixing. On the basis of hydrographic surveys, buoy data, and a simple but elegant model, [Price \(1981\)](#) deduced that most of the mixing that produces surface cooling results from the turbulent breakdown of the vertical shears associated with strong near-inertial currents. The key innovation in his model was the use of a parameterization of mixing based on detailed laboratory experiments by [Kato and Phillips \(1969\)](#) and [Kantha et al. \(1977\)](#). These showed that mixing induced by shear occurs when a bulk Richardson number based on the current strength, density stratification, and mixed layer depth falls below a critical value, and that the effect of the ensuing turbulence is to hold that Richardson number close to its critical value. The recognition that entrainment of cold water through the seasonal thermocline is dominated by shear-induced turbulence rather than directly by surface-wind-driven turbulence nicely explained the strong rightward bias of the observed surface cooling. Price's conception of the coupling of the near-inertial response to surface cooling forms the basis of today's understanding of the ocean response to tropical cyclones. [Figure 15-11](#) shows the observed ocean cooling owing to the passage of Atlantic Hurricane Gert in 1999. The near compensation of the surface cooling with warming at depth shows that most of the temperature change near the storm track is due to mixing rather than surface heat flux, as deduced by [Price \(1981\)](#) and others. The ocean mixed layer depth and surface currents associated with a uniformly translating tropical cyclone in a fully coupled model are shown in [Fig. 15-12](#).

The aforementioned observational analyses and the modeling study of [Price \(1981\)](#) showed that for storms translating at average speeds, the coldest water can be found in the wake of the storm, well removed from the central core where the surface fluxes are most important. Nevertheless, there is often enough mixing by the time the storm center arrives to reduce sea surface temperatures by 1°–3°C ([Schade and Emanuel 1999](#); [D'Asaro 2003](#)). Is this enough to have a noticeable effect on storm intensity? We can instead ask a closely related

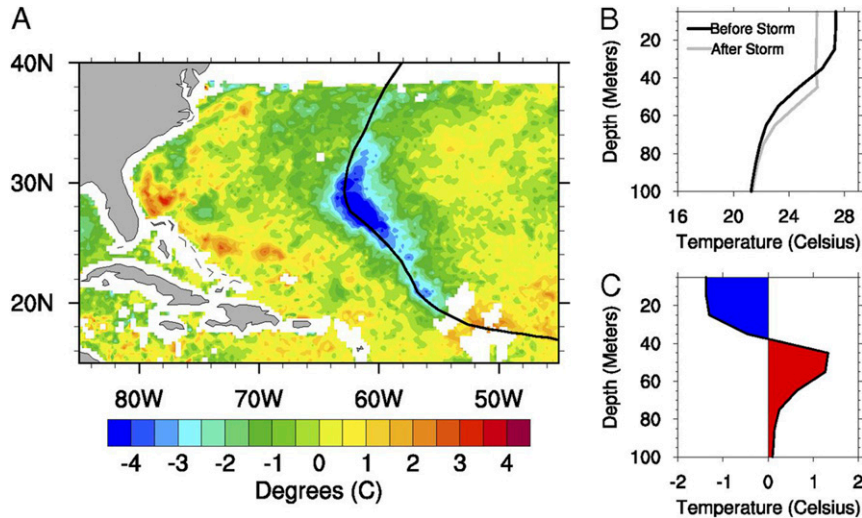


FIG. 15-11. Upper-ocean response to Hurricane Gert in 1999: (a) observed surface temperature anomaly showing cooling along the storm track primarily as a result of vertical ocean mixing [the data are from the NASA Tropical Rainfall Measuring Mission (TRMM) Microwave Imager], (b) vertical ocean temperature profiles averaged over Hurricane Gert's track before (black curve) and after (gray curve) the storm [analyzed using the NASA ocean reanalysis from Estimating the Circulation and Climate of the Ocean, Phase II (ECCO2)], and (c) the difference between the two temperature profiles shown in (b), highlighting the cool anomaly (above 40 m) and warm anomaly (below 40 m) that resulted from vertical ocean mixing following storm passage. [Source: The figure and caption (before AMS editing) are from [Srifer \(2013\)](#).]

question: How much sea surface temperature decrease would it take to make it impossible for the boundary layer enthalpy to increase from the environment to the eyewall? That decrease,  $\Delta k_0^*$ , is given by

$$\Delta k_0^* = k_0^* - k_e, \tag{15-13}$$

where  $k_e$  is the boundary layer enthalpy of the undisturbed environment. Using the definition of moist

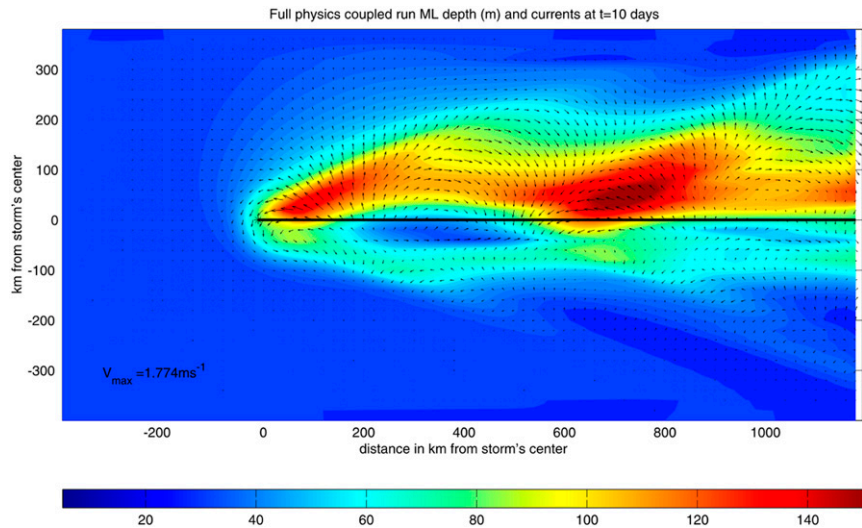


FIG. 15-12. Ocean mixed layer depth (color shading) and surface currents (black vectors) induced by a Northern Hemispheric tropical cyclone translating from right to left at a uniform speed of  $7 \text{ m s}^{-1}$ . The location of the cyclone center at the instant of the figure is at the left end of the black line. The model cyclone is fully coupled with the model ocean. (Source: [Korty 2002](#)).

enthalpy and the Clausius–Clapeyron equation, and assuming that the undisturbed boundary layer is at the same temperature as the undisturbed sea surface temperature and has a relative humidity  $\mathcal{H}$ , we can write (15-13) as

$$\Delta T_s = \frac{\Delta k_0^*}{c_p} = \frac{L_v q_s (1 - \mathcal{H})}{c_p + \frac{L_v^2 q_s}{R_v T_s^2}}, \quad (15-14)$$

where  $q_s$  is the undisturbed saturation specific humidity of the sea surface at temperature  $T_s$ ,  $L_v$  is the latent heat of vaporization,  $c_p$  is the heat capacity at constant pressure, and  $R_v$  is the gas constant for water vapor. For typical tropical values of surface temperature and humidity, this amounts to about 2.5°C. If decreasing the ocean temperature by this amount under the eyewall would kill the storm, then a drop of even 0.5°C can be expected to have a noticeable effect on storm intensity.

Sutyurin and Khain (1984) and Ginis et al. (1989) coupled axisymmetric tropical cyclones to three-dimensional ocean models to simulate the mutual interaction of a translating tropical cyclone and the ocean. They showed, contrary to expectations based on the results of Chang and Anthes (1979), that cooling of the ocean surface can have a substantial negative feedback on storm intensity. They also showed that, as expected, larger storms moving more slowly over shallower mixed layers experience more negative feedback on intensity.

With the realization that tropical cyclones can have important effects on the upper ocean and that the feedback to the storms can be substantial, many observational (e.g., Sanford et al. 1987; Shay and Elsberry 1987; Shay et al. 1989; Korolev et al. 1990; Shay et al. 1992; Lin et al. 2005; Sanford et al. 2007; Wu et al. 2007; Sanford et al. 2011) and modeling (e.g., Khain and Ginis 1991; Bender et al. 1993a; Schade and Emanuel 1999; Bender and Ginis 2000; Korty 2002; Lin et al. 2005; L. Wu et al. 2005; Morey et al. 2006; Sanford et al. 2007; Wu et al. 2007; Yablonsky and Ginis 2009; Blair et al. 2017) studies have further illuminated the nature of tropical cyclone interactions and feedbacks; these are nicely summarized in a review by Ginis (2002). Among the topics of recent interest are the idea that Langmuir circulations may play a role in mixed layer entrainment (Blair et al. 2017) and the effect of barrier layers (freshwater pools at the top of the mixed layer) on inhibiting mixing (Balaguru et al. 2012). The tropical cyclone model developed by NOAA's Geophysical Fluids Dynamics Laboratory (Bender et al. 1993b; Kurihara et al. 1993, 1995, 1998; Bender et al. 2007) was the first fully coupled model to be used for operational prediction of tropical cyclones and also the first model to be

competitive with purely statistical techniques (DeMaria and Kaplan 1994, 1997, 1999). A particular challenge for operational prediction of tropical cyclone intensity is the influence of ocean eddies and other subsurface thermal and density features on intensity (e.g., Lin et al. 2005; Wu et al. 2007; Mainelli et al. 2008; Jaimes and Shay 2009), given the difficulty of observing the subsurface ocean. It seems likely that improvement in tropical cyclone intensity prediction skill will depend in part on improved initialization of the oceanic component of prediction models.

#### *i. Interaction of tropical cyclones with their atmospheric environments*

Tropical cyclones interact strongly with their atmospheric environments. When the environmental horizontal wind varies with altitude, the distribution of clouds and precipitation is observed to become asymmetric and the intensity usually diminishes. External baroclinic disturbances, such as Rossby waves at the tropopause, alter the structure, motion, and intensity of tropical cyclones and if sustained lead to extratropical transition, which is covered in the next subsection.

Simpson and Riehl (1958) used aircraft observations to demonstrate that low-entropy air was ventilating the midlevel cores of two Atlantic hurricanes and suggested that the magnitude of ventilation was related to the baroclinity of the large-scale environments of the storms at middle levels. By the 1960s it had become clear that vertical shear of the horizontal wind exerts a strong control on the climatology of tropical cyclones (Gray 1968). Subsequent observational analyses (e.g., Merrill 1988b; Corbosiero and Molinari 2002; Knaff et al. 2004; Molinari et al. 2004) and modeling studies (e.g., Madala and Piacsek 1975; DeMaria 1996; Frank and Ritchie 1999; Smith et al. 2000; Frank and Ritchie 2001; Rogers et al. 2003; Braun and Wu 2007) established that convection and precipitation tend to be concentrated downshear from the storm core, and that large-scale shear tends to weaken tropical cyclones. Wind shear also affects storm motion (e.g., Wu and Emanuel 1995a,b) and can cause a leapfrog-like reformation of surface cyclones downshear from existing cyclone centers (Molinari et al. 2006). The presence of shear can greatly affect the intrinsic predictability of tropical cyclone intensity (Moskaitis 2009; Zhang and Tao 2013). A series of observational papers based upon eastern Pacific Hurricane Norbert (Houze et al. 1992; Marks et al. 1992; Gamache et al. 1993) provide observational support or confirmation for these ideas, as does a later paper on Hurricanes Olivia and Jimena (Black et al. 2002).

The basic dynamics underlying the downshear bias of convection is nicely described by Raymond (1992) and

illustrated in Fig. 15-13, which shows a tropical cyclone-like potential vorticity anomaly embedded in a large-scale shear flow as seen by an observer moving with the anomaly. Assuming for the moment that the vorticity anomaly (shading in Fig. 15-13) is not seriously deformed by the shear, the flow will be steady in this coordinate frame. Air approaches the anomaly from the right at low levels and from the left at high levels. Low-level flow approaching the anomaly from the right (downshear) must experience an increase in the vertical component of its absolute vorticity, requiring vertical stretching (positive values of  $\partial w/\partial z$ ). Flow receding from the anomaly to the right at upper levels must experience decreasing vorticity. Both these are consistent with upward motion downshear (to the right) of the anomaly. Conversely, air must subside to the left (upshear) of the anomaly. Note that the ascent is likely to be moist adiabatic, allowing air to ascend across potential temperature surfaces even at low levels, whereas the descent upshear of the anomaly may be closer to dry adiabatic, thus following the  $\theta$  surfaces. This is the basic reason that convection is usually concentrated on the downshear side of tropical cyclones.

The dynamics of tropical cyclones in shear are complex and have strong consequences for the storms' energy cycle. Much progress has been made in the last few decades in understanding both the dynamics and thermodynamics of these interactions.

One might begin by understanding the interaction between a simple environmental shear flow and vortices that do not contain convection or strong vertical flows. This was the approach taken by Jones (1995, 2000a,b) and by Smith et al. (2000). The Jones papers examined the behavior of initially barotropic and baroclinic vortices in a shear flow, as simulated by a three-dimensional hydrostatic model. She found that the upper-level vortex is initially displaced downshear from the surface cyclone, but then the mutual interaction of upper-level and lower-level cyclonic vorticity induces cyclone rotation of the tilted vorticity maximum around vertical axis, until the vortex is tilted at nearly right angles to the shear. In this configuration, the self-interaction of the tilted vortex monopole counters advection of vorticity by the environmental shear, and the gyration ceases, although the upper- and lower-level magnitude of the vortex tilt increase over time. Smith et al. (2000) simplified the problem to a two-layer model with an initially collocated point vortex in each layer, with a uniform translation of the upper layer with respect to the lower layer. For strong shear and/or weak vortices or weak vertical coupling, the upper and lower point vortices drift apart at right angles to the shear, as in the Jones work. For weaker shear and/or stronger vortices or stronger

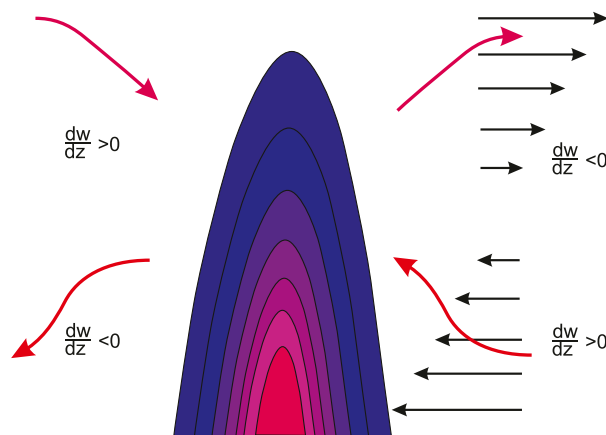


FIG. 15-13. Cyclonic potential vorticity anomaly (color shading) embedded in an environmental shear flow (black arrows) from left to right, as seen in a coordinate system moving with the anomaly. The red arrows show trajectories inferred from conservation of vorticity. See the text for a full description.

vertical coupling, the two vortices move downshear at some fraction of the upper-layer translation speed while gyrating around each other.

The dynamics of baroclinic (but perhaps initially barotropic) vortices in shear has been further elucidated in terms of Rossby waves traveling on radial potential vorticity gradients of tropical cyclones (Reasor and Montgomery 2001; Schecter et al. 2002; Schecter and Montgomery 2003; Reasor et al. 2004; Reasor and Montgomery 2015; Schecter 2015). Tilts of vortices away from the vertical can excite vortex Rossby waves through the mutual interaction of the vorticity anomalies at various levels, and the damping of such waves by radiation of wave energy away from the core can in turn damp the gyration of the system and reduce its vertical tilt. The vertical interaction of vortex Rossby waves is enhanced when phase change of water is included, leading to stronger resilience of tropical cyclones to wind shear (Schecter and Montgomery 2007; Reasor and Montgomery 2015; Schecter 2015). This body of theory, backed up by numerical simulations, suggests that tropical cyclones will eventually adjust to vertical shear toward a state in which the vortex tilts leftward with height, with respect to the background vertical shear vector (in the Northern Hemisphere). If the shear is too strong, relative to the strength of the vertical coupling, no steady state is achieved and the vortex may lose coherence.

The excitation of vortex Rossby waves by shear-induced tilt of the vortex leads to excursions of environmental air into the core of the storm. At midlevels, this air has low values of moist entropy, and if rained into, will cool and descend to the surface, quenching the

storm core with relatively low entropy air (Riemer et al. 2010, 2013). Ventilation of the core of tropical cyclones with low-entropy air was proposed by Simpson and Riehl (1958) as the main agent for shear-induced weakening of tropical cyclones, and this idea was quantified theoretically by Tang and Emanuel (2010) and explored further using a numerical model by Tang and Emanuel (2012a).

Thus, the weakening of tropical cyclones by environmental wind shear appears to result from a complex interplay of dynamic and thermodynamic process. Dynamical interactions mediated by the thermodynamics of vertical coupling result in vortex tilt and vortex Rossby waves, which can transport low-entropy environmental air into the core, either directly at middle levels or indirectly by first descending into the boundary layer in the form of evaporatively driven downdrafts. Either way, the low-entropy air reduces the efficiency of the energy cycle and results in storm weakening, which itself makes the whole system even more susceptible to the environmental shear.

It has long been recognized that the outflow layers of even the most axisymmetric tropical cyclones are typically highly asymmetric, with the outflow itself often concentrated in a small number of anticyclonically curved jets (e.g., Black and Anthes 1971; Merrill 1988a). The anticyclonic outflow has low inertial stability and thus is not as resilient to outside influences as the low-level cyclone flow (Rappin et al. 2011), thus vertical shear, even if weak and confined to the upper troposphere, can easily displace the low-potential-vorticity air downshear from the surface vortex (Wu and Emanuel 1994), where it becomes susceptible to distortion by environmental flow, the flow induced by the low-level cyclone, and, if blown into an elongated strip, barotropic/baroclinic instability.

Vortex lines are the characteristic surfaces along which information tends to propagate in an axisymmetric vortex (Schubert and Hack 1983). These lines tend to flare out to large radii at the top of a tropical cyclone, making them susceptible to environmental influences near the tropopause. Thus, relatively small amplitude disturbances in the upper troposphere appear to be able to influence the structure and intensity of tropical cyclones (Sadler 1976; Molinari and Vollaro 1989, 1990; Rodgers et al. 1990, 1991; Molinari et al. 1995; Shi et al. 1997; Rappin et al. 2011), and such interactions have been diagnosed in terms of eddy fluxes of angular momentum (Challa and Pfeffer 1980; Pfeffer and Challa 1981; Molinari and Vollaro 1989; DeMaria et al. 1993) and of potential vorticity (e.g., Molinari et al. 1995, 1998; Bosart et al. 2000; Hanley et al. 2001; Davis and Bosart 2003). The interactions are rather complex

and can have both positive and negative influences on tropical cyclone intensity. The superposition (along vortex lines) of a near-tropopause positive potential vorticity anomaly with the lower-tropospheric positive potential vorticity anomaly of the cyclone itself can boost the intensity of the storm, but increased inertial stability of the outflow (Rappin et al. 2011) and vertical wind shear can weaken it. The complexity of such interactions no doubt reduces the predictability of tropical cyclones influenced by such interactions. The interactions are strongly two way, with the tropical cyclones influencing (Kimball and Evans 2002) and, in some cases, creating upper-level disturbances (Ferreira and Schubert 1999).

When tropical cyclones travel into middle latitudes they often interact with the deep baroclinic flows found there, particularly late in the season when such flows migrate equatorward. For a given magnitude of vertical shear, baroclinity (horizontal temperature gradients) increases with latitude and with it so does the available potential energy. Depending to some extent on the phasing of the surface cyclone with baroclinic waves at higher latitudes, the tropical cyclone can tap into the available potential energy of the baroclinic zone and transform into an extratropical cyclone, in a process known as *extratropical transition* (ET). During ET, the system may extract energy from both surface enthalpy fluxes and baroclinic conversions. This is accompanied by sometimes dramatic changes in the movement of the storm and in the structure, size, and magnitude of the surface wind and rain fields, and in extreme cases the surface winds can amplify significantly, causing damage well removed from the coast. Hurricane Hazel of 1954 was an infamous example of ET, killing 81 people and causing much damage in Toronto, Canada, more than 1300 km from its landfall point (Gifford 2004). A more recent and notorious example was Hurricane Sandy, which devastated parts of New York City, coastal Long Island, and New Jersey in 2012 (Sobel 2014).

Extratropical transition is a complex process, involving a rich set of dynamic and thermodynamic interactions. The vertical shear interacts dynamically with the vorticity of the tropical cyclone and ventilates the core with low-entropy air, as described previously in this subsection. In addition, the circulation associated with the low-level, high-potential-vorticity core begins to advect the environmental potential vorticity and it dynamical equivalent, the surface potential temperature, thus producing and/or interacting with surface Eady edge waves and with the strong potential vorticity gradients found near the tropopause. The interaction is strongly two way, with the structure and movement of the low-level, high-potential-vorticity core strongly

affected by the ambient potential vorticity anomalies, and with the amplitude and propagation of the latter strongly modified by the circulation associated with the low-level, high-potential-vorticity core.

The character of ET is explored in a very extensive and growing body of literature, beginning with seminal papers exploring the complex physics of the process (Bosart et al. 2000; Harr and Elsberry 2000; Harr et al. 2000; Klein et al. 2000; Ritchie and Elsberry 2001; Kimball and Evans 2002; Klein et al. 2002; Ritchie and Elsberry 2003; Agusti-Panareda et al. 2004; Ritchie and Elsberry 2007; Davis et al. 2008) and extensive climatologies of the phenomenon (Hart and Evans 2001; Sinclair 2002; Wood and Ritchie 2014). ET can strongly affect the distribution of precipitation (Atallah and Bosart 2003; Colle 2003; Chen 2011) and surface wind (Abraham et al. 2004; Hart et al. 2006; Evans and Hart 2008; Harr 2012; Loridan et al. 2014), have significant consequences downstream of the region of transition (Riemer et al. 2008; Harr and Dea 2009; Riemer and Jones 2010; Torn and Hakim 2015), and strongly affect predictability (Anwender et al. 2008; Harr et al. 2008).

The ET process can work in the other direction, with extratropical cyclones making a transition to tropical cyclones in a process called *tropical transition* (Davis and Bosart 2004). Some events, like Hurricane Sandy, went through several periods in which the relative magnitudes of the surface enthalpy flux and baroclinic power sources oscillated through the life of the event (Galarnau et al. 2013; Halverson and Rabenhorst 2013).

In general, there is a continuum of cyclones from purely surface-flux-driven to purely baroclinic storms. A nice way to categorize a given cyclone at any point in its life cycle was developed by Hart (2003) by plotting storms in a phase plane in which the two axes consist of a measure of storm symmetry and a measure of the relative temperature of the core (warm core vs cold core). A cyclone phase diagram for Hurricane Sandy is shown in Fig. 15-14. This graphical depiction of extratropical transition has enjoyed widespread use in both research and operational forecasting and has been used, for example, in developing climatologies of ET (Evans and Hart 2003).

Comprehensive reviews of ET may be found in Jones et al. (2003), Harr (2012), and Evans et al. (2017).

#### *j. Tropical cyclone motion*

Since at least as far back as the early and middle twentieth century, it had been recognized both observationally (e.g., Riehl and Shafer 1944) and theoretically (e.g., Syōno 1955) that, to a first approximation, tropical cyclones move with the large-scale flow in which they are embedded. But the basic understanding of the

dynamics of vortices on a sphere dates to the work of Adem (1956) and Bogomolov (1977). This early work was specialized to tropical cyclone motion by Holland (1982), who treated the system as a barotropic cyclone on a  $\beta$  plane and found that the cyclonic circulation of the tropical cyclone advects background potential vorticity in such a way as to create a synoptic-scale anticyclonic gyre to the northeast and a cyclonic gyre to the southwest of a Northern Hemispheric storm. The circulation around these gyres then advects the storm poleward and westward, typically at about  $1\text{--}2\text{ ms}^{-1}$ . Analytic treatments of this so-called  $\beta$  drift have been developed by Chan and Williams (1987), Willoughby (1988b), Smith and Ulrich (1990), Smith (1991), Smith and Weber (1993), Sutyrin and Flierl (1994), Reznik and Dewar (1994), Llewellyn Smith (1997), and Schechter and Dubin (1999), among others. The barotropic framework is also the foundation of a basic understanding of the interaction of two or more cyclones (e.g., Holland and Dietachmayer 1993; Lander and Holland 1993; Ritchie and Holland 1993), sometimes known as the Fujiwhara effect (Fujiwhara 1921).

Actual tropical cyclones are strongly baroclinic vortices, and the potential vorticity environment through which they travel is highly inhomogeneous, both laterally and vertically (e.g., Molinari et al. 1997). This, all by itself, affects the propagation of concentrated vortices such as tropical cyclones (Tian and Luo 1994; Shapiro and Franklin 1999). The interactions of the cyclonic parts of tropical cyclones with shear flow and with external potential vorticity anomalies have been discussed in section 3i above, but these interactions also have effects on storm motion (e.g., Flatau et al. 1994; Wang and Holland 1996; Wu and Kurihara 1996; Dengler and Reeder 1997; Shapiro and Franklin 1999; Corbosiero and Molinari 2003). Displacement of the anticyclonic vorticity at the storm top from the position of the low-level cyclone can affect vortex motion with the same magnitude as  $\beta$  drift (Simpson 1946; Wu and Emanuel 1993, 1995a,b; Wu and Kurihara 1996; Corbosiero and Molinari 2003).

These advances, and results of a comprehensive field experiment on tropical cyclone motion (Elsberry et al. 1990), have led to significant improvements in our understanding of the problem, as reviewed by Chan (2005b), and, together with improvements in observations, modeling, and data assimilation, to a satisfying and still ongoing improvement in the skill of tropical cyclone forecasts (National Hurricane Center 2018).

#### *k. Genesis*

No aspect of tropical cyclones has proved as vexing and intractable as their formation. Much has been

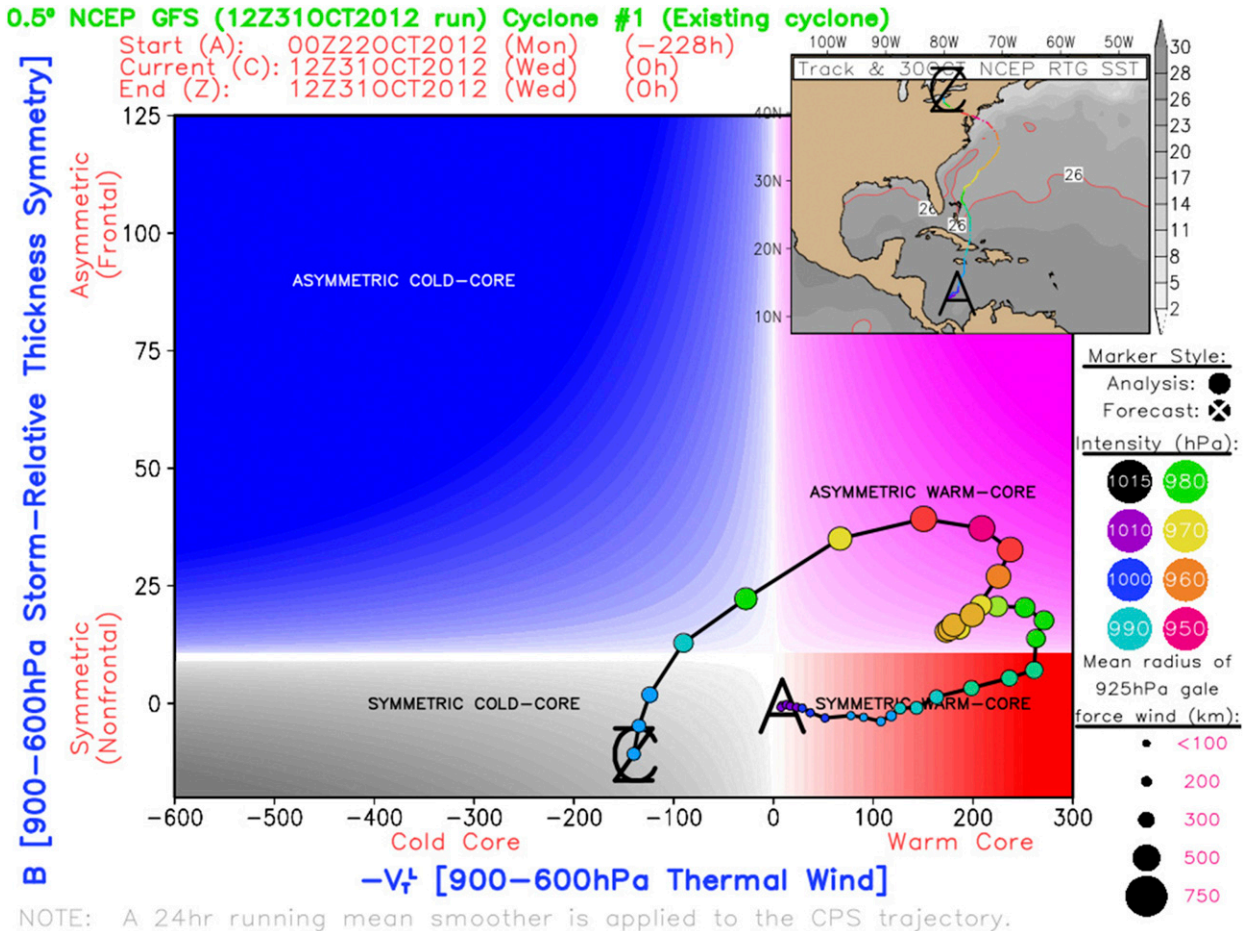


FIG. 15-14. Cyclone phase diagram showing the evolution of Hurricane Sandy, whose track (from A to C) is shown in the inset at upper right. The phase diagram has the magnitude and sign of the environmental thermal wind between 900 and 600 hPa on the abscissa (with negative values indicating a cold core) and a measure of the asymmetry of the low-level thermal field on the ordinate. The trajectory of the storm in this phase space extends from point A (0000 UTC 22 Oct, when Sandy was forming in the Caribbean Sea) to point C (1200 UTC 31 Oct, when Sandy’s remnant low had moved close to Lake Erie). Dots are plotted every 6 h, with redder colors denoting lower pressure as indicated by the scale at the right. At point A Sandy had the structure of a typical hurricane (symmetric warm core), but it became asymmetric as it intensified. Sandy quickly became an asymmetric cold-core low in the 12 h after landfall and a symmetric cold-core low as it decayed further over the next 24 h. The kink in the curve at the upper right of the phase diagram corresponds to the strengthening of Sandy’s inner core about a day before landfall. (Source: NCAR and UCAR News, <https://news.ucar.edu/8243/hybridization-sandy>; the image is provided through the courtesy of Robert Hart of Florida State University.)

written on the subject, and several field campaigns have been mounted to address the issue, including the Tropical Experiment in Mexico (TEXMEX; Bister and Emanuel 1997), the NASA Tropical Cloud Systems and Processes experiment (TCSP; Halverson et al. 2007), the Tropical Cyclone Structure field experiment (TCS08; Elsberry and Harr 2008), the NASA African Multidisciplinary Monsoon Analyses project (NAMMA; Zipser et al. 2009), the Pre-Depression Investigation of Cloud-Systems in the Tropics experiment (PREDICT; Montgomery et al. 2012), NASA’s Genesis and Rapid Intensification Processes field experiment (GRIP; Braun et al. 2013), and NOAA’s Hurricane Intensity

Forecasting Experiment (Rogers et al. 2013). Much has been learned, and many hypotheses advanced, but a clear understanding of the process remains elusive.

Research on tropical cyclogenesis has focused primarily on two aspects of the problem: the nature of the large-scale environments in which tropical cyclones form, and the dynamic and thermodynamic routes taken by particular observed and/or numerically simulated cyclones.

Gray (1975, 1979) was the first to develop an empirical relationship between the frequency of tropical cyclogenesis and climatological properties of the large-scale environment, beyond the sea surface temperature

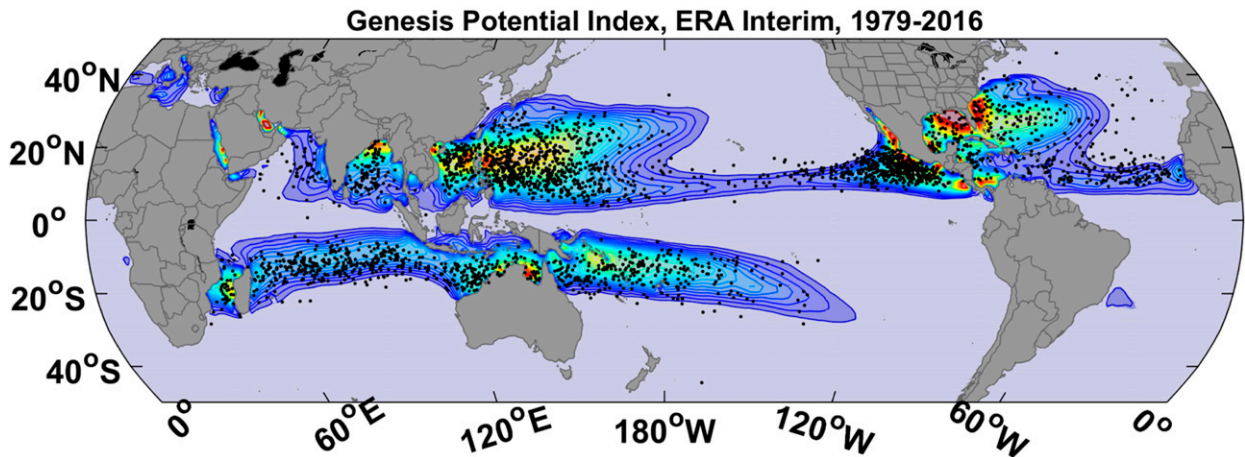


FIG. 15-15. Annual average of the sum over each year of the Emanuel (2010) genesis index (colored shading) calculated from monthly mean ERA-Interim data (Dee et al. 2011) over 1979–2016. The black dots show the locations of the first points recorded in historical tropical cyclone data (Knapp et al. 2010) over the same period.

criterion developed by Palmén (1948). He identified six environmental properties upon which genesis depends: the Coriolis parameter, low-level relative vorticity, shear of the horizontal wind through the depth of the troposphere, relative humidity of the middle troposphere, ocean thermal energy, and the difference between the equivalent potential temperatures at the surface and at 500 hPa. This last factor he mistook as a measure of the conditional instability of the tropical atmosphere. This error was corrected in a revised genesis index developed by DeMaria et al. (2001), specialized to the North Atlantic. They also dropped the factors depending on vorticity and ocean energy content. On the grounds of modeling results unavailable to Gray when he developed his genesis index, it is highly unlikely that subsurface ocean temperature and density are important influences on genesis even though they can have a substantial effect on developed storms. An important exception occurs when sea surface temperature is measured by surface infrared emissions; in that case, the surface temperature may not reflect conditions just below the surface, especially if surface winds are very light.

Other genesis indices have been developed in recent years (Emanuel and Nolan 2004; Emanuel 2010; Tippett et al. 2011; Bruyère et al. 2012). These have substituted potential intensity for sea surface temperature and reasserted the importance of vorticity, although the latter appears to enter as more of a threshold effect (Tippett et al. 2011). It also appears that genesis depends more nearly on the saturation deficit of the midtroposphere than on the relative humidity (Emanuel 2010). Tang and Emanuel (2012b) proposed that the humidity, shear, and potential intensity factors should enter as a particular

nondimensional ratio of the shear and the potential intensity, all multiplied by a nondimensional measure of the saturation deficit of the middle troposphere. This nondimensional ratio was previously shown by Rappin et al. (2010) to be highly correlated with the length of time for a weak initial vortex to begin to amplify at a substantial rate. Genesis indices have been found to correlate with modulation of tropical cyclones by El Niño–Southern Oscillation (ENSO; Camargo et al. 2007a) and the Madden Julian oscillation (MJO; Camargo et al. 2009), and to account for some aspects of climate change simulated by climate models (Camargo et al. 2007d; Zhang et al. 2010; Korty et al. 2012a,b; Camargo 2013; Emanuel 2013). A map of one particular genesis index (Emanuel 2010), calculated from monthly mean climatological data, is shown in Fig. 15-15 together with the locations of the starting points of tropical cyclones from historical data. The bulk of the climatological distribution of tropical cyclone origin points is captured by the genesis index, but there are some interesting exceptions. For example, there are many origin points located outside the regions of large genesis index in the North Atlantic. These are likely “subtropical cyclones” that typically develop under cold-core cyclones aloft, where the potential intensity is locally and transiently elevated over its normal seasonal values (see section 3I). Note also the large genesis index values in the Red Sea and Persian Gulf, where no tropical cyclones have been observed. These bodies of water are probably too small to permit tropical cyclones to form.

Genesis indices are purely empirical, although observations of individual storms, theory, and modeling results have been used to develop candidate environmental parameters, like midtropospheric humidity and

potential intensity, to use in developing the indices. Nevertheless, the (qualified) success of genesis indices should be consistent with any comprehensive theory of genesis.

Genesis theories date back to at least [Espy \(1841\)](#), who focused on the organized release of ambient conditional instability, an idea that persisted through the CISK era ([Charney and Eliassen 1964](#)) and arguably survives to this day (e.g., [Montgomery and Enagonio 1998](#); [Montgomery et al. 2006](#); [Kilroy et al. 2017](#)).<sup>9</sup> Objections to this idea were raised as early as 1901 by [von Hann \(1901\)](#), who pointed out “that since a thundercloud does not give any appreciable pressure-fall but generally even a pressure-rise, it would be unreasonable to assume that a magnifying of this process would cause the strongest pressure falls known” (quoted in [Bergeron 1954](#)). Indeed, [Rotunno and Emanuel \(1987\)](#) and [Emanuel \(1989\)](#) found that weak vortices placed in a normal tropical maritime environment decay with time owing to downdraft-induced cooling of the boundary layer in the core. Only when the free troposphere in the vortex core becomes sufficiently humid, thus limiting evaporatively cooled downdrafts, can the cyclone develop. Using much more comprehensive numerical simulations, [Nolan \(2007\)](#) and [Rappin et al. \(2010\)](#) found that reducing the saturation deficit of free tropospheric air in the core of an incipient cyclone is critical for intensification. [Sippel and Zhang \(2008\)](#) noted that in a mesoscale forecast model ensemble, those ensemble members with higher column humidity were more likely to develop. Today it is generally conceded that a nearly saturated mesoscale core is a prerequisite for tropical cyclone development (e.g., [Kilroy et al. 2017](#)), but how that core gets established and what happens afterward remain controversial.

While it is known that mature hurricanes are maintained by surface enthalpy fluxes ([Riehl 1950](#); [Kleinschmidt 1951](#); [Lilly and Emanuel 1985](#); [Emanuel 1986](#)), originators of theory dealing with the energetics of mature storms did not argue that the same process was responsible for their genesis, and [Emanuel \(1989\)](#) argued that the resting tropical atmosphere is linearly stable to perturbations that rely on surface fluxes for amplification. Indeed, early researchers were usually able to identify precursors to tropical cyclogenesis, in the form of African easterly waves, other wave disturbances both at low levels and near the tropopause, and

fronts ([Dunn 1940](#); [Riehl 1948a,b](#); [Dunn 1951](#); [Riehl 1951](#); [Ramage 1959](#); [Riehl 1975](#)). Today it is generally believed that tropical cyclogenesis must be triggered by an external disturbance, but as we shall see, this may prove to be among the last of the tropical cyclone shibboleths to fall.

If a nearly saturated mesoscale column of air is a prerequisite for tropical cyclone formation, how does one get to this state, starting from the normal thermodynamic state of the tropical atmosphere? This normal state, in regions susceptible to tropical cyclones, is one in which deep convection is frequent, and the atmosphere is maintained in a state that is nearly neutrally stable to parcel ascent from the boundary layer ([Betts 1986](#); [Xu and Emanuel 1989](#)). To a good approximation, this state has constant saturation moist static energy  $h^*$ , through the depth of the troposphere, while there is a broad minimum in the actual moist static energy  $h$  in the lower to middle troposphere. This state of affairs is illustrated in [Fig. 15-16a](#).

There are two, nonexclusive, routes to creating a saturated, moist-adiabatic column. The first assumes no input of energy to the column, and therefore the mass-weighted vertical integral of moist static energy must remain constant. Suppose, for example, that we insert a weak, barotropic cyclone through the depth of the troposphere so that Ekman pumping at the top of the boundary layer produces upward motion. Since the gross moist stability of the troposphere is usually positive, such a circulation would likely export moist static energy from the column, but for the sake of argument, we will assume neutral gross moist stability and thus no change in column-integrated moist static energy by advection. The upward motion excites anomalous convection, which mixes moist static energy. Taken to an extreme, this mixing would produce a saturated column of constant moist static energy, as illustrated in [Fig. 15-16b](#). Because of the shape of the initial moist static energy profile and conservation of vertically integrated moist static energy, however, such mixing would produce a net cooling of the column. If this happens strictly locally, then to maintain dynamical balance the cyclonic vorticity must increase with altitude, and therefore there is either an anticyclone at the surface or a cyclone aloft, or both. This new state is highly susceptible to tropical cyclogenesis because the column is already saturated so that downdrafts are no longer possible, and because the thermodynamic disequilibrium between the column and the underlying ocean is even greater than in the initial state. Heat transfer from the warm ocean will then lead to what [Bergeron \(1954\)](#) termed the “inverting” of the cyclone—that is, the formation of a cyclone at the surface at the expense of the

---

<sup>9</sup> Almost 70 years ago, [Riehl \(1951\)](#) wrote that “the classical thermodynamic (convective) theory of hurricane formation has few defenders today.” News of the death of the convective theory proved greatly exaggerated.

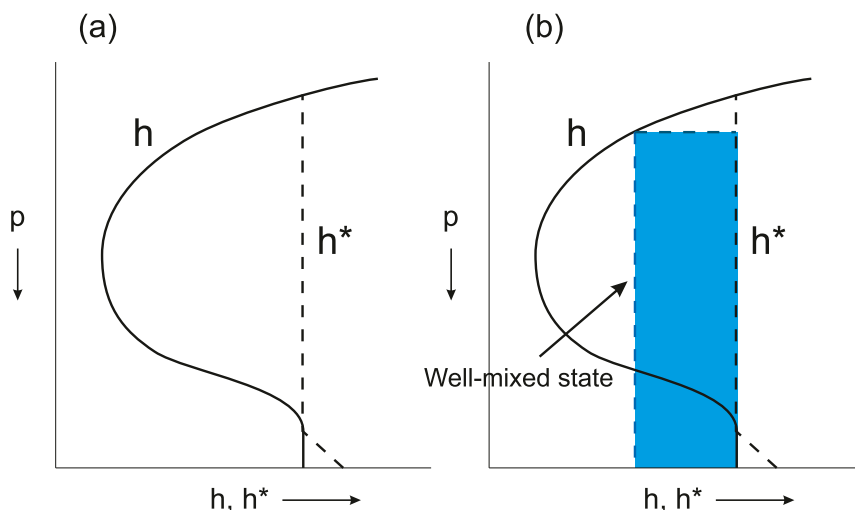


FIG. 15-16. (a) Typical thermodynamic state of the deep convecting tropical atmosphere. Moist static energy  $h$  is constant in the subcloud layer and decreases with altitude to a broad minimum in the lower-to-middle troposphere, increasing above that. The saturation moist static energy  $h^*$  is constant with height from the lifted condensation level to the tropopause, and therefore a parcel lifted from the subcloud layer is neutrally buoyant. (b) Vertical mixing of moist static energy—for example, by vigorous convection—produces constant moist static energy, whose value is that of the vertical average of the initial profile. Because this state is likely saturated through a deep layer, its  $h^*$  is clearly lower than that of the initial column, with the difference indicated by the blue shading.

circulation aloft—a process readily understandable using the tools of conservation and invertibility of potential vorticity.

The propensity of tropical cyclogenesis to originate in cold-core cyclones was first noted by Riehl (1963a) and later by many others [see the summary by Raymond (2014)]. Some tropical cyclones are observed to form from mesoscale convective complexes which commonly have cold-core cyclones at midlevels (Bartels and Maddox 1991). Such instances have been noted, for example, by McBride (1981), McBride and Zehr (1981), Velasco and Fritsch (1987), Davidson et al. (1990), and Laing and Fritsch (1993). A particularly interesting case of a strong mesoscale convective complex that first produced flash flooding in Pennsylvania and then formed a tropical cyclone once out over the Gulf Stream was documented by Bosart and Sanders (1981). The formation of a small-scale, intense surface cyclone underneath a cold-core cyclone aloft was observed by aircraft during the TEXMEX campaign (Bister and Emanuel 1997); this later developed into eastern North Pacific Hurricane Guillermo. The formation of a tropical cyclone from a mesoscale convective complex was simulated numerically by Chen and Frank (1993), and Nolan (2007) initialized their simulations of cyclogenesis using predefined cold-core vortices. The latter noticed that even when the model was initialized with a warm-core surface cyclone, the system developed a

cold-core, midlevel vortex before further development occurred. Bister and Emanuel (1997) initiated tropical cyclogenesis in an axisymmetric, cloud-permitting model simply by inserting an artificial “showerhead” in the middle troposphere; evaporation of the rain cooled and moistened the column spinning up a mesocyclone near the altitude of the showerhead. A warm-core, surface-based cyclone driven by WISHE then developed in the premoistened column. Raymond and Sessions (2007) and Raymond et al. (2011) noted that the saturation of the lower troposphere and the cessation of convective downdrafts lowers the locus of maximum convective heating, leading to a vertical velocity profile that imports moist static energy and is thus conducive to further development (see also Raymond 2014). It should be remarked that formation and maintenance of deep columns of nearly saturated air is made more robust to external influences, like shear, if they develop within rotating, and thus inertially confined, stagnation regions of the large-scale flow, which have come to be known as “pouches” (Dunkerton et al. 2009; Wang et al. 2010; Montgomery et al. 2012; Montgomery and Smith 2012; Wang et al. 2012).

Mixing of moist static energy and formation of cold-core cyclones is not the only possible route to genesis. Another way to achieve a nearly saturated column of air is to pump energy into the column, either through the bottom by surface heat transfer, or radiatively from the top

and bottom. In principle, adding energy to the column could achieve a nearly saturated, moist adiabatic state without necessarily going through a cold-core stage.

This is apparently what happens in the spontaneous aggregation of moist convection seen in many cloud-permitting simulations of radiative–convective equilibrium, dating back to those of Bretherton et al. (2005) [see the review by Wing et al. (2017)]. Diagnosis of nonrotating self-aggregation by Wing and Emanuel (2014) shows that enhanced surface enthalpy fluxes owing to convective downdrafts, together with decreased radiative cooling of the ascending moist and cloudy air, lead to an instability of the normal radiative–convective state, resulting in aggregation of convection. Diminution of radiative cooling by high, thick cirrus is particularly effective, as first conjectured by Riehl (1963a). Bretherton et al. (2005), Nolan et al. (2007b), Khairoutdinov and Emanuel (2013), and Wing et al. (2016) all showed that tropical cyclones can develop spontaneously in rotating, cloud-permitting radiative–convective simulations, and that the initial instability is driven by a combination of wind-dependent surface enthalpy fluxes and the interaction between both shortwave and longwave radiation and clouds and water vapor. It is important to recognize that the time for the initial radiative–convective equilibrium state to evolve to the point of hurricane-strength cyclones varies from 15 days in the Nolan et al. simulations to 25–65 days in the Wing et al. case, with the range spanning ensemble members that differ only in small-amplitude noise in the initial states. In these simulations, the maximum surface wind speed, after undergoing a ramp-up of indeterminate length, suddenly undergoes “ignition” and thereafter intensifies very rapidly. One might define “genesis” as the slow gestation period prior to ignition. The observed and modeled diurnal pulsing of tropical cyclone clouds and precipitation (Dunion et al. 2014; Bowman and Fowler 2015; Lepert and Cecil 2016; Navarro and Hakim 2016; Wu and Ruan 2016; O’Neill et al. 2017) provides further evidence of the importance of radiation in tropical cyclone evolution.

Whatever the thermodynamic route to genesis, observations and models clearly show that ambient wind shear has a strong effect on the process, as reviewed by Nolan and McGauley (2012). As discussed previously, wind shear enters genesis indices as a strictly negative effect, but histograms of wind shear at observed genesis locations, normalized by shear histograms at random locations in the tropics, hint that small shear may be more favorable than no shear at all. Observations and numerical simulations also suggest that the direction of shear, and the relative orientations of the shear and surface wind vectors, may enhance or suppress genesis,

possibly by changing the likelihood of convection in the high-vorticity cores of the developing cyclones (Nolan and McGauley 2012). Thus, we are left with a fascinating if incomplete picture of genesis. The dependence of radiative heating on clouds and water vapor, and the dependence of surface enthalpy fluxes on wind, can destabilize the tropical atmosphere and produce tropical cyclones, but it takes so long for this to happen that it is likely that, in nature, the process is accelerated by the action of external disturbances, as observations seem to suggest. Thus, one might postulate that the overall frequency of tropical cyclogenesis in a given climate is governed by some combination of the large-scale environmental susceptibility to genesis (as measured, for example, by a genesis index) and the frequency, structure, and amplitude of disturbances that serve as catalysts to the process.

In particular, the idea that all tropical cyclones originate in preexisting disturbances does not imply that, absent those disturbances, no tropical cyclones would develop. Recently, Patricola et al. (2018b) performed two 10-ensemble-member simulations using a regional model spanning the Atlantic from 5°S to 55°N and from 10° to 130°W, during the extremely active 2005 season. The eastern boundary lies just along the westernmost coast of Africa. About 75% of tropical cyclones in 2005 developed from African easterly waves (Beven et al. 2008). The model used prescribed (space and time varying) sea surface temperature, and the initial and boundary conditions were supplied from reanalysis data. The second ensemble simulation differed from the control in that waves entering the eastern boundary of the domain with periods between 2 and 10 days were filtered. Thus, the proximate catalysts of the 2005 Atlantic tropical cyclones, African easterly waves, were largely filtered. The result was no significant change in any of the tropical cyclone activity metrics calculated, including the overall frequency and accumulated cyclone energy from the control. The cyclones did seem to develop farther west, however. These experiments cast serious doubt on the proposition that *all* tropical cyclones in nature originate in preexisting disturbances, or that external perturbations are necessary to the existence of tropical cyclones in nature. Rather, they determine the timing and location of genesis events, serving as catalysts in an evolution that would anyway lead to genesis. This would also explain why some genesis indices, and the random seeding method of Emanuel et al. (2008b), produce good renditions of spatial, seasonal, and ENSO-driven variability even though they have no representations of external disturbance activity.

Thus, we may be at an interesting and productive turning point in research on tropical cyclogenesis,

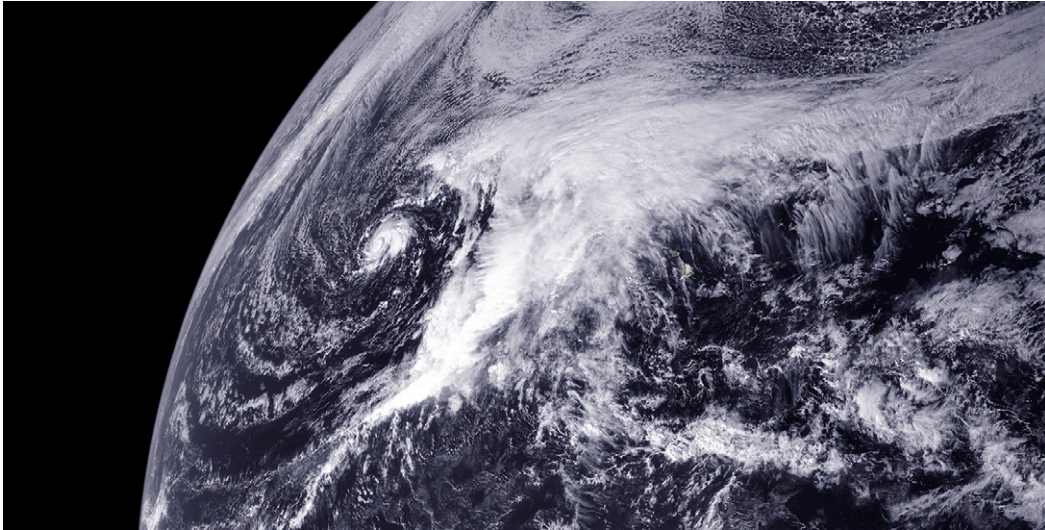


FIG. 15-17. A sub-tropical cyclone (the small cyclone to the left), northwest of Hawaii on 19 Dec 2010, within the much-larger-scale circulation of a synoptic-scale cold low aloft, following an occluded surface cyclone. This sub-tropical cyclone was later classified as Tropical Storm Omeka. (Source: the NOAA–NASA GOES Project; <https://goes.gsfc.nasa.gov/>.)

marked by the marriage of the global view pioneered by Erik Palmén (Palmén 1948) and William Gray (Gray 1968) to the numerous studies of how individual cyclones are generated, a union made possible by exciting new ideas about self-aggregation of moist convection.

#### *l. Subtropical storms, medicanes, polar lows, and agukabams*

The monthly mean genesis potential, shown in Fig. 15-15, encompasses the main regions of tropical cyclogenesis. But on submonthly time scales, excursions into the tropics or subtropics of colder air from high latitudes can transiently and locally elevate potential intensity. Simpson (1952a) was perhaps the first to notice that synoptic-scale cutoff low pressure systems at upper levels could trigger surface cyclones underneath them, based on his analysis of 76 “Kona storms” that form near Hawaii in winter (Daingerfield 1921). He showed that small-scale, warm-core storms resembling tropical cyclones developed within the large-scale, cold-core cyclones aloft and demonstrated that a parcel ascending from a saturated state at the surface could be quite a bit warmer than the air aloft, suggesting, in contemporary parlance, large potential intensity. Figure 15-17 shows an example of a tropical cyclone-like Kona storm within the much larger-scale circulation associated with a cutoff cyclone aloft. Since Simpson’s work, a rich literature on the subject of subtropical cyclones has developed (e.g., Ramage 1962; Cochran 1976; Bosart and Bartlo 1991; Davis and Bosart 2003, 2004; Guishard et al. 2007; Evans and Guishard 2009; Guishard et al. 2009; Evans

and Braun 2012; Bentley et al. 2016). The observed genesis points outside the regions of elevated genesis potential index in Fig. 15-15 are likely instances of subtropical cyclones.

Subtropical cyclones sometimes occur over the Mediterranean Sea, where they are known as “medicanes” (Ernst and Matson 1983; Mayengon 1984; Rasmussen and Zick 1987; Alpert and Neeman 1992; Pytharoulis et al. 2000; Homar et al. 2003; Emanuel 2005b; Lionello et al. 2006; Fita et al. 2007; Miglietta et al. 2008; Moscatello et al. 2008; Claud et al. 2010; Miglietta et al. 2013; Tous and Romero 2013; Tous et al. 2013; Cavicchia et al. 2014; Flaounas et al. 2015; Mazza et al. 2017; Pytharoulis et al. 2017).<sup>10</sup>

Simpson’s (1952a) observation that subtropical storms form under deep, cold-core, cutoff cyclones seems to be quite general. At the center of such disturbances, there is little horizontal temperature gradient or vertical wind shear, the air is anomalously cold relative to the sea surface temperature, and the core is often humid owing to a history of ascent. Emanuel (2005b) showed, using an axisymmetric, nonhydrostatic, cloud-permitting model, that such cold-core cyclones are ideal embryos in which to develop tropical cyclone-like vortices powered by surface enthalpy fluxes, and numerous model-based studies (e.g., Homar et al. 2003; Miglietta et al. 2008, 2013; Tous et al. 2013) underscore the importance of the

<sup>10</sup>Perhaps it was a medicanes that nearly sunk Ulysses’s ship in Book 5 of Homer’s *Odyssey*.

surface heat flux in such developments. The low dry static stability of the cold air favors storms of relatively small diameter.

Transient incursions of cold air over relatively warm water at high latitudes can also lead to the development of small-scale cyclones powered at least in part by surface heat fluxes, but such developments are often complicated by the presence of deep baroclinity. Ordinary baroclinic instability in atmospheres that have very low dry static stability through a deep layer will result in unusually small-scale and intense baroclinic cyclones (Stone 1966), with or without contributions from surface fluxes. On the other hand, strong surface fluxes underneath cutoff cyclones aloft can lead to subtropical cyclone-type development even without baroclinity. This led the present author to propose that there is a continuum of cyclone development between pure baroclinic instability and pure surface-flux-based development (see Rasmussen and Lystad 1987). Small-scale cyclones that develop over the oceans in cold air at high latitudes have come to be known as “polar lows” regardless of where they fit along this continuum, leading some to suggest that polar lows are primarily baroclinically powered (e.g., Harrold and Browning 1969; Reed and Duncan 1987) and others showing that pure surface-flux-driven cyclones are possible underneath deep cutoff cyclones in polar regions (Rasmussen 1979, 1981; Emanuel and Rotunno 1989; Nordeng 1990; Nordeng and Rasmussen 1992). The term “polar low” continues to be used to describe a variety of phenomena. Several climatologies of polar lows have appeared (e.g., Businger 1985; Rasmussen et al. 1992; Zhan and von Storch 2008; Yanase et al. 2016; Watanabe et al. 2018) and a conference was devoted to the subject (Rasmussen and Lystad 1987). The behavior of polar lows of various kinds has been described in a number of observationally based case studies (e.g., Rasmussen 1981, 1985; Nordeng and Rasmussen 1992) and their often complex developments explored with numerical simulations (e.g., Sardie and Warner 1985; Nordeng 1990). The topic is summarized in an entire book (Twitchell et al. 1989) and more recently in an extensive review (Rasmussen 2003).

Tropical cyclones generally develop over the sea because the rapid mixing of heat through the ocean’s mixed layer provides ample enthalpy flux through the surface to sustain such storms. The flow of heat through rock and soil is usually much too slow to sustain flux-driven cyclones (except perhaps on the scale of dust devils), and therefore storms almost always decay quasi exponentially over land (Tuleya 1994; Kaplan and DeMaria 1995). On some occasions, tropical cyclones are observed to redevelop over land in the absence of obvious baroclinic influences; this appears to be fairly

common over the deserts of northern Australia. Such redevelopments have been called “landphoons” and were named “agukabams” (from aboriginal roots translating to “land storms”) by Emanuel et al. (2008a), who showed that the flow of heat through certain soil types can be substantial, provided the soils are nearly water saturated. They were also able to simulate such redevelopments using a simple, axisymmetric tropical cyclone model coupled to a model of heat flow through wet, sandy soils. They argued that such storms would ultimately dissipate when they were far enough from an oceanic water source that their rainfall was insufficient to maintain a wet soil. A particularly fascinating case of inland redevelopment was that of Tropical Storm Erin of 2007. Evans et al. (2011) showed, using detailed numerical simulations, that the redevelopment of Erin over Oklahoma was driven by strong surface enthalpy fluxes, but in this case the soils were wet well before the arrival of the storm-related precipitation, which therefore played no part in the thermodynamics of the reintensification. A radar view of Erin (Fig. 15-18a) shows a reflectivity pattern similar to that of ordinary tropical cyclones. The storm passed right through the Oklahoma Mesonet, a dense array of observing stations developed by University of Oklahoma and Oklahoma State University, and maintained by the Oklahoma Climatological Survey.

The temporal evolution of the soil temperature at three depths, as measured at the Hinton, Oklahoma, mesonet site, is shown in Fig. 15-18b. As the core of Erin passed near this site early on 19 August, the soil temperatures dropped precipitously at all three depths. Given the heat capacity of the average soil type in this region and the depth through which and time interval over which the soil temperature dropped, it is straightforward to estimate a heat flux through the soil surface of at least  $200 \text{ W m}^{-2}$ , more than sufficient to maintain a tropical storm-strength tropical cyclone.

Kilroy et al. (2016) examined a case of tropical cyclone redevelopment over northern Australia in January of 2014 and showed that the system was maintained by surface enthalpy fluxes. The system eventually dissipated over land, perhaps because it strayed too far from the ocean to maintain wet soils or because the soil temperatures farther south were not sufficient to maintain it.

While thermally driven redevelopment over land appears to be unusual outside northern Australia, these cyclones can be intense enough to cause damage and flooding and an effort should be made to better understand their physics.

#### *m. Tropical cyclones and climate*

Interest in the influence of climate change on tropical cyclones dates back at least as far as the insightful work

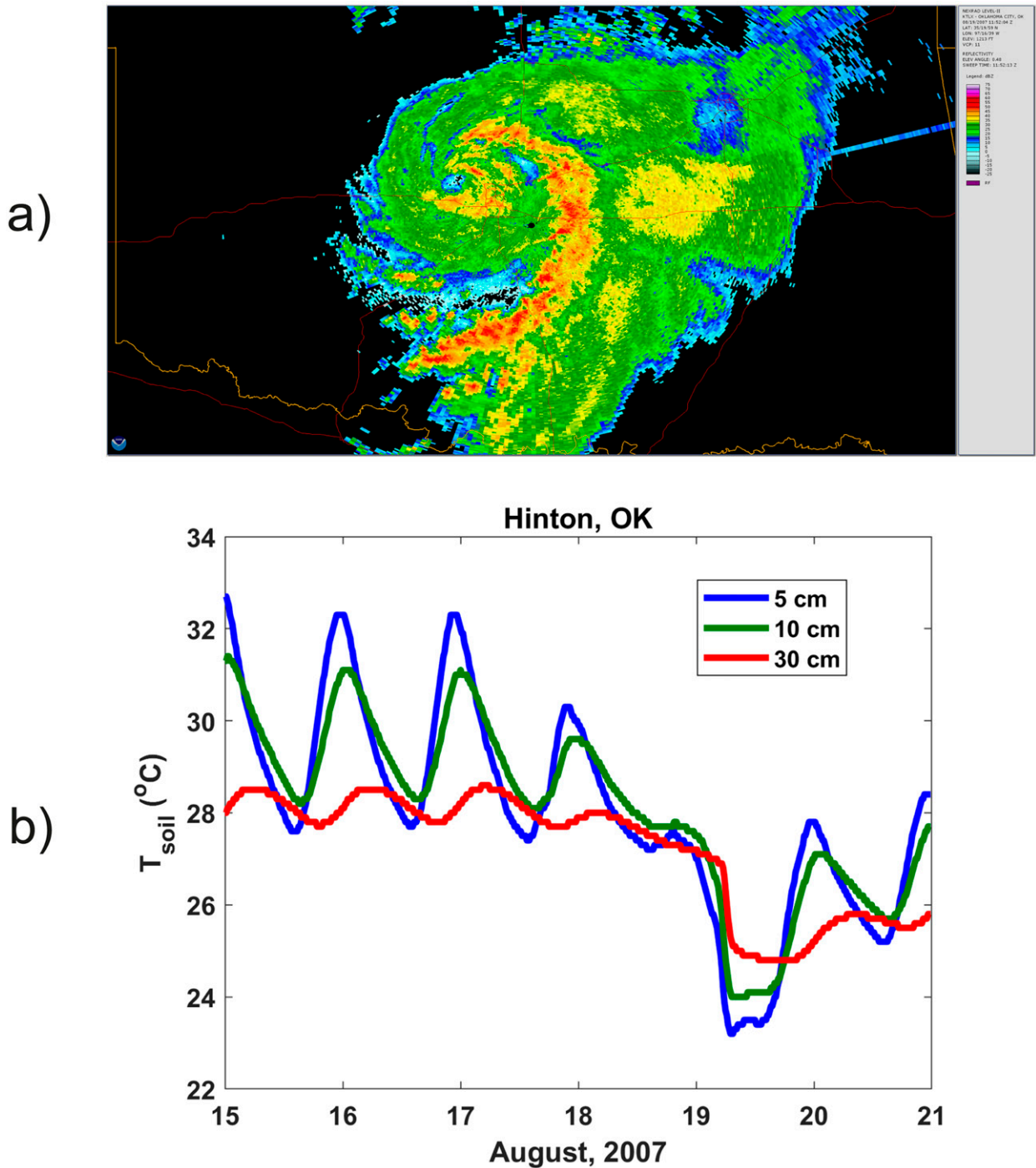


FIG. 15-18. (a) Radar reflectivity from the Oklahoma City NOAA/NEXRAD site at 1152 UTC 19 Aug 2007 (the software for the figure was obtained from <https://www.ncdc.noaa.gov/wct/install.php>). (b) Time evolution of soil temperature measured by the Hinton mesonet station at depths of 5 (blue), 10 (green), and 30 cm (red).

of Bergeron (1954), who speculated that the relatively small effects of changing distributions of sunlight or atmospheric composition could have noticeable effects on tropical cyclones. Emanuel (1987) pointed out that potential intensity increases with temperature and

calculated that increasing atmospheric carbon dioxide concentrations would yield a potential intensity increase of a few meters per second per Kelvin increase in sea surface temperature. The increase in North Atlantic hurricane activity that took place during the 1990s and

2000s stimulated renewed interest in the question of climate change effects on tropical cyclones and led to an explosion of publications on this issue. There are several reviews of the subject going back to [Lighthill et al. \(1994\)](#), [Henderson-Sellers et al. \(1998\)](#), and [Knutson et al. \(2010\)](#) and a number of edited volumes ([Murnane and Liu 2004](#); [Elsner and Jagger 2009](#); [Charabi 2010](#); [Diaz and Pulwarty 2012](#); [Elsner et al. 2014](#); [Walsh et al. 2016](#); [Collins and Walsh 2017](#)). As work on tropical cyclones and climate has been summarized in very recent comprehensive review papers ([Walsh et al. 2016](#); [Knutson et al. 2018](#), manuscript submitted to *Bull. Amer. Meteor. Soc.*), we here present only a cursory overview of this broad and interesting subject.

Climate fluctuations affect tropical cyclone genesis, tracks, and intensity presumably by modifying environmental conditions known to influence such storms; these include potential intensity, tropospheric humidity, and tropospheric winds, including wind shear. The influence of various combinations of these is evident in trends and variability in observed tropical cyclones. [Figure 15-19](#) shows the global annual number of tropical cyclones whose lifetime maximum winds equaled or exceeded 40 kt during an era of good global satellite surveillance, 1979–2016. An average of 78 storms of this magnitude occur each year, with a standard deviation of 8.9 storms, very close to the value of 8.8 that would be obtained from a pure Poisson process. There is clearly no long-term trend in global tropical cyclone counts. Despite the global stability in tropical cyclone numbers, there is evidence of substantial interannual and longer variations in activity within individual regions and some long-term trends in intensity and other metrics, as we shall see presently.

Connections between tropical cyclone activity and natural climate variability have been explored at least since the work of [Namias \(1955\)](#), who found that there are strong correlations between interannual fluctuations of Atlantic hurricane activity and changes in the general circulation, particularly in the pattern of long waves. This work was extended and particularized to individual parts of the Atlantic basin by [Ballenzweig \(1959\)](#). [Shapiro \(1982a,b\)](#) showed that Atlantic hurricane activity is modulated on interannual time scales by variability of sea surface temperatures and perhaps by the quasi-biennial oscillation.

It is by now well established that ENSO strongly modulates tropical cyclone activity in individual regions, although there tends to be global statistical compensation, with the various regions oscillating out of phase with each other. There is an extensive literature on ENSO effects on North Atlantic tropical cyclones (e.g., [Gray 1984](#); [Goldenberg and Shapiro 1996](#); [Bove et al. 1998](#); [Jones and Thorncroft 1998](#); [Pielke and Landsea](#)

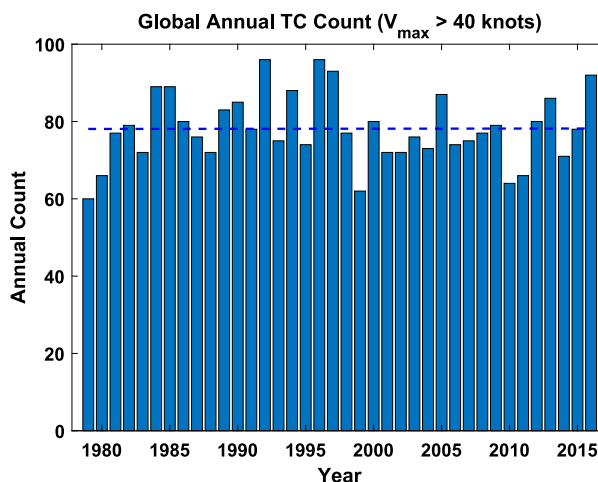


FIG. 15-19. Annual global number of tropical cyclones whose lifetime maximum winds equaled or exceeded 40 kt, from data from the National Hurricane Center for the Atlantic and eastern North Pacific regions and from the JTWC for the rest of the world, over 1979–2016. The horizontal dashed line shows the best-fit linear trend.

[1999](#); [Elsner et al. 2001](#); [Vitart and Anderson 2001](#); [Tang and Neelin 2004](#); [Donnelly and Woodruff 2007](#); [Iizuka and Matsuura 2009](#); [Ke 2009](#); [Klotzbach 2011a,b](#); [Patricola et al. 2014](#); [Wang et al. 2014](#); [Rodríguez-Fonseca et al. 2016](#)), with noticeable suppression of Atlantic storms during El Niño years and enhancement during the opposite La Niña phase. Recently, [Kossin \(2017\)](#) showed that even though Atlantic activity is suppressed in El Niño years, activity can be enhanced along the U.S. coast, demonstrating that basinwide metrics may not always be suitable proxies for coastal hazard risk. There is also an extensive literature on ENSO modulation of tropical cyclone activity in other basins, including the western North Pacific (e.g., [Chan 1985, 2000](#); [Saunders et al. 2000](#); [Sobel and Maloney 2000](#); [Wang and Chan 2002](#); [Wu et al. 2004](#); [Camargo and Sobel 2005](#); [Huang and Xu 2010](#); [Zhao et al. 2010](#); [Kim et al. 2011](#); [Li and Zhou 2012](#); [Zhang et al. 2012](#); [Yang et al. 2015](#); [Patricola et al. 2018a](#); [Zhao and Wang 2018](#)), the central and eastern North Pacific (e.g., [Chu and Wang 1997](#); [Hong et al. 2011](#); [Jin et al. 2014](#); [Jien et al. 2015](#)), the north Indian Ocean ([Liebmann et al. 1994](#); [Singh et al. 2000](#); [Charabi 2010](#); [Sumesh and Ramesh Kumar 2013](#)), and the Southern Hemisphere including the southwest Pacific region, Australia, and the south Indian Ocean (e.g., [Hastings 1990](#); [Evans and Allan 1992](#); [Hall et al. 2001](#); [Ho et al. 2006](#); [Kuleshov et al. 2009](#); [Chand and Walsh 2011](#)). Modulation of tropical cyclones by ENSO appears to occur through its influence on vertical wind shear (e.g., [Zhu et al. 2012](#)) and by transiently changing the temperature of the

atmosphere relative to that of the ocean (Tang and Neelin 2004).

There is increasing evidence that tropical cyclones are modulated by higher-frequency intraseasonal oscillations of the tropical atmosphere, including the MJO (Liebmann et al. 1994; Ferreira et al. 1996; Maloney and Hartmann 2000a,b; Mo 2000; Sobel and Maloney 2000; Hall et al. 2001; Hartmann and Maloney 2001; Maloney and Hartmann 2001; Bessafi and Wheeler 2006; Ho et al. 2006; Ayyer and Molinari 2008; Kim et al. 2008; Barrett and Leslie 2009; Chen et al. 2009; Vitart 2009; Chand and Walsh 2010; Kikuchi and Wang 2010; Klotzbach 2010; Huang et al. 2011; Schreck and Molinari 2011; Ventrice et al. 2011; Jiang et al. 2012; Krishnamohan et al. 2012; Klotzbach 2014; Wang and Moon 2017; Li and Zhou 2018). Presumably, the modulation is mediated by the effects of such oscillations on environmental wind shear, potential intensity, vertical motion, and tropospheric humidity. Longer-period phenomena, such as the Atlantic meridional mode (Kossin and Vimont 2007; Vimont and Kossin 2007; Zhang et al. 2017) and the Pacific decadal oscillation (Chan 2005a; Liu and Chan 2008; Lee et al. 2012), have also been implicated in regional variability of tropical cyclones.

Modulation of tropical cyclone genesis rates by the aforementioned phenomena is at least partially captured by genesis indices (see section 3k; Camargo et al. 2007a,d, 2009; Tippett et al. 2011; Wang and Moon 2017), suggesting that some of the modulation is by large-scale environmental factors, as opposed to seed disturbance characteristics.

Somewhat more controversial is the source of a multidecadal lull in North Atlantic tropical cyclone activity during the late twentieth century. In time series of both tropical Atlantic summertime sea surface temperatures and metrics of Atlantic tropical cyclone activity, there is a pronounced dip that began in the late 1950s and ended in the mid- to late 1990s. Most researchers (e.g., Gray et al. 1997; Goldenberg et al. 2001; Bell and Chelliah 2006; Zhang and Delworth 2006; Zhang et al. 2007; Chylek and Lesins 2008; Hetzinger et al. 2008; Klotzbach and Gray 2008; Wang et al. 2008; Enfield and Cid-Serrano 2010; Klotzbach 2011b; Caron et al. 2015) ascribe this to a phenomenon known as the Atlantic multidecadal oscillation (Delworth and Mann 2000; Gray et al. 2004), a coupled oscillatory mode that has maximum amplitude in the North Atlantic and is readily apparent in unforced simulations using global coupled climate models (e.g., Ting et al. 2015). On the other hand, the lull closely follows global sulfur emissions (Mann and Emanuel 2006), and modeling studies provide compelling evidence that the downturn was caused

by a regional cooling associated with sulfate aerosols (Booth et al. 2012; Dunstone et al. 2013). At the time of this writing, the cause of the late-twentieth-century depression of tropical Atlantic sea surface temperatures and tropical cyclone activity continues to be vigorously debated. The outcome of this debate is consequential as it bears on the future of tropical cyclone activity in the Atlantic region and elsewhere.

Patterns of tropical cyclone genesis and tracks have been illuminated by applying cluster analysis techniques to historical data (Blender et al. 1997; Camargo et al. 2007b,c; Nakamura et al. 2009; Ramsay et al. 2012). Such analyses can reveal patterns of tropical cyclone tracks related to natural climate fluctuations such as ENSO, the Atlantic meridional mode, the North Atlantic Oscillation, and the MJO (Kossin et al. 2010). The response of different clusters to modulation by climate fluctuations and trends offers clues about how such variability affects tropical cyclones.

Patterns of variability at centennial and longer time scales are beginning to show up in tropical cyclone proxies in the geological record, in a relatively new endeavor called paleotempestology. Duke (1985a,b) proposed that shallow marine deposits with a distinctive variable pattern known as hummocky cross stratification were created by strong winter storms and by tropical cyclones, and showed that the incidence of such deposits at tropical paleolatitudes are somewhat more common in sedimentary beds laid down during relatively warm climates (see also Duke et al. 1991). Liu and Fearn (1993) pioneered the use of overwash deposits as proxies for tropical cyclone surge events. These occur when storm surges wash sand and other material from immediate coastal environments back into nearshore lakes and marshes. Layers of this material are overlaid on organic layers deposited in the course of the normal sedimentation of such lakes and marshes and are in turn overlaid by organic material as the environments return to normal. The organic matter can be radiocarbon dated, establishing the time of the surge event. The dates of such layers correlate well with known historical events, and the technique can be applied as far back as 6000 years. Tropical cyclone variability related to past natural climate fluctuations has been documented at a variety of locations (Bravo et al. 1997; Liu and Fearn 2000; Donnelly et al. 2001a,b, 2004; Donnelly 2005; Lul and Liu 2005; Woodruff et al. 2006; Cheung et al. 2007; Donnelly and Woodruff 2007; Scileppi and Donnelly 2007; Woodruff et al. 2008; Boldt et al. 2010; Williams 2010; Liu et al. 2011; Brandon et al. 2013, 2014; Lin et al. 2014; Rogers et al. 2015; Baldini et al. 2016; van Hengstum et al. 2016; Soria et al. 2017; Hong et al. 2018; Soria et al. 2018). These records are beginning to reveal

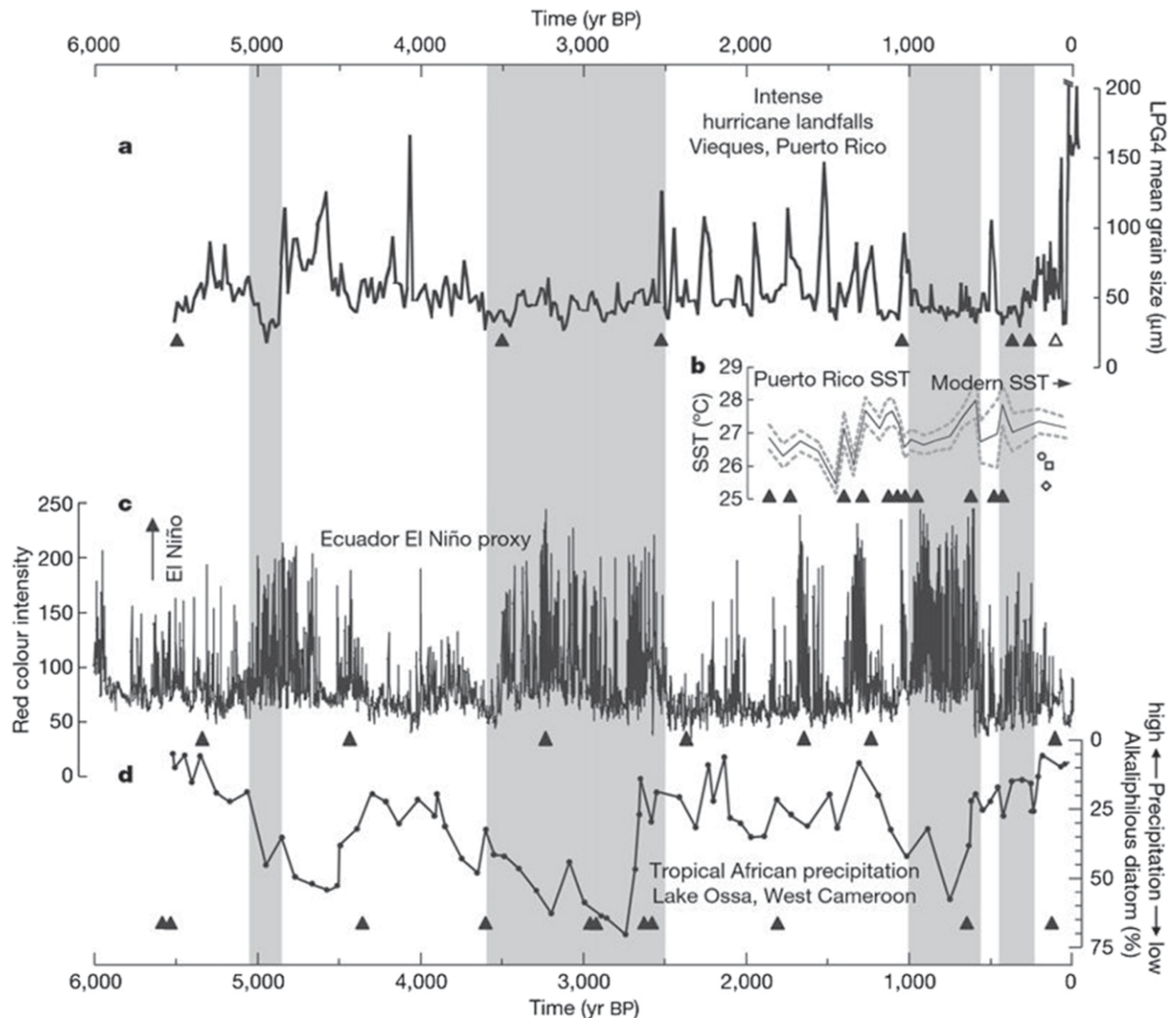


FIG. 15-20. (a) Mean bulk grain-size record from a core sample taken from a backbarrier lagoon on the Caribbean island of Vieques, Puerto Rico. Intervals of relatively few intense-hurricane-induced layers in all cores are noted with gray shading. (b) The thin line with the 2-std-dev uncertainty envelope (dashed lines) is a reconstruction of summer SSTs off Puerto Rico (core “PRP12”), and coral-based reconstruction of mean annual SSTs from La Parguera, Puerto Rico, are noted: 26.2°C for 1700–1705 (open circle), 25.3°C for 1780–85 (open diamond), and 26.0°C for 1800–05 (open square). The modern mean annual SST is noted with an arrow. (c) El Niño proxy reconstruction from Laguna Pallcacocha, Ecuador. Peaks in red color intensity are documented as allochthonous material washed into the lake, primarily during strong El Niño events. (d) Changes in precipitation in West Cameroon inferred from alkaliphilous diatoms (thriving in alkaline conditions) from Lake Ossa. Radiocarbon-age control points are noted with filled black triangles below (a)–(d). [Source: The figure and caption (before AMS editing) are from [Donnelly and Woodruff \(2007\)](#); reprinted by permission from Springer Nature.]

interesting trends and correlations with, for example, ENSO activity, as shown in [Fig. 15-20](#).

Much before 6000 years ago, rising sea levels associated with recovery from the last glacial period would have buried such overwash deposits. In some cases, such buried deposits are preserved and accessible in shallow water, as is the case with the “blue holes” found in the Bahamas ([van Hengstum et al. 2014](#)). Strong hurricanes can transport coarse sediment from shallow carbonate

platforms to the deep sea, and bank-edge sediments may therefore record tropical cyclone events, offering the possibility of reconstructing storm activity back to 7000 years ago and more ([Toomey et al. 2013](#)).

Surge and wave run-up onto beaches during tropical cyclones can result in the deposition of ridges of sediment, and these can be dated and used to reconstruct histories of tropical cyclone activity in suitable locations ([Nott et al. 2009](#); [Forsyth et al. 2010](#); [Nott 2011a](#); [Nott](#)

et al. 2013; Nott and Jagger 2013). Such records suggest that tropical cyclone activity in Australia is now lower than it has been in the past 500–1500 years (Haig et al. 2014).

Measurements of the isotopic composition of eyewall rain show that it is depleted in heavier isotopes, such as  $^{18}\text{O}$  (Lawrence and Gedzelman 1996; Gedzelman and Lawrence 2000). This is consistent with the thermodynamic requirement that little of the eyewall rain can evaporate, a process that concentrates heavier isotopes in the remaining liquid water. The ratio of heavier to lighter isotopes in rainwater can be preserved in trees, sediments, corals, and cave deposits under some circumstances, yielding a geochemical proxy for tropical cyclones; this has been used to develop tropical cyclone proxy records in a number of locations (Malmquist 1997; Miller et al. 2006; Frappier et al. 2007b; Mora et al. 2007; Hetzinger et al. 2008; van Soelen et al. 2013; Frappier et al. 2014; Munksgaard et al. 2015; Lane et al. 2017).

Given the short length and often-compromised quality of historical tropical cyclone records, paleotempestology offers some hope that climate signals can be detected in much longer objective records of storm activity. Several illuminating reviews of the field have appeared in recent years (Murnane and Liu 2004; Nott 2004; Frappier et al. 2007a; Liu 2007; Fan and Liu 2008; Liu et al. 2009; Nott 2011b; Nott and Jagger 2013; Baldini et al. 2016).

Somewhat more controversial is the response of tropical cyclone activity to global climate change, including paleoclimate variations and the anthropogenic effects of aerosols and greenhouse gases. This is a very extensive and active subject that has been recently reviewed comprehensively (Walsh et al. 2016; Knutson et al. 2018, manuscript submitted to *Bull. Amer. Meteor. Soc.*), and so only a broad overview is provided here.

Global climate change qualitatively differs from regional variability in that it can be expected to affect the temperature of the tropical troposphere above the boundary layer. Observations of tropical cyclones (e.g., Gray 1975) and simple models (Emanuel 1989, 1995) show that genesis is sensitive to midtropospheric humidity and, in particular, point to the importance of a nondimensional measure  $\chi_m$  of this humidity:

$$\chi_m \equiv \frac{s_m^* - s_m}{s_0^* - s_m^*}, \quad (15-15)$$

where  $s_m$  is the moist entropy of the middle troposphere,  $s_m^*$  is its saturation value, and  $s_0^*$  is the saturation entropy of the sea surface. [The original definition replaces  $s_m^*$  by  $s_b$  in the denominator of (15-15), but in a convectively neutral atmosphere these two quantities are nearly

equivalent.] This quantity is known from modeling studies to provide a measure of inhibition to tropical cyclone development; the larger its value is, the longer it takes to saturate a mesoscale column of the atmosphere, a prerequisite for intensification (see section 3k). The numerator of (15-15) can be written

$$s_m^* - s_m = \frac{L_v}{T_m} q_m^* (1 - \mathcal{H}), \quad (15-16)$$

where  $L_v$  is the latent heat of vaporization,  $T_m$  and  $q_m^*$  are the temperature and saturation specific humidity of the middle troposphere, and  $\mathcal{H}$  is now relative humidity of the middle troposphere.

If the global climate is stable, then the inability of the deep tropics to support strong, nontransient temperature gradients in the free troposphere (Sobel and Bretherton 2000) implies that  $T_m$  and  $q_m^*$  are virtually constant in space and time, and therefore variability of the saturation deficit given by (15-16) is almost entirely due to variations in relative humidity. Thus, the saturation deficit that appears in some genesis indices is tuned to handle variations of relative humidity, but, since the global climate has been relatively stable during the instrumental period, variations related to  $q_m^*$  have been very small. Yet, global temperature change can be expected to change  $q_m^*$  in ways that genesis indices cannot have been trained to deal with.

From a scaling standpoint, we expect  $q_m^*$  to increase nearly exponentially with midtropospheric temperature, according to the Clausius–Clapeyron equation. But the denominator of (15-15), which is proportional to the surface enthalpy flux, is constrained to equal the radiative cooling integrated over the troposphere, and this increases relatively slowly with global temperature. Thus, we may, in general, expect that the inhibition to tropical cyclone formation given by (15-15) increases with global temperature, assuming that midtropospheric relative humidity does not change much. Indeed, Emanuel (2013) showed that increasing  $\chi_m$  was the main brake on increasing genesis rates in his modeling study of the response of tropical cyclones to global warming.

While the thermodynamic inhibition to tropical cyclone formation increases with temperature, so too does the potential intensity. On time scales longer than that of the thermal equilibration of the ocean mixed layer (about 2 years), the mixed layer energy budget balances turbulent enthalpy fluxes from the surface with net surface radiative flux and convergence of heat transport in the ocean itself. This may be expressed

$$C_k \rho_a |\mathbf{V}| (k_0^* - k) = F_{\text{solar}} - F_{\text{IR}} - \int_0^h (\nabla \cdot \mathbf{Q}_{\text{ocean}}) dz, \quad (15-17)$$

where  $C_k$  is the surface enthalpy transfer coefficient,  $\rho_a$  is the surface air density,  $|\mathbf{V}|$  is the surface wind speed,  $k_0^*$  is the saturation enthalpy of the sea surface,  $k$  is the boundary layer enthalpy,  $F_{\text{solar}}$  is the net downward surface solar flux (accounting for reflection from the surface),  $F_{\text{IR}}$  is the net upward IR flux from the surface,  $h$  is the ocean mixed layer depth, and  $\mathbf{Q}_{\text{ocean}}$  is the three-dimensional ocean heat flux (including any turbulent fluxes through the base of the mixed layer).

If we eliminate  $k_0^* - k$  between (15-17) and the expression for potential intensity (15-7), the result is

$$|\mathbf{V}|^2 = \frac{T_s - T_o}{T_o} \frac{F_{\text{solar}} - F_{\text{IR}} - \int_0^h (\nabla \cdot \mathbf{Q}_{\text{ocean}}) dz}{C_D \rho_a |\mathbf{V}|}. \quad (15-18)$$

Thus, on time scales much more than a few years, potential intensity is controlled by surface radiative fluxes, ocean heat flux, and surface wind speed. It is important to note that sea surface temperature only enters in a minor way in the thermodynamic efficiency term [first term on right-hand side of (15-18)], although it plays a role as well in the net infrared flux. Models that specify rather than calculate ocean temperature will generally violate surface energy balance, leading to erroneous values of potential intensity. This calls into question the validity of applying atmosphere-only global models (AGCMs) to quantify the effects of climate change on tropical cyclone activity. Emanuel and Sobel (2013) explored the effects of varying surface wind, solar radiation, greenhouse gas concentration, and ocean heat flux on potential intensity and sea surface temperature, using a one-dimensional radiative-convective model, and showed that the functional relationship between surface temperature and potential intensity is very different depending on the type of forcing. Potential intensity cannot be expressed as a function of sea surface temperature alone.

In particular, greenhouse gas-induced warming produces a somewhat smaller response in potential intensity, per unit sea surface temperature change, than does solar forcing, and in some regions, increases in anthropogenic aerosols, which reduce surface insolation, have offset the effect of increasing greenhouse gases on potential intensity (Sobel et al. 2016). As more nations implement controls on aerosol-related pollution, potential intensity should rise with continued greenhouse warming, yielding the possibility of more intense tropical cyclones. How the frequency of such storms changes over time will depend on how the competition between increasing potential intensity and increasing thermodynamic inhibition (15-15) and other factors such as wind shear plays out. As of this writing,

most low-resolution global climate models predict a decline in the frequency of tropical cyclones, but some higher-resolution models and downscaling studies project an increase. The relatively few high-resolution models that have been applied to the climate change problem show an increase in high-intensity events, consistent with theory, and virtually all studies indicate an increase in tropical cyclone precipitation and related flooding as a consequence of the Clausius-Clapeyron increase in boundary layer water vapor, and perhaps other factors such as smaller translation speeds; indeed, observations suggest that translation speeds are decreasing (Kossin 2018). The record-breaking intensities of recent events such as Typhoon Haiyan of 2013, Hurricane Patricia of 2015, and Hurricane Irma of 2017 and the record rainfall of Hurricane Harvey of 2017 are consistent with these inferences and serve to remind us of the serious societal consequences of climate change impacts on tropical cyclones.

Last, changes in tropical cyclone activity may entail important feedbacks on the climate itself. All aggregation of moist convection, whether in the form of non-rotating clusters or tropical cyclones, serves to dry the free troposphere above the boundary layer (Bretherton and Khairoutdinov 2004), and the reduction in the infrared and solar radiative effects of water vapor cools the system, providing a negative feedback on tropical climate change (Khairoutdinov and Emanuel 2010). Observations support this negative feedback (Tobin et al. 2012). The thermal recovery of cold ocean wakes created by cyclone-induced upper-ocean mixing entails large column-integrated heating which, in the long-time mean, must be compensated by ocean export (Emanuel 2001) or released back to the atmosphere in subsequent cool seasons (Pasquero and Emanuel 2008; Jansen et al. 2010). More detailed analyses of cold-wake recovery (Srifer et al. 2008; Mei and Pasquero 2012, 2013; Mei et al. 2013) indicate that the net global ocean warming induced by tropical cyclones is on the order of 0.5 PW, a substantial fraction of the peak ocean heat transport of approximately 2 PW (Ganachaud and Wunsch 2000). Whether this added heat is transported away by ocean currents or transferred back to the atmosphere during subsequent cool seasons, the climate effects of cyclone-induced ocean mixing can be substantial (Korty et al. 2008; Pasquero and Emanuel 2008; Jansen and Ferrari 2009; Fedorov et al. 2010; Srifer et al. 2010; Hart 2011; Scoccimarro et al. 2011). This feedback loop will likely continue to be an exciting and productive avenue of research.

Cyclone-induced upper-ocean mixing also brings nutrients to the surface in tropical regions that are typically nutrient depleted, inducing prominent phytoplankton

blooms (Subrahmanyam et al. 2002; Lin et al. 2003; Venkateswrlu and Rao 2004; Lotliker et al. 2014) and locally increasing primary productivity. The possible effects on global biogeochemical cycles present an interesting topic for further research.

#### *n. Tropical cyclone forecasting*

Research on tropical cyclones not only represents a triumph of scientific discovery but has led, in tandem with technological advances, to vast improvements in forecasts. Eighty years ago, a violent hurricane struck New England with no warning. Today, such a forecast failure is inconceivable, although forecasters may still not anticipate that a tropical storm at sunset may be a category-4 hurricane at sunrise. Forecast improvements together with more effective ways of communicating and preparing for the hazard (including evacuation, if necessary) and of managing the aftermath have greatly reduced mortality and suffering from tropical cyclone disasters. This is particularly important in view of the near tripling of the global population exposed to tropical cyclone hazards since 1970 (Peduzzi et al. 2012).

The history of technical and scientific progress that led to the advanced state of tropical cyclone forecasting that we enjoy today is far too extensive to review here; instead, a brief overview of the topic is provided. As with other aspects of weather forecasting, advances in tropical cyclone prediction have been driven by improved physical understanding, better numerical techniques, rapidly increasing computational power, better and more observations, and improved ways of assimilating them into numerical models. Bauer et al. (2015) provide an excellent recent overview of what they refer to as the “quiet revolution” in numerical weather prediction in general.

Perhaps the first systematic attempt to forecast Atlantic hurricanes was made by Father Benito Viñes and his fellow Jesuit seminarians in Cuba in the late nineteenth century. They had developed a rudimentary network of weather stations around the Caribbean, and observations were telegraphed to Havana’s Belen Observatory. There Viñes’s team attempted to deduce the location of cyclonic centers in what might be regarded as an early example of synoptic map analysis, and by comparing the current analysis with previous maps they deduced the direction and speed of storm translation. Armed with this information and their extensive knowledge of hurricane climatology, they projected the storm’s future track. Today we might call this an example of “nowcasting.” By 1900 the Cuban Jesuits were good enough at this to excite the envy of the then chief of the U.S. Weather Bureau Willis Moore, who issued an edict forbidding the transmission of West Indian storm reports from the Bureau’s Havana office to its New

Orleans office. This resulted in wildly erroneous forecasts of the 1900 Galveston hurricane, thereby contributing to the worst hurricane disaster in U.S. history (Larson 1999).

By the early twentieth century, the weather services of most nations affected by tropical cyclones were doing what they could with available observations to forecast the paths of the storms and warn their citizens accordingly. The advent of radar and systematic aircraft reconnaissance during and after WWII led the U.S. Navy to found a center dedicated to tropical cyclone observations and forecasting; this later became the Joint Typhoon Warning Center (JTWC), which continues to monitor and forecast tropical cyclones today. This was followed in the 1950s by the establishment of the National Hurricane Research Program, a branch of which ultimately became the National Hurricane Center. Today, many nations (e.g., Japan, China, Australia, India, and France) affected by tropical cyclones have forecast centers or units dedicated to forecasting their tracks and intensities as well as associated phenomenon such as storm surges, freshwater flooding, and tornadoes.

From the 1930s onward, radiosonde networks were established to provide upper-air observations in support of weather forecasting. The spatial density of these networks and the frequency with which observations were made were predicated in part on the spatial scales of baroclinic systems as depicted so well by the Norwegian school of synoptic analysis. By the early 1950s, the number and distribution of upper-air observations was sufficient to make possible the first successful numerical weather forecasts (Charney et al. 1950). The upper-air networks were not, however, able to resolve the structure of tropical cyclones whose spatial dimensions are considerably smaller than those of most baroclinic cyclones. Primarily for this reason, skillful numerical prediction of tropical cyclones lagged behind that for extratropical weather by several decades.

By the 1940s, it was widely recognized that tropical cyclones tend to move with a suitably defined vertical average of the large-scale flow in which they are embedded (see section 3j), and forecasters began to use predictions of the evolution of these large-scale flows as an aid to forecasting. Tropical cyclone track prediction gradually became more objective with the introduction, in the 1960s, of statistical track forecast schemes whose predictors included numerical forecasts of the large-scale flow (Miller and Chase 1966). The first operational numerical weather prediction model that showed useful skill in forecasting tropical cyclone tracks was an equivalent barotropic model that was based on the vertically integrated vorticity equation (Sanders and Burpee 1968). This model and statistical models continued to serve through the early

1990s as the primary objective bases for prediction of tropical cyclone tracks.

None of these track-forecasting techniques could get very far without an adequate definition of the initial position and, to a lesser extent, intensity of the storms themselves. At the dawn of statistical and equivalent barotropic track forecasting, definition of the initial tropical cyclone relied almost exclusively on observations from reconnaissance aircraft, and these began to be supplemented by satellite-based observations in the 1970s. [Section 3a](#) describes in greater detail the evolution of the observational technology that is used to monitor tropical cyclones. There is little question that data acquired from aircraft missions improve forecasts ([Franklin and DeMaria 1992](#); [Burpee et al. 1996](#); [Christophersen et al. 2017](#)), and the advent of adjoint-based sensitivity estimates and inexpensive measurements from unmanned platforms offers the promise of further improvements through adaptive sampling.

The first fully baroclinic model used for operational tropical cyclone prediction was originally developed as a research model by Yoshio Kurihara and his associates at NOAA's Geophysical Fluid Dynamics Laboratory (GFDL; e.g., [Kurihara et al. 1998](#); [Bender et al. 2007](#)). By the early 1990s, the track forecast skill of what became known as the GFDL model had overtaken that of the best statistical models and had become a cornerstone of U.S hurricane prediction guidance.

Several particular physical attributes of tropical cyclones make them challenging to simulate numerically. The strongly frontogenetical flow in the eyewall means that the entropy gradients that control the storm's intensity span a few tens of kilometers or less, while the storm itself may be 1000 km in diameter. Thus, proper simulation of tropical cyclones requires both high resolution, at least in the core, and large domains. One strategy, adopted by GFDL and subsequent regional forecast models, is to nest grids of increasingly fine resolution within one another. While this may cause spurious wave reflection and other problems at subdomain boundaries, the strategy has proven generally effective.

The comparatively small scale of tropical cyclones translates to high Rossby numbers in their cores, and therefore reinitialization of such models (or assimilation of sparse data) may cause large imbalances and consequent emission of internal waves, etc. This led to the development of special techniques for handling initial conditions for tropical cyclones (e.g., [Kurihara et al. 1993](#)), although this problem has been greatly ameliorated by contemporary data assimilation techniques (e.g., [Weng and Zhang 2016](#)).

The development of advanced models for tropical cyclone forecasting has been accelerated by programs to encourage both model-related research and the transition of research models to operations, culminating in the community-led and community-supported Hurricane Research and Forecast model ([Atlas et al. 2015](#); [Bernaret et al. 2015](#)). Today's advanced models partially resolve convection, use multiply-nested grids, are used to generate modestly large real-time forecast ensembles, and can use ensemble-based techniques such as ensemble Kalman filters to assimilate detailed observations by, for example, airborne Doppler radar ([Weng and Zhang 2012](#); [Zhang and Weng 2015](#); [Weng and Zhang 2016](#)). Together with advances in observational technology ([section 3a](#)) and improved physics, such advances have led to a satisfying increase in the skill of tropical cyclone track forecasts, as shown in [Fig. 15-21a](#). There are even some indications that we are nearing intrinsic predictability limits of tropical cyclone tracks ([Landsea and Cangialosi 2018](#)).

Forecasting the intensity of tropical cyclones has proven much more difficult. Increased understanding of tropical cyclone physics and empirical relationships between tropical cyclone intensity and environmental predictors have yielded skillful statistical models ([Kaplan and DeMaria 1995](#); [DeMaria and Kaplan 1994, 1997, 1999](#)), and only very recently have deterministic models caught up with the skill of statistical forecasts. [Figure 15-21b](#) shows that there has been appreciable improvement in hurricane intensity forecasts over the relatively short period in which records are available ([DeMaria et al. 2014](#)). Challenges to progress in intensity forecasting include our incomplete understanding of boundary layer and air-sea exchange physics, lack of real-time measurements of ocean mixed layer properties ([Bender and Ginis 2000](#)), upscale error growth from convection ([Tao and Zhang 2015](#)), and incorrect forecasts of environmental conditions ([Emanuel and Zhang 2017](#)). As observations, models, and data assimilation continue to improve, one can hope for continued improvement in intensity forecasts and better quantification of forecast uncertainty through the use of large ensembles.

To date, most metrics of tropical cyclone forecast skill have focused on storm center position and maximum surface wind speed. Yet, in practice, these are far removed from the metrics of most utility to society, which are more concerned with the probabilities of hazardous conditions at fixed points in space. As large forecast ensembles become ever more feasible, such fixed-point probabilistic forecasts can be expected to become more widely used, both as effective ways of communicating risk and as better metrics by which model improvements may be judged.

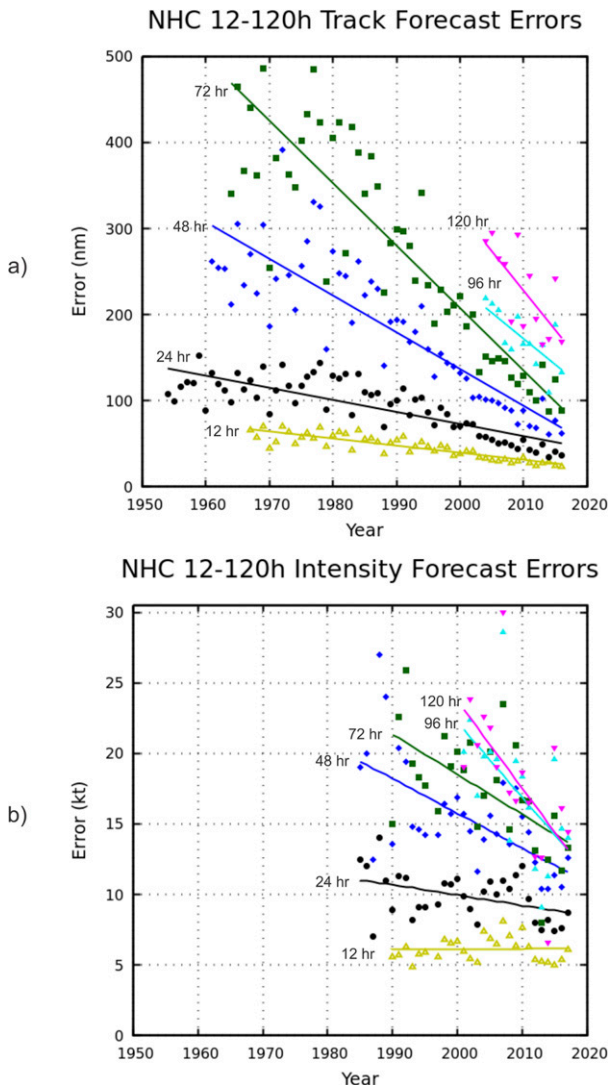


FIG. 15-21. NOAA National Hurricane Center Atlantic forecast errors: (a) track errors in nautical miles, from 1950 to 2017 and (b) intensity errors in knots from 1990 to 2017. Forecast lead times shown by numbered labels; linear regression lines are also shown. (Source: Courtesy of Hugh Willoughby, Florida International University.)

#### 4. Summary

Since the founding of the American Meteorological Society 100 years ago, there has been an explosion of research on tropical cyclones, leading to a far richer understanding of their behavior and physics. Such progress has been so deep and broad as to have been impossible to summarize well in a single chapter. Indeed, we have had to omit several important developments in the field, such as the increasingly fertile research on the socioeconomics of tropical cyclones [see the review by [Camargo and Hsiang \(2016\)](#)], which has delineated the economic and human costs of these

storms and provided guidance on how to cope with them. Nor have we discussed contemporary ideas for modifying tropical cyclones, such as the proposal by [Hoffman \(2002\)](#) to use the model adjoint-based sensitivity to design small perturbations which, when amplified by natural processes, would steer a hurricane harmlessly out to sea.

The field of tropical cyclone research shows every sign of increasing vitality over the coming decades, as many challenges remain. After decades of research, we still lack a full understanding of the physics of the air–sea interface at high wind speeds, a gap that impedes our ability to simulate the structure and intensity of hurricane-strength storms. The development of small-scale roll circulations and strong jets continues to challenge our command of tropical cyclone boundary layer physics, and we still lack a clear understanding of secondary eyewalls and spiral rainbands. Even though it has been clear, for at least one-quarter of a century, that the response of the upper ocean to passing storms has a strong feedback on them, models continue to be developed and run without regard for this connection; so too do some modelers fail to convert dissipated turbulence energy back into heat on the grounds that its inclusion can degrade some measures of model performance. Casting physics aside to achieve short-term gains in forecast model performance is a recipe for long-term failure.

The quasi-balanced interior flow of developed tropical cyclones demands boundary conditions at both the bottom and the top. The bottom condition is supplied by the complex and fascinating physics of the boundary layer, but the top condition received relatively little attention until the recent Office of Naval Research–sponsored Tropical Cyclone Intensity program ([Doyle et al. 2017](#)). Forecasters and researchers alike have long recognized the importance of tropical cyclone outflow, and accelerated research on its feedback to the rest of the system is needed to round out our basic understanding and perhaps to improve model skill.

There has been much progress in understanding the complex interactions between tropical cyclones and their kinematic and thermodynamic environments, but few researchers today would claim that we have an adequate command of such interactions, which can greatly affect intensity and structure. The ordinary spindown of tropical cyclones over land is relatively well understood, but the occasional inland rejuvenation of such storms, even in the absence of significant baroclinic interactions, needs to be better understood and modeled.

Tropical cyclogenesis remains enigmatic despite many field programs, theoretical developments, and the increasing success of forecast models in predicting genesis.

The growing appreciation of the roles of the interplay of terrestrial and solar radiation with the cloud and water vapor fields of nascent systems, their ability to develop spontaneously in cloud-system-resolving models, and the recent recognition that regional activity may not be tied to the character or even the existence of potential triggering disturbances, all offer potentially fruitful avenues of investigation that should be vigorously pursued.

As climate changes in response to anthropogenic and natural influences, it is particularly vital to improve our understanding and ability to project changes in tropical cyclone activity, not just globally but regionally. There is every reason to expect continued progress in quantifying past changes in storm activity through the developing field of paleotempestology, and as computational fire-power increases, global models will finally be able to resolve both the inner cores of developed tropical cyclones and the mesoscale processes involved in genesis, resulting in more consistent and believable projections.

Physical modeling is just beginning to be brought to bear on the problem of tropical cyclone risk, which has heretofore mostly been the province of a small number of catastrophe modeling firms. Globally, tropical cyclones are the leading cause of insured losses and a major source of suffering and mortality among natural hazards, and to make further progress, we now must move away from risk assessment based solely on historical storm statistics. To do so will require academic institutions to demolish some of the stovepipes (e.g., between science and engineering) that currently discourage basic researchers from more fully engaging in the practical problem of risk assessment, and hazard-modeling firms will need to form better and longer-lasting ties with academic researchers.

One hundred years of progress in tropical cyclone research is a tribute to scientific research in general, and to the American Meteorological Society in particular. We have every reason to believe that progress over the next hundred years will be even more remarkable.

*Acknowledgments.* In writing this chapter, I have borrowed lightly from a similar chapter I published in *Hurricane! Coping with Disaster* (Simpson et al. 2003), a tribute to Robert and Joanne Simpson published in 2003 by the American Geophysical Union. I am most grateful for careful and very helpful reviews by Jim Kossin, David Nolan, David Raymond, and Hugh Willoughby.

#### REFERENCES

- Abarca, S. F., and K. L. Corbosiero, 2011: Secondary eyewall formation in WRF simulations of Hurricanes Rita and Katrina (2005). *Geophys. Res. Lett.*, **38**, L07802, <https://doi.org/10.1029/2011GL047015>.
- , and M. T. Montgomery, 2013: Essential dynamics of secondary eyewall formation. *J. Atmos. Sci.*, **70**, 3216–3230, <https://doi.org/10.1175/JAS-D-12-0318.1>.
- Abdullah, A. J., 1966: The spiral bands of a hurricane: A possible dynamic explanation. *J. Atmos. Sci.*, **23**, 367–375, [https://doi.org/10.1175/1520-0469\(1966\)023<0367:TSBOAH>2.0.CO;2](https://doi.org/10.1175/1520-0469(1966)023<0367:TSBOAH>2.0.CO;2).
- Abraham, J., J. W. Strapp, C. Fogarty, and M. Wolde, 2004: Extratropical transition of Hurricane Michael: An aircraft investigation. *Bull. Amer. Meteor. Soc.*, **85**, 1323–1340, <https://doi.org/10.1175/BAMS-85-9-1323>.
- Ackerman, S., and Coauthors, 2019: Satellites see the world's atmosphere. *A Century of Progress in Atmospheric and Related Sciences: Celebrating the American Meteorological Society Centennial*, Meteor. Monogr., No. 59, Amer. Meteor. Soc., <https://doi.org/10.1175/AMSMONOGRAPHS-D-18-0009>.
- Adem, J., 1956: A series solution for the barotropic vorticity equation and its application to the study of atmospheric vortices. *Tellus*, **8**, 364–376, <https://doi.org/10.3402/tellusa.v8i3.9010>.
- Agusti-Panareda, A., C. D. Thorncroft, G. C. Craig, and S. L. Gray, 2004: The extratropical transition of Hurricane Irene (1999): A potential-vorticity perspective. *Quart. J. Roy. Meteor. Soc.*, **130**, 1047–1074, <https://doi.org/10.1256/qj.02.140>.
- Aiyyer, A., and J. Molinari, 2008: MJO and tropical cyclogenesis in the Gulf of Mexico and eastern Pacific: Case study and idealized numerical modeling. *J. Atmos. Sci.*, **65**, 2691–2704, <https://doi.org/10.1175/2007JAS2348.1>.
- Alpert, P., and B. U. Neeman, 1992: Cold small-scale cyclones over the eastern Mediterranean. *Tellus*, **44A**, 173–179, <https://doi.org/10.3402/tellusa.v44i2.14952>.
- Andreas, E. L., 2004: Spray stress revisited. *J. Phys. Oceanogr.*, **34**, 1429–1440, [https://doi.org/10.1175/1520-0485\(2004\)034<1429:SSR>2.0.CO;2](https://doi.org/10.1175/1520-0485(2004)034<1429:SSR>2.0.CO;2).
- , 2010: Spray-mediated enthalpy flux to the atmosphere and salt flux to the ocean in high winds. *J. Phys. Oceanogr.*, **40**, 608–619, <https://doi.org/10.1175/2009JPO4232.1>.
- , and K. Emanuel, 2001: Effects of sea spray on tropical cyclone intensity. *J. Atmos. Sci.*, **58**, 3741–3751, [https://doi.org/10.1175/1520-0469\(2001\)058<3741:ELOSSOT>2.0.CO;2](https://doi.org/10.1175/1520-0469(2001)058<3741:ELOSSOT>2.0.CO;2).
- , and J. Decosmo, 2002: The signature of sea spray in the HEXOS turbulent heat flux data. *Bound.-Layer Meteor.*, **103**, 303–333, <https://doi.org/10.1023/A:1014564513650>.
- , P. O. G. Persson, and J. E. Hare, 2008: A bulk turbulent air–sea flux algorithm for high-wind, spray conditions. *J. Phys. Oceanogr.*, **38**, 1581–1596, <https://doi.org/10.1175/2007JPO3813.1>.
- , L. Mahrt, and D. Vickers, 2015: An improved bulk air–sea surface flux algorithm, including spray-mediated transfer. *Quart. J. Roy. Meteor. Soc.*, **141**, 642–654, <https://doi.org/10.1002/qj.2424>.
- Anthes, R. A., Ed., 1982: *Tropical Cyclones: Their Evolution, Structure and Effects*. Meteor. Monogr., No. 41, Amer. Meteor. Soc., 298 pp.
- Anwender, D., P. A. Harr, and S. C. Jones, 2008: Predictability associated with the downstream impacts of the extratropical transition of tropical cyclones: Case studies. *Mon. Wea. Rev.*, **136**, 3226–3247, <https://doi.org/10.1175/2008MWR2249.1>.
- Atallah, E. H., and L. F. Bosart, 2003: The extratropical transition and precipitation distribution of Hurricane Floyd (1999). *Mon. Wea. Rev.*, **131**, 1063–1081, [https://doi.org/10.1175/1520-0493\(2003\)131<1063:TETAPD>2.0.CO;2](https://doi.org/10.1175/1520-0493(2003)131<1063:TETAPD>2.0.CO;2).
- Atlas, R., V. Tallapragada, and S. Gopalakrishnan, 2015: Advances in tropical cyclone intensity forecasts. *Mar. Technol. Soc. J.*, **49**, 149–160, <https://doi.org/10.4031/MTSJ.49.6.2>.

- Balaguru, K., P. Chang, R. Saravanan, L. R. Leung, Z. Xu, M. Li, and J.-S. Hsieh, 2012: Ocean barrier layers' effect on tropical cyclone intensification. *Proc. Natl. Acad. Sci. USA*, **109**, 14 343–14 347, <https://doi.org/10.1073/pnas.1201364109>.
- Baldini, L. M., and Coauthors, 2016: Persistent northward North Atlantic tropical cyclone track migration over the past five centuries. *Sci. Rep.*, **6**, 37522, <https://doi.org/10.1038/srep37522>.
- Ballenzweig, E. M., 1959: Relation of long-period circulation anomalies to tropical storm formation and motion. *J. Meteor.*, **16**, 121–139, [https://doi.org/10.1175/1520-0469\(1959\)016<0121:ROLPCA>2.0.CO;2](https://doi.org/10.1175/1520-0469(1959)016<0121:ROLPCA>2.0.CO;2).
- Bao, J.-W., C. W. Fairall, S. A. Michelson, and L. Bianco, 2011: Parameterizations of sea-spray impact on the air–sea momentum and heat fluxes. *Mon. Wea. Rev.*, **139**, 3781–3797, <https://doi.org/10.1175/MWR-D-11-00007.1>.
- Barnes, G. M., and K. Sieckman, 1984: The environment of fast- and slow-moving tropical mesoscale convective cloud lines. *Mon. Wea. Rev.*, **112**, 1782–1794, [https://doi.org/10.1175/1520-0493\(1984\)112<1782:TEOFAS>2.0.CO;2](https://doi.org/10.1175/1520-0493(1984)112<1782:TEOFAS>2.0.CO;2).
- , E. J. Zipser, D. Jorgensen, and F. Marks Jr., 1983: Mesoscale and convective structure of a hurricane rainband. *J. Atmos. Sci.*, **40**, 2125–2137, [https://doi.org/10.1175/1520-0469\(1983\)040<2125:MACSOA>2.0.CO;2](https://doi.org/10.1175/1520-0469(1983)040<2125:MACSOA>2.0.CO;2).
- Barrett, B. S., and L. M. Leslie, 2009: Links between tropical cyclone activity and Madden–Julian oscillation phase in the North Atlantic and northeast Pacific basins. *Mon. Wea. Rev.*, **137**, 727–744, <https://doi.org/10.1175/2008MWR2602.1>.
- Bartels, D. L., and R. A. Maddox, 1991: Midlevel cyclonic vortices generated by mesoscale convective systems. *Mon. Wea. Rev.*, **119**, 104–118, [https://doi.org/10.1175/1520-0493\(1991\)119<0104:MCVGBM>2.0.CO;2](https://doi.org/10.1175/1520-0493(1991)119<0104:MCVGBM>2.0.CO;2).
- Bauer, P., A. Thorpe, and G. Brunet, 2015: The quiet revolution of numerical weather prediction. *Nature*, **525**, 47, <https://doi.org/10.1038/nature14956>.
- Bell, G. D., and M. Chelliah, 2006: Leading tropical modes associated with interannual and multidecadal fluctuations in North Atlantic hurricane activity. *J. Climate*, **19**, 590–612, <https://doi.org/10.1175/JCLI3659.1>.
- Bell, M. M., and M. T. Montgomery, 2008: Observed structure, evolution, and potential intensity of category 5 Hurricane Isabel (2003) from 12 to 14 September. *Mon. Wea. Rev.*, **136**, 2023–2046, <https://doi.org/10.1175/2007MWR1858.1>.
- , —, and K. Emanuel, 2012: Air–sea enthalpy and momentum exchange at major hurricane wind speeds observed during CBLAST. *J. Atmos. Sci.*, **69**, 3197–3222, <https://doi.org/10.1175/JAS-D-11-0276.1>.
- Bender, M. A., and I. Ginis, 2000: Real-case simulations of hurricane–ocean interaction using a high-resolution coupled model: Effects on hurricane intensity. *Mon. Wea. Rev.*, **128**, 917–946, [https://doi.org/10.1175/1520-0493\(2000\)128<0917:RCOHO>2.0.CO;2](https://doi.org/10.1175/1520-0493(2000)128<0917:RCOHO>2.0.CO;2).
- , —, and Y. Kurihara, 1993a: Numerical simulations of tropical cyclone–ocean interaction with a high-resolution coupled model. *J. Geophys. Res.*, **98**, 23 245–23 263, <https://doi.org/10.1029/93JD02370>.
- , R. J. Ross, R. E. Tuleya, and Y. Kurihara, 1993b: Improvements in tropical cyclone track and intensity forecasts using the GFDL initialization system. *Mon. Wea. Rev.*, **121**, 2046–2061, [https://doi.org/10.1175/1520-0493\(1993\)121<2046:ITCTA>2.0.CO;2](https://doi.org/10.1175/1520-0493(1993)121<2046:ITCTA>2.0.CO;2).
- , I. Ginis, R. Tuleya, B. Thomas, and T. Marchok, 2007: The operational GFDL coupled hurricane–ocean prediction system and a summary of its performance. *Mon. Wea. Rev.*, **135**, 3965–3989, <https://doi.org/10.1175/2007MWR2032.1>.
- Bennetts, D. A., and B. J. Hoskins, 1979: Conditional symmetric instability—A possible explanation for frontal rainbands. *Quart. J. Roy. Meteor. Soc.*, **105**, 945–962, <https://doi.org/10.1002/qj.49710544615>.
- Bentley, A. M., D. Keyser, and L. F. Bosart, 2016: A dynamically based climatology of subtropical cyclones that undergo tropical transition in the North Atlantic basin. *Mon. Wea. Rev.*, **144**, 2049–2068, <https://doi.org/10.1175/MWR-D-15-0251.1>.
- Bergeron, T., 1954: The problem of tropical hurricanes. *Quart. J. Roy. Meteor. Soc.*, **80**, 131–164, <https://doi.org/10.1002/qj.49708034402>.
- Bernaret, L., and Coauthors, 2015: Community support and transition of research to operations for the Hurricane Research and Forecast (HWRF) Model. *Bull. Amer. Meteor. Soc.*, **96**, 953–960, <https://doi.org/10.1175/BAMS-D-13-00093.1>.
- Bessafi, M., and M. C. Wheeler, 2006: Modulation of south Indian Ocean tropical cyclones by the Madden–Julian oscillation and convectively coupled equatorial waves. *Mon. Wea. Rev.*, **134**, 638–656, <https://doi.org/10.1175/MWR3087.1>.
- Betts, A. K., 1986: A new convective adjustment scheme. Part I: Observational and theoretical basis. *Quart. J. Roy. Meteor. Soc.*, **112**, 677–691, <https://doi.org/10.1002/qj.49711247307>.
- Beven, J., Jr., and Coauthors, 2008: Atlantic hurricane season of 2005. *Mon. Wea. Rev.*, **136**, 1109–1173, <https://doi.org/10.1175/2007MWR2074.1>.
- Bishop, C. H., and A. J. Thorpe, 1994: Frontal wave stability during moist deformation frontogenesis. Part I: Linear wave dynamics. *J. Atmos. Sci.*, **51**, 852–873, [https://doi.org/10.1175/1520-0469\(1994\)051<0852:FWSMDM>2.0.CO;2](https://doi.org/10.1175/1520-0469(1994)051<0852:FWSMDM>2.0.CO;2).
- Bister, M., and K. A. Emanuel, 1997: The genesis of Hurricane Guillermo: TEXMEX analyses and a modeling study. *Mon. Wea. Rev.*, **125**, 2662–2682, [https://doi.org/10.1175/1520-0493\(1997\)125<2662:TGOHGT>2.0.CO;2](https://doi.org/10.1175/1520-0493(1997)125<2662:TGOHGT>2.0.CO;2).
- , and —, 1998: Dissipative heating and hurricane intensity. *Meteor. Atmos. Phys.*, **65**, 233–240, <https://doi.org/10.1007/BF01030791>.
- , and —, 2002: Low frequency variability of tropical cyclone potential intensity: 1. Interannual to interdecadal variability. *J. Geophys. Res.*, **107**, 4801, <https://doi.org/10.1029/2001JD000776>.
- Bjerknes, J., 1938: Saturated-adiabatic ascent of air through dry-adiabatically descending environment. *Quart. J. Roy. Meteor. Soc.*, **64**, 325–330.
- Black, M. L., J. F. Gamache, F. D. Marks Jr., C. E. Samsury, and H. E. Willoughby, 2002: Eastern Pacific Hurricanes Jimena of 1991 and Olivia of 1994: The effects of vertical shear on structure and intensity. *Mon. Wea. Rev.*, **130**, 2291–2312, [https://doi.org/10.1175/1520-0493\(2002\)130<2291:EPHJOA>2.0.CO;2](https://doi.org/10.1175/1520-0493(2002)130<2291:EPHJOA>2.0.CO;2).
- Black, P. G., and R. A. Anthes, 1971: On the asymmetric structure of the tropical cyclone outflow layer. *J. Atmos. Sci.*, **28**, 1348–1366, [https://doi.org/10.1175/1520-0469\(1971\)028<1348:OTASOT>2.0.CO;2](https://doi.org/10.1175/1520-0469(1971)028<1348:OTASOT>2.0.CO;2).
- , and F. Marks, 1991: The structure of an eyewall meso-vortex in Hurricane Hugo. Preprints, *19th Conf. on Hurricanes and Tropical Meteorology*, Miami, FL, Amer. Meteor. Soc., 579–582.
- , and Coauthors, 2007: Air–sea exchange in hurricanes: Synthesis of observations from the coupled boundary layer air–sea

- transfer experiment. *Bull. Amer. Meteor. Soc.*, **88**, 357–374, <https://doi.org/10.1175/BAMS-88-3-357>.
- Blair, A., I. Ginis, T. Hara, and E. Ulhorn, 2017: Impact of Langmuir turbulence on upper ocean response to Hurricane Edouard: Model and observations. *J. Geophys. Res. Oceans*, **122**, 9712–9724, <https://doi.org/10.1002/2017JC012956>.
- Blender, R., K. Fraedrich, and F. Lunkeit, 1997: Identification of cyclone-track regimes in the North Atlantic. *Quart. J. Roy. Meteor. Soc.*, **123**, 727–741, <https://doi.org/10.1002/qj.49712353910>.
- Bluestein, H. B., 1976: Synoptic-scale deformation and tropical cloud bands. Ph.D. thesis, Dept. of Meteorology, Massachusetts Institute of Technology, 208 pp.
- , and M. H. Jain, 1985: Formation of mesoscale lines of precipitation: Severe squall lines in Oklahoma during the spring. *J. Atmos. Sci.*, **42**, 1711–1732, [https://doi.org/10.1175/1520-0469\(1985\)042<1711:FOMLOP>2.0.CO;2](https://doi.org/10.1175/1520-0469(1985)042<1711:FOMLOP>2.0.CO;2).
- , and F. D. Marks Jr., 1987: On the structure of the eyewall of Hurricane Diana (1984): Comparison of radar and visual characteristics. *Mon. Wea. Rev.*, **115**, 2542–2552, [https://doi.org/10.1175/1520-0493\(1987\)115<2542:OTSOTE>2.0.CO;2](https://doi.org/10.1175/1520-0493(1987)115<2542:OTSOTE>2.0.CO;2).
- Bode, L., and R. K. Smith, 1975: A parameterization of the boundary layer of a tropical cyclone. *Bound.-Layer Meteor.*, **8**, 3–19, <https://doi.org/10.1007/BF02579390>.
- Bogomolov, V. A., 1977: Dynamics of vorticity on a sphere. *Fluid Dyn.*, **12**, 863–870, <https://doi.org/10.1007/BF01090320>.
- Boldt, K. V., P. Lane, J. D. Woodruff, and J. P. Donnelly, 2010: Calibrating a sedimentary record of overwash from southeastern New England using modeled historic hurricane surges. *Mar. Geol.*, **275**, 127–139, <https://doi.org/10.1016/j.margeo.2010.05.002>.
- Booth, B. B. B., N. J. Dunstone, P. R. Halloran, T. Andrews, and N. Bellouin, 2012: Aerosols implicated as a prime driver of twentieth-century North Atlantic climate variability. *Nature*, **484**, 228–232, <https://doi.org/10.1038/nature10946>.
- Bosart, L. F., and F. Sanders, 1981: The Johnstown flood of July 1977: A long-lived convective system. *J. Atmos. Sci.*, **38**, 1616–1642, [https://doi.org/10.1175/1520-0469\(1981\)038<1616:TJFOJA>2.0.CO;2](https://doi.org/10.1175/1520-0469(1981)038<1616:TJFOJA>2.0.CO;2).
- , and J. A. Bartlo, 1991: Tropical storm formation in a baroclinic environment. *Mon. Wea. Rev.*, **119**, 1979–2013, [https://doi.org/10.1175/1520-0493\(1991\)119<1979:TSFIAB>2.0.CO;2](https://doi.org/10.1175/1520-0493(1991)119<1979:TSFIAB>2.0.CO;2).
- , W. E. Bracken, J. Molinari, C. S. Velden, and P. G. Black, 2000: Environmental influences on the rapid intensification of Hurricane Opal (1995) over the Gulf of Mexico. *Mon. Wea. Rev.*, **128**, 322–352, [https://doi.org/10.1175/1520-0493\(2000\)128<0322:EIOTRI>2.0.CO;2](https://doi.org/10.1175/1520-0493(2000)128<0322:EIOTRI>2.0.CO;2).
- Bove, M. C., J. B. Elsner, C. W. Landsea, X. Niu, and J. J. O'Brien, 1998: Effect of El Niño on U.S. landfalling hurricanes, revisited. *Bull. Amer. Meteor. Soc.*, **79**, 2477–2482, [https://doi.org/10.1175/1520-0477\(1998\)079<2477:EOENOO>2.0.CO;2](https://doi.org/10.1175/1520-0477(1998)079<2477:EOENOO>2.0.CO;2).
- Bowman, K. P., and M. D. Fowler, 2015: The diurnal cycle of precipitation in tropical cyclones. *J. Climate*, **28**, 5325–5334, <https://doi.org/10.1175/JCLI-D-14-00804.1>.
- Brandon, C. M., J. D. Woodruff, D. P. Lane, and J. P. Donnelly, 2013: Tropical cyclone wind speed constraints from resultant storm surge deposition: A 2500 year reconstruction of hurricane activity from St. Marks, FL. *Geochem. Geophys. Geosyst.*, **14**, 2993–3008, <https://doi.org/10.1002/ggge.20217>.
- , —, J. P. Donnelly, and R. M. Sullivan, 2014: How unique was Hurricane Sandy? Sedimentary reconstructions of extreme flooding from New York harbor. *Sci. Rep.*, **4**, 7366, <https://doi.org/10.1038/srep07366>.
- Braun, S. A., and W.-K. Tao, 2000: Sensitivity of high-resolution simulations of Hurricane Bob (1991) to planetary boundary layer parameterizations. *Mon. Wea. Rev.*, **128**, 3941–3961, [https://doi.org/10.1175/1520-0493\(2000\)129<3941:SOHRSO>2.0.CO;2](https://doi.org/10.1175/1520-0493(2000)129<3941:SOHRSO>2.0.CO;2).
- , and L. Wu, 2007: A numerical study of Hurricane Erin (2001). Part II: Shear and the organization of eyewall vertical motion. *Mon. Wea. Rev.*, **135**, 1179–1194, <https://doi.org/10.1175/MWR3336.1>.
- , and Coauthors, 2013: NASA's Genesis and Rapid Intensification Processes (GRIP) field experiment. *Bull. Amer. Meteor. Soc.*, **94**, 345–363, <https://doi.org/10.1175/BAMS-D-11-00232.1>.
- Bravo, J., J. P. Donnelly, and J. Dowling, 1997: Sedimentary evidence for the 1938 hurricane in southern New England. Preprints, 22nd Conf. on Hurricanes and Tropical Meteorology, Ft. Collins, CO, Amer. Meteor. Soc., 395–396.
- Bretherton, C. S., and M. F. Khairoutdinov, 2004: Convective self-aggregation in large cloud-resolving model simulations of radiative convective equilibrium. 26th Conf. on Hurricanes and Tropical Meteorology, Miami Beach, FL, Amer. Meteor. Soc., 12B.4, [https://ams.confex.com/ams/26HURR/techprogram/paper\\_76059.htm](https://ams.confex.com/ams/26HURR/techprogram/paper_76059.htm).
- , P. N. Blossey, and M. F. Khairoutdinov, 2005: An energy-balance analysis of deep convective self-aggregation above uniform SST. *J. Atmos. Sci.*, **62**, 4273–4292, <https://doi.org/10.1175/JAS3614.1>.
- Bruyère, C. L., G. J. Holland, and E. Towler, 2012: Investigating the use of a genesis potential index for tropical cyclones in the North Atlantic basin. *J. Climate*, **25**, 8611–8626, <https://doi.org/10.1175/JCLI-D-11-00619.1>.
- Bryan, G. H., 2012: Effects of surface exchange coefficients and turbulence length scales on the intensity and structure of numerically simulated hurricanes. *Mon. Wea. Rev.*, **140**, 1125–1143, <https://doi.org/10.1175/MWR-D-11-00231.1>.
- , and R. Rotunno, 2009a: Evaluation of an analytical model for the maximum intensity of tropical cyclones. *J. Atmos. Sci.*, **66**, 3042–3060, <https://doi.org/10.1175/2009JAS3038.1>.
- , and —, 2009b: The maximum intensity of tropical cyclones in axisymmetric numerical model simulations. *Mon. Wea. Rev.*, **137**, 1770–1789, <https://doi.org/10.1175/2008MWR2709.1>.
- Burpee, R. W., J. L. Franklin, S. J. Lord, R. E. Tuleya, and S. D. Aberson, 1996: The impact of omega dropwindsondes on operational hurricane track forecast models. *Bull. Amer. Meteor. Soc.*, **77**, 925–933, [https://doi.org/10.1175/1520-0477\(1996\)077<0925:TIOODO>2.0.CO;2](https://doi.org/10.1175/1520-0477(1996)077<0925:TIOODO>2.0.CO;2).
- Businger, S., 1985: The synoptic climatology of polar low outbreaks. *Tellus*, **37A**, 419–432, <https://doi.org/10.3402/tellusa.v37i5.11686>.
- Byers, H. R., 1944: *General Meteorology*. McGraw-Hill, 645 pp.
- , and R. R. Braham Jr., 1948: Thunderstorm structure and circulation. *J. Meteor.*, **5**, 71–86, [https://doi.org/10.1175/1520-0469\(1948\)005<0071:TSAC>2.0.CO;2](https://doi.org/10.1175/1520-0469(1948)005<0071:TSAC>2.0.CO;2).
- Camargo, S. J., 2013: Global and regional aspects of tropical cyclone activity in the CMIP5 models. *J. Climate*, **26**, 9880–9902, <https://doi.org/10.1175/JCLI-D-12-00549.1>.
- , and A. H. Sobel, 2005: Western North Pacific tropical cyclone intensity and ENSO. *J. Climate*, **18**, 2996–3006, <https://doi.org/10.1175/JCLI3457.1>.
- , and S. M. Hsiang, 2016: Tropical cyclones: From the influence of climate to their socioeconomic impacts. *Extreme Events: Observations, Modeling, and Economics*, M. Chavez, M. Ghil, and J. Urrutia-Fucugauchi, Eds., Wiley-Blackwell, 438 pp.

- , K. A. Emanuel, and A. H. Sobel, 2007a: Use of a genesis potential index to diagnose ENSO effects on tropical cyclone genesis. *J. Climate*, **20**, 4819–4834, <https://doi.org/10.1175/JCLI4282.1>.
- , A. W. Robertson, S. J. Gaffney, P. Smyth, and M. Ghil, 2007b: Cluster analysis of typhoon tracks. Part I: General properties. *J. Climate*, **20**, 3635–3653, <https://doi.org/10.1175/JCLI4188.1>.
- , —, —, —, and —, 2007c: Cluster analysis of typhoon tracks. Part II: Large-scale circulation and ENSO. *J. Climate*, **20**, 3654–3676, <https://doi.org/10.1175/JCLI4203.1>.
- , A. H. Sobel, A. G. Barnston, and K. A. Emanuel, 2007d: Tropical cyclone genesis potential index in climate models. *Tellus*, **59A**, 428–443, <https://doi.org/10.1111/j.1600-0870.2007.00238.x>.
- , M. C. Wheeler, and A. H. Sobel, 2009: Diagnosis of the MJO modulation of tropical cyclogenesis using an empirical index. *J. Atmos. Sci.*, **66**, 3061–3074, <https://doi.org/10.1175/2009JAS3101.1>.
- Caron, L. P., M. Boudreault, and C. L. Bruyere, 2015: Changes in large-scale controls of Atlantic tropical cyclone activity with the phases of the Atlantic multidecadal oscillation. *Climate Dyn.*, **44**, 1801–1821, <https://doi.org/10.1007/s00382-014-2186-5>.
- Cavicchia, L., H. von Storch, and S. Gualdi, 2014: A long-term climatology of medicanes. *Climate Dyn.*, **43**, 1183–1195, <https://doi.org/10.1007/s00382-013-1893-7>.
- Challa, M., and R. L. Pfeffer, 1980: Effects of eddy fluxes of angular momentum on model hurricane development. *J. Atmos. Sci.*, **37**, 1603–1618, [https://doi.org/10.1175/1520-0469\(1980\)037<1603:EOEFOA>2.0.CO;2](https://doi.org/10.1175/1520-0469(1980)037<1603:EOEFOA>2.0.CO;2).
- Chan, J. C. L., 1985: Tropical cyclone activity in the northwest Pacific in relation to the El Niño/Southern Oscillation phenomenon. *Mon. Wea. Rev.*, **113**, 599–606, [https://doi.org/10.1175/1520-0493\(1985\)113<0599:TCAITN>2.0.CO;2](https://doi.org/10.1175/1520-0493(1985)113<0599:TCAITN>2.0.CO;2).
- , 2000: Tropical cyclone activity over the western North Pacific associated with El Niño and La Niña events. *J. Climate*, **13**, 2960–2972, [https://doi.org/10.1175/1520-0442\(2000\)013<2960:TCAOTW>2.0.CO;2](https://doi.org/10.1175/1520-0442(2000)013<2960:TCAOTW>2.0.CO;2).
- , 2005a: Interannual and interdecadal variations of tropical cyclone activity over the western North Pacific. *Meteor. Atmos. Phys.*, **89**, 143–152, <https://doi.org/10.1007/s00703-005-0126-y>.
- , 2005b: The physics of tropical cyclone motion. *Annu. Rev. Fluid Mech.*, **37**, 99–128, <https://doi.org/10.1146/annurev.fluid.37.061903.175702>.
- , and R. T. Williams, 1987: Analytical and numerical studies of the beta-effect in tropical cyclone motion. Part I: Zero mean flow. *J. Atmos. Sci.*, **44**, 1257–1265, [https://doi.org/10.1175/1520-0469\(1987\)044<1257:AANSOT>2.0.CO;2](https://doi.org/10.1175/1520-0469(1987)044<1257:AANSOT>2.0.CO;2).
- Chand, S. S., and K. J. E. Walsh, 2010: The influence of the Madden–Julian oscillation on tropical cyclone activity in the Fiji region. *J. Climate*, **23**, 868–886, <https://doi.org/10.1175/2009JCLI3316.1>.
- , and —, 2011: Influence of ENSO on tropical cyclone intensity in the Fiji region. *J. Climate*, **24**, 4096–4108, <https://doi.org/10.1175/2011JCLI4178.1>.
- Chane Ming, F., C. Ibrahim, C. Barthe, S. Jolivet, P. Keckhut, Y. A. Liou, and Y. Kuleshov, 2014: Observation and a numerical study of gravity waves during tropical cyclone Ivan (2008). *Atmos. Chem. Phys.*, **14**, 641–658, <https://doi.org/10.5194/acp-14-641-2014>.
- Chang, S. W., and R. A. Anthes, 1979: Mutual response of the tropical cyclone and the ocean. *J. Phys. Oceanogr.*, **9**, 128–135, [https://doi.org/10.1175/1520-0485\(1979\)009<0128:TMROTT>2.0.CO;2](https://doi.org/10.1175/1520-0485(1979)009<0128:TMROTT>2.0.CO;2).
- Charabi, Y., Ed., 2010: *Indian Ocean Tropical Cyclones and Climate Change*. Springer, 373 pp.
- Charney, J. G., and M. E. Stern, 1962: On the stability of internal baroclinic jets in a rotating atmosphere. *J. Atmos. Sci.*, **19**, 159–172, [https://doi.org/10.1175/1520-0469\(1962\)019<0159:OTSOIB>2.0.CO;2](https://doi.org/10.1175/1520-0469(1962)019<0159:OTSOIB>2.0.CO;2).
- , and A. Eliassen, 1964: On the growth of the hurricane depression. *J. Atmos. Sci.*, **21**, 68–75, [https://doi.org/10.1175/1520-0469\(1964\)021<0068:OTGOTH>2.0.CO;2](https://doi.org/10.1175/1520-0469(1964)021<0068:OTGOTH>2.0.CO;2).
- , R. Fjørtoft, and J. Von Neumann, 1950: Numerical integration of the barotropic vorticity equation. *Tellus*, **2**, 237–254, <https://doi.org/10.3402/tellusa.v2i4.8607>.
- Chavas, D. R., and K. A. Emanuel, 2010: A QuickSCAT climatology of tropical cyclone size. *Geophys. Res. Lett.*, **37**, L18816, <https://doi.org/10.1029/2010GL044558>.
- , and —, 2014: Equilibrium tropical cyclone size in an idealized state of axisymmetric radiative–convective equilibrium. *J. Atmos. Sci.*, **71**, 1663–1680, <https://doi.org/10.1175/JAS-D-13-0155.1>.
- Chen, G., 2011: A comparison of precipitation distribution of two landfalling tropical cyclones during the extratropical transition. *Adv. Atmos. Sci.*, **28**, 1390, <https://doi.org/10.1007/s00376-011-0148-y>.
- Chen, S. S., and W. M. Frank, 1993: A numerical study of the genesis of extratropical convective mesovortices. Part I: Evolution and dynamics. *J. Atmos. Sci.*, **50**, 2401–2426, [https://doi.org/10.1175/1520-0469\(1993\)050<2401:ANSOTG>2.0.CO;2](https://doi.org/10.1175/1520-0469(1993)050<2401:ANSOTG>2.0.CO;2).
- Chen, T.-C., S.-Y. Wang, M.-C. Yen, and A. J. Clark, 2009: Impact of the intraseasonal variability of the western North Pacific large-scale circulation on tropical cyclone tracks. *Wea. Forecasting*, **24**, 646–666, <https://doi.org/10.1175/2008WAF2222186.1>.
- Chen, Y., G. Brunet, and M. K. Yau, 2003: Spiral bands in a simulated hurricane. Part II: Wave activity diagnostics. *J. Atmos. Sci.*, **60**, 1239–1256, [https://doi.org/10.1175/1520-0469\(2003\)60<1239:SBIASH>2.0.CO;2](https://doi.org/10.1175/1520-0469(2003)60<1239:SBIASH>2.0.CO;2).
- Cheung, K. F., L. Tang, J. P. Donnelly, E. M. Scileppi, K.-B. Liu, X.-Z. Mao, S. H. Houston, and R. J. Murnane, 2007: Numerical modeling and field evidence of coastal overwash in southern New England from Hurricane Bob and implications for paleotempestology. *J. Geophys. Res.*, **112**, F03024, <https://doi.org/10.1029/2006JF000612>.
- Christophersen, H., A. Aksoy, J. Dunion, and K. Sellwood, 2017: The impact of NASA Global Hawk unmanned aircraft dropwindsonde observations on tropical cyclone track, intensity, and structure: Case studies. *Mon. Wea. Rev.*, **145**, 1817–1830, <https://doi.org/10.1175/MWR-D-16-0332.1>.
- Chu, P.-S., and J. Wang, 1997: Tropical cyclone occurrences in the vicinity of Hawaii: Are the differences between El Niño and non-El Niño years significant? *J. Climate*, **10**, 2683–2689, [https://doi.org/10.1175/1520-0442\(1997\)010<2683:TCOITV>2.0.CO;2](https://doi.org/10.1175/1520-0442(1997)010<2683:TCOITV>2.0.CO;2).
- Chylek, P., and G. Lesins, 2008: Multidecadal variability of Atlantic hurricane activity: 1851–2007. *J. Geophys. Res.*, **113**, D22106, <https://doi.org/10.1029/2008JD010036>.
- Cione, J. J., E. A. Kalina, E. W. Uhlhorn, A. M. Farber, and B. Damiano, 2016: Coyote unmanned aircraft system observations in Hurricane Edouard (2014). *Earth Space Sci.*, **3**, 370–380, <https://doi.org/10.1002/2016EA000187>.
- Claud, C., B. Alhammoud, B. M. Funatsu, and J.-P. Chaboureaud, 2010: Mediterranean hurricanes: Large-scale environment and convective and precipitating areas from satellite microwave observations. *Nat. Hazards Earth Syst. Sci.*, **10**, 2199–2213, <https://doi.org/10.5194/nhess-10-2199-2010>.

- Cochran, D. R., 1976: Unusual tropical development from a mid-Pacific cold low. *Mon. Wea. Rev.*, **104**, 804–808, [https://doi.org/10.1175/1520-0493\(1976\)104<0804:UTDFAM>2.0.CO;2](https://doi.org/10.1175/1520-0493(1976)104<0804:UTDFAM>2.0.CO;2).
- Colle, B. A., 2003: Numerical simulations of the extratropical transition of Floyd (1999): Structural evolution and responsible mechanisms for the heavy rainfall over the northeast United States. *Mon. Wea. Rev.*, **131**, 2905–2926, [https://doi.org/10.1175/1520-0493\(2003\)131<2905:NSOTET>2.0.CO;2](https://doi.org/10.1175/1520-0493(2003)131<2905:NSOTET>2.0.CO;2).
- Collins, J. M., and K. Walsh, Eds., 2017: *Hurricanes and Climate Change*. Vol. 3, Springer, 255 pp.
- Corbosiero, K. L., and J. Molinari, 2002: The effects of vertical wind shear on the distribution of convection in tropical cyclones. *Mon. Wea. Rev.*, **130**, 2110–2123, [https://doi.org/10.1175/1520-0493\(2002\)130<2110:TEOVWS>2.0.CO;2](https://doi.org/10.1175/1520-0493(2002)130<2110:TEOVWS>2.0.CO;2).
- , and —, 2003: The relationship between storm motion, vertical wind shear, and convective asymmetries in tropical cyclones. *J. Atmos. Sci.*, **60**, 366–376, [https://doi.org/10.1175/1520-0469\(2003\)060<0366:TRBSMV>2.0.CO;2](https://doi.org/10.1175/1520-0469(2003)060<0366:TRBSMV>2.0.CO;2).
- , —, A. R. Aiyyer, and M. L. Black, 2006: The structure and evolution of Hurricane Elena (1985). Part II: Convective asymmetries and evidence for vortex Rossby waves. *Mon. Wea. Rev.*, **134**, 3073–3091, <https://doi.org/10.1175/MWR3250.1>.
- Craig, G. C., and S. L. Gray, 1996: CISK or WISHE as the mechanism for tropical cyclone intensification. *J. Atmos. Sci.*, **53**, 3528–3540, [https://doi.org/10.1175/1520-0469\(1996\)053<3528:COWATM>2.0.CO;2](https://doi.org/10.1175/1520-0469(1996)053<3528:COWATM>2.0.CO;2).
- Daingerfield, L. H., 1921: Kona storms. *Mon. Wea. Rev.*, **49**, 327–329, [https://doi.org/10.1175/1520-0493\(1921\)49<327:KS>2.0.CO;2](https://doi.org/10.1175/1520-0493(1921)49<327:KS>2.0.CO;2).
- D'Asaro, E. A., 2003: The ocean boundary layer below Hurricane Dennis. *J. Phys. Oceanogr.*, **33**, 561–579, [https://doi.org/10.1175/1520-0485\(2003\)033<0561:TOBLBH>2.0.CO;2](https://doi.org/10.1175/1520-0485(2003)033<0561:TOBLBH>2.0.CO;2).
- Davidson, N. E., G. J. Holland, J. L. McBride, and T. D. Keenan, 1990: On the formation of AMEX tropical cyclones Irma and Jason. *Mon. Wea. Rev.*, **118**, 1981–2000, [https://doi.org/10.1175/1520-0493\(1990\)118<1981:OTFOAT>2.0.CO;2](https://doi.org/10.1175/1520-0493(1990)118<1981:OTFOAT>2.0.CO;2).
- Davis, C. A., and L. F. Bosart, 2003: Baroclinically induced tropical cyclogenesis. *Mon. Wea. Rev.*, **131**, 2730–2747, [https://doi.org/10.1175/1520-0493\(2003\)131<2730:BITC>2.0.CO;2](https://doi.org/10.1175/1520-0493(2003)131<2730:BITC>2.0.CO;2).
- , and L. Bosart, 2004: The TT problem. *Bull. Amer. Meteor. Soc.*, **85**, 1657–1662, <https://journals.ametsoc.org/doi/pdf/10.1175/BAMS-85-11-1657>.
- , S. C. Jones, and M. Riemer, 2008: Hurricane vortex dynamics during Atlantic extratropical transition. *J. Atmos. Sci.*, **65**, 714–736, <https://doi.org/10.1175/2007JAS2488.1>.
- Dean, L., K. Emanuel, and D. R. Chavas, 2009: On the size distribution of Atlantic tropical cyclones. *Geophys. Res. Lett.*, **36**, L14803, <https://doi.org/10.1029/2009GL039051>.
- DeCosmo, J., K. B. Katsaros, S. D. Smith, R. J. Anderson, W. A. Oost, K. Bumke, and H. Chadwick, 1996: Air-sea exchange of water vapor and sensible heat: The Humidity Exchange Over the Sea (HEXOS) results. *J. Geophys. Res.*, **101**, 12 001–12 016, <https://doi.org/10.1029/95JC03796>.
- Dee, D. P., and Coauthors, 2011: The ERA-interim reanalysis: Configuration and performance of the data assimilation system. *Quart. J. Roy. Meteor. Soc.*, **137**, 553–597, <https://doi.org/10.1002/qj.828>.
- Delworth, T. L., and M. E. Mann, 2000: Observed and simulated multidecadal variability in the Northern Hemisphere. *Climate Dyn.*, **16**, 661–676, <https://doi.org/10.1007/s003820000075>.
- DeMaria, M., 1996: The effect of vertical shear on tropical cyclone intensity change. *J. Atmos. Sci.*, **53**, 2076–2088, [https://doi.org/10.1175/1520-0469\(1996\)053<2076:TEOVSO>2.0.CO;2](https://doi.org/10.1175/1520-0469(1996)053<2076:TEOVSO>2.0.CO;2).
- , and J. Kaplan, 1994: A Statistical Hurricane Intensity Prediction Scheme (SHIPS) for the Atlantic basin. *Wea. Forecasting*, **9**, 209–220, [https://doi.org/10.1175/1520-0434\(1994\)009<0209:ASHIPS>2.0.CO;2](https://doi.org/10.1175/1520-0434(1994)009<0209:ASHIPS>2.0.CO;2).
- , and —, 1997: An operational evaluation of a Statistical Hurricane Intensity Prediction Scheme (SHIPS). Preprints, *22nd Conf. on Hurricanes and Tropical Meteorology*, Ft. Collins, CO, Amer. Meteor. Soc., 280–281.
- , and —, 1999: An updated Statistical Hurricane Intensity Prediction Scheme (SHIPS) for the Atlantic and eastern North Pacific basins. *Wea. Forecasting*, **14**, 326–337, [https://doi.org/10.1175/1520-0434\(1999\)014<0326:AUSHIP>2.0.CO;2](https://doi.org/10.1175/1520-0434(1999)014<0326:AUSHIP>2.0.CO;2).
- , —, and J.-J. Baik, 1993: Upper-level eddy angular momentum fluxes and tropical cyclone intensity change. *J. Atmos. Sci.*, **50**, 1133–1147, [https://doi.org/10.1175/1520-0469\(1993\)050<1133:ULEAMF>2.0.CO;2](https://doi.org/10.1175/1520-0469(1993)050<1133:ULEAMF>2.0.CO;2).
- , J. A. Knaff, and B. H. Connell, 2001: A tropical cyclone genesis parameter for the tropical Atlantic. *Wea. Forecasting*, **16**, 219–233, [https://doi.org/10.1175/1520-0434\(2001\)016<0219:ATCGPF>2.0.CO;2](https://doi.org/10.1175/1520-0434(2001)016<0219:ATCGPF>2.0.CO;2).
- , C. R. Sampson, J. A. Knaff, and K. D. Musgrave, 2014: Is tropical cyclone intensity guidance improving? *Bull. Amer. Meteor. Soc.*, **95**, 387–398, <https://doi.org/10.1175/BAMS-D-12-00240.1>.
- Demuth, J. L., M. DeMaria, and J. A. Knaff, 2006: Improvement of Advanced Microwave Sounding Unit tropical cyclone intensity and size estimation algorithms. *J. Appl. Meteor. Climatol.*, **45**, 1573–1581, <https://doi.org/10.1175/JAM2429.1>.
- Dengler, K., and M. J. Reeder, 1997: The effects of convection and baroclinicity on the motion of tropical-cyclone-like vortices. *Quart. J. Roy. Meteor. Soc.*, **123**, 699–725, <https://doi.org/10.1002/qj.49712353909>.
- Diaz, H. F., and R. S. Pulwarty, Eds., 2012: *Climate and Socio-economic Impacts*. Springer, 292 pp.
- Didlake, A. C., Jr., and R. A. Houze Jr., 2013: Dynamics of the stratiform sector of a tropical cyclone rainband. *J. Atmos. Sci.*, **70**, 1891–1911, <https://doi.org/10.1175/JAS-D-12-0245.1>.
- Diercks, J. W., and R. A. Anthes, 1976: Diagnostic studies of spiral rainbands in a nonlinear hurricane model. *J. Atmos. Sci.*, **33**, 959–975, [https://doi.org/10.1175/1520-0469\(1976\)033<0959:DSOSRI>2.0.CO;2](https://doi.org/10.1175/1520-0469(1976)033<0959:DSOSRI>2.0.CO;2).
- Donelan, M. A., B. K. Haus, N. Reul, W. J. Plant, M. Stiassnie, H. C. Graber, O. B. Brown, and E. S. Saltzman, 2004: On the limiting aerodynamic roughness of the ocean in very strong winds. *Geophys. Res. Lett.*, **31**, L18306, <https://doi.org/10.1029/2004GL019460>.
- Donnelly, J. P., 2005: Evidence of past intense tropical cyclones from backbarrier salt pond sediments: A case study from Isla de Culebrita, Puerto Rico, USA. *J. Coastal Res.*, **S142**, 201–210, <https://www.jstor.org/stable/25736985>.
- , and J. D. Woodruff, 2007: Intense hurricane activity over the past 5,000 years controlled by El Niño and the west African monsoon. *Nature*, **447**, 465–468, <https://doi.org/10.1038/nature05834>.
- , and Coauthors, 2001a: 700 yr sedimentary record of intense hurricane landfalls in southern New England. *Geol. Soc. Amer. Bull.*, **113**, 714–727, [https://doi.org/10.1130/0016-7606\(2001\)113<0714:YSROIH>2.0.CO;2](https://doi.org/10.1130/0016-7606(2001)113<0714:YSROIH>2.0.CO;2).
- , S. Roll, M. Wengren, J. Butler, R. Lederer, and T. Webb III, 2001b: Sedimentary evidence of intense hurricane strikes from

- New Jersey. *Geology*, **29**, 615–618, [https://doi.org/10.1130/0091-7613\(2001\)029<0615:SEOIHS>2.0.CO;2](https://doi.org/10.1130/0091-7613(2001)029<0615:SEOIHS>2.0.CO;2).
- , J. Butler, S. Roll, M. Wengren, and T. Webb, 2004: A back-barrier overwash record of intense storms from Brigantine, New Jersey. *Mar. Geol.*, **210**, 107–121, <https://doi.org/10.1016/j.margeo.2004.05.005>.
- Doyle, J. D., and Coauthors, 2017: A view of tropical cyclones from above: The tropical cyclone intensity experiment. *Bull. Amer. Meteor. Soc.*, **98**, 2113–2134, <https://doi.org/10.1175/BAMS-D-16-0055.1>.
- Duke, W. L., 1985a: Hummocky cross-stratification, tropical hurricanes, and intense winter storms. *Sedimentology*, **32**, 167–194, <https://doi.org/10.1111/j.1365-3091.1985.tb00502.x>.
- , 1985b: The paleogeography of Paleozoic and Mesozoic storm depositional systems: A discussion. *J. Geol.*, **93**, 88–90, <https://doi.org/10.1086/628923>.
- , R. W. C. Arnott, and R. J. Cheel, 1991: Shelf sandstones and hummocky cross-stratification: New insights on a stormy debate. *Geology*, **19**, 625–628, [https://doi.org/10.1130/0091-7613\(1991\)019<0625:SSAHCS>2.3.CO;2](https://doi.org/10.1130/0091-7613(1991)019<0625:SSAHCS>2.3.CO;2).
- Junion, J. P., C. D. Thorncroft, and C. S. Velden, 2014: The tropical cyclone diurnal cycle of mature hurricanes. *Mon. Wea. Rev.*, **142**, 3900–3919, <https://doi.org/10.1175/MWR-D-13-00191.1>.
- Dunkerton, T. J., M. T. Montgomery, and Z. Wang, 2009: Tropical cyclogenesis in a tropical wave critical layer: Easterly waves. *Atmos. Chem. Phys.*, **9**, 5587–5646, <https://doi.org/10.5194/acp-9-5587-2009>.
- Dunn, G. E., 1940: Cyclogenesis in the tropical Atlantic. *Bull. Amer. Meteor. Soc.*, **21**, 215–229, <https://doi.org/10.1175/1520-0477-21.6.215>.
- , 1951: Tropical cyclones. *Compendium of Meteorology*, T. F. Malone, Ed., Amer. Meteor. Soc., 887–901.
- Dunstone, N. J., D. M. Smith, B. B. Booth, L. Hermanson, and R. Eade, 2013: Anthropogenic aerosol forcing of Atlantic tropical storms. *Nat. Geosci.*, **6**, 534–539, <https://doi.org/10.1038/ngeo1854>.
- Dvorak, V. F., 1975: Tropical cyclone intensity analysis and forecasting from satellite imagery. *Mon. Wea. Rev.*, **103**, 420–430, [https://doi.org/10.1175/1520-0493\(1975\)103<0420:TCIAAF>2.0.CO;2](https://doi.org/10.1175/1520-0493(1975)103<0420:TCIAAF>2.0.CO;2).
- , 1984: Tropical cyclone intensity analysis using satellite data. NOAA Tech. Rep. NESDIS 11, 45 pp., [http://satepsanone.nesdis.noaa.gov/pub/Publications/Tropical/Dvorak\\_1984.pdf](http://satepsanone.nesdis.noaa.gov/pub/Publications/Tropical/Dvorak_1984.pdf).
- Ellis, R., and S. Businger, 2010: Helical circulations in the typhoon boundary layer. *J. Geophys. Res.*, **115**, D06205, <https://doi.org/10.1029/2009JD011819>.
- Elsberry, R. L., and P. A. Harr, 2008: Tropical cyclone structure (TCS08) field experiment: Science basis, observational platforms, and strategy. *Asia-Pac. J. Atmos. Sci.*, **44**, 209–231.
- , T. S. Fraim, and R. N. Trapnell, 1976: A mixed layer model of the oceanic thermal response to hurricanes. *J. Geophys. Res.*, **81**, 1153–1162, <https://doi.org/10.1029/JC081i006p01153>.
- , B. C. Diehl, J. C.-L. Chan, P. A. Harr, G. J. Holland, M. Lander, T. Neta, and D. Thom, 1990: ONR tropical cyclone motion research initiative: Field experiment summary. Tech. Rep. NPS-MR-91-001, 107 pp., <http://www.dtic.mil/dtic/tr/fulltext/u2/a231152.pdf>.
- Elsner, J. B., and T. H. Jagger, Eds., 2009: *Hurricanes and Climate Change*. Vol. 1, Springer, 419 pp.
- , B. H. Bossak, and X. F. Niu, 2001: Secular changes to the ENSO-U.S. Hurricane relationship. *Geophys. Res. Lett.*, **28**, 4123–4126, <https://doi.org/10.1029/2001GL013669>.
- , R. E. Hodges, J. C. Malmstadt, and K. N. Scheitlin, Eds., 2014: *Hurricanes and Climate Change*. Vol. 2, Springer, 255 pp.
- Emanuel, K. A., 1986: An air-sea interaction theory for tropical cyclones. Part I: Steady state maintenance. *J. Atmos. Sci.*, **43**, 585–605, [https://doi.org/10.1175/1520-0469\(1986\)043<0585:AASITF>2.0.CO;2](https://doi.org/10.1175/1520-0469(1986)043<0585:AASITF>2.0.CO;2).
- , 1987: The dependence of hurricane intensity on climate. *Nature*, **326**, 483–485, <https://doi.org/10.1038/326483a0>.
- , 1988: The maximum intensity of hurricanes. *J. Atmos. Sci.*, **45**, 1143–1155, [https://doi.org/10.1175/1520-0469\(1988\)045<1143:TMIOH>2.0.CO;2](https://doi.org/10.1175/1520-0469(1988)045<1143:TMIOH>2.0.CO;2).
- , 1989: The finite-amplitude nature of tropical cyclogenesis. *J. Atmos. Sci.*, **46**, 3431–3456, [https://doi.org/10.1175/1520-0469\(1989\)046<3431:TFANOT>2.0.CO;2](https://doi.org/10.1175/1520-0469(1989)046<3431:TFANOT>2.0.CO;2).
- , 1995: The behavior of a simple hurricane model using a convective scheme based on subcloud-layer entropy equilibrium. *J. Atmos. Sci.*, **52**, 3960–3968, [https://doi.org/10.1175/1520-0469\(1995\)052<3960:TBOASH>2.0.CO;2](https://doi.org/10.1175/1520-0469(1995)052<3960:TBOASH>2.0.CO;2).
- , 1997: Some aspects of hurricane inner-core dynamics and energetics. *J. Atmos. Sci.*, **54**, 1014–1026, [https://doi.org/10.1175/1520-0469\(1997\)054<1014:SAOHC>2.0.CO;2](https://doi.org/10.1175/1520-0469(1997)054<1014:SAOHC>2.0.CO;2).
- , 2000: A statistical analysis of tropical cyclone intensity. *Mon. Wea. Rev.*, **128**, 1139–1152, [https://doi.org/10.1175/1520-0493\(2000\)128<1139:ASAOTC>2.0.CO;2](https://doi.org/10.1175/1520-0493(2000)128<1139:ASAOTC>2.0.CO;2).
- , 2001: The contribution of tropical cyclones to the oceans’ meridional heat transport. *J. Geophys. Res.*, **106**, 14 771–14 781, <https://doi.org/10.1029/2000JD900641>.
- , 2003: A similarity hypothesis for air-sea exchange at extreme wind speeds. *J. Atmos. Sci.*, **60**, 1420–1428, [https://doi.org/10.1175/1520-0469\(2003\)060<1420:ASHFAE>2.0.CO;2](https://doi.org/10.1175/1520-0469(2003)060<1420:ASHFAE>2.0.CO;2).
- , 2004: Tropical cyclone energetics and structure. *Atmospheric Turbulence and Mesoscale Meteorology*, E. Federovich, R. Rotunno, and B. Stevens, Eds., Cambridge University Press, 165–192, <https://doi.org/10.1017/CBO9780511735035.010>.
- , 2005a: *Divine Wind: The History and Science of Hurricanes*. Oxford University Press, 304 pp.
- , 2005b: Genesis and maintenance of “Mediterranean hurricanes.” *Adv. Geosci.*, **2**, 217–220, <https://doi.org/10.5194/adgeo-2-217-2005>.
- , 2010: Tropical cyclone activity downscaled from NOAA-CIRES reanalysis, 1908–1958. *J. Adv. Model. Earth Syst.*, **2**, <https://doi.org/10.3894/JAMES.2010.2.1>.
- , 2012: Self-stratification of tropical cyclone outflow: Part II: Implications for storm intensification. *J. Atmos. Sci.*, **69**, 988–996, <https://doi.org/10.1175/JAS-D-11-0177.1>; Corrigendum, **75**, 2155–2156, <https://doi.org/10.1175/JAS-D-18-0047.1>.
- , 2013: Downscaling CMIP5 climate models shows increased tropical cyclone activity over the 21st century. *Proc. Natl. Acad. Sci. USA*, **110**, 12 219–12 224, <https://doi.org/10.1073/pnas.1301293110>.
- , and R. Rotunno, 1989: Polar lows as arctic hurricanes. *Tellus*, **41A**, 1–17, <https://doi.org/10.1111/j.1600-0870.1989.tb00362.x>.
- , and D. Nolan, 2004: Tropical cyclone activity and global climate. *26th Conf. on Hurricanes and Tropical Meteorology*, Miami Beach, FL, Amer. Meteor. Soc., 10A.2, [https://ams.confex.com/ams/26HURR/techprogram/paper\\_75463.htm](https://ams.confex.com/ams/26HURR/techprogram/paper_75463.htm).
- , and R. Rotunno, 2011: Self-stratification of tropical cyclone outflow. Part I: Implications for storm structure. *J. Atmos. Sci.*, **68**, 2236–2249, <https://doi.org/10.1175/JAS-D-10-05024.1>.
- , and A. H. Sobel, 2013: Response of tropical sea surface temperature, precipitation, and tropical cyclone-related variables to changes in global and local forcing. *J. Adv. Model. Earth Syst.*, **5**, 447–458, <https://doi.org/10.1002/jame.20032>.

- , and F. Zhang, 2017: The role of inner-core moisture in tropical cyclone predictability and practical forecast skill. *J. Atmos. Sci.*, **74**, 2315–2324, <https://doi.org/10.1175/JAS-D-17-0008.1>.
- , R. Rotunno, and D. K. Lilly, 1985: An air-sea interaction theory for tropical cyclones. Preprints, *16th Conf. on Hurricanes and Tropical Meteorology*, Houston, TX, Amer. Meteor. Soc., 27–28.
- , K. Speer, R. Rotunno, R. Srivastava, and M. Molina, 1995: Hypercanes: A possible link in global extinction scenarios. *J. Geophys. Res.*, **100**, 13 755–13 765, <https://doi.org/10.1029/95JD01368>.
- , J. Callaghan, and P. Otto, 2008a: A hypothesis for the redevelopment of warm-core cyclones over northern Australia. *Mon. Wea. Rev.*, **136**, 3863–3872, <https://doi.org/10.1175/2008MWR2409.1>.
- , R. Sundararajan, and J. Williams, 2008b: Hurricanes and global warming: Results from downscaling IPCC AR4 simulations. *Bull. Amer. Meteor. Soc.*, **89**, 347–367, <https://doi.org/10.1175/BAMS-89-3-347>.
- Enfield, D. B., and L. Cid-Serrano, 2010: Secular and multidecadal warmings in the North Atlantic and their relationships with major hurricane activity. *Int. J. Climatol.*, **30**, 174–184, <https://doi.org/10.1002/joc.1881>.
- Ernst, J. A., and M. Matson, 1983: A Mediterranean tropical storm? *Weather*, **38**, 332–337, <https://doi.org/10.1002/j.1477-8696.1983.tb04818.x>.
- Espy, J. P., 1841: *The Philosophy of Storms*. Little and Brown, 552 pp.
- Evans, C., and R. E. Hart, 2008: Analysis of the wind field evolution associated with the extratropical transition of Bonnie (1998). *Mon. Wea. Rev.*, **136**, 2047–2065, <https://doi.org/10.1175/2007MWR2051.1>.
- , R. S. Schumacher, and T. J. Galarneau Jr., 2011: Sensitivity in the overland reintensification of tropical cyclone Erin (2007) to near-surface soil moisture characteristics. *Mon. Wea. Rev.*, **139**, 3848–3870, <https://doi.org/10.1175/2011MWR3593.1>.
- , and Coauthors, 2017: The extratropical transition of tropical cyclones. Part I: Cyclone evolution and direct impacts. *Mon. Wea. Rev.*, **145**, 4317–4344, <https://doi.org/10.1175/MWR-D-17-0027.1>.
- Evans, J. L., and R. J. Allan, 1992: El Niño/Southern Oscillation modification to the structure of the monsoon and tropical cyclone activity in the Australasian region. *Int. J. Climatol.*, **12**, 611–623, <https://doi.org/10.1002/joc.3370120607>.
- , and R. E. Hart, 2003: Objective indicators of the life cycle evolution of extratropical transition for Atlantic tropical cyclones. *Mon. Wea. Rev.*, **131**, 909–925, [https://doi.org/10.1175/1520-0493\(2003\)131<0909:OIOTLC>2.0.CO;2](https://doi.org/10.1175/1520-0493(2003)131<0909:OIOTLC>2.0.CO;2).
- , and M. P. Guishard, 2009: Atlantic subtropical storms. Part I: Diagnostic criteria and composite analysis. *Mon. Wea. Rev.*, **137**, 2065–2080, <https://doi.org/10.1175/2009MWR2468.1>.
- , and A. Braun, 2012: A climatology of subtropical cyclones in the South Atlantic. *J. Climate*, **25**, 7328–7340, <https://doi.org/10.1175/JCLI-D-11-00212.1>.
- Fairall, C. W., E. F. Bradley, J. E. Hare, A. A. Grachev, and J. B. Edson, 2003: Bulk parameterization of air–sea fluxes: Updates and verification for the COARE algorithm. *J. Climate*, **16**, 571–591, [https://doi.org/10.1175/1520-0442\(2003\)016<0571:BPOASF>2.0.CO;2](https://doi.org/10.1175/1520-0442(2003)016<0571:BPOASF>2.0.CO;2).
- Faller, A., 1963: An experimental study of the instability of the laminar Ekman boundary layer. *J. Fluid Mech.*, **15**, 560–576, <https://doi.org/10.1017/S0022112063000458>.
- Fan, D. D., and K. B. Liu, 2008: Perspectives on the linkage between typhoon activity and global warming from recent research advances in paleotempestology. *Chin. Sci. Bull.*, **53**, 2907–2922, <https://doi.org/10.1007/s11434-008-0341-2>.
- Federov, K. N., A. Varfolomeev, A. I. Ginzburg, A. G. Zatsepin, A. Krasnopevtsev, A. G. Ostrovsky, and V. E. Sklyarov, 1979: Thermal reaction of the ocean on the passage of Hurricane Ella. *Okeanologiya*, **19**, 992–1001.
- Fedorov, A. V., C. M. Brierley, and K. Emanuel, 2010: Tropical cyclones and permanent El Niño in the early Pliocene epoch. *Nature*, **463**, 1066–1070, <https://doi.org/10.1038/nature08831>.
- Ferreira, R. N., and W. H. Schubert, 1999: The role of tropical cyclones in the formation of tropical upper-tropospheric troughs. *J. Atmos. Sci.*, **56**, 2891–2907, [https://doi.org/10.1175/1520-0469\(1999\)056<2891:TROTCI>2.0.CO;2](https://doi.org/10.1175/1520-0469(1999)056<2891:TROTCI>2.0.CO;2).
- , —, and J. J. Hack, 1996: Dynamical aspects of twin tropical cyclones associated with the Madden-Julian oscillation. *J. Atmos. Sci.*, **53**, 929–945, [https://doi.org/10.1175/1520-0469\(1996\)053<0929:DAOTTC>2.0.CO;2](https://doi.org/10.1175/1520-0469(1996)053<0929:DAOTTC>2.0.CO;2).
- Firing, E., and R. C. Beardsley, 1976: The behavior of a barotropic eddy on a  $\beta$ -plane. *J. Phys. Oceanogr.*, **6**, 57–65, [https://doi.org/10.1175/1520-0485\(1976\)006<0057:TBOABE>2.0.CO;2](https://doi.org/10.1175/1520-0485(1976)006<0057:TBOABE>2.0.CO;2).
- Fita, L., R. Romero, A. Luque, K. Emanuel, and C. Ramis, 2007: Analysis of the environments of seven Mediterranean tropical-like storms using an axisymmetric, nonhydrostatic, cloud resolving model. *Nat. Hazards Earth Syst. Sci.*, **7**, 41–56, <https://doi.org/10.5194/nhess-7-41-2007>.
- Fjørtoft, R., 1950: Application of integral theorems in deriving criteria of stability for laminar flows and for the baroclinic circular vortex. *Geophys. Publ.*, **17**, 1–52.
- Flaounas, E., S. Raveh-Rubin, H. Wernli, P. Drobinski, and S. Bastin, 2015: The dynamical structure of intense Mediterranean cyclones. *Climate Dyn.*, **44**, 2411–2427, <https://doi.org/10.1007/s00382-014-2330-2>.
- Flatau, M., W. H. Schubert, and D. E. Stevens, 1994: The role of baroclinic processes in tropical cyclone motion: The influence of vertical tilt. *J. Atmos. Sci.*, **51**, 2589–2601, [https://doi.org/10.1175/1520-0469\(1994\)051<2589:TROBPI>2.0.CO;2](https://doi.org/10.1175/1520-0469(1994)051<2589:TROBPI>2.0.CO;2).
- Ford, R., 1994: The instability of an axisymmetric vortex with monotonic potential vorticity in rotating shallow water. *J. Fluid Mech.*, **280**, 303–334, <https://doi.org/10.1017/S0022112094002946>.
- Forsyth, A. J., J. Nott, and M. D. Bateman, 2010: Beach ridge plain evidence of a variable late-Holocene tropical cyclone climate, north Queensland, Australia. *Palaeogeogr. Palaeoclimatol. Palaeoecol.*, **297**, 707–716, <https://doi.org/10.1016/j.palaeo.2010.09.024>.
- Fortner, L. E., 1958: Typhoon Sarah, 1956. *Bull. Amer. Meteor. Soc.*, **39**, 633–639, <https://doi.org/10.1175/1520-0477-39.12.633>.
- Foster, R. C., 2009: Boundary-layer similarity under an axisymmetric, gradient wind vortex. *Bound.-Layer Meteor.*, **131**, 321–344, <https://doi.org/10.1007/s10546-009-9379-1>.
- Frank, W. M., 1977a: Structure and energetics of the tropical cyclone: I. Storm structure. *Mon. Wea. Rev.*, **105**, 1119–1135, [https://doi.org/10.1175/1520-0493\(1977\)105<1119:TSAEOT>2.0.CO;2](https://doi.org/10.1175/1520-0493(1977)105<1119:TSAEOT>2.0.CO;2).
- , 1977b: Structure and energetics of the tropical cyclone: II. Dynamics and energetics. *Mon. Wea. Rev.*, **105**, 1136–1150, [https://doi.org/10.1175/1520-0493\(1977\)105<1136:TSAEOT>2.0.CO;2](https://doi.org/10.1175/1520-0493(1977)105<1136:TSAEOT>2.0.CO;2).
- , and E. A. Ritchie, 1999: Effects of environmental flow upon tropical cyclone structure. *Mon. Wea. Rev.*, **127**, 2044–2061, [https://doi.org/10.1175/1520-0493\(1999\)127<2044:EOEFUT>2.0.CO;2](https://doi.org/10.1175/1520-0493(1999)127<2044:EOEFUT>2.0.CO;2).

- , and —, 2001: Effects of vertical wind shear on the intensity and structure of numerically simulated hurricanes. *Mon. Wea. Rev.*, **129**, 2249–2269, [https://doi.org/10.1175/1520-0493\(2001\)129<2249:EOVWSO>2.0.CO;2](https://doi.org/10.1175/1520-0493(2001)129<2249:EOVWSO>2.0.CO;2).
- Franklin, J. L., and M. DeMaria, 1992: The impact of omega dropwindsonde observations on barotropic hurricane track forecasts. *Mon. Wea. Rev.*, **120**, 381–391, [https://doi.org/10.1175/1520-0493\(1992\)120<0381:TIOODO>2.0.CO;2](https://doi.org/10.1175/1520-0493(1992)120<0381:TIOODO>2.0.CO;2).
- , S. J. Lord, and F. D. Marks Jr., 1988: Dropwindsonde and radar observations of the eye of Hurricane Gloria (1985). *Mon. Wea. Rev.*, **116**, 1237–1244, [https://doi.org/10.1175/1520-0493\(1988\)116<1237:DAROOT>2.0.CO;2](https://doi.org/10.1175/1520-0493(1988)116<1237:DAROOT>2.0.CO;2).
- Frappier, A. B., T. R. Knutson, K.-B. Liu, and K. Emanuel, 2007a: Perspective: Coordinating paleoclimate research on tropical cyclones with hurricane-climate theory and modelling. *Tellus*, **59A**, 529–527, <https://doi.org/10.1111/j.1600-0870.2007.00250.x>.
- , D. Sahagian, S. J. Carpenter, L. A. Gonzalez, and B. R. Frappier, 2007b: Stalagmite stable isotope record of recent tropical cyclone events. *Geology*, **35**, 111–114, <https://doi.org/10.1130/G23145A.1>.
- , J. Pyburn, A. D. Pinkey-Drobnis, X. F. Wang, D. R. Corbett, and B. H. Dahlin, 2014: Two millennia of tropical cyclone-induced mud layers in a northern Yucatan stalagmite: Multiple overlapping climatic hazards during the Maya terminal classic “megadroughts.” *Geophys. Res. Lett.*, **41**, 5148–5157, <https://doi.org/10.1002/2014GL059882>.
- Frisius, T., and D. Schönemann, 2012: An extended model for the potential intensity of tropical cyclones. *J. Atmos. Sci.*, **69**, 641–661, <https://doi.org/10.1175/JAS-D-11-064.1>.
- Fu, L.-L., T. Lee, W. T. Liu, and R. Kwok, 2019: 50 years of satellite remote sensing of the ocean. *A Century of Progress in Atmospheric and Related Sciences: Celebrating the American Meteorological Society Centennial*, Meteor. Monogr., No. 59, Amer. Meteor. Soc., <https://doi.org/10.1175/AMSMONOGRAPHS-D-18-0010>.
- Fujiwhara, S., 1921: The natural tendency towards symmetry of motion and its application as a principle in meteorology. *Quart. J. Roy. Meteor. Soc.*, **47**, 287–292, <https://doi.org/10.1002/qj.49704720010>.
- Fung, I. Y.-S., 1977: The organization of spiral rainbands in a hurricane. Sc.D. thesis, Dept. of Meteorology, Massachusetts Institute of Technology, 140 pp., <http://hdl.handle.net/1721.1/16337>.
- Galarneau, T. J., Jr., C. A. Davis, and M. A. Shapiro, 2013: Intensification of Hurricane Sandy (2012) through extratropical warm core seclusion. *Mon. Wea. Rev.*, **141**, 4296–4321, <https://doi.org/10.1175/MWR-D-13-00181.1>.
- Gall, J. S., W. M. Frank, and Y. Kwon, 2008: Effects of sea spray on tropical cyclones simulated under idealized conditions. *Mon. Wea. Rev.*, **136**, 1686–1705, <https://doi.org/10.1175/2007MWR2183.1>.
- Gall, R., J. Tuttle, and P. Hildebrand, 1998: Small-scale spiral bands observed in Hurricanes Andrew, Hugo, and Erin. *Mon. Wea. Rev.*, **126**, 1749–1766, [https://doi.org/10.1175/1520-0493\(1998\)126<1749:SSBOI>2.0.CO;2](https://doi.org/10.1175/1520-0493(1998)126<1749:SSBOI>2.0.CO;2).
- Gamache, J. F., R. A. Houze Jr., and F. D. Marks Jr., 1993: Dual aircraft investigation of the inner core of Hurricane Norbert. Part III: Water budget. *J. Atmos. Sci.*, **50**, 3221–3243, [https://doi.org/10.1175/1520-0469\(1993\)050<3221:DAIOTI>2.0.CO;2](https://doi.org/10.1175/1520-0469(1993)050<3221:DAIOTI>2.0.CO;2).
- Ganachaud, A., and C. Wunsch, 2000: Improved estimates of global ocean circulation, heat transport and mixing from hydrological data. *Nature*, **408**, 453–457, <https://doi.org/10.1038/35044048>.
- Getzelman, S. D., and J. R. Lawrence, 2000: Stable isotope ratios and the extratropical transition of tropical cyclones. Preprints, *24th Conf. on Hurricanes and Tropical Meteorology*, Ft. Lauderdale, FL, Amer. Meteor. Soc., 288–289.
- Geisler, J. E., 1970: Linear theory of the response of a two layer ocean to a moving hurricane. *Geophys. Fluid Dyn.*, **1**, 249–272, <https://doi.org/10.1080/03091927009365774>.
- Gentry, R. C., 1970: Hurricane Debbie modification experiments, August 1969. *Science*, **168**, 473–475, <https://doi.org/10.1126/science.168.3930.473>.
- , 1983: Genesis of tornadoes associated with hurricanes. *Mon. Wea. Rev.*, **111**, 1793–1805, [https://doi.org/10.1175/1520-0493\(1983\)111<1793:GOTAWH>2.0.CO;2](https://doi.org/10.1175/1520-0493(1983)111<1793:GOTAWH>2.0.CO;2).
- Gifford, J., 2004: *Hurricane Hazel: Canada's Storm of the Century*. Dundurn, 104 pp.
- Ginis, I., 2002: Tropical cyclone–ocean interactions. *Atmosphere–Ocean Interactions*, Vol. 1, Advances in Fluid Mechanics Series, No. 33, WIT Press, 83–114.
- , K. Z. Dikinov, and A. P. Khain, 1989: Three dimensional coupled model of the atmosphere and the ocean in the zone of typhoon. *Dokl. Akad. Sci.*, **307**, 333–337.
- Goldenberg, S. B., and L. J. Shapiro, 1996: Physical mechanisms for the association of El Niño and West African rainfall with Atlantic major hurricane activity. *J. Climate*, **9**, 1169–1187, [https://doi.org/10.1175/1520-0442\(1996\)009<1169:PMFTAO>2.0.CO;2](https://doi.org/10.1175/1520-0442(1996)009<1169:PMFTAO>2.0.CO;2).
- , C. W. Landsea, A. M. Mestas-Núñez, and W. M. Gray, 2001: The recent increase in Atlantic hurricane activity: Causes and implications. *Science*, **293**, 474–479, <https://doi.org/10.1126/science.1060040>.
- Gray, S. L., 1994: Theory of mature tropical cyclones: A comparison between Kleinschmidt (1951) and Emanuel (1986). Joint Centre for Mesoscale Meteorology Internal Rep. 40, 50 pp.
- Gray, S. T., L. J. Graumlich, J. L. Betancourt, and G. T. Pedersen, 2004: A tree-ring based reconstruction of the Atlantic multi-decadal oscillation since 1567 A.D. *Geophys. Res. Lett.*, **31**, L12205, <https://doi.org/10.1029/2004GL019932>.
- Gray, W. M., 1968: Global view of the origin of tropical disturbances and storms. *Mon. Wea. Rev.*, **96**, 669–700, [https://doi.org/10.1175/1520-0493\(1968\)096<0669:GVOTOO>2.0.CO;2](https://doi.org/10.1175/1520-0493(1968)096<0669:GVOTOO>2.0.CO;2).
- , 1975: Tropical cyclone genesis. Colorado State University Dept. of Atmospheric Science Paper 234, 121 pp., [https://mountainscholar.org/bitstream/handle/10217/247/0234\\_Bluebook.pdf?sequence=1&isAllowed=y](https://mountainscholar.org/bitstream/handle/10217/247/0234_Bluebook.pdf?sequence=1&isAllowed=y).
- , 1979: Hurricanes: Their formation, structure, and likely role in the tropical circulation. *Meteorology over the Tropical Oceans*, D. B. Shaw, Ed., Royal Meteorological Society, 155–218.
- , 1984: Atlantic seasonal hurricane frequency. Part I: El Niño and 30 mb quasi-biennial oscillation influences. *Mon. Wea. Rev.*, **112**, 1649–1668, [https://doi.org/10.1175/1520-0493\(1984\)112<1649:ASHFPI>2.0.CO;2](https://doi.org/10.1175/1520-0493(1984)112<1649:ASHFPI>2.0.CO;2).
- , and D. J. Shea, 1973: The hurricane’s inner core region. II. Thermal stability and dynamic characteristics. *J. Atmos. Sci.*, **30**, 1565–1576, [https://doi.org/10.1175/1520-0469\(1973\)030<1565:THICRI>2.0.CO;2](https://doi.org/10.1175/1520-0469(1973)030<1565:THICRI>2.0.CO;2).
- , J. D. Sheaffer, and C. W. Landsea, 1997: Climate trends associated with multidecadal variability of Atlantic hurricane activity. *Hurricanes: Climate and Socioeconomic Impacts*, H. F. Diaz, and R. S. Pulwarty, Eds., Springer, 15–53.
- Green, B. W., and F. Zhang, 2013: Impacts of air–sea flux parameterizations on the intensity and structure of tropical cyclones. *Mon. Wea. Rev.*, **141**, 2308–2324, <https://doi.org/10.1175/MWR-D-12-00274.1>.

- Guadalupe, L. E. R., 2014: *Father Benito Viñes: The 19th-Century Life and Contributions of a Cuban Hurricane Observer and Scientist*. Amer. Meteor. Soc., 184 pp.
- Guinn, T. A., and W. H. Schubert, 1993: Hurricane spiral bands. *J. Atmos. Sci.*, **50**, 3380–3403, [https://doi.org/10.1175/1520-0469\(1993\)050<3380:HSB>2.0.CO;2](https://doi.org/10.1175/1520-0469(1993)050<3380:HSB>2.0.CO;2).
- Guishard, M. P., E. A. Nelson, J. L. Evans, R. E. Hart, and D. G. O'Connell, 2007: Bermuda subtropical storms. *Meteor. Atmos. Phys.*, **97**, 239–253, <https://doi.org/10.1007/s00703-006-0255-y>.
- , J. L. Evans, and R. E. Hart, 2009: Atlantic subtropical storms. Part II: Climatology. *J. Climate*, **22**, 3574–3594, <https://doi.org/10.1175/2008JCL12346.1>.
- Haig, J., J. Nott, and G. J. Reichert, 2014: Australian tropical cyclone activity lower than at any time over the past 550–1,500 years. *Nature*, **505**, 667–671, <https://doi.org/10.1038/nature12882>.
- Hakim, G. J., 2011: The mean state of axisymmetric hurricanes in statistical equilibrium. *J. Atmos. Sci.*, **68**, 1364–1376, <https://doi.org/10.1175/2010JAS3644.1>.
- Hall, J. D., A. J. Matthews, and D. J. Karoly, 2001: The modulation of tropical cyclone activity in the Australian region by the Madden–Julian oscillation. *Mon. Wea. Rev.*, **129**, 2970–2982, [https://doi.org/10.1175/1520-0493\(2001\)129<2970:TMOTCA>2.0.CO;2](https://doi.org/10.1175/1520-0493(2001)129<2970:TMOTCA>2.0.CO;2).
- Halverson, J. B., and T. Rabenhorst, 2013: Hurricane Sandy: The science and impacts of a superstorm. *Weatherwise*, **66**, 14–23, <https://doi.org/10.1080/00431672.2013.762838>.
- , J. Simpson, G. Heymsfield, H. Pierce, T. Hock, and L. Ritchie, 2006: Warm core structure of Hurricane Erin diagnosed from high altitude dropsondes during CAMEX-4. *J. Atmos. Sci.*, **63**, 309–324, <https://doi.org/10.1175/JAS3596.1>.
- Halverson, J., and Coauthors, 2007: NASA's Tropical Cloud Systems and Processes experiment: Investigating tropical cyclogenesis and hurricane intensity change. *Bull. Amer. Meteor. Soc.*, **88**, 867–882, <https://doi.org/10.1175/BAMS-88-6-867>.
- Hanley, D., J. Molinari, and D. Keyser, 2001: A composite study of the interactions between tropical cyclones and upper-tropospheric troughs. *Mon. Wea. Rev.*, **129**, 2570–2584, [https://doi.org/10.1175/1520-0493\(2001\)129<2570:ACSOTI>2.0.CO;2](https://doi.org/10.1175/1520-0493(2001)129<2570:ACSOTI>2.0.CO;2).
- Harr, P. A., 2012: The extratropical transition of tropical cyclones: Structural characteristics, downstream impacts, and forecast challenges. *Global Perspectives on Tropical Cyclones: From Science to Mitigation*, J. C. L. Chan and J. D. Kepert, Eds., World Scientific, 149–174, [https://doi.org/10.1142/9789814293488\\_0005](https://doi.org/10.1142/9789814293488_0005).
- , and R. L. Elsberry, 2000: Extratropical transition of tropical cyclones over the western North Pacific. Part I: Evolution of structural characteristics during the transition process. *Mon. Wea. Rev.*, **128**, 2613–2633, [https://doi.org/10.1175/1520-0493\(2000\)128<2613:ETOTCO>2.0.CO;2](https://doi.org/10.1175/1520-0493(2000)128<2613:ETOTCO>2.0.CO;2).
- , and J. M. Dea, 2009: Downstream development associated with the extratropical transition of tropical cyclones over the western North Pacific. *Mon. Wea. Rev.*, **137**, 1295–1319, <https://doi.org/10.1175/2008MWR2558.1>.
- , R. L. Elsberry, and T. F. Hogan, 2000: Extratropical transition of tropical cyclones over the western North Pacific. Part II: The impact of midlatitude circulation characteristics. *Mon. Wea. Rev.*, **128**, 2634–2653, [https://doi.org/10.1175/1520-0493\(2000\)128<2634:ETOTCO>2.0.CO;2](https://doi.org/10.1175/1520-0493(2000)128<2634:ETOTCO>2.0.CO;2).
- , D. Anwender, and S. C. Jones, 2008: Predictability associated with the downstream impacts of the extratropical transition of tropical cyclones: Methodology and a case study of Typhoon Nabi (2005). *Mon. Wea. Rev.*, **136**, 3205–3225, <https://doi.org/10.1175/2008MWR2248.1>.
- Harrold, T. W., and K. A. Browning, 1969: The polar low as a baroclinic disturbance. *Quart. J. Roy. Meteor. Soc.*, **95**, 710–723, <https://doi.org/10.1002/qj.49709540605>.
- Hart, R. E., 2003: A cyclone phase space derived from thermal wind and thermal asymmetry. *Mon. Wea. Rev.*, **131**, 585–616, [https://doi.org/10.1175/1520-0493\(2003\)131<0585:ACPSDF>2.0.CO;2](https://doi.org/10.1175/1520-0493(2003)131<0585:ACPSDF>2.0.CO;2).
- , 2011: An inverse relationship between aggregate Northern Hemisphere tropical cyclone activity and subsequent winter climate. *Geophys. Res. Lett.*, **38**, L01705, <https://doi.org/10.1029/2010GL045612>.
- , and J. L. Evans, 2001: A climatology of the extratropical transition of Atlantic tropical cyclones. *J. Climate*, **14**, 546–564, [https://doi.org/10.1175/1520-0442\(2001\)014<0546:ACOTET>2.0.CO;2](https://doi.org/10.1175/1520-0442(2001)014<0546:ACOTET>2.0.CO;2).
- , and J. H. Cossuth, 2013: A family tree of tropical meteorology's academic community and its proposed expansion. *Bull. Amer. Meteor. Soc.*, **94**, 1837–1848, <https://doi.org/10.1175/BAMS-D-12-00110.1>.
- , J. L. Evans, and C. Evans, 2006: Synoptic composites of the extratropical transition life cycle of North Atlantic tropical cyclones: Factors determining posttransition evolution. *Mon. Wea. Rev.*, **134**, 553–578, <https://doi.org/10.1175/MWR3082.1>.
- Hartmann, D. L., and E. D. Maloney, 2001: The Madden–Julian oscillation, barotropic dynamics, and North Pacific tropical cyclone formation. Part II: Stochastic barotropic modeling. *J. Atmos. Sci.*, **58**, 2559–2570, [https://doi.org/10.1175/1520-0469\(2001\)058<2559:TMOBJD>2.0.CO;2](https://doi.org/10.1175/1520-0469(2001)058<2559:TMOBJD>2.0.CO;2).
- Hastings, P. A., 1990: Southern Oscillation influences on tropical cyclone activity in the Australian/south-west Pacific region. *Int. J. Climatol.*, **10**, 291–298, <https://doi.org/10.1002/joc.3370100306>.
- Haurwitz, B., 1935: The height of tropical cyclones and of the “eye” of the storm. *Mon. Wea. Rev.*, **63**, 45–49, [https://doi.org/10.1175/1520-0493\(1935\)63<45:THOTCA>2.0.CO;2](https://doi.org/10.1175/1520-0493(1935)63<45:THOTCA>2.0.CO;2).
- Haus, B. K., D. Jeong, M. A. Donelan, J. A. Zhang, and I. Savelyev, 2010: Relative rates of sea-air heat transfer and frictional drag in very high winds. *Geophys. Res. Lett.*, **37**, L07802, <https://doi.org/10.1029/2009GL042206>.
- Hawkins, H. F., and D. T. Rubsam, 1968: Hurricane Hilda, 1964: II. Structure and budgets of the hurricane on October 1, 1964. *Mon. Wea. Rev.*, **96**, 617–636, [https://doi.org/10.1175/1520-0493\(1968\)096<0617:HH>2.0.CO;2](https://doi.org/10.1175/1520-0493(1968)096<0617:HH>2.0.CO;2).
- , and S. M. Imbembo, 1976: The structure of a small, intense hurricane—Inez 1966. *Mon. Wea. Rev.*, **104**, 418–442, [https://doi.org/10.1175/1520-0493\(1976\)104<0418:TOSASI>2.0.CO;2](https://doi.org/10.1175/1520-0493(1976)104<0418:TOSASI>2.0.CO;2).
- Hawkins, J. D., and M. Helveston, 2004: Tropical cyclone multiple eyewall characteristics. *26th Conf. on Hurricanes and Tropical Meteorology*, Miami Beach, FL, Amer. Meteor. Soc., P1.7, [https://ams.confex.com/ams/26HURR/techprogram/paper\\_76084.htm](https://ams.confex.com/ams/26HURR/techprogram/paper_76084.htm).
- Henderson-Sellers, A., and Coauthors, 1998: Tropical cyclones and global climate change: A post-IPCC assessment. *Bull. Amer. Meteor. Soc.*, **79**, 19–38, [https://doi.org/10.1175/1520-0477\(1998\)079<0019:TCAGCC>2.0.CO;2](https://doi.org/10.1175/1520-0477(1998)079<0019:TCAGCC>2.0.CO;2).
- Hendricks, E. A., M. T. Montgomery, and C. A. Davis, 2004: The role of “vortical” hot towers in the formation of tropical cyclone Diana (1984). *J. Atmos. Sci.*, **61**, 1209–1232, [https://doi.org/10.1175/1520-0469\(2004\)061<1209:TROVHT>2.0.CO;2](https://doi.org/10.1175/1520-0469(2004)061<1209:TROVHT>2.0.CO;2).
- Hetzinger, S., M. Pfeiffer, W. C. Dullo, N. Keenlyside, M. Latif, and J. Zinke, 2008: Caribbean coral tracks

- Atlantic multidecadal oscillation and past hurricane activity. *Geology*, **36**, 11–14, <https://doi.org/10.1130/G24321A.1>.
- Ho, C. H., J. H. Kim, J. H. Jeong, H. S. Kim, and D. Chen, 2006: Variation of tropical cyclone activity in the South Indian ocean: El Niño–Southern Oscillation and Madden-Julian Oscillation effects. *J. Geophys. Res.*, **111**, D22101, <https://doi.org/10.1029/2006JD007289>.
- Hoffman, R. N., 2002: Controlling the global weather. *Bull. Amer. Meteor. Soc.*, **83**, 241–248, [https://doi.org/10.1175/1520-0477\(2002\)083<0241:CTGW>2.3.CO;2](https://doi.org/10.1175/1520-0477(2002)083<0241:CTGW>2.3.CO;2).
- Holland, G. J., 1980: Analytic model of the wind and pressure profiles in hurricanes. *Mon. Wea. Rev.*, **108**, 1212–1218, [https://doi.org/10.1175/1520-0493\(1980\)108<1212:AAMOTW>2.0.CO;2](https://doi.org/10.1175/1520-0493(1980)108<1212:AAMOTW>2.0.CO;2).
- , 1982: Tropical cyclone motion: Environmental interaction plus a beta effect. Colorado State University Dept. of Atmospheric Science Paper 348, 47 pp., [https://tropical.colostate.edu/media/sites/111/2016/10/348\\_Holland.pdf](https://tropical.colostate.edu/media/sites/111/2016/10/348_Holland.pdf).
- , 1983: Tropical cyclone motion: Environmental interaction plus a beta effect. *J. Atmos. Sci.*, **40**, 328–342, [https://doi.org/10.1175/1520-0469\(1983\)040<0328:TCMEIP>2.0.CO;2](https://doi.org/10.1175/1520-0469(1983)040<0328:TCMEIP>2.0.CO;2).
- , 1997: The maximum potential intensity of tropical cyclones. *J. Atmos. Sci.*, **54**, 2519–2541, [https://doi.org/10.1175/1520-0469\(1997\)054<2519:TMPIOT>2.0.CO;2](https://doi.org/10.1175/1520-0469(1997)054<2519:TMPIOT>2.0.CO;2).
- , and G. S. Dietachmayer, 1993: On the interaction of tropical-cyclone-scale vortices. III: Continuous barotropic vortices. *Quart. J. Roy. Meteor. Soc.*, **119**, 1381–1398, <https://doi.org/10.1002/qj.49711951408>.
- , J. I. Belanger, and A. Fritz, 2010: A revised model for radial profiles of hurricane winds. *Mon. Wea. Rev.*, **138**, 4393–4406, <https://doi.org/10.1175/2010MWR3317.1>.
- Holthuijsen, L. H., M. D. Powell, and J. D. Pietrzak, 2012: Wind and waves in extreme hurricanes. *J. Geophys. Res.*, **117**, C09003, <https://doi.org/10.1029/2012JC007983>.
- Homar, V., R. Romero, D. J. Stensrud, C. Ramis, and S. Alonso, 2003: Numerical diagnosis of a small, quasi-tropical cyclone over the western Mediterranean: Dynamical vs. Boundary factors. *Quart. J. Roy. Meteor. Soc.*, **129**, 1469–1490, <https://doi.org/10.1256/qj.01.91>.
- Hong, C. C., Y. H. Li, T. Li, and M. Y. Lee, 2011: Impacts of central Pacific and eastern Pacific El Niños on tropical cyclone tracks over the western North Pacific. *Geophys. Res. Lett.*, **38**, L16712, <https://doi.org/10.1029/2011GL048821>.
- Hong, I., and Coauthors, 2018: Sedimentological characteristics of the 2015 Tropical Cyclone Pam overwash sediments from Vanuatu, South Pacific. *Mar. Geol.*, **396**, 205–214, <https://doi.org/10.1016/j.margeo.2017.05.011>.
- Hoskins, B. J., and F. P. Bretherton, 1972: Atmospheric frontogenesis models: Mathematical formulation and solution. *J. Atmos. Sci.*, **29**, 11–37, [https://doi.org/10.1175/1520-0469\(1972\)029<0011:AFMMFA>2.0.CO;2](https://doi.org/10.1175/1520-0469(1972)029<0011:AFMMFA>2.0.CO;2).
- Houze, R. A., Jr., 2010: Clouds in tropical cyclones. *Mon. Wea. Rev.*, **138**, 293–344, <https://doi.org/10.1175/2009MWR2989.1>.
- , F. D. Marks Jr., and R. A. Black, 1992: Dual aircraft investigation of the inner core of Hurricane Norbert. Part II: Mesoscale distribution of ice particles. *J. Atmos. Sci.*, **49**, 943–962, [https://doi.org/10.1175/1520-0469\(1992\)049<0943:DAIOTI>2.0.CO;2](https://doi.org/10.1175/1520-0469(1992)049<0943:DAIOTI>2.0.CO;2).
- , S. S. Chen, B. F. Smull, W.-C. Lee, and M. M. Bell, 2007: Hurricane intensity and eyewall replacement. *Science*, **315**, 1235–1239, <https://doi.org/10.1126/science.1135650>.
- , and Coauthors, 2006: The hurricane rainband and intensity change experiment: Observations and modeling of hurricanes Katrina, Ophelia, and Rita. *Bull. Amer. Meteor. Soc.*, **87**, 1503–1522, <https://doi.org/10.1175/BAMS-87-11-1503>.
- Huang, F., and S. Xu, 2010: Super typhoon activity over the western North Pacific and its relationship with ENSO. *J. Ocean Univ. China*, **9**, 123–128, <https://doi.org/10.1007/s11802-010-0123-8>.
- Huang, P., C. Chou, and R. Huang, 2011: Seasonal modulation of tropical intraseasonal oscillations on tropical cyclone genesis in the western North Pacific. *J. Climate*, **24**, 6339–6352, <https://doi.org/10.1175/2011JCLI4200.1>.
- Huang, Y. J., M. T. Montgomery, and C. C. Wu, 2012: Concentric eyewall formation in Typhoon Sinlaku (2008). Part II: Axisymmetric dynamical processes. *J. Atmos. Sci.*, **69**, 662–674, <https://doi.org/10.1175/JAS-D-11-0114.1>.
- Ichiye, T., 1977: Response of a two-layer ocean with a baroclinic current to a moving storm, part II. *J. Oceanogr. Soc. Japan*, **33**, 169–182, <https://doi.org/10.1007/BF02109689>.
- Iizuka, S., and T. Matsuura, 2009: Relationship between ENSO and North Atlantic tropical cyclone frequency simulated in a coupled general circulation model. *Hurricanes and Climate Change*, J. B. Elsner and T. H. Jagger, Eds., Springer, 323–338, [https://doi.org/10.1007/978-0-387-09410-6\\_17](https://doi.org/10.1007/978-0-387-09410-6_17).
- Jaimes, B., and L. K. Shay, 2009: Mixed layer cooling in mesoscale oceanic eddies during Hurricanes Katrina and Rita. *Mon. Wea. Rev.*, **137**, 4188–4207, <https://doi.org/10.1175/2009MWR2849.1>.
- Jansen, M. F., and R. Ferrari, 2009: Impact of the latitudinal distribution of tropical cyclones on ocean heat transport. *Geophys. Res. Lett.*, **36**, L06604, <https://doi.org/10.1029/2008GL036796>.
- , —, and T. A. Mooring, 2010: Seasonal versus permanent thermocline warming by tropical cyclones. *Geophys. Res. Lett.*, **37**, L03602, <https://doi.org/10.1029/2009GL041808>.
- Jarosch, E., D. A. Mitchell, D. W. Wang, and W. J. Teague, 2007: Bottom-up determination of air-sea momentum exchange under a major tropical cyclone. *Science*, **315**, 1707–1709, <https://doi.org/10.1126/science.1136466>.
- Jeong, D., B. K. Haus, and M. A. Donelan, 2012: Enthalpy transfer across the air–water interface in high winds including spray. *J. Atmos. Sci.*, **69**, 2733–2748, <https://doi.org/10.1175/JAS-D-11-0260.1>.
- Jiang, X., M. Zhao, and D. E. Waliser, 2012: Modulation of tropical cyclones over the eastern Pacific by the intraseasonal variability simulated in an AGCM. *J. Climate*, **25**, 6524–6538, <https://doi.org/10.1175/JCLI-D-11-00531.1>.
- Jien, J. Y., W. A. Gough, and K. Butler, 2015: The influence of El Niño–Southern Oscillation on tropical cyclone activity in the eastern North Pacific basin. *J. Climate*, **28**, 2459–2474, <https://doi.org/10.1175/JCLI-D-14-00248.1>.
- Jin, F. F., J. Boucharel, and I. I. Lin, 2014: Eastern Pacific tropical cyclones intensified by El Niño delivery of subsurface ocean heat. *Nature*, **516**, 82–85, <https://doi.org/10.1038/nature13958>.
- Jones, C. G., and C. D. Thorncroft, 1998: The rôle of El Niño in Atlantic tropical cyclone activity. *Weather*, **53**, 324–336, <https://doi.org/10.1002/j.1477-8696.1998.tb06409.x>.
- Jones, S. C., 1995: The evolution of vortices in vertical shear. I: Initially barotropic vortices. *Quart. J. Roy. Meteor. Soc.*, **121**, 821–851, <https://doi.org/10.1002/qj.49712152406>.
- , 2000a: The evolution of vortices in vertical shear. II: Large-scale asymmetries. *Quart. J. Roy. Meteor. Soc.*, **126**, 3137–3159, <https://doi.org/10.1002/qj.49712657008>.
- , 2000b: The evolution of vortices in vertical shear. III: Baroclinic vortices. *Quart. J. Roy. Meteor. Soc.*, **126**, 3161–3185, <https://doi.org/10.1002/qj.49712657009>.

- , and Coauthors, 2003: The extratropical transition of tropical cyclones: Forecast challenges, current understanding, and future directions. *Wea. Forecasting*, **18**, 1052–1092, [https://doi.org/10.1175/1520-0434\(2003\)018<1052:TETOTC>2.0.CO;2](https://doi.org/10.1175/1520-0434(2003)018<1052:TETOTC>2.0.CO;2).
- Jordan, C. L., 1961: Marked changes in the characteristics of the eye of intense typhoons between the deepening and filling stages. *J. Meteor.*, **18**, 779–789, [https://doi.org/10.1175/1520-0469\(1961\)018<0779:MCITCO>2.0.CO;2](https://doi.org/10.1175/1520-0469(1961)018<0779:MCITCO>2.0.CO;2).
- Kantha, L. H., O. M. Phillips, and R. S. Azad, 1977: On turbulent entrainment at a stable density interface. *J. Fluid Mech.*, **79**, 753–768, <https://doi.org/10.1017/S0022112077000433>.
- Kaplan, J., and M. DeMaria, 1995: A simple empirical model for predicting the decay of tropical cyclone winds after landfall. *J. Appl. Meteor.*, **34**, 2499–2512, [https://doi.org/10.1175/1520-0450\(1995\)034<2499:ASEMFP>2.0.CO;2](https://doi.org/10.1175/1520-0450(1995)034<2499:ASEMFP>2.0.CO;2).
- Kasahara, A., 1957: The numerical prediction of hurricane movement with the barotropic model. *J. Meteor.*, **14**, 386–402, [https://doi.org/10.1175/1520-0469\(1957\)014<0386:TNP0HM>2.0.CO;2](https://doi.org/10.1175/1520-0469(1957)014<0386:TNP0HM>2.0.CO;2).
- , 1961: A numerical experiment on the development of a tropical cyclone. *J. Meteor.*, **18**, 259–282, [https://doi.org/10.1175/1520-0469\(1961\)018<0259:ANEOTD>2.0.CO;2](https://doi.org/10.1175/1520-0469(1961)018<0259:ANEOTD>2.0.CO;2).
- Kato, H., and O. M. Phillips, 1969: On the penetration of a turbulent layer into stratified fluid. *J. Fluid Mech.*, **37**, 643–655, <https://doi.org/10.1017/S0022112069000784>.
- Katsaros, K. B., P. W. Vachon, P. G. Black, P. P. Dodge, and E. W. Uhlhorn, 2000: Wind fields from SAR: Could they improve our understanding of storm dynamics? *Johns Hopkins APL Tech. Dig.*, **21**, 86–93.
- Ke, F., 2009: Linkage between the Atlantic tropical hurricane frequency and the Antarctic oscillation in the Western Hemisphere. *Atmos. Ocean. Sci. Lett.*, **2**, 159–164, <https://doi.org/10.1080/16742834.2009.11446796>.
- Keper, J. D., 2010: Slab- and height-resolving models of the tropical cyclone boundary layer. Part I: Comparing the simulations. *Quart. J. Roy. Meteor. Soc.*, **136**, 1686–1699, <https://doi.org/10.1002/qj.667>.
- , 2013: How does the boundary layer contribute to eyewall replacement cycles in axisymmetric tropical cyclones? *J. Atmos. Sci.*, **70**, 2808–2830, <https://doi.org/10.1175/JAS-D-13-0046.1>.
- Khain, A., and I. Ginis, 1991: The mutual response of a moving tropical cyclone and the ocean. *Beitr. Phys. Atmos.*, **64**, 125–141.
- Khairoutdinov, M. F., and K. Emanuel, 2010: Aggregated convection and the regulation of tropical climate. *29th Conf. on Hurricanes and Tropical Meteorology*, Tucson, AZ, Amer. Meteor. Soc., P2.69, [https://ams.confex.com/ams/29Hurricanes/techprogram/paper\\_168418.htm](https://ams.confex.com/ams/29Hurricanes/techprogram/paper_168418.htm).
- , and —, 2013: Rotating radiative-convective equilibrium simulated by a cloud-resolving model. *J. Adv. Model. Earth Syst.*, **5**, 816–825, <https://doi.org/10.1002/2013MS000253>.
- Kikuchi, K., and B. Wang, 2010: Formation of tropical cyclones in the northern Indian Ocean associated with two types of tropical intraseasonal oscillation modes. *J. Meteor. Soc. Japan*, **88**, 475–496, <https://doi.org/10.2151/jmsj.2010-313>.
- Kilroy, G., R. K. Smith, M. T. Montgomery, B. Lynch, and C. Earl-Spurr, 2016: A case-study of a monsoon low that formed over the sea and intensified over land as seen in ECMWF analyses. *Quart. J. Roy. Meteor. Soc.*, **142**, 2244–2255, <https://doi.org/10.1002/qj.2814>.
- , —, and —, 2017: A unified view of tropical cyclogenesis and intensification. *Quart. J. Roy. Meteor. Soc.*, **143**, 450–462, <https://doi.org/10.1002/qj.2934>.
- Kim, H.-M., P. J. Webster, and J. A. Curry, 2011: Modulation of North Pacific tropical cyclone activity by three phases of ENSO. *J. Climate*, **24**, 1839–1849, <https://doi.org/10.1175/2010JCLI3939.1>.
- Kim, J.-H., C.-H. Ho, H.-S. Kim, C.-H. Sui, and S. K. Park, 2008: Systematic variation of summertime tropical cyclone activity in the western North Pacific in relation to the Madden–Julian oscillation. *J. Climate*, **21**, 1171–1191, <https://doi.org/10.1175/2007JCLI1493.1>.
- Kimball, S. K., and J. L. Evans, 2002: Idealized numerical simulations of hurricane–trough interaction. *Mon. Wea. Rev.*, **130**, 2210–2227, [https://doi.org/10.1175/1520-0493\(2002\)130<2210:INSOHT>2.0.CO;2](https://doi.org/10.1175/1520-0493(2002)130<2210:INSOHT>2.0.CO;2).
- Klein, P. M., P. A. Harr, and R. L. Elsberry, 2000: Extratropical transition of western North Pacific tropical cyclones: An overview and conceptual model of the transformation stage. *Wea. Forecasting*, **15**, 373–395, [https://doi.org/10.1175/1520-0434\(2000\)015<0373:ETOWNP>2.0.CO;2](https://doi.org/10.1175/1520-0434(2000)015<0373:ETOWNP>2.0.CO;2).
- , —, and —, 2002: Extratropical transition of western North Pacific tropical cyclones: Midlatitude and tropical cyclone contributions to reintensification. *Mon. Wea. Rev.*, **130**, 2240–2259, [https://doi.org/10.1175/1520-0493\(2002\)130<2240:ETOWNP>2.0.CO;2](https://doi.org/10.1175/1520-0493(2002)130<2240:ETOWNP>2.0.CO;2).
- Kleinschmidt, E., Jr., 1951: Grundlagen einer theorie der tropischen zyklonen. *Arch. Meteor. Geophys. Bioklimatol.*, **4A**, 53–72, <https://doi.org/10.1007/BF02246793>.
- Klotzbach, P. J., 2010: On the Madden–Julian oscillation–Atlantic hurricane relationship. *J. Climate*, **23**, 282–293, <https://doi.org/10.1175/2009JCLI2978.1>.
- , 2011a: El Niño–Southern Oscillation’s impact on Atlantic basin hurricanes and U.S. landfalls. *J. Climate*, **24**, 1252–1263, <https://doi.org/10.1175/2010JCLI3799.1>.
- , 2011b: The influence of El Niño–Southern Oscillation and the Atlantic multidecadal oscillation on Caribbean tropical cyclone activity. *J. Climate*, **24**, 721–731, <https://doi.org/10.1175/2010JCLI3705.1>.
- , 2014: The Madden–Julian Oscillation’s impacts on worldwide tropical cyclone activity. *J. Climate*, **27**, 2317–2330, <https://doi.org/10.1175/JCLI-D-13-00483.1>.
- , and W. M. Gray, 2008: Multidecadal variability in North Atlantic tropical cyclone activity. *J. Climate*, **21**, 3929–3935, <https://doi.org/10.1175/2008JCLI2162.1>.
- Knaff, J. A., S. A. Seseske, M. DeMaria, and J. L. Demuth, 2004: On the influences of vertical wind shear on symmetric tropical cyclone structure derived from AMSU. *Mon. Wea. Rev.*, **132**, 2503–2510, [https://doi.org/10.1175/1520-0493\(2004\)132<2503:OTIOVW>2.0.CO;2](https://doi.org/10.1175/1520-0493(2004)132<2503:OTIOVW>2.0.CO;2).
- Knapp, K. R., M. C. Kruk, D. H. Levinson, H. J. Diamond, and C. J. Neumann, 2010: The International Best Track Archive for Climate Stewardship (IBTrACS): Unifying tropical cyclone best track data. *Bull. Amer. Meteor. Soc.*, **91**, 363–376, <https://doi.org/10.1175/2009BAMS2755.1>.
- Knutson, T., and Coauthors, 2010: Tropical cyclones and climate change. *Nat. Geosci.*, **3**, 157–163, <https://doi.org/10.1038/ngeo779>.
- Korolev, V. S., S. A. Petrichenko, and V. D. V. D. Pudov, 1990: Heat and moisture exchange between the ocean and atmosphere in tropical storms Tess and Skip. *Sov. Meteor. Hydrol.*, **3**, 92–94.
- Korty, R. L., 2002: Processes affecting the ocean’s feedback on the intensity of a hurricane. *25th Conf. on Hurricane and Tropical Meteorology*, San Diego, CA, Amer. Meteor. Soc., 14D.2, <https://ams.confex.com/ams/25HURR/webprogram/Paper35849.html>.

- , K. A. Emanuel, and J. R. Scott, 2008: Tropical cyclone-induced upper ocean mixing and climate: Application to equable climates. *J. Climate*, **21**, 638–654, <https://doi.org/10.1175/2007JCLI1659.1>.
- , S. J. Camargo, and J. Galewsky, 2012a: Tropical cyclone genesis factors in simulations of the last glacial maximum. *J. Climate*, **25**, 4348–4365, <https://doi.org/10.1175/JCLI-D-11-00517.1>.
- , —, and —, 2012b: Variations in tropical cyclone genesis factors in simulations of the Holocene epoch. *J. Climate*, **25**, 8196–8211, <https://doi.org/10.1175/JCLI-D-12-00033.1>.
- Kossin, J. P., 2002: Daily hurricane variability inferred from GOES infrared imagery. *Mon. Wea. Rev.*, **130**, 2260–2270, [https://doi.org/10.1175/1520-0493\(2002\)130<2260:DHVIFG>2.0.CO;2](https://doi.org/10.1175/1520-0493(2002)130<2260:DHVIFG>2.0.CO;2).
- , 2017: Hurricane intensification along United States coast suppressed during active hurricane periods. *Nature*, **541**, 390–393, <https://doi.org/10.1038/nature20783>.
- , 2018: A global slowdown of tropical cyclone translation speed. *Nature*, **558**, 104–107, <https://doi.org/10.1038/s41586-018-0158-3>.
- , and M. D. Eastin, 2001: Two distinct regimes in the kinematic and thermodynamic structure of the hurricane eye and eyewall. *J. Atmos. Sci.*, **58**, 1079–1090, [https://doi.org/10.1175/1520-0469\(2001\)058<1079:TDRITK>2.0.CO;2](https://doi.org/10.1175/1520-0469(2001)058<1079:TDRITK>2.0.CO;2).
- , and W. H. Schubert, 2001: Mesovortices, polygonal flow patterns, and rapid pressure falls in hurricane-like vortices. *J. Atmos. Sci.*, **58**, 2196–2209, [https://doi.org/10.1175/1520-0469\(2001\)058<2196:MPFPAR>2.0.CO;2](https://doi.org/10.1175/1520-0469(2001)058<2196:MPFPAR>2.0.CO;2).
- , and —, 2003: Diffusion versus advective rearrangement of a circular vortex sheet. *J. Atmos. Sci.*, **60**, 586–589, [https://doi.org/10.1175/1520-0469\(2003\)060<0586:DVAROA>2.0.CO;2](https://doi.org/10.1175/1520-0469(2003)060<0586:DVAROA>2.0.CO;2).
- , and D. J. Vimont, 2007: A more general framework for understanding Atlantic hurricane variability and trends. *Bull. Amer. Meteor. Soc.*, **88**, 1767–1782, <https://doi.org/10.1175/BAMS-88-11-1767>.
- , and M. Sitkowski, 2009: An objective model for identifying secondary eyewall formation in hurricanes. *Mon. Wea. Rev.*, **137**, 876–892, <https://doi.org/10.1175/2008MWR2701.1>.
- , J. A. Knaff, H. I. Berger, D. C. Herndon, T. A. Cram, C. S. Velden, R. J. Murnane, and J. D. Hawkins, 2007: Estimating hurricane wind structure in the absence of aircraft reconnaissance. *Wea. Forecasting*, **22**, 89–101, <https://doi.org/10.1175/WAF985.1>.
- , S. J. Camargo, and M. Sitkowski, 2010: Climate modulation of North Atlantic hurricane tracks. *J. Climate*, **23**, 3057–3076, <https://doi.org/10.1175/2010JCLI3497.1>.
- Kowch, R., and K. Emanuel, 2015: Are special processes at work in the rapid intensification of tropical cyclones? *Mon. Wea. Rev.*, **143**, 878–882, <https://doi.org/10.1175/MWR-D-14-00360.1>.
- Krishnamohan, K. S., K. Mohanakumar, and P. V. Joseph, 2012: The influence of Madden–Julian oscillation in the genesis of north Indian Ocean tropical cyclones. *Theor. Appl. Climatol.*, **109**, 271–282, <https://doi.org/10.1007/s00704-011-0582-x>.
- Kuleshov, Y., F. Chane-Ming, L. Qi, I. Chouaibou, C. Hoareau, and F. Roux, 2009: Tropical cyclone genesis in the southern hemisphere and its relationship with the ENSO. *Ann. Geophys.*, **27**, 2523–2538, <https://doi.org/10.5194/angeo-27-2523-2009>.
- Kuo, H.-C., L.-Y. Lin, C.-P. Chang, and R. T. Williams, 2004: The formation of concentric vorticity structures in typhoons. *J. Atmos. Sci.*, **61**, 2722–2734, <https://doi.org/10.1175/JAS3286.1>.
- , W. H. Schubert, C.-L. Tsai, and Y.-F. Kuo, 2008: Vortex interactions and barotropic aspects of concentric eyewall formation. *Mon. Wea. Rev.*, **136**, 5183–5198, <https://doi.org/10.1175/2008MWR2378.1>.
- Kuo, H.-L., 1965: On formation and intensification of tropical cyclones through latent heat release by cumulus convection. *J. Atmos. Sci.*, **22**, 40–63, [https://doi.org/10.1175/1520-0469\(1965\)022<0040:OFAIOT>2.0.CO;2](https://doi.org/10.1175/1520-0469(1965)022<0040:OFAIOT>2.0.CO;2).
- Kurihara, Y., 1976: On the development of spiral bands in a tropical cyclone. *J. Atmos. Sci.*, **33**, 940–958, [https://doi.org/10.1175/1520-0469\(1976\)033<0940:OTDOSB>2.0.CO;2](https://doi.org/10.1175/1520-0469(1976)033<0940:OTDOSB>2.0.CO;2).
- , M. A. Bender, and R. J. Ross, 1993: An initialization scheme of hurricane models by vortex specification. *Mon. Wea. Rev.*, **121**, 2030–2045, [https://doi.org/10.1175/1520-0493\(1993\)121<2030:AISOHM>2.0.CO;2](https://doi.org/10.1175/1520-0493(1993)121<2030:AISOHM>2.0.CO;2).
- , —, R. E. Tuleya, and R. J. Ross, 1995: Improvements in the GFDL hurricane prediction system. *Mon. Wea. Rev.*, **123**, 2791–2801, [https://doi.org/10.1175/1520-0493\(1995\)123<2791:ITGHP>2.0.CO;2](https://doi.org/10.1175/1520-0493(1995)123<2791:ITGHP>2.0.CO;2).
- , R. E. Tuleya, and M. A. Bender, 1998: The GFDL hurricane prediction system and its performance in the 1995 hurricane season. *Mon. Wea. Rev.*, **126**, 1306–1322, [https://doi.org/10.1175/1520-0493\(1998\)126<1306:TGHPSA>2.0.CO;2](https://doi.org/10.1175/1520-0493(1998)126<1306:TGHPSA>2.0.CO;2).
- Kutzbach, G., 1979: *The Thermal Theory of Cyclones*. Amer. Meteor. Soc., 255 pp.
- Kwon, Y. C., and W. M. Frank, 2008: Dynamic instabilities of simulated hurricane-like vortices and their impacts on the core structure of hurricanes. Part II: Moist experiments. *J. Atmos. Sci.*, **65**, 106–122, <https://doi.org/10.1175/2007JAS2132.1>.
- Laing, A. G., and J. M. Fritsch, 1993: Mesoscale convective complexes in Africa. *Mon. Wea. Rev.*, **121**, 2254–2263, [https://doi.org/10.1175/1520-0493\(1993\)121<2254:MCCIA>2.0.CO;2](https://doi.org/10.1175/1520-0493(1993)121<2254:MCCIA>2.0.CO;2).
- Lander, M., and G. J. Holland, 1993: On the interaction of tropical-cyclone-scale vortices. I: Observations. *Quart. J. Roy. Meteor. Soc.*, **119**, 1347–1361, <https://doi.org/10.1002/qj.49711951406>.
- Landsea, C. W., and J. P. Cangialosi, 2018: Have we reached the limits of predictability for tropical cyclone track forecasting? *Bull. Amer. Meteor. Soc.*, <https://doi.org/10.1175/BAMS-D-17-0136.1>, in press.
- Lane, C. S., B. Hildebrandt, L. M. Kennedy, A. LeBlanc, K. B. Liu, A. J. Wagner, and A. D. Hawkes, 2017: Verification of tropical cyclone deposits with oxygen isotope analyses of coeval ostracod valves. *J. Paleolimnol.*, **57**, 245–255, <https://doi.org/10.1007/s10933-017-9943-5>.
- Larson, E., 1999: *Isaac's Storm: A Man, a Time, and the Deadliest Hurricane in History*. Crown Publishers, 336 pp.
- Lawrence, J. R., and S. D. Gedzelman, 1996: Low stable isotope ratios of tropical cyclone rains. *Geophys. Res. Lett.*, **23**, 527–530, <https://doi.org/10.1029/96GL00425>.
- Le Dizes, S., M. Rossi, and H. K. Moffat, 1996: On the three-dimensional instability of elliptical vortex subjected to stretching. *Phys. Fluids*, **8**, 2084–2090, <https://doi.org/10.1063/1.868982>.
- Lee, H. S., T. Yamashita, and T. Mishima, 2012: Multi-decadal variations of ENSO, the Pacific decadal oscillation and tropical cyclones in the western North Pacific. *Progress Oceanogr.*, **105**, 67–80, <https://doi.org/10.1016/j.pocean.2012.04.009>.
- Leibovich, S., and K. Stewartson, 1983: A sufficient condition for the instability of columnar vortices. *J. Fluid Mech.*, **126**, 335–356, <https://doi.org/10.1017/S0022112083000191>.
- Leipper, D. F., 1967: Observed ocean conditions and Hurricane Hilda, 1964. *J. Atmos. Sci.*, **24**, 182–196, [https://doi.org/10.1175/1520-0469\(1967\)024<0182:OOCANH>2.0.CO;2](https://doi.org/10.1175/1520-0469(1967)024<0182:OOCANH>2.0.CO;2).
- Leppert, K. D., II, and D. J. Cecil, 2016: Tropical cyclone diurnal cycle as observed by TRMM. *Mon. Wea. Rev.*, **144**, 2793–2808, <https://doi.org/10.1175/MWR-D-15-0358.1>.

- Leslie, L. M., and R. K. Smith, 1970: The surface boundary layer of a hurricane. II. *Tellus*, **22**, 288–297, <https://doi.org/10.3402/tellusa.v22i3.10222>.
- Lewis, B. M., and H. F. Hawkins, 1982: Polygonal eye walls and rainbands in hurricanes. *Bull. Amer. Meteor. Soc.*, **63**, 1294–1300, [https://doi.org/10.1175/1520-0477\(1982\)063<1294:PEWARI>2.0.CO;2](https://doi.org/10.1175/1520-0477(1982)063<1294:PEWARI>2.0.CO;2).
- Lewis, J. M., M. G. Fearon, and H. E. Klieforth, 2012: Herbert Riehl: Intrepid and enigmatic scholar. *Bull. Amer. Meteor. Soc.*, **93**, 963–985, <https://doi.org/10.1175/BAMS-D-11-00224.1>.
- Li, R. C. Y., and W. Zhou, 2012: Changes in western Pacific tropical cyclones associated with the El Niño–Southern Oscillation cycle. *J. Climate*, **25**, 5864–5878, <https://doi.org/10.1175/JCLI-D-11-00430.1>.
- , and —, 2018: Revisiting the intraseasonal, interannual and interdecadal variability of tropical cyclones in the western North Pacific. *Atmos. Ocean. Sci. Lett.*, **11**, 198–208, <https://doi.org/10.1080/16742834.2018.1459460>.
- Liebmann, B., H. H. Hendon, and J. D. Glick, 1994: The relationship between tropical cyclones of the western Pacific and Indian Oceans and the Madden-Julian oscillation. *J. Meteor. Soc. Japan*, **72**, 401–412, [https://doi.org/10.2151/jmsj1965.72.3\\_401](https://doi.org/10.2151/jmsj1965.72.3_401).
- Lighthill, J., G. Holland, W. Gray, C. Landsea, G. Craig, J. Evans, Y. Kurihara, and C. Guard, 1994: Global climate change and tropical cyclones. *Bull. Amer. Meteor. Soc.*, **75**, 2147–2157, <https://doi.org/10.1175/1520-0477-75.11.2147>.
- , 1999: Ocean spray and the thermodynamics of tropical cyclones. *J. Eng. Math.*, **35**, 11–42, <https://doi.org/10.1023/A:1004383430896>.
- Lilly, D. K., 1960: On the theory of disturbances in a conditionally unstable atmosphere. *Mon. Wea. Rev.*, **88**, 1–17, [https://doi.org/10.1175/1520-0493\(1960\)088<0001:OTTODI>2.0.CO;2](https://doi.org/10.1175/1520-0493(1960)088<0001:OTTODI>2.0.CO;2).
- , 1966: On the instability of Ekman boundary flow. *J. Atmos. Sci.*, **23**, 481–494, [https://doi.org/10.1175/1520-0469\(1966\)023<0481:OTTOEB>2.0.CO;2](https://doi.org/10.1175/1520-0469(1966)023<0481:OTTOEB>2.0.CO;2).
- , and K. Emanuel, 1985: A steady-state hurricane model. Preprints, *16th Conf. on Hurricanes and Tropical Meteorology*, Houston, TX, Amer. Meteor. Soc., 142–143.
- Lin, I.-I., and Coauthors, 2003: New evidence for enhanced ocean primary production triggered by tropical cyclone. *Geophys. Res. Lett.*, **30**, 1718, <https://doi.org/10.1029/2003GL017141>.
- , C.-C. Wu, K. Emanuel, I.-H. Lee, C.-R. Wu, and I.-F. Pun, 2005: The interaction of supertyphoon Maemi (2003) with a warm ocean eddy. *Mon. Wea. Rev.*, **133**, 2635–2649, <https://doi.org/10.1175/MWR3005.1>.
- , and Coauthors, 2013: An ocean coupling potential intensity index for tropical cyclones. *Geophys. Res. Lett.*, **40**, 1878–1882, <https://doi.org/10.1002/grl.50091>.
- Lin, N., P. Lane, K. A. Emanuel, R. Sullivan, and J. P. Donnelly, 2014: Heightened hurricane surge risk in northwest Florida revealed from climatological-hydrodynamic modeling and paleorecord reconstruction. *J. Geophys. Res. Atmos.*, **119**, 8606–8623, <https://doi.org/10.1002/2014JD021584>.
- Lionello, P., and Coauthors, 2006: Cyclones in the Mediterranean region: Climatology and effects on the environment. *Developments in Earth and Environmental Sciences*, Vol. 4, P. Lionello, P. Malanotte-Rizzoli, and R. Boscolo, Eds., Elsevier, 325–372, [https://doi.org/10.1016/S1571-9197\(06\)80009-1](https://doi.org/10.1016/S1571-9197(06)80009-1).
- Liu, K.-B., 2007: Paleotempestology. *Encyclopedia of Quaternary Science*, S. Elias, Ed., Elsevier, 1978–1986.
- , and M. L. Fearn, 1993: Lake-sediment record of late Holocene hurricane activities from coastal Alabama. *Geology*, **21**, 793–796, [https://doi.org/10.1130/0091-7613\(1993\)021<0793:LSROLH>2.3.CO;2](https://doi.org/10.1130/0091-7613(1993)021<0793:LSROLH>2.3.CO;2).
- , and —, 2000: Reconstruction of prehistoric landfall frequencies of catastrophic hurricanes in northwestern Florida from lake sediment records. *Quat. Res.*, **54**, 238–245, <https://doi.org/10.1006/qres.2000.2166>.
- , H. Y. Lu, and C. M. Shen, 2009: Some fundamental misconceptions about paleotempestology. *Quat. Res.*, **71**, 253–254, <https://doi.org/10.1016/j.yqres.2008.11.001>.
- , C. Li, T. A. Bianchette, T. A. McCloskey, Q. Yao, and E. Weeks, 2011: Storm deposition in a coastal backbarrier lake in Louisiana caused by hurricanes Gustav and Ike. *J. Coastal Res.*, **64**, 1866–1870.
- Liu, K. S., and J. C. L. Chan, 2008: Interdecadal variability of western North Pacific tropical cyclone tracks. *J. Climate*, **21**, 4464–4476, <https://doi.org/10.1175/2008JCLI2207.1>.
- Llewellyn Smith, S. G., 1997: The motion of a non-isolated vortex on the beta-plane. *J. Fluid Mech.*, **346**, 149–179, <https://doi.org/10.1017/S0022112097006290>.
- Loridan, T., E. Scherer, M. Dixon, E. Bellone, and S. Khare, 2014: Cyclone wind field asymmetries during extratropical transition in the western North Pacific. *J. Appl. Meteor. Climatol.*, **53**, 421–428, <https://doi.org/10.1175/JAMC-D-13-0257.1>.
- Lotliker, A. A., T. S. Kumar, V. S. Reddem, and S. Nayak, 2014: Cyclone Phailin enhanced the productivity following its passage: Evidence from satellite data. *Curr Sci India*, **106**, 360–361.
- Lul, H.-Y., and K.-B. Liu, 2005: Phytolith assemblages as indicators of coastal environmental changes and hurricane overwash deposition. *Holocene*, **15**, 965–972, <https://doi.org/10.1191/0959683605h1870ra>.
- MacDonald, N. J., 1968: The evidence for the existence of Rossby-like waves in the hurricane vortex. *Tellus*, **20**, 138–150, <https://doi.org/10.3402/tellusa.v20i1.9993>.
- Madala, R. V., and S. A. Piacsek, 1975: Numerical simulation of asymmetric hurricanes on a  $\beta$ -plane with vertical shear. *Tellus*, **27**, 453–468, <https://doi.org/10.3402/tellusa.v27i5.10172>.
- Mainelli, M., M. DeMaria, L. K. Shay, and G. Goni, 2008: Application of oceanic heat content estimation to operational forecasting of recent Atlantic category 5 hurricanes. *Wea. Forecasting*, **23**, 3–16, <https://doi.org/10.1175/2007WAF2006111.1>.
- Makariev, A. M., V. G. Gorshkov, A. V. Nefiodov, A. V. Chikunov, D. Sheil, A. D. Nobre, and B.-L. Li, 2018: Hurricane’s maximum potential intensity and the gravitational power of precipitation. ArXiv, 15 pp., <https://arxiv.org/abs/1801.06833>.
- Malkus, J. S., and H. Riehl, 1960: On the dynamics and energy transformations in steady-state hurricanes. *Tellus*, **12**, 1–20, <https://doi.org/10.3402/tellusa.v12i1.9351>.
- Malmquist, D. L., 1997: Oxygen isotopes in cave stalagmites as a proxy record of past tropical cyclone activity. Preprints, *22nd Conf. on Hurricanes and Tropical Meteorology*, Ft. Collins, CO, Amer. Meteor. Soc., 393–394.
- Maloney, E. D., and D. L. Hartmann, 2000a: Modulation of eastern North Pacific hurricanes by the Madden-Julian oscillation. *J. Climate*, **13**, 1451–1460, [https://doi.org/10.1175/1520-0442\(2000\)013<1451:MOENPH>2.0.CO;2](https://doi.org/10.1175/1520-0442(2000)013<1451:MOENPH>2.0.CO;2).
- , and —, 2000b: Modulation of hurricane activity in the Gulf of Mexico by the Madden-Julian oscillation. *Science*, **287**, 2002–2004, <https://doi.org/10.1126/science.287.5460.2002>.
- , and —, 2001: The Madden-Julian oscillation, barotropic dynamics, and North Pacific tropical cyclone formation. Part I:

- Observations. *J. Atmos. Sci.*, **58**, 2545–2558, [https://doi.org/10.1175/1520-0469\(2001\)058<2545:TMJOBDD>2.0.CO;2](https://doi.org/10.1175/1520-0469(2001)058<2545:TMJOBDD>2.0.CO;2).
- Mann, M. E., and K. A. Emanuel, 2006: Atlantic hurricane trends linked to climate change. *Eos, Trans. Amer. Geophys. Union*, **87**, 233–244, <https://doi.org/10.1029/2006EO240001>.
- Marks, F. D., Jr., and R. A. Houze Jr., 1984: Airborne Doppler radar observations in Hurricane Debby. *Bull. Amer. Meteor. Soc.*, **65**, 569–582, [https://doi.org/10.1175/1520-0477\(1984\)065<0569:ADROIH>2.0.CO;2](https://doi.org/10.1175/1520-0477(1984)065<0569:ADROIH>2.0.CO;2).
- , —, and J. F. Gamache, 1992: Dual aircraft investigation of the inner core of Hurricane Norbert. Part I: Kinematic structure. *J. Atmos. Sci.*, **49**, 919–942, [https://doi.org/10.1175/1520-0469\(1992\)049<0919:DAIOTI>2.0.CO;2](https://doi.org/10.1175/1520-0469(1992)049<0919:DAIOTI>2.0.CO;2).
- Mayengon, R., 1984: Warm core cyclones in the Mediterranean. *Mariners Weather Log*, Vol. 28, National Weather Service, Silver Spring, MD, 6–9.
- Mazza, E., U. Ulbrich, and R. Klein, 2017: The tropical transition of the October 1996 medicane in the western Mediterranean Sea: A warm seclusion event. *Mon. Wea. Rev.*, **145**, 2575–2595, <https://doi.org/10.1175/MWR-D-16-0474.1>.
- McBride, J. L., 1981: Observational analysis of tropical cyclone formation. Part III: Budget analysis. *J. Atmos. Sci.*, **38**, 1152–1166, [https://doi.org/10.1175/1520-0469\(1981\)038<1152:OAOTCF>2.0.CO;2](https://doi.org/10.1175/1520-0469(1981)038<1152:OAOTCF>2.0.CO;2).
- , and R. M. Zehr, 1981: Observational analysis of tropical cyclone formation. Part II: Comparison of non-developing versus developing systems. *J. Atmos. Sci.*, **38**, 1132–1151, [https://doi.org/10.1175/1520-0469\(1981\)038<1132:OAOTCF>2.0.CO;2](https://doi.org/10.1175/1520-0469(1981)038<1132:OAOTCF>2.0.CO;2).
- McCaul, E. W., Jr., 1991: Buoyancy and shear characteristics of hurricane-tornado environments. *Mon. Wea. Rev.*, **119**, 1954–1978, [https://doi.org/10.1175/1520-0493\(1991\)119<1954:BASCOH>2.0.CO;2](https://doi.org/10.1175/1520-0493(1991)119<1954:BASCOH>2.0.CO;2).
- McWilliams, J. C., and G. R. Flierl, 1979: On the evolution of isolated, nonlinear vortices. *J. Phys. Oceanogr.*, **9**, 1155–1182, [https://doi.org/10.1175/1520-0485\(1979\)009<1155:OTEOIN>2.0.CO;2](https://doi.org/10.1175/1520-0485(1979)009<1155:OTEOIN>2.0.CO;2).
- Mei, W., and C. Pasquero, 2012: Restratification of the upper ocean after the passage of a tropical cyclone: A numerical study. *J. Phys. Oceanogr.*, **42**, 1377–1401, <https://doi.org/10.1175/JPO-D-11-0209.1>.
- , and —, 2013: Spatial and temporal characterization of sea surface temperature response to tropical cyclones. *J. Climate*, **26**, 3745–3765, <https://doi.org/10.1175/JCLI-D-12-00125.1>.
- , F. Primeau, J. C. McWilliams, and C. Pasquero, 2013: Sea surface height evidence for long-term warming effects of tropical cyclones on the ocean. *Proc. Natl. Acad. Sci. USA*, **110**, 15 207–15 210, <https://doi.org/10.1073/pnas.1306753110>.
- Merrill, R. T., 1984: A comparison of large and small tropical cyclones. *Mon. Wea. Rev.*, **112**, 1408–1418, [https://doi.org/10.1175/1520-0493\(1984\)112<1408:ACOLAS>2.0.CO;2](https://doi.org/10.1175/1520-0493(1984)112<1408:ACOLAS>2.0.CO;2).
- , 1988a: Characteristics of the upper-tropospheric environmental flow around hurricanes. *J. Atmos. Sci.*, **45**, 1665–1677, [https://doi.org/10.1175/1520-0469\(1988\)045<1665:COTUTE>2.0.CO;2](https://doi.org/10.1175/1520-0469(1988)045<1665:COTUTE>2.0.CO;2).
- , 1988b: Environmental influences on hurricane intensification. *J. Atmos. Sci.*, **45**, 1678–1687, [https://doi.org/10.1175/1520-0469\(1988\)045<1678:EIOHI>2.0.CO;2](https://doi.org/10.1175/1520-0469(1988)045<1678:EIOHI>2.0.CO;2).
- Miglietta, M. M., S. Davolio, A. Moscatello, F. Pacifico, and R. Rotunno, 2008: The role of surface fluxes in the development of a tropical-like cyclone in southern Italy. *Adv. Sci. Res.*, **2**, 35–39, <https://doi.org/10.5194/asr-2-35-2008>.
- , S. Laviola, A. Malvaldi, D. Conte, V. Levizzani, and C. Price, 2013: Analysis of tropical-like cyclones over the Mediterranean Sea through a combined modeling and satellite approach. *Geophys. Res. Lett.*, **40**, 2400–2405, <https://doi.org/10.1002/grl.50432>.
- Miller, B. I., 1958: On the maximum intensity of hurricanes. *J. Meteor.*, **15**, 184–195, [https://doi.org/10.1175/1520-0469\(1958\)015<0184:OTMIOH>2.0.CO;2](https://doi.org/10.1175/1520-0469(1958)015<0184:OTMIOH>2.0.CO;2).
- , and P. P. Chase, 1966: Prediction of hurricane motion by statistical methods. *Mon. Wea. Rev.*, **94**, 399–405, [https://doi.org/10.1175/1520-0493\(1966\)094<0399:POHMBS>2.3.CO;2](https://doi.org/10.1175/1520-0493(1966)094<0399:POHMBS>2.3.CO;2).
- Miller, D. L., C. I. Mora, H. D. Grissino-Mayer, C. J. Mock, M. E. Uhle, and Z. Sharp, 2006: Tree-ring isotope records of tropical cyclone activity. *Proc. Natl. Acad. Sci. USA*, **103**, 14 294–14 297, <https://doi.org/10.1073/pnas.0606549103>.
- Miyamoto, Y., and T. Takemi, 2013: A transition mechanism for the spontaneous axisymmetric intensification of tropical cyclones. *J. Atmos. Sci.*, **70**, 112–129, <https://doi.org/10.1175/JAS-D-11-0285.1>.
- Mo, K. C., 2000: The association between intraseasonal oscillations and tropical storms in the Atlantic basin. *Mon. Wea. Rev.*, **128**, 4097–4107, [https://doi.org/10.1175/1520-0493\(2000\)129<4097:TABIOA>2.0.CO;2](https://doi.org/10.1175/1520-0493(2000)129<4097:TABIOA>2.0.CO;2).
- Molinari, J., and D. Vollaro, 1989: External influences on hurricane intensity. Part I: Outflow layer eddy angular momentum fluxes. *J. Atmos. Sci.*, **46**, 1093–1105, [https://doi.org/10.1175/1520-0469\(1989\)046<1093:EIOHIP>2.0.CO;2](https://doi.org/10.1175/1520-0469(1989)046<1093:EIOHIP>2.0.CO;2).
- , and —, 1990: External influences on hurricane intensity. Part II: Vertical structure and response of the hurricane vortex. *J. Atmos. Sci.*, **47**, 1902–1918, [https://doi.org/10.1175/1520-0469\(1990\)047<1902:EIOHIP>2.0.CO;2](https://doi.org/10.1175/1520-0469(1990)047<1902:EIOHIP>2.0.CO;2).
- , S. Skubis, and D. Vollaro, 1995: External influences on hurricane intensity. Part III: Potential vorticity structure. *J. Atmos. Sci.*, **52**, 3593–3606, [https://doi.org/10.1175/1520-0469\(1995\)052<3593:EIOHIP>2.0.CO;2](https://doi.org/10.1175/1520-0469(1995)052<3593:EIOHIP>2.0.CO;2).
- , D. Knight, M. Dickinson, D. Vollaro, and S. Skubis, 1997: Potential vorticity, easterly waves, and eastern Pacific tropical cyclogenesis. *Mon. Wea. Rev.*, **125**, 2699–2708, [https://doi.org/10.1175/1520-0493\(1997\)125<2699:PVEWAE>2.0.CO;2](https://doi.org/10.1175/1520-0493(1997)125<2699:PVEWAE>2.0.CO;2).
- , S. Skubis, D. Vollaro, F. Alsheimer, and H. E. Willoughby, 1998: Potential vorticity analysis of tropical cyclone intensification. *J. Atmos. Sci.*, **55**, 2632–2644, [https://doi.org/10.1175/1520-0469\(1998\)055<2632:PVAOTC>2.0.CO;2](https://doi.org/10.1175/1520-0469(1998)055<2632:PVAOTC>2.0.CO;2).
- , D. Vollaro, and K. L. Corbosiero, 2004: Tropical cyclone formation in a sheared environment: A case study. *J. Atmos. Sci.*, **61**, 2493–2509, <https://doi.org/10.1175/JAS3291.1>.
- , P. Dodge, D. Vollaro, K. L. Corbosiero, and F. Marks Jr., 2006: Mesoscale aspects of the downshear reformation of a tropical cyclone. *J. Atmos. Sci.*, **63**, 341–354, <https://doi.org/10.1175/JAS3591.1>.
- Möller, J. D., and M. T. Montgomery, 2000: Tropical cyclone evolution via potential vorticity anomalies in a three-dimensional balance model. *J. Atmos. Sci.*, **57**, 3366–3387, [https://doi.org/10.1175/1520-0469\(2000\)057<3366:TCEVPV>2.0.CO;2](https://doi.org/10.1175/1520-0469(2000)057<3366:TCEVPV>2.0.CO;2).
- Montgomery, M. T., and L. J. Shapiro, 1995: Generalized Charney–Stern and Fjortoft theorems for rapidly rotating vortices. *J. Atmos. Sci.*, **52**, 1829–1833, [https://doi.org/10.1175/1520-0469\(1995\)052<1829:GCAFTF>2.0.CO;2](https://doi.org/10.1175/1520-0469(1995)052<1829:GCAFTF>2.0.CO;2).
- , and R. Kallenback, 1997: A theory for vortex Rossby-waves and its application to spiral bands and intensity changes in hurricanes. *Quart. J. Roy. Meteor. Soc.*, **123**, 435–465, <https://doi.org/10.1002/qj.49712353810>.
- , and J. Enagonio, 1998: Tropical cyclogenesis via convectively forced vortex Rossby waves in a three-dimensional quasigeostrophic model. *J. Atmos. Sci.*, **55**, 3176–3207, [https://doi.org/10.1175/1520-0469\(1998\)055<3176:TCVCFV>2.0.CO;2](https://doi.org/10.1175/1520-0469(1998)055<3176:TCVCFV>2.0.CO;2).

- , and R. K. Smith, 2012: The genesis of Typhoon Nuri as observed during the tropical cyclone structure 2008 (TCS08) field experiment. Part 2: Observations of the convective environment. *Atmos. Chem. Phys.*, **12**, 4001–4009, <https://doi.org/10.5194/acp-12-4001-2012>.
- , and —, 2014: Paradigms for tropical cyclone intensification. *Aust. Meteor. Ocean J.*, **64**, 37–66, <https://doi.org/10.22499/2.6401.005>.
- , H. D. Snell, and Z. Yang, 2001: Axisymmetric spindown dynamics of hurricane-like vortices. *J. Atmos. Sci.*, **58**, 421–435, [https://doi.org/10.1175/1520-0469\(2001\)058<0421:ASDOHL>2.0.CO;2](https://doi.org/10.1175/1520-0469(2001)058<0421:ASDOHL>2.0.CO;2).
- , M. E. Nicholls, T. A. Cram, and A. B. Saunders, 2006: A vortical hot tower route to tropical cyclogenesis. *J. Atmos. Sci.*, **63**, 355–386, <https://doi.org/10.1175/JAS3604.1>.
- , R. Smith, and N. van Sang, 2010: Sensitivity of tropical cyclone models to the surface drag coefficient. *Quart. J. Roy. Meteor. Soc.*, **136**, 1945–1953, <https://doi.org/10.1002/qj.702>.
- , and Coauthors, 2012: The Pre-Depression Investigation of Cloud-Systems in the Tropics (PREDICT) experiment: Scientific basis, new analysis tools, and some first results. *Bull. Amer. Meteor. Soc.*, **93**, 153–172, <https://doi.org/10.1175/BAMS-D-11-00046.1>.
- Moon, I.-J., I. Ginis, and T. Hara, 2004: Effect of surface waves on air–sea momentum exchange. Part II: Behavior of drag coefficient under tropical cyclones. *J. Atmos. Sci.*, **61**, 2334–2348, [https://doi.org/10.1175/1520-0469\(2004\)061<2334:EOSWOA>2.0.CO;2](https://doi.org/10.1175/1520-0469(2004)061<2334:EOSWOA>2.0.CO;2).
- Moon, Y., and D. S. Nolan, 2015a: Spiral rainbands in a numerical simulation of Hurricane Bill (2009). Part I: Structures and comparisons to observations. *J. Atmos. Sci.*, **72**, 164–190, <https://doi.org/10.1175/JAS-D-14-0058.1>.
- , and —, 2015b: Spiral rainbands in a numerical simulation of Hurricane Bill (2009). Part II: Propagation of inner rainbands. *J. Atmos. Sci.*, **72**, 191–215, <https://doi.org/10.1175/JAS-D-14-0056.1>.
- Mora, C. I., D. L. Miller, and H. D. Grissino-Mayer, 2007: Oxygen isotope proxies in tree-ring cellulose: Tropical cyclones, drought, and climate oscillations. *Terr. Ecol.*, **1**, 63–75, [https://doi.org/10.1016/S1936-7961\(07\)01005-6](https://doi.org/10.1016/S1936-7961(07)01005-6).
- Morey, S. L., M. A. Bourassa, D. S. Dukhovskoy, and J. J. O'Brien, 2006: Modeling studies of the upper ocean response to a tropical cyclone. *Ocean Dyn.*, **56**, 594–606, <https://doi.org/10.1007/s10236-006-0085-y>.
- Morrison, I., S. Businger, F. Marks, P. Dodge, and J. A. Businger, 2005: An observational case for the prevalence of roll vortices in the hurricane boundary layer. *J. Atmos. Sci.*, **62**, 2662–2673, <https://doi.org/10.1175/JAS3508.1>.
- Moscatello, A., M. M. Miglietta, and R. Rotunno, 2008: Observational analysis of a Mediterranean ‘hurricane’ over south-eastern Italy. *Weather*, **63**, 306–311, <https://doi.org/10.1002/wea.231>.
- Moskatis, J. R., 2009: Toward improved tropical cyclone intensity forecasts: Probabilistic prediction, predictability, and the role of verification. Ph.D. thesis, Dept. of Earth, Atmospheric, and Planetary Sciences, Massachusetts Institute of Technology, 214 pp., <http://hdl.handle.net/1721.1/47846>.
- Mrowiec, A. A., S. T. Garner, and O. M. Pauluis, 2011: Axisymmetric hurricane in a dry atmosphere: Theoretical framework and numerical experiments. *J. Atmos. Sci.*, **68**, 1607–1619, <https://doi.org/10.1175/2011JAS3639.1>.
- Munksgaard, N. C., C. Zwart, N. Kurita, A. Bass, J. Nott, and M. I. Bird, 2015: Stable isotope anatomy of Tropical Cyclone Ita, north-eastern Australia, April 2014. *PLOS ONE*, **10**, <https://doi.org/10.1371/journal.pone.0119728>.
- Muramatsu, T., 1986: The structure of polygonal eye of a typhoon. *J. Meteor. Soc. Japan*, **64**, 913–921, [https://doi.org/10.2151/jmsj1965.64.6\\_913](https://doi.org/10.2151/jmsj1965.64.6_913).
- Murnane, R., and K.-B. Liu, Eds., 2004: *Hurricanes and Typhoons: Past, Present, and Future*. Columbia University Press, 464 pp.
- Nakamura, J., U. Lall, Y. Kushnir, and S. J. Camargo, 2009: Classifying North Atlantic tropical cyclone tracks by mass moments. *J. Climate*, **22**, 5481–5494, <https://doi.org/10.1175/2009JCLI2828.1>.
- Namias, J., 1955: Tropical cyclones related to the atmosphere’s general circulation. *Trans. N. Y. Acad. Sci. Ser. II*, **17**, 346–349.
- National Hurricane Center, 2018: National Hurricane Center forecast verification: Official error trends. <https://www.nhc.noaa.gov/verification/verify5.shtml>.
- Navarro, E. L., and G. J. Hakim, 2016: Idealized numerical modeling of the diurnal cycle of tropical cyclones. *J. Atmos. Sci.*, **73**, 4189–4201, <https://doi.org/10.1175/JAS-D-15-0349.1>.
- Naylor, J., and D. A. Schecter, 2014: Evaluation of the impact of moist convection on the development of asymmetric inner core instabilities in simulated tropical cyclones. *J. Adv. Model. Earth Syst.*, **6**, 1027–1048, <https://doi.org/10.1002/2014MS000366>.
- Nolan, D. S., 2001: The stabilizing effects of axial stretching on turbulent vortex dynamics. *Phys. Fluids*, **13**, 1724–1738, <https://doi.org/10.1063/1.1370390>.
- , 2007: What is the trigger for tropical cyclogenesis? *Aust. Meteor. Mag.*, **56**, 241–266, <http://www.bom.gov.au/jshess/docs/2007/nolan.pdf>.
- , and B. F. Farrell, 1999: Generalized stability analyses of asymmetric disturbances in one- and two-celled vortices maintained by radial inflow. *J. Atmos. Sci.*, **56**, 1282–1307, [https://doi.org/10.1175/1520-0469\(1999\)056<1282:GSAOAD>2.0.CO;2](https://doi.org/10.1175/1520-0469(1999)056<1282:GSAOAD>2.0.CO;2).
- , and M. T. Montgomery, 2002: Nonhydrostatic, three-dimensional perturbations to balanced, hurricane-like vortices. Part I: Linearized formulation, stability, and evolution. *J. Atmos. Sci.*, **59**, 2989–3020, [https://doi.org/10.1175/1520-0469\(2002\)059<2989:NTDPTB>2.0.CO;2](https://doi.org/10.1175/1520-0469(2002)059<2989:NTDPTB>2.0.CO;2).
- , and L. D. Grasso, 2003: Nonhydrostatic, three-dimensional perturbations to balanced, hurricane-like vortices. Part II: Symmetric response and nonlinear simulations. *J. Atmos. Sci.*, **60**, 2717–2745, [https://doi.org/10.1175/1520-0469\(2003\)060<2717:NTPTBH>2.0.CO;2](https://doi.org/10.1175/1520-0469(2003)060<2717:NTPTBH>2.0.CO;2).
- , and M. G. McGauley, 2012: Tropical cyclogenesis in wind shear: Climatological relationships and physical processes. *Cyclones: Formation, Triggers, and Control*, K. Oouchi and H. Fudeyasu, Eds., Nova Science Publishers, 1–36.
- , and J. A. Zhang, 2017: Spiral gravity waves radiating from tropical cyclones. *Geophys. Res. Lett.*, **44**, 3924–3931, <https://doi.org/10.1002/2017GL073572>.
- , Y. Moon, and D. P. Stern, 2007a: Tropical cyclone intensification from asymmetric convection: Energetics and efficiency. *J. Atmos. Sci.*, **64**, 3377–3405, <https://doi.org/10.1175/JAS3988.1>.
- , E. D. Rappin, and K. A. Emanuel, 2007b: Tropical cyclogenesis sensitivity to environmental parameters in radiative–convective equilibrium. *Quart. J. Roy. Meteor. Soc.*, **133**, 2085–2107, <https://doi.org/10.1002/qj.170>.
- Nong, S., and K. Emanuel, 2003: Concentric eyewalls in hurricanes. *Quart. J. Roy. Meteor. Soc.*, **129**, 3323–3338, <https://doi.org/10.1256/qj.01.132>.

- Nordeng, T. E., 1990: A model-based diagnostic study of the development and maintenance mechanism of two polar lows. *Tellus*, **42A**, 92–108, <https://doi.org/10.3402/tellusa.v42i1.11863>.
- , and E. A. Rasmussen, 1992: A most beautiful polar low. A case study of a polar low development in the Bear Island region. *Tellus*, **44A**, 81–99, <https://doi.org/10.3402/tellusa.v44i2.14947>.
- Nott, J., 2004: Palaeotempestology: The study of and implications review article prehistoric tropical cyclones—A review for hazard assessment. *Environ. Int.*, **30**, 433–447, <https://doi.org/10.1016/j.envint.2003.09.010>.
- , 2011a: A 6000 year tropical cyclone record from Western Australia. *Quat. Sci. Rev.*, **30**, 713–722, <https://doi.org/10.1016/j.quascirev.2010.12.004>.
- , 2011b: Tropical cyclones, global climate change and the role of Quaternary studies. *J. Quat. Sci.*, **26**, 468–473, <https://doi.org/10.1002/jqs.1524>.
- , and T. H. Jagger, 2013: Deriving robust return periods for tropical cyclone inundations from sediments. *Geophys. Res. Lett.*, **40**, 370–373, <https://doi.org/10.1029/2012GL054455>.
- , S. Smithers, K. Walsh, and E. Rhodes, 2009: Sand beach ridges record 6000 year history of extreme tropical cyclone activity in northeastern Australia. *Quat. Sci. Rev.*, **28**, 1511–1520, <https://doi.org/10.1016/j.quascirev.2009.02.014>.
- , C. Chague-Goff, J. Goff, C. Sloss, and N. Riggs, 2013: Anatomy of sand beach ridges: Evidence from severe Tropical Cyclone Yasi and its predecessors, northeast Queensland, Australia. *J. Geophys. Res. Earth Surf.*, **118**, 1710–1719, <https://doi.org/10.1002/jgrf.20122>.
- O'Brien, J. J., 1967: The non-linear response of a two-layer, baroclinic ocean to a stationary, axially-symmetric hurricane. Part II. Upwelling and mixing induced by momentum transfer. *J. Atmos. Sci.*, **24**, 208–214, [https://doi.org/10.1175/1520-0469\(1967\)024<0208:TNLROA>2.0.CO;2](https://doi.org/10.1175/1520-0469(1967)024<0208:TNLROA>2.0.CO;2).
- , and R. O. Reid, 1967: The non-linear response of a two-layer, baroclinic ocean to a stationary, axially-symmetric hurricane: Part I. Upwelling induced by momentum transfer. *J. Atmos. Sci.*, **24**, 197–207, [https://doi.org/10.1175/1520-0469\(1967\)024<0197:TNLROA>2.0.CO;2](https://doi.org/10.1175/1520-0469(1967)024<0197:TNLROA>2.0.CO;2).
- Olander, T. L., and C. S. Velden, 2007: The advanced Dvorak technique: Continued development of an objective scheme to estimate tropical cyclone intensity using geostationary infrared satellite imagery. *Wea. Forecasting*, **22**, 287–298, <https://doi.org/10.1175/WAF975.1>.
- Onderlinde, M. J., and H. E. Fuelberg, 2014: A parameter for forecasting tornadoes associated with landfalling tropical cyclones. *Wea. Forecasting*, **29**, 1238–1255, <https://doi.org/10.1175/WAF-D-13-00086.1>.
- O'Neill, M. E., K. A. Emanuel, and G. R. Flierl, 2015: Polar vortex formation in giant-planet atmospheres due to moist convection. *Nat. Geosci.*, **8**, 523–526, <https://doi.org/10.1038/ngeo2459>.
- , D. Perez-Betancourt, and A. A. Wing, 2017: Accessible environments for diurnal-period waves in simulated tropical cyclones. *J. Atmos. Sci.*, **74**, 2489–2502, <https://doi.org/10.1175/JAS-D-16-0294.1>.
- Ooyama, K., 1964: A dynamical model for the study of tropical cyclone development. *Geofis. Int.*, **4**, 187–198.
- , 1969: Numerical simulation of the life-cycle of tropical cyclones. *J. Atmos. Sci.*, **26**, 3–40, [https://doi.org/10.1175/1520-0469\(1969\)026<0003:NSOTLC>2.0.CO;2](https://doi.org/10.1175/1520-0469(1969)026<0003:NSOTLC>2.0.CO;2).
- Ortiz, F., 1947: *El Huracán: Su Mitología y Sus Símbolos*. Fondo de Cultura Económica, 686 pp.
- Palmén, E., 1948: On the formation and structure of tropical hurricanes. *Geophysica*, **3**, 26–39.
- , 1985: In my opinion. . . . *Geophysica*, **21**, 5–18.
- Pasquero, C., and K. Emanuel, 2008: Tropical cyclones and transient upper-ocean warming. *J. Climate*, **21**, 149–162, <https://doi.org/10.1175/2007JCLI1550.1>.
- Patricola, C. M., R. Saravanan, and P. Chang, 2014: The impact of the El Niño–Southern Oscillation and Atlantic Meridional Mode on seasonal Atlantic tropical cyclone activity. *J. Climate*, **27**, 5311–5328, <https://doi.org/10.1175/JCLI-D-13-00687.1>.
- , S. J. Camargo, P. J. Klotzbach, R. Saravanan, and P. Chang, 2018a: The influence of ENSO flavors on western North Pacific tropical cyclone activity. *J. Climate*, **31**, 5395–5416, <https://doi.org/10.1175/JCLI-D-17-0678.1>.
- , R. Saravanan, and P. Chang, 2018b: The response of Atlantic tropical cyclones to suppression of African easterly waves. *Geophys. Res. Lett.*, **45**, 471–479, <https://doi.org/10.1002/2017GL076081>.
- Patterson, M. C. L., D. Osbrink, A. Brescia, D. Downer, J. Etro, and J. Cione, 2014: Atmospheric and ocean boundary layer profiling with unmanned air platforms. *Oceans 2014*, St. Johns, NL, Canada, IEEE, 7 pp., <https://doi.org/10.1109/OCEANS.2014.7002978>.
- Peduzzi, P., B. Chatenoux, H. Dao, A. De Bono, C. Herold, J. Kossin, F. Mouton, and O. Nordbeck, 2012: Global trends in tropical cyclone risk. *Nat. Climate Change*, **2**, 289–294, <https://doi.org/10.1038/nclimate1410>.
- Peng, K., R. Rotunno, and G. H. Bryan, 2018: Evaluation of a time-dependent model for the intensification of tropical cyclones. *J. Atmos. Sci.*, **75**, 2125–2138, <https://doi.org/10.1175/JAS-D-17-0382.1>.
- Peng, M. S., B.-F. Jeng, and R. T. Williams, 1999: A numerical study on tropical cyclone intensification. Part I: Beta effect and mean flow effect. *J. Atmos. Sci.*, **56**, 1404–1423, [https://doi.org/10.1175/1520-0469\(1999\)056<1404:ANSOTC>2.0.CO;2](https://doi.org/10.1175/1520-0469(1999)056<1404:ANSOTC>2.0.CO;2).
- Persing, J., and M. T. Montgomery, 2003: Hurricane superintensity. *J. Atmos. Sci.*, **60**, 2349–2371, [https://doi.org/10.1175/1520-0469\(2003\)060<2349:HS>2.0.CO;2](https://doi.org/10.1175/1520-0469(2003)060<2349:HS>2.0.CO;2).
- Pfeffer, R. L., and M. Challa, 1981: A numerical study of the role of eddy fluxes of momentum in the development of Atlantic hurricanes. *J. Atmos. Sci.*, **38**, 2393–2398, [https://doi.org/10.1175/1520-0469\(1981\)038<2393:ANSOTR>2.0.CO;2](https://doi.org/10.1175/1520-0469(1981)038<2393:ANSOTR>2.0.CO;2).
- Piddington, H., 1848: *The Sailor's Horn-Book for the Law of Storms*. 1st ed., Smith, Elder and Co., 292 pp.
- Pielke, R. A., Jr., and C. N. Landsea, 1999: La Niña, El Niño, and Atlantic hurricane damages in the United States. *Bull. Amer. Meteor. Soc.*, **80**, 2027–2034, [https://doi.org/10.1175/1520-0477\(1999\)080<2027:LNAENO>2.0.CO;2](https://doi.org/10.1175/1520-0477(1999)080<2027:LNAENO>2.0.CO;2).
- Powell, M. D., 1990: Boundary layer structure and dynamics in outer hurricane rainbands. Part II: Downdraft modification and mixed layer recovery. *Mon. Wea. Rev.*, **118**, 918–938, [https://doi.org/10.1175/1520-0493\(1990\)118<0918:BLSADI>2.0.CO;2](https://doi.org/10.1175/1520-0493(1990)118<0918:BLSADI>2.0.CO;2).
- , P. J. Vickery, and T. A. Reinhold, 2003: Reduced drag coefficients for high wind speeds in tropical cyclones. *Nature*, **422**, 279–283, <https://doi.org/10.1038/nature01481>.
- Price, J. F., 1981: Upper ocean response to a hurricane. *J. Phys. Oceanogr.*, **11**, 153–175, [https://doi.org/10.1175/1520-0485\(1981\)011<0153:UORTAH>2.0.CO;2](https://doi.org/10.1175/1520-0485(1981)011<0153:UORTAH>2.0.CO;2).
- Pudov, V. D., and A. A. V. K. N. Federov, 1979: Vertical structure of the wake of a typhoon in the upper ocean. *Okeanologiya*, **21**, 142–146.
- Pytharoulis, I., G. C. Craig, and S. P. Ballard, 2000: The hurricane-like Mediterranean cyclone of January 1995. *Meteor. Appl.*, **7**, 261–279, <https://doi.org/10.1017/S1350482700001511>.

- , I. T. Matsangouras, I. Tegoulas, S. Kotsopoulos, T. S. Karacostas, and P. T. Nastos, 2017: Numerical study of the medicane of November 2014. *Perspectives on Atmospheric Sciences*, T. Karacostas, A. Bais, and P. Nastos, Eds., Springer, 115–121, [https://doi.org/10.1007/978-3-319-35095-0\\_17](https://doi.org/10.1007/978-3-319-35095-0_17).
- Ramage, C. S., 1959: Hurricane development. *J. Meteor.*, **16**, 227–237, [https://doi.org/10.1175/1520-0469\(1959\)016<0227:HD>2.0.CO;2](https://doi.org/10.1175/1520-0469(1959)016<0227:HD>2.0.CO;2).
- , 1962: The subtropical cyclone. *J. Geophys. Res.*, **67**, 1401–1411, <https://doi.org/10.1029/JZ067i004p01401>.
- Ramsay, H. A., S. J. Camargo, and D. Kim, 2012: Cluster analysis of tropical cyclone tracks in the southern hemisphere. *Climate Dyn.*, **39**, 897–917, <https://doi.org/10.1007/s00382-011-1225-8>.
- Rappin, E. D., D. S. Nolan, and K. A. Emanuel, 2010: Thermodynamic control of tropical cyclogenesis in environments of radiative-convective equilibrium with shear. *Quart. J. Roy. Meteor. Soc.*, **136**, 1954–1971, <https://doi.org/10.1002/qj.706>.
- , M. C. Morgan, and G. J. Tripoli, 2011: The impact of outflow environment on tropical cyclone intensification and structure. *J. Atmos. Sci.*, **68**, 177–194, <https://doi.org/10.1175/2009JAS2970.1>.
- Rasmussen, E., 1979: The polar low as an extratropical CISK disturbance. *Quart. J. Roy. Meteor. Soc.*, **105**, 531–549, <https://doi.org/10.1002/qj.49710544504>.
- , 1981: An investigation of a polar low with a spiral cloud structure. *J. Atmos. Sci.*, **38**, 1785–1792, [https://doi.org/10.1175/1520-0469\(1981\)038<1785:AIOAPL>2.0.CO;2](https://doi.org/10.1175/1520-0469(1981)038<1785:AIOAPL>2.0.CO;2).
- , 1985: A case study of a polar low development over the Barents Sea. *Tellus*, **37A**, 407–418, <https://doi.org/10.1111/j.1600-0870.1985.tb00440.x>.
- , 2003: Polar lows. *A Half Century of Progress in Meteorology: A Tribute to Richard Reed*, Meteor. Monogr., No. 53, Amer. Meteor. Soc., 61–78.
- , and M. Lystad, 1987: The Norwegian polar lows project: A summary of the international conference on polar lows, 20–23 May 1986, Oslo, Norway. *Bull. Amer. Meteor. Soc.*, **68**, 801–816, <https://doi.org/10.1175/1520-0477-68.7.783>.
- , and C. Zick, 1987: A subsynoptic vortex over the Mediterranean with some resemblance to polar lows. *Tellus*, **39A**, 408–425, <https://doi.org/10.1111/j.1600-0870.1987.tb00318.x>.
- , T. B. Pedersen, L. T. Pedersen, and J. Turner, 1992: Polar lows and arctic instability lows in the Bear Island region. *Tellus*, **44A**, 133–154, <https://doi.org/10.3402/tellusa.v44i2.14950>.
- Raymond, D. J., 1992: Nonlinear balance and potential-vorticity thinking at large Rossby number. *Quart. J. Roy. Meteor. Soc.*, **118**, 987–1015, <https://doi.org/10.1002/qj.49711850708>.
- , and S. L. Sessions, 2007: Evolution of convection during tropical cyclogenesis. *Geophys. Res. Lett.*, **34**, L06811, <https://doi.org/10.1029/2006GL028607>.
- , —, and C. L. Carrillo, 2011: Thermodynamics of tropical cyclogenesis in the northwest Pacific. *J. Geophys. Res.*, **116**, D18101, <https://doi.org/10.1029/2011JD015624>.
- , S. Gjorgjievska, S. Sessions, and Z. Fuchs, 2014: Tropical cyclogenesis and mid-level vorticity. *Aust. Meteor. Mag.*, **64**, 11–25, <http://www.bom.gov.au/jshess/docs/2014/ramond.pdf>.
- Reasor, P. D., and M. T. Montgomery, 2001: Three-dimensional alignment and corotation of weak, TC-like vortices via linear vortex Rossby waves. *J. Atmos. Sci.*, **58**, 2306–2330, [https://doi.org/10.1175/1520-0469\(2001\)058<2306:TDAACO>2.0.CO;2](https://doi.org/10.1175/1520-0469(2001)058<2306:TDAACO>2.0.CO;2).
- , and —, 2015: Evaluation of a heuristic model for tropical cyclone resilience. *J. Atmos. Sci.*, **72**, 1765–1782, <https://doi.org/10.1175/JAS-D-14-0318.1>.
- , —, and L. D. Grasso, 2004: A new look at the problem of tropical cyclones in vertical shear flow: Vortex resiliency. *J. Atmos. Sci.*, **61**, 3–22, [https://doi.org/10.1175/1520-0469\(2004\)061<0003:ANLATP>2.0.CO;2](https://doi.org/10.1175/1520-0469(2004)061<0003:ANLATP>2.0.CO;2).
- Reed, R. J., and C. N. Duncan, 1987: Baroclinic instability as a mechanism for the serial development of polar lows: A case study. *Tellus*, **39A**, 376–384, <https://doi.org/10.3402/tellusa.v39i4.11766>.
- Reznik, G. M., and W. K. Dewar, 1994: An analytical theory of distributed axisymmetric barotropic vortices on the beta-plane. *J. Fluid Mech.*, **269**, 301–321, <https://doi.org/10.1017/S0022112094001576>.
- Richter, D. H., and D. P. Stern, 2014: Evidence of spray-mediated air-sea enthalpy flux within tropical cyclones. *Geophys. Res. Lett.*, **41**, 2997–3003, <https://doi.org/10.1002/2014GL059746>.
- Riehl, H., 1948a: On the formation of typhoons. *J. Meteor.*, **5**, 247–265, [https://doi.org/10.1175/1520-0469\(1948\)005<0247:OTFOT>2.0.CO;2](https://doi.org/10.1175/1520-0469(1948)005<0247:OTFOT>2.0.CO;2).
- , 1948b: On the formation of west Atlantic hurricanes. University of Chicago Dept. of Meteorology Misc. Rep. 24, 64 pp.
- , 1950: A model of hurricane formation. *J. Appl. Phys.*, **21**, 917–925, <https://doi.org/10.1063/1.1699784>.
- , 1951: Aerology of tropical storms. *Compendium of Meteorology*, T. F. Malone, Ed., Amer. Meteor. Soc., 902–913.
- , 1954: *Tropical Meteorology*. McGraw-Hill, 392 pp.
- , 1963a: On the origin and possible modification of hurricanes. *Science*, **141**, 1001–1010, <https://doi.org/10.1126/science.141.3585.1001>.
- , 1963b: Some relations between wind and thermal structure of steady state hurricanes. *J. Atmos. Sci.*, **20**, 276–287, [https://doi.org/10.1175/1520-0469\(1963\)020<0276:SRBWAT>2.0.CO;2](https://doi.org/10.1175/1520-0469(1963)020<0276:SRBWAT>2.0.CO;2).
- , 1975: Further studies on the origin of hurricanes. Colorado State University Dept. of Atmospheric Science Rep. 235, 24 pp., <http://hermes.cde.state.co.us/drupal/islandora/object/co%3A9028>.
- , and R. J. Shafer, 1944: The recurvature of tropical storms. *J. Meteor.*, **1**, 42–54, [https://doi.org/10.1175/1520-0469\(1944\)001<0001:TROTS>2.0.CO;2](https://doi.org/10.1175/1520-0469(1944)001<0001:TROTS>2.0.CO;2).
- Riemer, M., and S. C. Jones, 2010: The downstream impact of tropical cyclones on a developing baroclinic wave in idealized scenarios of extratropical transition. *Quart. J. Roy. Meteor. Soc.*, **136**, 617–637, <https://doi.org/10.1002/qj.605>.
- , —, and C. A. Davis, 2008: The impact of extratropical transition on the downstream flow: An idealized modelling study with a straight jet. *Quart. J. Roy. Meteor. Soc.*, **134**, 69–91, <https://doi.org/10.1002/qj.189>.
- , M. T. Montgomery, and M. E. Nicholls, 2010: A new paradigm for intensity modification of tropical cyclones: Thermodynamic impact of vertical wind shear on the inflow layer. *Atmos. Chem. Phys.*, **10**, 3163–3188, <https://doi.org/10.5194/acp-10-3163-2010>.
- , —, and —, 2013: Further examination of the thermodynamic modification of the inflow layer of tropical cyclones by vertical wind shear. *Atmos. Chem. Phys.*, **13**, 327–346, <https://doi.org/10.5194/acp-13-327-2013>.
- Ritchie, E. A., and G. J. Holland, 1993: On the interaction of tropical-cyclone-scale vortices. II: Discrete vortex patches. *Quart. J. Roy. Meteor. Soc.*, **119**, 1363–1379, <https://doi.org/10.1002/qj.49711951407>.
- , and R. L. Elsberry, 2001: Simulations of the transformation stage of the extratropical transition of tropical cyclones. *Mon. Wea. Rev.*, **129**, 1462–1480, [https://doi.org/10.1175/1520-0493\(2001\)129<1462:SOTTSSO>2.0.CO;2](https://doi.org/10.1175/1520-0493(2001)129<1462:SOTTSSO>2.0.CO;2).
- , and —, 2003: Simulations of the extratropical transition of tropical cyclones: Contributions by the midlatitude

- upper-level trough to reintensification. *Mon. Wea. Rev.*, **131**, 2112–2128, [https://doi.org/10.1175/1520-0493\(2003\)131<2112:SOTETO>2.0.CO;2](https://doi.org/10.1175/1520-0493(2003)131<2112:SOTETO>2.0.CO;2).
- , and —, 2007: Simulations of the extratropical transition of tropical cyclones: Phasing between the upper-level trough and tropical cyclones. *Mon. Wea. Rev.*, **135**, 862–876, <https://doi.org/10.1175/MWR3303.1>.
- Robe, F. R., and K. Emanuel, 1996: Dependence of tropical convection on radiative forcing. *J. Atmos. Sci.*, **53**, 3265–3275, [https://doi.org/10.1175/1520-0469\(1996\)053<3265:MCSSIF>2.0.CO;2](https://doi.org/10.1175/1520-0469(1996)053<3265:MCSSIF>2.0.CO;2).
- Rodgers, E. B., J. Stout, J. Steranka, and S. Chang, 1990: Tropical cyclone-upper atmospheric interaction as inferred from satellite total ozone observations. *J. Appl. Meteor.*, **29**, 934–954, [https://doi.org/10.1175/1520-0450\(1990\)029<0934:TCUAI>2.0.CO;2](https://doi.org/10.1175/1520-0450(1990)029<0934:TCUAI>2.0.CO;2).
- , S. W. Chang, J. Stout, J. Steranka, and J.-J. Shi, 1991: Satellite observations of variations in tropical cyclone convection caused by upper-tropospheric troughs. *J. Appl. Meteor.*, **30**, 1163–1184, [https://doi.org/10.1175/1520-0450\(1991\)030<1163:SOOVIT>2.0.CO;2](https://doi.org/10.1175/1520-0450(1991)030<1163:SOOVIT>2.0.CO;2).
- Rodríguez-Fonseca, B., and Coauthors, 2016: A review of ENSO influence on the North Atlantic. A non-stationary signal. *Atmosphere*, **7**, 87, <https://doi.org/10.3390/atmos7070087>.
- Rogers, L. J., L. J. Moore, E. B. Goldstein, C. J. Hein, J. Lorenzo-Trueba, and A. D. Ashton, 2015: Anthropogenic controls on overwash deposition: Evidence and consequences. *J. Geophys. Res. Earth Surf.*, **120**, 2609–2624, <https://doi.org/10.1002/2015JF003634>.
- Rogers, R., S. Chen, J. Tenerelli, and H. E. Willoughby, 2003: A numerical study of the impact of vertical shear on the distribution of rainfall in Hurricane Bonnie (1998). *Mon. Wea. Rev.*, **131**, 1577–1599, <https://doi.org/10.1175/2546.1>.
- , and Coauthors, 2013: NOAA's Hurricane Intensity Forecasting Experiment: A progress report. *Bull. Amer. Meteor. Soc.*, **94**, 859–882, <https://doi.org/10.1175/BAMS-D-12-00089.1>.
- Rosenthal, S. L., 1964: Some attempts to simulate the development of tropical cyclones by numerical methods. *Mon. Wea. Rev.*, **92**, 1–21, [https://doi.org/10.1175/1520-0493\(1964\)092<0001:SATSTD>2.3.CO;2](https://doi.org/10.1175/1520-0493(1964)092<0001:SATSTD>2.3.CO;2).
- , 1971: The response of a tropical cyclone model to variations in boundary layer parameters, initial conditions, lateral boundary conditions and domain size. *Mon. Wea. Rev.*, **99**, 767–777, [https://doi.org/10.1175/1520-0493\(1971\)099<0767:TROATC>2.3.CO;2](https://doi.org/10.1175/1520-0493(1971)099<0767:TROATC>2.3.CO;2).
- Rossby, C.-G., 1948: On displacement and intensity changes of atmospheric vortices. *J. Mar. Res.*, **7**, 175–187.
- Rotunno, R., 1978: A note on the stability of a cylindrical vortex sheet. *J. Fluid Mech.*, **87**, 761–771, <https://doi.org/10.1017/S0022112078001871>.
- , and K. A. Emanuel, 1987: An air–sea interaction theory for tropical cyclones. Part II: Evolutionary study using a non-hydrostatic axisymmetric numerical model. *J. Atmos. Sci.*, **44**, 542–561, [https://doi.org/10.1175/1520-0469\(1987\)044<0542:AAITFT>2.0.CO;2](https://doi.org/10.1175/1520-0469(1987)044<0542:AAITFT>2.0.CO;2).
- , and G. H. Bryan, 2012: Effects of parameterized diffusion on simulated hurricanes. *J. Atmos. Sci.*, **69**, 2284–2299, <https://doi.org/10.1175/JAS-D-11-0204.1>.
- , J. B. Klemp, and M. L. Weisman, 1988: A theory for strong, long-lived squall lines. *J. Atmos. Sci.*, **45**, 463–485, [https://doi.org/10.1175/1520-0469\(1988\)045<0463:ATFSL>2.0.CO;2](https://doi.org/10.1175/1520-0469(1988)045<0463:ATFSL>2.0.CO;2).
- Rozoff, C. M., D. S. Nolan, J. P. Kossin, F. Zhang, and J. Fang, 2012: The roles of an expanding wind field and inertial stability in tropical cyclone secondary eyewall formation. *J. Atmos. Sci.*, **69**, 2621–2643, <https://doi.org/10.1175/JAS-D-11-0326.1>.
- Ruf, C. S., and Coauthors, 2016: New ocean winds satellite mission to probe hurricanes and tropical convection. *Bull. Amer. Meteor. Soc.*, **97**, 385–395, <https://doi.org/10.1175/BAMS-D-14-00218.1>.
- Sabuwala, T., G. Gioia, and P. Chakraborty, 2015: Effect of rain-power on hurricane intensity. *Geophys. Res. Lett.*, **42**, 3024–3029, <https://doi.org/10.1002/2015GL063785>.
- Sadler, J. C., 1976: A role of the tropical upper tropospheric trough in early season typhoon development. *Mon. Wea. Rev.*, **104**, 1266–1278, [https://doi.org/10.1175/1520-0493\(1976\)104<1266:AROTTU>2.0.CO;2](https://doi.org/10.1175/1520-0493(1976)104<1266:AROTTU>2.0.CO;2).
- Sanders, F., and R. W. Burpee, 1968: Experiments in barotropic hurricane track forecasting. *J. Appl. Meteor.*, **7**, 313–323, [https://doi.org/10.1175/1520-0450\(1968\)007<0313:EIBHTF>2.0.CO;2](https://doi.org/10.1175/1520-0450(1968)007<0313:EIBHTF>2.0.CO;2).
- Sanford, T. B., P. G. Black, J. R. Haustein, J. W. Feeney, G. Z. Forristall, and J. F. Price, 1987: Ocean response to a hurricane. Part I: Observations. *J. Phys. Oceanogr.*, **17**, 2065–2083, [https://doi.org/10.1175/1520-0485\(1987\)017<2065:ORTAHP>2.0.CO;2](https://doi.org/10.1175/1520-0485(1987)017<2065:ORTAHP>2.0.CO;2).
- , J. F. Price, J. B. Girton, and D. C. Webb, 2007: Highly resolved observations and simulations of the ocean response to a hurricane. *Geophys. Res. Lett.*, **34**, L13604, <https://doi.org/10.1029/2007GL029679>.
- , —, and —, 2011: Upper-ocean response to Hurricane Frances (2004) observed by profiling EM-APEX floats. *J. Phys. Oceanogr.*, **41**, 1041–1056, <https://doi.org/10.1175/2010JPO4313.1>.
- Sardie, J. M., and T. T. Warner, 1985: A numerical study of the development mechanisms of polar lows. *Tellus*, **37A**, 460–477, <https://doi.org/10.1111/j.1600-0870.1985.tb00444.x>.
- Sasaki, Y., and K. Miyakoda, 1954: Numerical forecasting of the movement of cyclone. *J. Meteor. Soc. Japan*, **32**, 325–335, [https://doi.org/10.2151/jmsj1923.32.11-12\\_325](https://doi.org/10.2151/jmsj1923.32.11-12_325).
- Saunders, M. A., R. E. Chandler, C. J. Merchant, and F. P. Roberts, 2000: Atlantic hurricanes and NW Pacific typhoons: ENSO spatial impacts on occurrence and landfall. *Geophys. Res. Lett.*, **27**, 1147–1150, <https://doi.org/10.1029/1999GL010948>.
- Schade, L. R., and K. A. Emanuel, 1999: The ocean's effect on the intensity of tropical cyclones: Results from a simple coupled atmosphere–ocean model. *J. Atmos. Sci.*, **56**, 642–651, [https://doi.org/10.1175/1520-0469\(1999\)056<0642:TOSEOT>2.0.CO;2](https://doi.org/10.1175/1520-0469(1999)056<0642:TOSEOT>2.0.CO;2).
- Schechter, D. A., 2015: Response of a simulated hurricane to misalignment forcing compared to the predictions of a simple theory. *J. Atmos. Sci.*, **72**, 1235–1260, <https://doi.org/10.1175/JAS-D-14-0149.1>.
- , and D. H. E. Dubin, 1999: Vortex motion driven by a background vorticity gradient. *Phys. Rev. Lett.*, **83**, 2191–2194, <https://doi.org/10.1103/PhysRevLett.83.2191>.
- , and M. T. Montgomery, 2003: On the symmetrization rate of an intense geophysical vortex. *Dyn. Atmos. Oceans*, **37**, 55–88, [https://doi.org/10.1016/S0377-0265\(03\)00015-0](https://doi.org/10.1016/S0377-0265(03)00015-0).
- , and —, 2007: Waves in a cloudy vortex. *J. Atmos. Sci.*, **64**, 314–337, <https://doi.org/10.1175/JAS3849.1>.
- , —, and P. D. Reasor, 2002: A theory for the vertical alignment of a quasigeostrophic vortex. *J. Atmos. Sci.*, **59**, 150–168, [https://doi.org/10.1175/1520-0469\(2002\)059<0150:ATFTVA>2.0.CO;2](https://doi.org/10.1175/1520-0469(2002)059<0150:ATFTVA>2.0.CO;2).
- Schreck, C. J., III, and J. Molinari, 2011: Tropical cyclogenesis associated with Kelvin waves and the Madden–Julian oscillation. *Mon. Wea. Rev.*, **139**, 2723–2734, <https://doi.org/10.1175/MWR-D-10-05060.1>.
- Schubert, W. H., and J. J. Hack, 1983: Transformed Eliassen-balanced vortex model. *J. Atmos. Sci.*, **40**, 1571–1583, [https://doi.org/10.1175/1520-0469\(1983\)040<1571:TEBVM>2.0.CO;2](https://doi.org/10.1175/1520-0469(1983)040<1571:TEBVM>2.0.CO;2).

- , M. T. Montgomery, R. K. Taft, T. A. Guinn, S. R. Fulton, J. P. Kossin, and J. P. Edwards, 1999: Polygonal eyewalls, asymmetric eye contraction, and potential vorticity mixing in hurricanes. *J. Atmos. Sci.*, **56**, 1197–1223, [https://doi.org/10.1175/1520-0469\(1999\)056<1197:PEAECA>2.0.CO;2](https://doi.org/10.1175/1520-0469(1999)056<1197:PEAECA>2.0.CO;2).
- Schultz, L. A., and D. J. Cecil, 2009: Tropical cyclone tornadoes, 1950–2007. *Mon. Wea. Rev.*, **137**, 3471–3484, <https://doi.org/10.1175/2009MWR2896.1>.
- Scileppi, E., and J. P. Donnelly, 2007: Sedimentary evidence of hurricane strikes in western long island, New York. *Geochem. Geophys. Geosyst.*, **8**, Q06011, <https://doi.org/10.1029/2006GC001463>.
- Scoccimarro, E., and Coauthors, 2011: Effects of tropical cyclones on ocean heat transport in a high-resolution coupled general circulation model. *J. Climate*, **24**, 4368–4384, <https://doi.org/10.1175/2011JCLI4104.1>.
- Senn, H. V., and H. W. Hiser, 1959: On the origin of hurricane spiral rain bands. *J. Meteor.*, **16**, 419–426, [https://doi.org/10.1175/1520-0469\(1959\)016<0419:OTOOHS>2.0.CO;2](https://doi.org/10.1175/1520-0469(1959)016<0419:OTOOHS>2.0.CO;2).
- Shapiro, L. J., 1982a: Hurricane climatic fluctuations. Part I: Patterns and cycles. *Mon. Wea. Rev.*, **110**, 1007–1013, [https://doi.org/10.1175/1520-0493\(1982\)110<1007:HCFPIP>2.0.CO;2](https://doi.org/10.1175/1520-0493(1982)110<1007:HCFPIP>2.0.CO;2).
- , 1982b: Hurricane climatic fluctuations. Part II: Relation to large-scale circulation. *Mon. Wea. Rev.*, **110**, 1014–1023, [https://doi.org/10.1175/1520-0493\(1982\)110<1014:HCFPIR>2.0.CO;2](https://doi.org/10.1175/1520-0493(1982)110<1014:HCFPIR>2.0.CO;2).
- , 1983: The asymmetric boundary layer flow under a translating hurricane. *J. Atmos. Sci.*, **40**, 1984–1998, [https://doi.org/10.1175/1520-0469\(1983\)040<1984:TABLFU>2.0.CO;2](https://doi.org/10.1175/1520-0469(1983)040<1984:TABLFU>2.0.CO;2).
- , and J. L. Franklin, 1999: Potential vorticity asymmetries and tropical cyclone motion. *Mon. Wea. Rev.*, **127**, 124–131, [https://doi.org/10.1175/1520-0493\(1999\)127<0124:PVAATC>2.0.CO;2](https://doi.org/10.1175/1520-0493(1999)127<0124:PVAATC>2.0.CO;2).
- Shay, L. K., and R. L. Elsberry, 1987: Near-inertial ocean current response to Hurricane Frederic. *J. Phys. Oceanogr.*, **17**, 1249–1269, [https://doi.org/10.1175/1520-0485\(1987\)017<1249:NIOCRT>2.0.CO;2](https://doi.org/10.1175/1520-0485(1987)017<1249:NIOCRT>2.0.CO;2).
- , —, and P. G. Black, 1989: Vertical structure of the ocean current response to a hurricane. *J. Phys. Oceanogr.*, **19**, 649–669, [https://doi.org/10.1175/1520-0485\(1989\)019<0649:VSOTOC>2.0.CO;2](https://doi.org/10.1175/1520-0485(1989)019<0649:VSOTOC>2.0.CO;2).
- , P. G. Black, A. J. Mariano, J. D. Hawkins, and R. L. Elsberry, 1992: Upper ocean response to Hurricane Gilbert. *J. Geophys. Res.*, **97**, 20 227–20 248, <https://doi.org/10.1029/92JC01586>.
- Shea, D. J., and W. M. Gray, 1973: The hurricane's inner core region. I. Symmetric and asymmetric structure. *J. Atmos. Sci.*, **30**, 1544–1564, [https://doi.org/10.1175/1520-0469\(1973\)030<1544:THICRI>2.0.CO;2](https://doi.org/10.1175/1520-0469(1973)030<1544:THICRI>2.0.CO;2).
- Shi, J. J., S. Chang, and S. Raman, 1997: Interaction between Hurricane Florence (1988) and an upper-tropospheric westerly trough. *J. Atmos. Sci.*, **54**, 1231–1247, [https://doi.org/10.1175/1520-0469\(1997\)054<1231:IBHFAA>2.0.CO;2](https://doi.org/10.1175/1520-0469(1997)054<1231:IBHFAA>2.0.CO;2).
- Shutts, G. J., 1981: Hurricane structure and the zero potential vorticity approximation. *Mon. Wea. Rev.*, **109**, 324–329, [https://doi.org/10.1175/1520-0493\(1981\)109<0324:HSATZP>2.0.CO;2](https://doi.org/10.1175/1520-0493(1981)109<0324:HSATZP>2.0.CO;2).
- Simpson, R. H., 1946: On the movement of tropical cyclones. *Eos, Trans. Amer. Geophys. Union*, **27**, 641–655, <https://doi.org/10.1029/TR027i005p00641>.
- , 1952a: Evolution of the Kona storm, a subtropical cyclone. *J. Meteor.*, **9**, 24–35, [https://doi.org/10.1175/1520-0469\(1952\)009<0024:EOTKSA>2.0.CO;2](https://doi.org/10.1175/1520-0469(1952)009<0024:EOTKSA>2.0.CO;2).
- , 1952b: Exploring eye of Typhoon “Marge,” 1951. *Bull. Amer. Meteor. Soc.*, **33**, 286–298, <https://doi.org/10.1175/1520-0477-33.7.286>.
- , and H. Riehl, 1958: Mid-tropospheric ventilation as a constraint on hurricane development and maintenance. Preprints, *Tech. Conf. on Hurricanes*, Miami Beach, FL, Amer. Meteor. Soc., D4-1–D4-10.
- , and J. S. Malkus, 1963: An experiment in hurricane modification: Preliminary results. *Science*, **142**, 498–498, <https://doi.org/10.1126/science.142.3591.498>.
- , R. Anthes, M. Garstang, and J. Simpson, Eds., 2003: Hurricane! *Coping with Disaster: Progress and Challenges since Galveston, 1900*. Amer. Geophys. Union, 360 pp.
- Sinclair, M. R., 2002: Extratropical transition of southwest Pacific tropical cyclones. Part I: Climatology and mean structure changes. *Mon. Wea. Rev.*, **130**, 590–609, [https://doi.org/10.1175/1520-0493\(2002\)130<0590:ETOSPT>2.0.CO;2](https://doi.org/10.1175/1520-0493(2002)130<0590:ETOSPT>2.0.CO;2).
- Singh, O. P., T. M. A. Khan, and M. S. Rahman, 2000: Changes in the frequency of tropical cyclones over the north Indian Ocean. *Meteor. Atmos. Phys.*, **75**, 11–20, <https://doi.org/10.1007/s007030070011>.
- Sippel, J. A., and F. Zhang, 2008: A probabilistic analysis of the dynamics and predictability of tropical cyclogenesis. *J. Atmos. Sci.*, **65**, 3440–3459, <https://doi.org/10.1175/2008JAS2597.1>.
- Smith, R. K., 1968: The surface boundary layer of a hurricane. *Tellus*, **20**, 473–484.
- , 1980: Tropical cyclone eye dynamics. *J. Atmos. Sci.*, **37**, 1227–1232, [https://doi.org/10.1175/1520-0469\(1980\)037<1227:TCED>2.0.CO;2](https://doi.org/10.1175/1520-0469(1980)037<1227:TCED>2.0.CO;2).
- , 1991: An analytic theory of tropical-cyclone motion in a barotropic shear flow. *Quart. J. Roy. Meteor. Soc.*, **117**, 685–714, <https://doi.org/10.1002/qj.49711750003>.
- , 2003: A simple model of the hurricane boundary layer. *Quart. J. Roy. Meteor. Soc.*, **129**, 1007–1027, <https://doi.org/10.1256/qj.01.197>.
- , 2005: Why must hurricanes have eyes? *Weather*, **60**, 326–328, <https://doi.org/10.1256/wea.34.05>.
- , and W. Ulrich, 1990: An analytical theory of tropical cyclone motion using a barotropic model. *J. Atmos. Sci.*, **47**, 1973–1986, [https://doi.org/10.1175/1520-0469\(1990\)047<1973:AAOTOC>2.0.CO;2](https://doi.org/10.1175/1520-0469(1990)047<1973:AAOTOC>2.0.CO;2).
- , and H. C. Weber, 1993: An extended analytic theory of tropical-cyclone motion in a barotropic shear flow. *Quart. J. Roy. Meteor. Soc.*, **119**, 1149–1166, <https://doi.org/10.1002/qj.49711951314>.
- , and S. Vogl, 2008: A simple model of the hurricane boundary layer revisited. *Quart. J. Roy. Meteor. Soc.*, **134**, 337–351, <https://doi.org/10.1002/qj.216>.
- , and M. T. Montgomery, 2015: Toward clarity on understanding tropical cyclone intensification. *J. Atmos. Sci.*, **72**, 3020–3031, <https://doi.org/10.1175/JAS-D-15-0017.1>.
- , W. Ulrich, and G. Sneddon, 2000: On the dynamics of hurricane-like vortices in vertical-shear flows. *Quart. J. Roy. Meteor. Soc.*, **126**, 2653–2670, <https://doi.org/10.1002/qj.49712656903>.
- , M. T. Montgomery, and S. Vogl, 2008: A critique of Emanuel's hurricane model and potential intensity theory. *Quart. J. Roy. Meteor. Soc.*, **134**, 551–561, <https://doi.org/10.1002/qj.241>.
- , —, and N. V. Sang, 2009: Tropical cyclone spin-up revisited. *Quart. J. Roy. Meteor. Soc.*, **135**, 1321–1335, <https://doi.org/10.1002/qj.428>.
- Smith, S. D., and Coauthors, 1992: Sea surface wind stress and drag coefficients: The HEXOS results. *Bound.-Layer Meteor.*, **60**, 109–142, <https://doi.org/10.1007/BF00122064>.
- Sobel, A. H., 2014: *Storm Surge: Hurricane Sandy, Our Changing Climate, and Extreme Weather of the Past and Future*. 1st ed. Harper Wave, 336 pp.

- , and C. S. Bretherton, 2000: Modeling tropical precipitation in a single column. *J. Climate*, **13**, 4378–4392, [https://doi.org/10.1175/1520-0442\(2000\)013<4378:MTPIAS>2.0.CO;2](https://doi.org/10.1175/1520-0442(2000)013<4378:MTPIAS>2.0.CO;2).
- , and E. D. Maloney, 2000: Effect of ENSO and the MJO on western North Pacific tropical cyclones. *Geophys. Res. Lett.*, **27**, 1739–1742, <https://doi.org/10.1029/1999GL011043>.
- , S. J. Camargo, T. M. Hall, C. Y. Lee, M. K. Tippett, and A. A. Wing, 2016: Human influence on tropical cyclone intensity. *Science*, **353**, 242–246, <https://doi.org/10.1126/science.aaf6574>.
- Soloviev, A. V., and R. Lukas, 2010: Effects of bubbles and sea spray on air–sea exchange in hurricane conditions. *Bound.-Layer Meteor.*, **136**, 365–376, <https://doi.org/10.1007/s10546-010-9505-0>.
- , —, M. A. Donelan, B. K. Haus, and I. Ginis, 2014: The air–sea interface and surface stress under tropical cyclones. *Sci. Rep.*, **4**, 5306, <https://doi.org/10.1038/srep05306>.
- , —, —, —, and —, 2017: Is the state of the air–sea interface a factor in rapid intensification and rapid decline of tropical cyclones? *J. Geophys. Res. Oceans*, **122**, 10 174–10 183, <https://doi.org/10.1002/2017JC013435>.
- Soria, J. L. A., A. D. Switzer, J. E. Pilarczyk, F. P. Siringan, N. S. Khan, and H. M. Fritz, 2017: Typhoon Haiyan overwash sediments from Leyte Gulf coastlines show local spatial variations with hybrid storm and tsunami signatures. *Sediment. Geol.*, **358**, 121–138, <https://doi.org/10.1016/j.sedgeo.2017.06.006>.
- , and Coauthors, 2018: Surf beat-induced overwash during Typhoon Haiyan deposited two distinct sediment assemblages on the carbonate coast of Hernani, Samar, central Philippines. *Mar. Geol.*, **396**, 215–230, <https://doi.org/10.1016/j.margeo.2017.08.016>.
- Sliver, R. L., 2013: Observational evidence supports the role of tropical cyclones in regulating climate. *Proc. Natl. Acad. Sci. USA*, **110**, 15 173–15 174, <https://doi.org/10.1073/pnas.1314721110>.
- , M. Huber, and J. Nusbaumer, 2008: Investigating tropical cyclone–climate feedbacks using the TRMM Microwave Imager and the Quick Scatterometer. *Geochem. Geophys. Geosyst.*, **9**, Q09V11, <https://doi.org/10.1029/2007GC001842>.
- , M. Goes, M. E. Mann, and K. Keller, 2010: Climate response to tropical cyclone-induced ocean mixing in an Earth system model of intermediate complexity. *J. Geophys. Res.*, **115**, C10042, <https://doi.org/10.1029/2010JC006106>.
- Staley, D. O., and R. L. Gall, 1984: Hydrodynamic instability of small eddies in a tornado vortex. *J. Atmos. Sci.*, **41**, 422–429, [https://doi.org/10.1175/1520-0469\(1984\)041<0422:HIOSSEI>2.0.CO;2](https://doi.org/10.1175/1520-0469(1984)041<0422:HIOSSEI>2.0.CO;2).
- Stern, D. P., and F. Zhang, 2013: How does the eye warm? Part I: A potential temperature budget analysis of an idealized tropical cyclone. *J. Atmos. Sci.*, **70**, 73–90, <https://doi.org/10.1175/JAS-D-11-0329.1>.
- Stith, J. L., and Coauthors, 2019: 100 years of progress in atmospheric observing systems. *A Century of Progress in Atmospheric and Related Sciences: Celebrating the American Meteorological Society Centennial*, Meteor. Monogr., No. 59, Amer. Meteor. Soc., <https://doi.org/10.1175/AMSMONOGRAPHS-D-18-0006.1>.
- Stone, P. H., 1966: On non-geostrophic baroclinic stability. *J. Atmos. Sci.*, **23**, 390–400, [https://doi.org/10.1175/1520-0469\(1966\)023<0390:ONGBS>2.0.CO;2](https://doi.org/10.1175/1520-0469(1966)023<0390:ONGBS>2.0.CO;2).
- Subrahmanyam, B., K. H. Rao, N. S. Rao, V. S. N. Murty, and R. J. Sharp, 2002: Influence of a tropical cyclone on chlorophyll-a concentration in the Arabian Sea. *Geophys. Res. Lett.*, **29**, 2065, <https://doi.org/10.1029/2002GL015892>.
- Sumesh, K. G., and M. R. Ramesh Kumar, 2013: Tropical cyclones over north Indian Ocean during El-Niño Modoki years. *Nat. Hazards*, **68**, 1057–1074, <https://doi.org/10.1007/s11069-013-0679-x>.
- Sutyryn, G. G., and A. P. Khain, 1984: Effect of the ocean–atmosphere interaction on the intensity of a moving tropical cyclone. *Atmos. Ocean. Phys.*, **20**, 697–703.
- , and G. R. Flierl, 1994: Intense vortex motion on the beta plane: Development of the beta gyres. *J. Atmos. Sci.*, **51**, 773–790, [https://doi.org/10.1175/1520-0469\(1994\)051<0773:IVMOTB>2.0.CO;2](https://doi.org/10.1175/1520-0469(1994)051<0773:IVMOTB>2.0.CO;2).
- Syono, S., 1955: On the motion of a typhoon. *J. Meteor. Soc. Japan*, **33**, 245–261, [https://doi.org/10.2151/jmsj1923.33.6\\_245](https://doi.org/10.2151/jmsj1923.33.6_245).
- Tang, B., and K. Emanuel, 2010: Midlevel ventilation’s constraint on tropical cyclone intensity. *J. Atmos. Sci.*, **67**, 1817–1830, <https://doi.org/10.1175/2010JAS3318.1>.
- , and —, 2012a: Sensitivity of tropical cyclone intensity to ventilation in an axisymmetric model. *J. Atmos. Sci.*, **69**, 2394–2413, <https://doi.org/10.1175/JAS-D-11-0232.1>.
- , and —, 2012b: A ventilation index for tropical cyclones. *Bull. Amer. Meteor. Soc.*, **93**, 1901–1912, <https://doi.org/10.1175/BAMS-D-11-00165.1>.
- Tang, B. H., and D. J. Neelin, 2004: ENSO influence on Atlantic hurricanes via tropospheric warming. *Geophys. Res. Lett.*, **31**, L24204, <https://doi.org/10.1029/2004GL021072>.
- Tao, D., and F. Zhang, 2015: Effects of vertical wind shear on the predictability of tropical cyclones: Practical versus intrinsic limit. *J. Adv. Model. Earth Syst.*, **7**, 1534–1553, <https://doi.org/10.1002/2015MS000474>.
- Tatro, P., and E. Mollo-Christensen, 1967: Experiments on Ekman layer instability. *J. Fluid Mech.*, **28**, 531–543, <https://doi.org/10.1017/S0022112067002289>.
- Thorpe, A. J., 1992: An appreciation of the meteorological research of Ernst Kleinschmidt. Joint Centre for Mesoscale Meteorology Internal Rep. 11, 22 pp.
- , M. J. Miller, and M. W. Moncrieff, 1982: Two-dimensional convection in non-constant shear: A model of mid-latitude squall lines. *Quart. J. Roy. Meteor. Soc.*, **108**, 739–762, <https://doi.org/10.1002/qj.49710845802>.
- Tian, Y., and Z. Luo, 1994: Vertical structure of beta gyres and its effect on tropical cyclone motion. *Adv. Atmos. Sci.*, **11**, 43–50, <https://doi.org/10.1007/BF02656992>.
- Ting, M., S. J. Camargo, C. Li, and Y. Kushnir, 2015: Natural and forced North Atlantic hurricane potential intensity change in CMIP5 models. *J. Climate*, **28**, 3926–3942, <https://doi.org/10.1175/JCLI-D-14-00520.1>.
- Tippett, M. K., S. Camargo, and A. H. Sobel, 2011: A Poisson regression index for tropical cyclone genesis and the role of large-scale vorticity in genesis. *J. Climate*, **24**, 2335–2357, <https://doi.org/10.1175/2010JCLI3811.1>.
- Tobin, I., S. Bony, and R. Roca, 2012: Observational evidence for relationships between the degree of aggregation of deep convection, water vapor, surface fluxes, and radiation. *J. Climate*, **25**, 6885–6904, <https://doi.org/10.1175/JCLI-D-11-00258.1>.
- Toomey, M. R., W. B. Curry, J. P. Donnelly, and P. J. van Hengstum, 2013: Reconstructing 7000 years of North Atlantic hurricane variability using deep-sea sediment cores from the western Great Bahama Bank. *Paleoceanography*, **28**, <https://doi.org/10.1002/palo.20012>.
- Torn, R. D., and G. J. Hakim, 2015: Comparison of wave packets associated with extratropical transition and winter cyclones. *Mon. Wea. Rev.*, **143**, 1782–1803, <https://doi.org/10.1175/MWR-D-14-00006.1>.

- Tous, M., and R. Romero, 2013: Meteorological environments associated with medicane development. *Int. J. Climatol.*, **33**, 1–14, <https://doi.org/10.1002/joc.3428>.
- , —, and C. Ramis, 2013: Surface heat fluxes influence on medicane trajectories and intensification. *Atmos. Res.*, **123**, 400–411, <https://doi.org/10.1016/j.atmosres.2012.05.022>.
- Tuleya, R. E., 1994: Tropical storm development and decay: Sensitivity to surface boundary conditions. *Mon. Wea. Rev.*, **122**, 291–304, [https://doi.org/10.1175/1520-0493\(1994\)122<0291:TSDADS>2.0.CO;2](https://doi.org/10.1175/1520-0493(1994)122<0291:TSDADS>2.0.CO;2).
- Twitchell, P. F., E. A. Rasmussen, and K. L. Davidson, Eds., 1989: *Polar and Arctic Lows*. A. Deepak, 421 pp.
- van Hengstum, P. J., J. P. Donnelly, M. R. Toomey, N. A. Albury, P. Lane, and B. Kakuk, 2014: Heightened hurricane activity on the Little Bahama Bank from 1350 to 1650 AD. *Cont. Shelf Res.*, **86**, 103–115, <https://doi.org/10.1016/j.csr.2013.04.032>.
- , —, P. L. Fall, M. R. Toomey, N. A. Albury, and B. Kakuk, 2016: The intertropical convergence zone modulates intense hurricane strikes on the western North Atlantic margin. *Sci. Rep.*, **6**, 21728, <https://doi.org/10.1038/srep21728>.
- van Soelen, E. E., F. Wagner-Cremer, J. S. S. Damste, and G. J. Reichert, 2013: Reconstructing tropical cyclone frequency using hydrogen isotope ratios of sedimentary n-alkanes in northern Queensland, Australia. *Palaeogeogr., Palaeoclimatol., Palaeoecol.*, **376**, 66–72, <https://doi.org/10.1016/j.palaeo.2013.02.019>.
- Velasco, I., and J. M. Fritsch, 1987: Mesoscale convective complexes in the Americas. *J. Geophys. Res.*, **92**, 9591–9613, <https://doi.org/10.1029/JD092iD08p09591>.
- Velden, C. S., and Coauthors, 2006: The Dvorak tropical cyclone intensity estimation technique: A satellite-based method that has endured for over 30 years. *Bull. Amer. Meteor. Soc.*, **87**, 1195–1210, <https://doi.org/10.1175/BAMS-87-9-1195>.
- Venkateswrlu, P., and K. H. Rao, 2004: A study on cyclone induced productivity in south-western Bay of Bengal during November–December 2000 using MODIS data products. *2004 International Geoscience and Remote Sensing Symp.*, Anchorage, AK, IEEE, 3496–3499, <https://doi.org/10.1109/IGARSS.2004.1370462>.
- Ventrice, M. J., C. D. Thorncroft, and P. E. Roundy, 2011: The Madden–Julian oscillation’s influence on African easterly waves and downstream tropical cyclogenesis. *Mon. Wea. Rev.*, **139**, 2704–2722, <https://doi.org/10.1175/MWR-D-10-05028.1>.
- Vimont, D. J., and J. P. Kossin, 2007: The Atlantic Meridional Mode and hurricane activity. *Geophys. Res. Lett.*, **34**, L07709, <https://doi.org/10.1029/2007GL029683>.
- Viñes, B., 1885: Practical hints in regard to West Indian hurricanes. U.S. Hydrographic Office, Bureau of Navigation Paper 77, U. S. Government Printing Office, 15 pp.
- Vitart, F., 2009: Impact of the Madden Julian Oscillation on tropical storms and risk of landfall in the ECMWF forecast system. *Geophys. Res. Lett.*, **36**, L15802, <https://doi.org/10.1029/2009GL039089>.
- , and J. L. Anderson, 2001: Sensitivity of Atlantic tropical storm frequency to ENSO and interdecadal variability of SSTs in an ensemble of AGCM integrations. *J. Climate*, **14**, 533–545, [https://doi.org/10.1175/1520-0442\(2001\)014<0533:SOATSF>2.0.CO;2](https://doi.org/10.1175/1520-0442(2001)014<0533:SOATSF>2.0.CO;2).
- von Hann, J., 1901: *Lehrbuch der Meteorologie (Textbook of Meteorology)*. C. H. Tauchnitz, 847 pp.
- Walsh, K. J. E., and Coauthors, 2016: Tropical cyclones and climate change. *Wiley Interdiscip. Rev. Climate Change*, **7**, 65–89, <https://doi.org/10.1002/wcc.371>.
- Wang, B., and J. C. L. Chan, 2002: How strong ENSO events affect tropical storm activity over the western North Pacific. *J. Climate*, **15**, 1643–1658, [https://doi.org/10.1175/1520-0442\(2002\)015<1643:HSEEAT>2.0.CO;2](https://doi.org/10.1175/1520-0442(2002)015<1643:HSEEAT>2.0.CO;2).
- , and J.-Y. Moon, 2017: An anomalous genesis potential index for MJO modulation of tropical cyclones. *J. Climate*, **30**, 4021–4035, <https://doi.org/10.1175/JCLI-D-16-0749.1>.
- Wang, C. Z., S. K. Lee, and D. B. Enfield, 2008: Atlantic warm pool acting as a link between Atlantic multidecadal oscillation and Atlantic tropical cyclone activity. *Geochem. Geophys. Geosyst.*, **9**, Q05V03, <https://doi.org/10.1029/2007GC001809>.
- Wang, H., and Coauthors, 2014: How well do global climate models simulate the variability of Atlantic tropical cyclones associated with ENSO? *J. Climate*, **27**, 5673–5692, <https://doi.org/10.1175/JCLI-D-13-00625.1>.
- Wang, Y., 2002: Vortex Rossby waves in a numerically simulated tropical cyclone. Part I: Overall structure, potential vorticity, and kinetic energy budgets. *J. Atmos. Sci.*, **59**, 1213–1238, [https://doi.org/10.1175/1520-0469\(2002\)059<1213:VRWIAN>2.0.CO;2](https://doi.org/10.1175/1520-0469(2002)059<1213:VRWIAN>2.0.CO;2).
- , 2009: How do outer spiral rainbands affect tropical cyclone structure and intensity? *J. Atmos. Sci.*, **66**, 1250–1273, <https://doi.org/10.1175/2008JAS2737.1>.
- , and G. J. Holland, 1996: Tropical cyclone motion and evolution in vertical shear. *J. Atmos. Sci.*, **53**, 3313–3332, [https://doi.org/10.1175/1520-0469\(1996\)053<3313:TCMAEI>2.0.CO;2](https://doi.org/10.1175/1520-0469(1996)053<3313:TCMAEI>2.0.CO;2).
- , J. D. Kepert, and G. Holland, 2001: The effect of sea spray evaporation on tropical cyclone boundary layer structure and intensity. *Mon. Wea. Rev.*, **129**, 2481–2500, [https://doi.org/10.1175/1520-0493\(2001\)129<2481:TEOSSE>2.0.CO;2](https://doi.org/10.1175/1520-0493(2001)129<2481:TEOSSE>2.0.CO;2).
- Wang, Z., M. T. Montgomery, and T. J. Dunkerton, 2010: Genesis of pre-hurricane Felix (2007). Part I: The role of the easterly wave critical layer. *J. Atmos. Sci.*, **67**, 1711–1729, <https://doi.org/10.1175/2009JAS3420.1>.
- , —, and C. Fritz, 2012: A first look at the structure of the wave pouch during the 2009 PREDICT–GRIP dry runs over the Atlantic. *Mon. Wea. Rev.*, **140**, 1144–1163, <https://doi.org/10.1175/MWR-D-10-05063.1>.
- Watanabe, S.-I., H. Niino, and W. Yanase, 2018: Composite analysis of polar mesocyclones over the western part of the Sea of Japan. *Mon. Wea. Rev.*, **146**, 985–1004, <https://doi.org/10.1175/MWR-D-17-0107.1>.
- Weatherford, C. L., and W. M. Gray, 1988a: Typhoon structure as revealed by aircraft reconnaissance. Part I: Data analysis and climatology. *Mon. Wea. Rev.*, **116**, 1032–1043, [https://doi.org/10.1175/1520-0493\(1988\)116<1032:TSARBA>2.0.CO;2](https://doi.org/10.1175/1520-0493(1988)116<1032:TSARBA>2.0.CO;2).
- , and —, 1988b: Typhoon structure as revealed by aircraft reconnaissance. Part II: Structural variability. *Mon. Wea. Rev.*, **116**, 1044–1056, [https://doi.org/10.1175/1520-0493\(1988\)116<1044:TSARBA>2.0.CO;2](https://doi.org/10.1175/1520-0493(1988)116<1044:TSARBA>2.0.CO;2).
- Weng, Y., and F. Zhang, 2012: Assimilating airborne Doppler radar observations with an ensemble Kalman filter for convection-permitting hurricane initialization and prediction: Katrina (2005). *Mon. Wea. Rev.*, **140**, 841–859, <https://doi.org/10.1175/2011MWR3602.1>.
- , and —, 2016: Advances in convection-permitting tropical cyclone analysis and prediction through EnKF assimilation of reconnaissance aircraft observations. *J. Meteor. Soc. Japan*, **94**, 345–358, <https://doi.org/10.2151/jmsj.2016-018>.
- Wexler, H., 1945: The structure of the September, 1944, hurricane when off Cape Henry, Virginia. *Bull. Amer. Meteor. Soc.*, **26**, 156–159, <https://doi.org/10.1175/1520-0477-26.5.156>.
- , 1947: Structure of hurricanes as determined by radar. *Ann. N. Y. Acad. Sci.*, **48**, 821–844, <https://doi.org/10.1111/j.1749-6632.1947.tb38495.x>.

- Wheeler, M., and G. N. Kiladis, 1999: Convectively coupled equatorial waves: Analysis of clouds and temperature in the wavenumber-frequency domain. *J. Atmos. Sci.*, **56**, 374–399, [https://doi.org/10.1175/1520-0469\(1999\)056<0374:CCEWAO>2.0.CO;2](https://doi.org/10.1175/1520-0469(1999)056<0374:CCEWAO>2.0.CO;2).
- Williams, G. J., R. K. Taft, B. D. McNoldy, and W. H. Schubert, 2013: Shock-like structures in the tropical cyclone boundary layer. *J. Adv. Model. Earth Syst.*, **5**, 338–353, <https://doi.org/10.1002/jame.20028>.
- Williams, H. F. L., 2010: Storm surge deposition by Hurricane Ike on the McFaddin National Wildlife Refuge, Texas: Implications for paleotempestology studies. *J. Foraminiferal Res.*, **40**, 210–219, <https://doi.org/10.2113/gsjfr.40.3.210>.
- Willoughby, H. E., 1977: Inertia-buoyancy waves in hurricanes. *J. Atmos. Sci.*, **34**, 1028–1039, [https://doi.org/10.1175/1520-0469\(1977\)034<1028:IBWIH>2.0.CO;2](https://doi.org/10.1175/1520-0469(1977)034<1028:IBWIH>2.0.CO;2).
- , 1988a: The dynamics of the tropical hurricane core. *Aust. Meteor. Mag.*, **36**, 183–191, <http://www.bom.gov.au/jshess/docs/1988/willoughby.pdf>.
- , 1988b: Linear motion of a shallow water, barotropic vortex. *J. Atmos. Sci.*, **45**, 1906–1928, [https://doi.org/10.1175/1520-0469\(1988\)045<1906:LMOASW>2.0.CO;2](https://doi.org/10.1175/1520-0469(1988)045<1906:LMOASW>2.0.CO;2).
- , 1998: Tropical cyclone eye thermodynamics. *Mon. Wea. Rev.*, **126**, 3053–3067, [https://doi.org/10.1175/1520-0493\(1998\)126<3053:TCET>2.0.CO;2](https://doi.org/10.1175/1520-0493(1998)126<3053:TCET>2.0.CO;2).
- , J. A. Clos, and M. G. Shoreibah, 1982: Concentric eyes, secondary wind maxima, and the evolution of the hurricane vortex. *J. Atmos. Sci.*, **39**, 395–411, [https://doi.org/10.1175/1520-0469\(1982\)039<0395:CEWSWM>2.0.CO;2](https://doi.org/10.1175/1520-0469(1982)039<0395:CEWSWM>2.0.CO;2).
- , D. P. Jorgensen, R. A. Black, and S. L. Rosenthal, 1985: Project STORMFURY: A scientific chronicle 1962–1983. *Bull. Amer. Meteor. Soc.*, **66**, 505–514, [https://doi.org/10.1175/1520-0477\(1985\)066<0505:PSASC>2.0.CO;2](https://doi.org/10.1175/1520-0477(1985)066<0505:PSASC>2.0.CO;2).
- Wing, A. A., and K. A. Emanuel, 2014: Physical mechanisms controlling self-aggregation of convection in idealized numerical modeling simulations. *J. Adv. Model. Earth Syst.*, **6**, 59–74, <https://doi.org/10.1002/2013MS000269>.
- , S. J. Camargo, and A. H. Sobel, 2016: Role of radiative-convective feedbacks in spontaneous tropical cyclogenesis in idealized numerical simulations. *J. Atmos. Sci.*, **73**, 2633–2642, <https://doi.org/10.1175/JAS-D-15-0380.1>.
- , K. Emanuel, C. E. Holloway, and C. Muller, 2017: Convective self-aggregation in numerical simulations: A review. *Surv. Geophys.*, **38**, 1173–1197, <https://doi.org/10.1007/s10712-017-9408-4>.
- Wood, K. M., and E. A. Ritchie, 2014: A 40-year climatology of extratropical transition in the eastern North Pacific. *J. Climate*, **27**, 5999–6015, <https://doi.org/10.1175/JCLI-D-13-00645.1>.
- Woodruff, J. D., J. P. Donnelly, and D. Mohrig, 2006: Grain-size distributions and flow parameter estimates for a prehistoric overwash event within a backbarrier lagoon, Vieques, Puerto Rico. *Eos, Trans. Amer. Geophys. Union*, **87** (Ocean Science Meeting Suppl.), Abstract OS26M-08.
- , —, —, and W. R. Geyer, 2008: Reconstructing relative flooding intensities responsible for hurricane-induced deposits from laguna Playa Grande, Vieques, Puerto Rico. *Geology*, **36**, 391–394, <https://doi.org/10.1130/G24731A.1>.
- Wright, C. W., and Coauthors, 2001: Hurricane directional wave spectrum spatial variation in the open ocean. *J. Phys. Oceanogr.*, **31**, 2472–2488, [https://doi.org/10.1175/1520-0485\(2001\)031<2472:HDWSSV>2.0.CO;2](https://doi.org/10.1175/1520-0485(2001)031<2472:HDWSSV>2.0.CO;2).
- Wu, C.-C., and K. A. Emanuel, 1993: Interaction of a baroclinic vortex with background shear: Application to hurricane movement. *J. Atmos. Sci.*, **50**, 62–76, [https://doi.org/10.1175/1520-0469\(1993\)050<0062:IOABVW>2.0.CO;2](https://doi.org/10.1175/1520-0469(1993)050<0062:IOABVW>2.0.CO;2).
- , and —, 1994: On hurricane outflow structure. *J. Atmos. Sci.*, **51**, 1995–2003, [https://doi.org/10.1175/1520-0469\(1994\)051<1995:OHOS>2.0.CO;2](https://doi.org/10.1175/1520-0469(1994)051<1995:OHOS>2.0.CO;2).
- , and —, 1995a: Potential vorticity diagnostics of hurricane movement. Part I: A case study of Hurricane Bob (1991). *Mon. Wea. Rev.*, **123**, 69–92, [https://doi.org/10.1175/1520-0493\(1995\)123<0069:PVDOHM>2.0.CO;2](https://doi.org/10.1175/1520-0493(1995)123<0069:PVDOHM>2.0.CO;2).
- , and —, 1995b: Potential vorticity diagnostics of hurricane movement. Part II: Tropical Storm Ana (1991) and Hurricane Andrew (1992). *Mon. Wea. Rev.*, **123**, 93–109, [https://doi.org/10.1175/1520-0493\(1995\)123<0093:PVDOHM>2.0.CO;2](https://doi.org/10.1175/1520-0493(1995)123<0093:PVDOHM>2.0.CO;2).
- , and Y. Kurihara, 1996: A numerical study of the feedback mechanisms of hurricane-environment interaction on hurricane movement from the potential vorticity perspective. *J. Atmos. Sci.*, **53**, 2264–2282, [https://doi.org/10.1175/1520-0469\(1996\)053<2264:ANSOTF>2.0.CO;2](https://doi.org/10.1175/1520-0469(1996)053<2264:ANSOTF>2.0.CO;2).
- , and Coauthors, 2005: Dropwindsonde observations for typhoon surveillance near the Taiwan region (DOTSTAR): An overview. *Bull. Amer. Meteor. Soc.*, **86**, 787–790, <https://doi.org/10.1175/BAMS-86-6-787>.
- , C.-Y. Lee, and I.-I. Lin, 2007: The effect of the ocean eddy on tropical cyclone intensity. *J. Atmos. Sci.*, **64**, 3562–3578, <https://doi.org/10.1175/JAS4051.1>.
- Wu, J., 1990: On parameterization of sea spray. *J. Geophys. Res.*, **95**, 18 269–18 279, <https://doi.org/10.1029/JC095iC10p18269>.
- Wu, L., B. Wang, and S. A. Braun, 2005: Impacts of air–sea interaction on tropical cyclone track and intensity. *Mon. Wea. Rev.*, **133**, 3299–3314, <https://doi.org/10.1175/MWR3030.1>.
- Wu, M. C., W. L. Chang, and W. M. Leung, 2004: Impacts of El Niño–Southern Oscillation events on tropical cyclone land-falling activity in the western North Pacific. *J. Climate*, **17**, 1419–1428, [https://doi.org/10.1175/1520-0442\(2004\)017<1419:IOENOE>2.0.CO;2](https://doi.org/10.1175/1520-0442(2004)017<1419:IOENOE>2.0.CO;2).
- Wu, Q., and Z. Ruan, 2016: Diurnal variations of the areas and temperatures in tropical cyclone clouds. *Quart. J. Roy. Meteor. Soc.*, **142**, 2788–2796, <https://doi.org/10.1002/qj.2868>.
- Wurman, J., and J. Winslow, 1998: Intense sub-kilometer-scale boundary layer rolls observed in Hurricane Fran. *Science*, **280**, 555–557, <https://doi.org/10.1126/science.280.5363.555>.
- Xu, K.-M., and K. A. Emanuel, 1989: Is the tropical atmosphere conditionally unstable? *Mon. Wea. Rev.*, **117**, 1471–1479, [https://doi.org/10.1175/1520-0493\(1989\)117<1471:ITTACU>2.0.CO;2](https://doi.org/10.1175/1520-0493(1989)117<1471:ITTACU>2.0.CO;2).
- Yablonsky, R. M., and I. Ginis, 2009: Limitation of one-dimensional ocean models for coupled hurricane–ocean model forecasts. *Mon. Wea. Rev.*, **137**, 4410–4419, <https://doi.org/10.1175/2009MWR2863.1>.
- Yamasaki, M., 1968: Numerical simulation of tropical cyclone development with the use of primitive equations. *J. Meteor. Soc. Japan*, **46**, 178–201, [https://doi.org/10.2151/jmsj1965.46.3\\_178](https://doi.org/10.2151/jmsj1965.46.3_178).
- , 1977: A preliminary experiment of the tropical cyclone without parameterizing the effects of cumulus convection. *J. Meteor. Soc. Japan*, **55**, 11–31, [https://doi.org/10.2151/jmsj1965.55.1\\_11](https://doi.org/10.2151/jmsj1965.55.1_11).
- Yanai, M., 1964: Formation of tropical cyclones. *Rev. Geophys.*, **2**, 367–414, <https://doi.org/10.1029/RG002i002p0367>.
- Yanase, W., and Coauthors, 2016: Climatology of polar lows over the Sea of Japan using the JRA-55 reanalysis. *J. Climate*, **29**, 419–437, <https://doi.org/10.1175/JCLI-D-15-0291.1>.
- Yang, Y.-T., H.-C. Kuo, E. A. Hendricks, Y.-C. Liu, and M. S. Peng, 2015: Relationship between typhoons with concentric

- eyewalls and ENSO in the western North Pacific basin. *J. Climate*, **28**, 3612–3623, <https://doi.org/10.1175/JCLI-D-14-00541.1>.
- Zhan, M., and H. von Storch, 2008: A long-term climatology of North Atlantic polar lows. *Geophys. Res. Lett.*, **35**, L22702, <https://doi.org/10.1029/2008GL035769>.
- Zhang, F., and D. Tao, 2013: Effects of vertical wind shear on the predictability of tropical cyclones. *J. Atmos. Sci.*, **70**, 975–983, <https://doi.org/10.1175/JAS-D-12-0133.1>.
- , and Y. Weng, 2015: Predicting hurricane intensity and associated hazards. *Bull. Amer. Meteor. Soc.*, **96**, 25–33, <https://doi.org/10.1175/BAMS-D-13-00231.1>.
- Zhang, R., and T. L. Delworth, 2006: Impact of Atlantic multidecadal oscillations on India/Sahel rainfall and Atlantic hurricanes. *Geophys. Res. Lett.*, **33**, L17712, <https://doi.org/10.1029/2006GL026267>.
- , —, and I. M. Held, 2007: Can the Atlantic Ocean drive the observed multidecadal variability in Northern Hemisphere mean temperature? *Geophys. Res. Lett.*, **34**, L02709, <https://doi.org/10.1029/2006GL028683>.
- Zhang, W., H.-F. Graf, Y. Leung, and M. Herzog, 2012: Different El Niño types and tropical cyclone landfall in East Asia. *J. Climate*, **25**, 6510–6523, <https://doi.org/10.1175/JCLI-D-11-00488.1>.
- , G. A. Vecchi, G. Villarini, H. Murakami, A. Rosati, X. Yang, L. Jia, and F. Zeng, 2017: Modulation of western North Pacific tropical cyclone activity by the Atlantic Meridional Mode. *Climate Dyn.*, **48**, 631–647, <https://doi.org/10.1007/s00382-016-3099-2>.
- Zhang, Y., H. Wang, J. Sun, and H. Drange, 2010: Changes in the tropical cyclone genesis potential index over the western North Pacific in the SRES A2 scenario. *Adv. Atmos. Sci.*, **27**, 1246–1258, <https://doi.org/10.1007/s00376-010-9096-1>.
- Zhao, H., and C. Wang, 2018: On the relationship between ENSO and tropical cyclones in the western North Pacific during the boreal summer. *Climate Dyn.*, <https://doi.org/10.1007/s00382-018-4136-0>, in press.
- , L. Wu, and W. Zhou, 2010: Assessing the influence of the ENSO on tropical cyclone prevailing tracks in the western North Pacific. *Adv. Atmos. Sci.*, **27**, 1361–1371, <https://doi.org/10.1007/s00376-010-9161-9>.
- Zhong, W., D.-L. Zhang, and H.-C. Lu, 2009: A theory for mixed vortex Rossby–gravity waves in tropical cyclones. *J. Atmos. Sci.*, **66**, 3366–3381, <https://doi.org/10.1175/2009JAS3060.1>.
- Zhu, P., 2008: Simulation and parameterization of the turbulent transport in the hurricane boundary layer by large eddies. *J. Geophys. Res.*, **113**, D17104, <https://doi.org/10.1029/2007JD009643>.
- Zhu, X., R. Saravanan, and P. Chang, 2012: Influence of mean flow on the ENSO–vertical wind shear relationship over the northern tropical Atlantic. *J. Climate*, **25**, 858–864, <https://doi.org/10.1175/JCLI-D-11-00213.1>.
- Zipser, E. J., and Coauthors, 2009: The Saharan air layer and the fate of African easterly waves—NASA’s AMMA field study of tropical cyclogenesis. *Bull. Amer. Meteor. Soc.*, **90**, 1137–1156, <https://doi.org/10.1175/2009BAMS2728.1>.
- Zweers, N. C., V. K. Makin, J. W. de Vries, and V. N. Kudryavtsev, 2015: The impact of spray-mediated enhanced enthalpy and reduced drag coefficients in the modelling of tropical cyclones. *Bound.-Layer Meteor.*, **155**, 501–514, <https://doi.org/10.1007/s10546-014-9996-1>.